RAPPORT DE CAMPAGNE

CAMPAGNE MD188

11 Janvier 2005-23 Février 2005

Kerguelen: Etude comparée de l'Océan et du Plateau dans les eaux de Surface

KErguelen : compared study of Ocean and Plateau in Surface waters

Chef de projet :

Prof. Stéphane Blain

Laboratoire d'Océanographie Microbienne (LOMIC)
UMR 7621 CNRS UPMC
avenue du Fontaulé
66650 Banyuls sur mer

☎ 04 68 88 73 44
🖷 04 68 88 73 95
stephane.blain@obs-banyuls.fr

Chef de mission :

Prof. Bernard quéguiner

Institut Méditerranéen d'Océanologie (MIO)
UMR 7294 CNRS /UAM
Campus de Luminy
13288 Marseille Cedex 09

☎ 04 91 82 91 05
🖷 04 91 82 19 91
bernard.queguiner@univ-amu.fr

REMERCIEMENTS

Le responsable du projet, le chef de mission et l'équipe scientifique et technique de KEOPS sont très reconnaissants à Yves FRENOT, directeur de l'IPEV, et à Hélène LEAU, responsable du Département "moyens navals et instrumentation embarquée", pour avoir oeuvré à la programmation puis à la réalisation de la campagne KEOPS 2.

Nous tenons également à remercier toutes les personnes de l'IPEV qui ont contribué au succés de la campagne aussi bien à terre qu'en mer et en particuliers Pierre Sangiardi, OPEA pendant KEOPS.

Nous remercions également l'ANR pour le soutien apporté à ce projet au travers du programme "Blanc SIMI 6" ainsi que l'INSU pour le soutien apporté à ce projet au travers du programme "LEFE/CYBER".

Nos remerciements vont également au Commandant B. Lassiette et à l'équipage du Marion Dufresne pour avoir permis la réalisation de l'intensif programme d'opérations prévues malgré les aléas météorologiques.

Content

List of participants to the KEOPS 2 cruise

Name	Nationality	Affiliation	Country of Affiliation
Armand Leanne	Australian	McQuarie Univ	Australia
Batailler Nicole	French	LOMIC	France
Blain Stéphane	French	LOMIC	France
Bowie Andy	English	Univ of Tasmania	Australia
Caparros Jocelyne	French	LOMIC	France
Carlotti François	French	MIO	France
Cavagna Anne–Julie	French	VUB	Belgium
Chever Fanny	French	LEMAR	France
Chirurgien Laure	French	LMGEM	France
Christaki Urania	Greek	LOG	France
Closset Ivia	French	LOCEAN	France
Cornet–Barthaux Véronique	French	MIO	France
Cotté Cédric	French	CEBC/Mammifères	France
Davies Diana	Australian	Univ of Tasmania	Australia
Dehairs Frank	Belgian	VUB	Belgium
Delgard Marie–Lise	French	EPOC	France
d'Ovidio Francesco	Italian	LOCEAN	France
Durand Isabelle	French	LOCEAN	France
Fernandez Camila	Chilean	LOMIC	France
Flores–Leiva Lennis	Colombian	COPAS	Chile
Fourquez Marion	French	LOMIC	France
Garcia Solsona Ester		LEGOS	France
Gueneugues Audrey	French	LOMIC	France
Hartmann Manuela	German	NOCS	United Kindom
Jae-Hak Lee	South Korean	KORDI	South Korea
Jouandet Marie–Paule	French	MIO	France
Kestenare Elodie	French	LEGOS	France
Landa Marine	French	LOMIC	France
Lansard Bruno	French	LEGOS	France
Lasbleiz Marine	French	MIO	France
Laurenceau Emmanuel	French	Univ of Tasmania	Australia
Leblanc Karine	French	MIO	France
Lefevre Dominique	French	LMGEM	France
Llort Joan		LOCEAN/OISO	France
Lo Monaco Claire	French	LOCEAN/OISO	France
Obernosterer Ingrid	Austrian	LOMIC	France
Oriol Louise	French	LOMIC	France
Ousshain Mustapha	French	LOV	France
Park Young Hyang	French	LOCEAN	France
Peralta Veronica	Australian	McQuarie Univ	Australia
Planchon Frédéric	French	VUB	Belgium
Quéguiner Bernard	French	MIO	France
Quéroué Fabien	French	LEMAR	France
Rougier Gilles	French	MIO	France
Royer Anne	French	DT INSU Brest	France
Sarthou Géraldine	French	LEMAR	France
Scouarnec Lionel	French	DT INSU Brest	France
Trull Tom	USA	Univ of Tasmania	Australia
Van beek Pieter	French	LEGOS	France
Van Dermerwe Pier	Australian	Univ of Tasmania	Australia
Zhou Meng	USA	U. Mass. / MIO	France
Zhu Yiwu	USA	U. Mass. / MIO	France

1 KEOPS 2 Log-Book

Principal investigators

Bernard Quéguiner (Chief Sceintist)
MIO, Campus de Luminy, Case 901, 13288 Marseille cedex 9
☎+33 491 829 105
🖷 +33 491 821 991
sbernard.queguiner@obs-banyuls.fr

Stéphane Blain (Project Leader)
LOMIC, Observatoire océanologique de Banyuls,avenue du Fontaulé,
66650 Banyuls sur mer. France
☎+33 468 887 343
stephane.blain@obs-banyuls.fr

31 stations have been sampled during KEOPS 2. Some of them have been visited several times. The HNLC reference station (R) has been visited twice. The Kerguelen Plateau bloom reference station of KEOPS 1 (A3) has also been visited twice. The East Kerguelen reference station (E) has been visited three times at the same location and then splitted in two (Eat and West) for the fourth visit ana fith visit was finally made at the end of the cruise. Another long-term stations (F) was also carried out to sample the Polar Front Eastern bloom. Apart from these long-term stations extra stations have been made to document the meridional and zonal extensions of the East Kerguelen bloom and, occasionally, during deployment and recovery of drifting moorings. Fianlly, stations dedicated to geochemical measurements have been also conducted (G). In the following Log-book, the letters refer to the station and the following number to the sequential occupations.

During KEOPS 2, 302 deck operations have been conducted. Codes are as following :

- CTD — Rosette profiles including CTD (as well as other sensors, see individual reports for details),
- BONGO — Mesozooplankton Bongo net deployment
- PHYTONET — Microphytoplankton net deployment
- DRIFT–PART–TRAP — Drifting particle traps
- GEL–TRAP — Drifting particule gel–sampled traps
- IODA — *In situ* Oxygen Dynamic Auto-sampler deployed on a drifting mooring
- IODA–SED–TRAP — combination of IODA and particle trap drifting mooring
- ISP-QMA-SUPOR — *In situ* pumps
- MOORED SED TRAP — deployment of moored sediment traps
- MULTICORER — deployment of the OKTOPUS INSU corer
- MULTINET — Deployment of the combined nano– maicroplankton nets NOC system
- TMR — Deployment of the ACE–CRC Trace–metal clean rosette
- TURBOMAP — Deploymenyt of the KORDI turbulence profiler

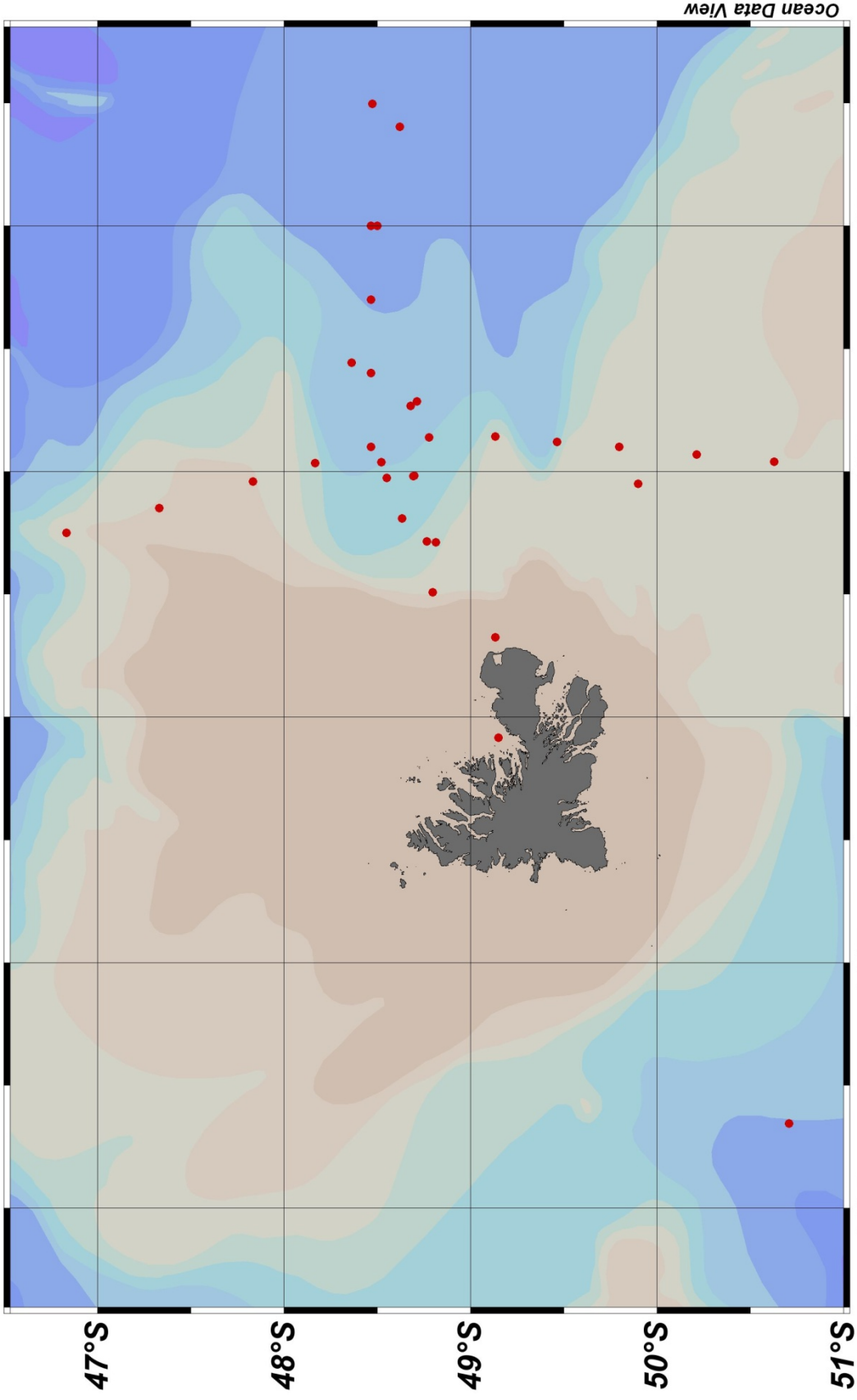

Figure 1 : Map of the study area and location of the stations sampled during KEOPS 2.

Table I : Log-book of operations

			start of station				end of station			
Station	Code of opération	OP #	date	time	position	sounder	date	time	position	sounder
TEST	CTD-000	1	10/10/2011		50° 37.8000' S 072° 04.8000' E		10/10/2011		50° 37.8200' S 072° 04.8200' E	
OISO-6	CTD-001	2	15/10/2011	02:55	44° 59.9800' S 052° 06.0400' E	3 250 m	15/10/2011	04:37	44° 59.9900' S 052° 06.0400' E	3 258 m
OISO7	CTD-002	3	16/10/2011	12:08	47° 40.0000' S 058° 00.3000' E		16/10/2011	13:54		
OISO7	BONGO-01	4	16/10/2011	14:20			16/10/2011	14:42		
OISO7	PHYTONET-01	5	16/10/2011	15:00			16/10/2011	15:20		
OISO7	MULTINET-1	6	16/10/2011	15:35			16/10/2011	16:00	47° 40.0000' S 058° 00.3000' E	
R	IODA-DEP-1	7	17/10/2011	22:00	50° 41.9849' S 066° 42.1192' E	2 923 m	17/10/2011	23:27	50° 42.4528' S 066° 41.6945' E	2 605 m
R	DRIFT-PART-TRAP-1	8	18/10/2011	00:56	50° 42.5729' S 066° 41.4721' E	2 605 m	18/10/2011	02:06	50° 42.8582' S 066° 40.7117' E	2 839 m
A3-1	–	9	18/10/2011	18:50	50° 37.8000' S 072° 04.8000' E		18/10/2011	19:00	50° 37.8000' S 072° 04.8000' E	
A3-1	CTD-003	10	19/10/2011	19:35	50° 37.7781' S 072° 04.8296' E	535 m	19/10/2011	21:02	50° 37.7400' S 072° 04.8000' E	
A3-1	ISP-QMA-SUPOR-01	11	19/10/2011	22:05	50° 37.7574' S 072° 04.8193' E	530 m	19/10/2011	02:26	50° 37.6635' S 072° 04.8316' E	533 m
A3-1	BONGO-02	12	20/10/2011	03:03	50° 37.8000' S 072° 04.8000' E	524 m	20/10/2011	03:55	50° 37.7678' S 072° 04.8232' E	525 m
A3-1	CTD-004	13	20/10/2011	05:32	50° 37.7715' S 072° 04.8233' E	530 m	20/10/2011	06:31	50° 37.7686' S 072° 04.8253' E	529 m
A3-1	TMR-PROCESS-01	14	20/10/2011	08:41	50° 37.8821' S 072° 04.9934' E	532 m	20/10/2011	09:15	50° 37.8826' S 072° 04.9900' E	531 m
A3-1	MOORED SED TRAP-1	15	20/10/2011	10:14	50° 38.0766' S 072° 05.0765' E	533 m	20/10/2011	12:49	50° 38.3062' S 072° 02.5748' E	526 m

Table I **(continued)**

			start of station				end of station			
Station	**Code of opération**	**OP #**	**date**	**time**	**position**	**sounder**	**date**	**time**	**position**	**sounder**
A3-1	TMR-PROCESS-02	16	20/10/2011	13:30	50° 38.6154' S 072° 02.7086' E	524 m	20/10/2011	14:26	50° 38.5923' S 072° 02.7023' E	523 m
A3-1	BONGO-03	17	20/10/2011	14:51	50° 38.5904' S 072° 02.7020' E	527 m	20/10/2011	15:57	50° 38.7178' S 072° 01.8330' E	525 m
A3-1	PHYTONET-02	18	20/10/2011	16:07	50° 38.7100' S 072° 01.8300' E		20/10/2011	16:20	50° 38.7194' S 072° 01.8335' E	524 m
A3-1	MULTINET-2	19	20/10/2011	16:54	50° 38.7100' S 072° 01.8300' E	535 m	20/10/2011	17:10	50° 38.7200' S 072° 01.8300' E	
A3-1	TMR-PROCESS-03	20	20/10/2011	17:50	50° 38.7257' S 072° 01.8390' E		20/10/2011	18:54	50° 38.7263' S 072° 01.8368' E	536 m
A3-1	MULTICORER-1	21	20/10/2011	20:10	50° 38.7205' S 072° 01.8425' E	535 m	20/10/2011	21:30		
A3-1	TMR-PROD-01	22	20/10/2011	21:54			21/10/2011	01:15		
A3-1	TURBOMAP-01	23	21/10/2011	01:25			21/10/2011	01:40		
A3-1	CTD-005	24	21/10/2011	02:22			21/10/2011	03:10	50° 36.2000' S 072° 03.5000' E	
TNS-10	CTD-006	25	21/10/2011	07:28	50° 12.8530' S 072° 07.9180' E	565 m	21/10/2011	08:27	50° 12.8600' S 072° 07.9100' E	558 m
TNS-10	BONGO-04	26	21/10/2011	09:09	50° 12.8633' S 072° 07.9136' E	563 m	21/10/2011	09:29	50° 12.8660' S 072° 07.9097' E	569 m
TNS-10	TURBOMAP-02	27	21/10/2011	10:04	50° 12.8516' S 072° 08.2460' E	557 m	21/10/2011	10:26	50° 13.0737' S 072° 08.7228' E	558 m
TNS-9	CTD-007	28	21/10/2011	13:40	49° 47.9440' S 072° 12.0110' E	615 m	21/10/2011	14:23	49° 47.9410' S 072° 12.0108' E	622 m
TNS-9	BONGO-05	29	21/10/2011	14:38	49° 47.9013' S 072° 12.0177' E	625 m	21/10/2011	15:03	49° 47.9429' S 072° 12.0121' E	625 m
TNS-9	TURBOMAP-03	30	21/10/2011	15:17	49° 47.9629' S 072° 12.0022' E	602 m	21/10/2011	15:41	49° 48.4428' S 072° 12.6557' E	612 m
TNS-8	CTD-008	31	21/10/2011	18:48	49° 27.7700' S 072° 14.4050' E	1 030 m	21/10/2011	19:43	49° 27.7700' S 072° 14.3000' E	1 030 m

Table I **(continued)**

			start of station				end of station			
Station	**Code of opération**	**OP #**	**date**	**time**	**position**	**sounder**	**date**	**time**	**position**	**sounder**
TNS-8	BONGO-06	32	21/10/2011	20:11	49° 27.7700' S 072° 14.3900' E	1 026 m	21/10/2011	20:30	49° 27.7700' S 072° 14.2900' E	1 030 m
TNS-8	TURBOMAP-04	33	21/10/2011	20:48	49° 27.9000' S 072° 14.4300' E	1 026 m	21/10/2011	21:19	49° 28.5900' S 072° 15.3100' E	1 034 m
TNS-7	CTD-009	34	22/10/2011	01:31	49° 08.0057' S 072° 17.0125' E	1 890 m	22/10/2011	02:53	49° 08.0044' S 072° 17.0177' E	1 888 m
TNS-7	BONGO-07	35	22/10/2011	03:13	49° 08.0070' S 072° 17.0196' E	1 878 m	22/10/2011	03:33	49° 08.0048' S 072° 17.0160' E	1 884 m
TNS-7	TURBOMAP-05	36	22/10/2011	03:44	49° 08.3440' S 072° 16.9877' E	1 882 m	22/10/2011	04:23	49° 09.1448' S 072° 17.0446' E	1 882 m
TNS-6	MOORED SED TRAP-2	37	22/10/2011	07:15	48° 47.9344' S 072° 18.0364' E	1 867 m	22/10/2011	08:47	48° 47.2072' S 072° 18.0787' E	1 911 m
TNS-6	CTD-010	38	22/10/2011	11:18	48° 46.7860' S 072° 16.7720' E	1 885 m	22/10/2011	12:54	48° 46.7265' S 072° 16.6484' E	1 885 m
TNS-6	BONGO-08	39	22/10/2011	13:11	48° 46.7226' S 072° 16.6447' E	1 891 m	22/10/2011	13:33	48° 46.7100' S 072° 16.3600' E	1 891 m
TNS-6	PHYTONET-03	40	22/10/2011	13:42	48° 46.7207' S 072° 16.6387' E	1 883 m	22/10/2011	13:53	48° 46.6900' S 072° 16.4200' E	1 883 m
TNS-5	CTD-011	41	22/10/2011	16:56	48° 28.0642' S 072° 12.1061' E	2 060 m	22/10/2011	18:36	48° 28.0633' S 072° 12.1017' E	2 060 m
TNS-5	BONGO-09	42	22/10/2011	19:14	48° 28.0625' S 072° 12.1115' E	2 065 m	22/10/2011	19:36		
TNS-5	TURBOMAP-06	43	22/10/2011	19:57			22/10/2011	20:34	48° 28.3000' S 072° 12.2000' E	
TNS-4	CTD-012	44	23/10/2011	00:44	48° 09.9700' S 072° 03.9300' E	1 800 m	23/10/2011	02:10	48° 09.9700' S 072° 03.9300' E	1 809 m
TNS-4	BONGO-10	45	23/10/2011	02:18	48° 09.9700' S 072° 03.9300' E	1 802 m	23/10/2011	02:48	48° 09.9700' S 072° 03.9300' E	1 809 m
TNS-4	TURBOMAP-07	46	23/10/2011	02:56	48° 10.0700' S 072° 04.0000' E	1 800 m	23/10/2011	03:34	48° 10.2900' S 072° 04.2700' E	1 794 m
TNS-3	CTD-013	47	23/10/2011	06:41	47° 50.0145' S 071° 55.1745' E	540 m	23/10/2011	07:26	47° 50.0152' S 071° 55.1714' E	2 060 m

Table I **(continued)**

			start of station				end of station			
Station	**Code of opération**	**OP #**	**date**	**time**	**position**	**sounder**	**date**	**time**	**position**	**sounder**
TNS-3	BONGO-11	48	23/10/2011	07:46	47° 50.0107' S 071° 55.1740' E	542 m	23/10/2011	08:11	47° 50.0070' S 071° 55.1710' E	539 m
TNS-3	TURBOMAP-08	49	23/10/2011	08:33	47° 50.0624' S 071° 55.2554' E	541 m	23/10/2011	09:00	47° 50.1690' S 071° 55.2460' E	545 m
TNS-2	CTD-014	50	23/10/2011	12:06	47° 19.9075' S 071° 42.0755' E	520 m	23/10/2011	12:51	47° 19.9118' S 071° 42.0761' E	514 m
TNS-2	BONGO-12	51	23/10/2011	12:59	47° 19.9116' S 071° 42.0723' E	516 m	23/10/2011	13:22	47° 19.9128' S 071° 42.0697' E	514 m
TNS-2	TURBOMAP-09	52	23/10/2011	13:31	47° 19.8886' S 071° 42.1567' E	517 m	23/10/2011	13:53	46° 55.8000' S 071° 32.4000' E	
TNS-1	CTD-015	53	23/10/2011	17:13	46° 49.9994' S 071° 30.0636' E	2 280 m	23/10/2011	19:00	46° 49.9980' S 071° 30.0657' E	2 283 m
TNS-1	BONGO-13	54	23/10/2011	19:23	46° 49.9896' S 071° 30.0648' E	2 283 m	23/10/2011	19:45	46° 49.9903' S 071° 30.0656' E	2 282 m
TNS-1	PHYTONET-04	55	23/10/2011	19:52	46° 49.9892' S 071° 30.0643' E	2 281 m	23/10/2011	20:06	46° 50.0000' S 071° 30.0000' E	
TNS-1	TURBOMAP-10	56	23/10/2011	20:16	46° 49.9900' S 071° 30.1000' E	2 280 m	23/10/2011	20:32	46° 49.9700' S 071° 30.4200' E	2 261 m
R2 IODA	IODA-REC-1	57	25/10/2011			2 319 m	25/10/2011	13:45	50° 17.6586' S 066° 51.1489' E	2 280 m
R2 IODA	CTD-016	58	25/10/2011	14:58	50° 17.6598' S 066° 51.1493' E	2 280 m	25/10/2011	16:12	50° 17.6513' S 066° 51.1494' E	2 293 m
R2 IODA	TMR-TEST	59	25/10/2011				25/10/2011	18:25	50° 17.6522' S 066° 51.1421' E	2 297 m
R2	CTD-017	60	25/10/2011	22:59	50° 21.5229' S 066° 43.0052' E	2 531 m	26/10/2011	00:11	50° 21.5261' S 066° 43.0045' E	2 525 m
R2	BONGO-14	61	26/10/2011	00:37	50° 21.5261' S 066° 43.0040' E	2 524 m	26/10/2011	01:31	50° 21.5317' S 066° 42.9998' E	2 527 m
R2	CTD-018	62	26/10/2011	01:48	50° 21.5261' S 066° 43.0030' E	2 526 m	26/10/2011	02:09	50° 21.5265' S 066° 43.0019' E	2 527 m
R2	TMR-PROD-02	63	26/10/2011	03:15	50° 21.5300' S 066° 42.4400' E	2 528 m	26/10/2011	04:55	50° 21.5300' S 066° 42.4400' E	2 561 m

Table I **(continued)**

			start of station				end of station			
Station	**Code of opération**	**OP #**	**date**	**time**	**position**	**sounder**	**date**	**time**	**position**	**sounder**
R2	ISP-QMA-SUPOR-02	64	26/10/2011	05:32	50° 21.5200' S 066° 43.0000' E	2 535 m	26/10/2011	12:45	50° 21.5211' S 066° 42.9984' E	2 528 m
R2	CTD-019	65	26/10/2011	13:05	50° 21.5214' S 066° 42.9976' E	2 526 m	26/10/2011	13:25	50° 21.5249' S 066° 42.9971' E	2 527 m
R2	BONGO-15	66	26/10/2011	13:28	50° 21.5270' S 066° 42.9947' E	2 530 m	26/10/2011	14:53	50° 21.5222' S 066° 42.9942' E	2 525 m
R2	PHYTONET-05	67	26/10/2011	14:56	50° 21.5218' S 066° 42.9933' E	2 526 m	26/10/2011	15:06	50° 21.5810' S 066° 42.9946' E	2 525 m
R2	GEL-TRAP-1	68	26/10/2011	15:33	50° 21.5899' S 066° 42.9303' E	2 528 m				
R2	TMR-PROCESS-04	69	26/10/2011	17:45	50° 23.2746' S 066° 41.3642' E	2 455 m	26/10/2011	17:56	50° 23.2850' S 066° 41.3100' E	
R2	TURBOMAP-11	70	26/10/2011	18:25	50° 23.3879' S 066° 41.2096' E	2 433 m	26/10/2011	18:47	50° 23.3718' S 066° 41.4585' E	2 440 m
R2	CTD-020	71	26/10/2011	19:19	50° 23.3729' S 066° 41.5943' E	2 445 m	26/10/2011	21:32	50° 23.3708' S 066° 41.5980' E	2 423 m
R2	MULTICORER2	72	26/10/2011	21:59	50° 23.3711' S 066° 41.6010' E	2 445 m	27/10/2011	00:14	50° 23.3700' S 066° 41.5750' E	2 445 m
R2	TMR-PROCESS-05	73	27/10/2011	00:38	50° 23.3700' S 066° 41.5700' E	2 463 m	27/10/2011	00:52	50° 23.3700' S 066° 41.5800' E	2 445 m
R2	CTD-021	74	27/10/2011	01:18	50° 23.3700' S 066° 41.5670' E	2 456 m	27/10/2011	01:40	50° 23.3700' S 066° 41.5800' E	2 445 m
R2	TMR-ISOTOPES-1	75	27/10/2011	02:30			27/10/2011	03:34	50° 23.3700' S 066° 41.5600' E	2 459 m
R2	CTD-022	76	27/10/2011	04:31	50° 23.3723' S 066° 41.5646' E	2 450 m	27/10/2011	05:00	50° 23.3751' S 066° 41.5660' E	2 450 m
R2	MULTINET-3	77	27/10/2011	05:41	50° 23.3600' S 066° 41.5500' E	2 445 m	27/10/2011	06:00	50° 23.3700' S 066° 41.5600' E	2 467 m
R2	ISP-QMA-SUPOR-03	78	27/10/2011	06:24	50° 23.3725' S 066° 41.5602' E	2 445 m	27/10/2011	12:10	50° 23.3725' S 066° 41.5389' E	2 442 m
R2	BONGO-16	79	27/10/2011	12:16	50° 23.3736' S 066° 41.5578' E	2 447 m	27/10/2011			

Table I **(continued)**

			start of station				end of station			
Station	**Code of opération**	**OP #**	**date**	**time**	**position**	**sounder**	**date**	**time**	**position**	**sounder**
R2	GEL-TRAP-1	80	27/10/2011	13:33	50° 20.1046' S 066° 40.6930' E	2 459 m	27/10/2011	14:56	50° 18.4084' S 066° 40.3462' E	2 460 m
E-1	IRIDIUM -DEP	81	28/10/2011	18:07	48° 27.9810' S 072° 11.9597' E	2 064 m	28/10/2011	18:09	48° 27.9389' S 072° 12.0824' E	2 063 m
E-1	PHYTONET-06	82	28/10/2011	18:27	48° 27.9051' S 072° 12.3144' E	2 060 m	28/10/2011	18:37	48° 27.9020' S 072° 12.3237' E	
E-1	CTD-023	83	28/10/2011	19:10	48° 27.9040' S 072° 12.3100' E	2 060 m	28/10/2011	20:40	48° 27.9130' S 072° 12.3080' E	2 060 m
E-1	GEL-TRAP-2	84	28/10/2011				28/10/2011		48° 28.7180' S 072° 12.6830' E	2 065 m
E-1	ISP-QMA-SUPOR-04	85	28/10/2011	23:24	48° 29.5728' S 072° 14.1467' E	2 081 m	29/10/2011	07:20		
E-1	CTD-024	86	29/10/2011	07:46	48° 29.5695' S 072° 14.1527' E	2 075 m	29/10/2011	09:07	48° 29.5730' S 072° 14.1470' E	2 075 m
E-1	TMR-PROCESS-06	87	29/10/2011	09:36	48° 29.5370' S 072° 14.1466' E	2 080 m	29/10/2011	09:52	48° 29.5740' S 072° 14.1450' E	2 080 m
E-1	IODA-SED-TRAP-1	88	29/10/2011	10:35	48° 29.6590' S 072° 14.2822' E	2 082 m	29/10/2011	11:33	48° 30.0780' S 072° 14.6690' E	2 075 m
E-1	CTD-025	89	29/10/2011	11:53	48° 30.6840' S 072° 15.1669' E	2 058 m	29/10/2011	12:28	48° 30.6840' S 072° 15.1720' E	2 058 m
E-1	BONGO-17	90	29/10/2011	12:50	48° 30.6837' S 072° 15.1723' E	2 054 m	29/10/2011	13:53	48° 30.6810' S 072° 15.1713' E	2 083 m
E-1	PHYTONET-07	91	29/10/2011	14:02	48° 30.6848' S 072° 15.1699' E	2 073 m	29/10/2011	14:05	48° 30.6851' S 072° 15.1688' E	2 082 m
E-1	CTD-026	92	29/10/2011	14:15	48° 30.6807' S 072° 15.1675' E	2 083 m	29/10/2011	14:36	48° 30.6847' S 072° 15.1719' E	2 085 m
E-1	ISP-QMA-SUPOR-05	93	29/10/2011	15:21	48° 28.0126' S 072° 11.8506' E	2 057 m	29/10/2011	21:36	48° 28.0387' S 072° 11.8462' E	2 032 m
E-1	TURBOMAP-12	94	29/10/2011	21:54	48° 27.6224' S 072° 11.4298' E	2 066 m	29/10/2011	22:17	48° 27.5094' S 072° 11.2427' E	2 066 m
E-1	CTD-027	95	29/10/2011	22:46	48° 27.4700' S 072° 11.2100' E	2 056 m	30/10/2011	00:05	48° 27.4730' S 072° 11.2177' E	2 056 m

Table I **(continued)**

			start of station				end of station			
Station	**Code of opération**	**OP #**	**date**	**time**	**position**	**sounder**	**date**	**time**	**position**	**sounder**
E-1	BONGO-18	96	30/10/2011	01:05	48° 27.4360' S 072° 11.2620' E	2 049 m	30/10/2011	02:01	48° 27.4378' S 072° 11.2675' E	
E-1	CTD-028	97	30/10/2011	02:21	48° 27.4390' S 072° 11.2645' E	2 050 m	30/10/2011	02:42	48° 27.4370' S 072° 11.2640' E	2 050 m
E-1	TMR-PROD-03	98	30/10/2011	03:26	48° 27.4360' S 072° 11.2587' E	2 047 m	30/10/2011	04:50	48° 27.4370' S 072° 11.2700' E	2 058 m
E-1	GEL-TRAP-2	99	30/10/2011	05:00	48° 27.4750' S 072° 11.2650' E		30/10/2011	07:01	48° 29.8800' S 072° 10.6600' E	2 055 m
E-1	CTD-029	100	30/10/2011	07:26	48° 29.8810' S 072° 10.6610' E	2 050 m	30/10/2011	07:53	48° 29.8797' S 072° 10.6620' E	2 057 m
E-1	MULTINET-4	101	30/10/2011	08:18	48° 29.8809' S 072° 10.6594' E	2 051 m	30/10/2011	08:45	48° 29.8779' S 072° 10.6614' E	2 051 m
E-1	CTD-030	102	30/10/2011	09:15	48° 29.8780' S 072° 10.6620' E	2 058 m	30/10/2011	11:07	48° 29.8790' S 072° 10.6610' E	2 058 m
E-1	CTD-031	103	30/10/2011	12:15	48° 29.8750' S 072° 10.6620' E	2 051 m	30/10/2011	12:35	48° 29.8790' S 072° 10.6610' E	2 058 m
E-1	TMR-ISOTOPES-2	104	30/10/2011	13:00	48° 29.8760' S 072° 10.6610' E	2 030 m	30/10/2011	14:17	48° 29.8790' S 072° 10.6580' E	2 025 m
E-1	CTD-032	105	30/10/2011	14:30	48° 29.8760' S 072° 10.6610' E	2 033 m	30/10/2011	15:30	48° 29.8630' S 072° 10.6500' E	2 033 m
E-1	CTD-033	106	30/10/2011	16:20	48° 29.8670' S 072° 10.6520' E	2 050 m	30/10/2011	16:57	48° 29.8680' S 072° 10.6560' E	2 050 m
E-1	CTD-034	107	30/10/2011	18:32	48° 29.3872' S 072° 10.6610' E	2 050 m	30/10/2011	19:15	48° 29.8670' S 072° 10.6560' E	2 050 m
TEW-1	MULTICORER-3	108	31/10/2011	08:02	49° 09.0142' S 069° 49.9403' E	84 m	31/10/2011	08:37	49° 08.9890' S 069° 50.0110' E	85 m
TEW-1	CTD-035	109	31/10/2011	08:51	49° 08.9890' S 069° 50.0096' E	86 m	31/10/2011	09:21	49° 08.9880' S 069° 50.0110' E	86 m
TEW-1	BONGO-19	110	31/10/2011	09:40	49° 08.9900' S 069° 50.0100' E	86 m	31/10/2011	09:48	49° 08.9890' S 069° 50.0080' E	86 m
TEW-1	PHYTONET-08	111	31/10/2011	10:00	49° 08.9910' S 069° 50.0080' E	86 m	31/10/2011	10:10	49° 08.9850' S 069° 50.0090' E	86 m

Table I **(continued)**

			start of station					end of station				
Station	**Code of opération**	**OP #**	**date**	**time**	**position**		**sounder**	**date**	**time**	**position**		**sounder**
TEW-1	CTD-036	112	31/10/2011	10:36	49° 08.9880' S	069° 50.0110' E	86 m	31/10/2011	10:54	49° 08.9890' S	069° 50.0100' E	86 m
TEW-1	TMR-PROD-04	113	31/10/2011	11:42	49° 08.9860' S	069° 50.0090' E	86 m	31/10/2011	11:50	49° 08.9870' S	069° 50.0120' E	86 m
TEW-2	CTD-037	114	31/10/2011	15:19	48° 53.9666' S	070° 39.9785' E	84 m	31/10/2011	15:40	48° 53.9670' S	070° 39.9700' E	85 m
TEW-2	TMR-PROD-05	115	31/10/2011	16:00	48° 53.9638' S	070° 39.9733' E	85 m	31/10/2011	16:16	48° 53.9591' S	070° 39.9795' E	85 m
TEW-2	BONGO-20	116	31/10/2011	16:26	48° 53.9640' S	070° 39.9718' E	85 m	31/10/2011	16:32	48° 53.9617' S	070° 39.9734' E	85 m
TEW-2	PHYTONET-09	117	31/10/2011	16:41	48° 53.9603' S	070° 39.9730' E	85 m	31/10/2011	16:47	48° 53.9647' S	070° 39.9695' E	85 m
TEW-3	CTD-038	118	31/10/2011	18:41	48° 47.9485' S	071° 01.0554' E	565 m	31/10/2011	19:40	48° 47.9441' S	071° 01.0775' E	565 m
TEW-3	BONGO-21	119	31/10/2011	19:57	48° 47.9146' S	071° 01.0498' E	556 m	31/10/2011	20:23	48° 47.9154' S	071° 01.0471' E	556 m
TEW-3	PHYTONET-10	120	31/10/2011	20:35	48° 47.9142' S	071° 01.0524' E	557 m	31/10/2011	20:48	48° 47.9160' S	071° 01.0485' E	557 m
TEW-3	CTD-039	121	31/10/2011	21:15	48° 47.9165' S	071° 01.0460' E	557 m	31/10/2011	21:21	48° 47.9180' S	071° 01.0460' E	557 m
TEW-3	TMR-PROD-06	122	31/10/2011	21:58	48° 47.9160' S	071° 01.0460' E	557 m	31/10/2011	22:26	48° 47.9150' S	071° 01.0450' E	557 m
TEW-3	CTD-040	123	31/10/2011	22:57	48° 47.9120' S	071° 01.0460' E	557 m	31/10/2011	23:19	48° 47.9120' S	071° 01.0480' E	557 m
TEW-3	CTD-041	124	01/11/2011	00:07	48° 47.8790' S	071° 01.0080' E	561 m	01/11/2011	00:44	48° 47.8210' S	071° 00.8580' E	569 m
TEW-4	CTD-042	125	01/11/2011	05:19	48° 37.9840' S	071° 37.0200' E	1 585 m	01/11/2011	06:48	48° 37.9800' S	071° 37.0270' E	1 601 m
TEW-4	TMR-PROD-07	126	01/11/2011	07:10	48° 37.9800' S	071° 37.0000' E	1 600 m	01/11/2011	08:38	48° 37.9800' S	071° 37.0270' E	1 595 m
TEW-4	BONGO-22	127	01/11/2011	08:54	48° 37.9800' S	071° 37.0200' E	1 603 m	01/11/2011	09:28	48° 37.9840' S	071° 37.0240' E	1 603 m

Table I **(continued)**

			start of station				end of station			
Station	**Code of opération**	**OP #**	**date**	**time**	**position**	**sounder**	**date**	**time**	**position**	**sounder**
TEW-4	PHYTONET-11	128	01/11/2011	09:43	48° 37.9800' S 071° 37.0250' E	1 603 m	01/11/2011	09:51	48° 37.9800' S 071° 37.0200' E	1 603 m
E-2	CTD-043	129	01/11/2011	12:00	48° 31.4060' S 072° 04.6250' E	2 003 m	01/11/2011	13:30	48° 31.4000' S 072° 04.6270' E	2 003 m
E-2	BONGO-23	130	01/11/2011	13:38	48° 31.4010' S 072° 04.6230' E	2 003 m	01/11/2011	14:03	48° 31.4000' S 072° 04.6270' E	2 003 m
E-2	PHYTONET-12	131	01/11/2011	14:06	48° 31.4010' S 072° 04.6251' E	2 003 m	01/11/2011	14:19	48° 31.4020' S 072° 04.6220' E	2 003 m
E-2	TMR-PROD-08	132	01/11/2011	14:35	48° 31.4030' S 072° 04.6200' E	2 003 m	01/11/2011	15:50	48° 31.4020' S 072° 04.6240' E	2 003 m
TEW-5	CTD-044	133	01/11/2011	19:00	48° 28.0680' S 072° 47.9800' E	2 275 m	01/11/2011	20:51	48° 28.0680' S 072° 47.9340' E	2 275 m
TEW-5	BONGO-24	134	01/11/2011	21:05	48° 28.0693' S 072° 47.9312' E	2 247 m	01/11/2011	21:27	48° 28.0721' S 072° 47.9302' E	2 245 m
TEW-5	PHYTONET-13	135	01/11/2011	21:43	48° 28.0744' S 072° 47.9291' E	2 244 m	01/11/2011	21:54	48° 28.0761' S 072° 47.9306' E	2 250 m
TEW-5	TMR-PROD-09	136	01/11/2011	22:14	48° 28.0870' S 072° 47.9299' E	2 273 m	01/11/2011	23:27	48° 28.0780' S 072° 47.9250' E	2 280 m
TEW-6	CTD-045	137	02/11/2011	03:59	48° 27.9713' S 073° 23.9883' E	2 415 m	02/11/2011	05:50	48° 27.9961' S 073° 23.9885' E	2 404 m
TEW-6	BONGO-25	138	02/11/2011	06:13	48° 27.9762' S 073° 23.9950' E	2 415 m	02/11/2011	06:40	48° 27.9708' S 073° 23.9892' E	2 407 m
TEW-6	PHYTONET-14	139	02/11/2011	06:15	48° 27.9697' S 073° 23.8884' E	2 404 m	02/11/2011	06:56	48° 27.9711' S 073° 23.9875' E	2 390 m
TEW-7	CTD-046	140	02/11/2011	09:34	48° 28.0000' S 073° 59.9530' E	2 510 m	02/11/2011	06:39	48° 28.0000' S 073° 59.9650' E	2 510 m
TEW-7	BONGO-26	141	02/11/2011	11:55	48° 27.9970' S 073° 59.9650' E	2 510 m	02/11/2011	12:15	48° 27.9900' S 073° 59.9600' E	2 510 m
TEW-7	PHYTONET-15	142	02/11/2011	12:22	48° 27.9900' S 073° 59.9600' E	2 497 m	02/11/2011	12:31	48° 27.9990' S 073° 59.9670' E	2 509 m
TEW-7	TMR-PROD-10	143	02/11/2011	12:50	48° 27.9980' S 073° 59.9640' E	2 505 m	02/11/2011	14:02	48° 27.9980' S 073° 59.9640' E	2 491 m

Table I **(continued)**

			start of station				end of station			
Station	**Code of opération**	**OP #**	**date**	**time**	**position**	**sounder**	**date**	**time**	**position**	**sounder**
TEW-8	CTD-047	144	02/11/2011	18:47	48° 28.0542' S 075° 00.1937' E	2 786 m	02/11/2011	21:20	48° 28.3900' S 074° 59.9600' E	2 784 m
TEW-8	BONGO-27	145	02/11/2011	21:39	48° 28.3850' S 074° 59.9500' E	2 784 m	02/11/2011	22:02	48° 28.3900' S 074° 59.9330' E	2 784 m
TEW-8	PHYTONET-16	146	02/11/2011	22:10	48° 28.4150' S 074° 59.8150' E	2 784 m	02/11/2011	22:22	48° 28.4350' S 074° 59.6890' E	2 784 m
TEW-8	CTD-048	147	02/11/2011	22:35	48° 28.4520' S 074° 59.6920' E	2 784 m	02/11/2011	22:43	48° 28.4630' S 074° 59.6890' E	2 784 m
E-3	CTD-049	148	03/11/2011	11:57	48° 41.9865' S 071° 58.0192' E	1 750 m	03/11/2011	12:49	48° 41.9890' S 071° 58.0180' E	1 750 m
E-3	TMR-ISOTOPES-3	149	03/11/2011	13:13	48° 41.9899' S 071° 58.0161' E	1 750 m	03/11/2011	14:14	48° 41.9870' S 071° 58.0150' E	1 750 m
E-3	GEL-TRAP-3	150	03/11/2011	14:30	48° 41.9184' S 071° 57.8907' E	1 875 m	03/11/2011	15:21	48° 41.4880' S 071° 57.5180' E	1 875 m
E-3	TURBOMAP-13	151	03/11/2011	15:35	48° 41.4740' S 071° 57.5000' E	1 876 m	03/11/2011	15:53	48° 41.4550' S 071° 57.7499' E	1 876 m
E-3	IODA-SED-TRAP-1	152	03/11/2011	18:14	48° 38.4387' S 071° 48.9911' E	1 776 m	03/11/2011	19:10	48° 37.8770' S 071° 48.5600' E	1 735 m
E-3	CTD-050	153	03/11/2011	20:58	48° 42.1290' S 071° 58.0097' E	1 914 m	03/11/2011	22:23	48° 42.1339' S 071° 58.0031' E	1 917 m
E-3	BONGO-28	154	03/11/2011	22:35	48° 42.1360' S 071° 58.0047' E	1 914 m	03/11/2011	23:38	48° 42.1320' S 071° 58.0050' E	1 925 m
E-3	TMR-PROD-11	155	03/11/2011	23:58	48° 42.1320' S 071° 58.0050' E	1 925 m	04/11/2011	01:10	48° 42.1340' S 071° 58.0010' E	1 926 m
E-3	CTD-051	156	04/11/2011	01:29	48° 42.1337' S 071° 58.0029' E	1 920 m	04/11/2011	01:49	48° 42.1343' S 071° 58.0055' E	1 905 m
E-3	ISP-QMA-SUPOR-06	157	04/11/2011	03:05	48° 42.1334' S 071° 58.0027' E	1 919 m	04/11/2011	09:22	48° 41.8220' S 071° 57.7760' E	1 905 m
E-3	CTD-052	158	04/11/2011	10:10	48° 42.2180' S 071° 58.2860' E	1 915 m	04/11/2011	10:39	48° 42.2230' S 071° 58.2320' E	1 915 m
E-3	BONGO-29	159	04/11/2011	10:56	48° 42.2450' S 071° 58.1940' E	1 916 m	04/11/2011	11:49	48° 42.2430' S 071° 58.2030' E	1 916 m

Table I **(continued)**

			start of station				end of station			
Station	**Code of opération**	**OP #**	**date**	**time**	**position**	**sounder**	**date**	**time**	**position**	**sounder**
E-3	PHYTONET-17	160	04/11/2011	12:03	48° 42.2430' S 071° 58.2020' E	1 916 m	04/11/2011	12:23	48° 42.2410' S 071° 58.1960' E	1 934 m
E-3	CTD-053	161	04/11/2011	12:34	48° 42.2440' S 071° 58.2040' E	1 932 m	04/11/2011	12:58	48° 42.2420' S 071° 58.2020' E	1 924 m
E-3	MULTINET-5	162	04/11/2011	13:15	48° 42.2420' S 071° 58.2060' E	1 932 m	04/11/2011	13:31	48° 42.2410' S 071° 58.2140' E	1 916 m
E-3	CTD-054	163	04/11/2011	13:58	48° 42.2400' S 071° 58.2120' E	1 923 m	04/11/2011	14:24	48° 42.2393' S 071° 58.2090' E	1 923 m
E-3	GEL-TRAP-3	164	04/11/2011	15:00	48° 43.8975' S 071° 56.6616' E	1 872 m	04/11/2011	16:26	48° 43.9192' S 071° 56.4900' E	1 861 m
E-3	CTD-055	165	04/11/2011	17:22	48° 42.0700' S 071° 58.0180' E	1 910 m	04/11/2011	19:10	48° 42.0715' S 071° 58.0160' E	1 900 m
E-3	TMR-PROCESS-07	166	04/11/2011	19:35	48° 42.0686' S 071° 58.0193' E	1 900 m	04/11/2011	19:50	48° 42.0730' S 071° 58.0200' E	1 900 m
E-3	ISP-QMA-SUPOR-07	167	04/11/2011	21:10	48° 42.0700' S 071° 58.0200' E	1 900 m	05/11/2011	04:45	48° 42.0761' S 071° 58.0019' E	1 919 m
E-3	MULTICORER-4	168	05/11/2011	04:55	48° 42.0790' S 071° 58.0044' E	1 920 m	05/11/2011	07:25	48° 42.0809' S 071° 58.0215' E	1 920 m
E-3	IODA-SED-TRAP-2	169	05/11/2011	07:52	48° 42.0616' S 071° 56.9628' E	1 910 m	05/11/2011	08:53	48° 41.8005' S 071° 56.9667' E	1 910 m
F-L	CTD-056	170	06/11/2011	00:35	48° 31.3930' S 074° 40.0370' E	2 690 m	06/11/2011	02:20	48° 31.3920' S 074° 40.0340' E	2 690 m
F-L	ISP-QMA-SUPOR-08	171	06/11/2011	03:43	48° 31.3940' S 074° 40.0360' E	2 690 m	06/11/2011	09:15	48° 31.3820' S 074° 40.0630' E	2 698 m
F-L	MULTINET-6	172	06/11/2011	09:40	48° 31.3835' S 074° 40.0645' E	2 702 m	06/11/2011	09:43	48° 31.3820' S 074° 40.0660' E	2 702 m
F-L	CTD-057	173	06/11/2011	10:20	48° 31.3829' S 074° 40.0674' E	2 684 m	06/11/2011	11:01	48° 31.3810' S 074° 40.0670' E	2 700 m
F-L	CTD-058	174	06/11/2011	11:59	48° 31.3815' S 074° 40.0690' E	2 700 m	06/11/2011	12:10	48° 31.3870' S 074° 40.0670' E	2 700 m
F-L	BONGO-30	175	06/11/2011	12:18	48° 31.3817' S 074° 40.0675' E	2 723 m	06/11/2011	13:16	48° 31.3848' S 074° 40.0722' E	2 723 m

Table I **(continued)**

			start of station				end of station			
Station	**Code of opération**	**OP #**	**date**	**time**	**position**	**sounder**	**date**	**time**	**position**	**sounder**
F-L	PHYTONET-18	176	06/11/2011	13:26	48° 31.3850' S 074° 40.0695' E	2 696 m	06/11/2011	13:37	48° 31.3825' S 074° 40.0699' E	2 961 m
F-L	CTD-059	177	06/11/2011	13:50	48° 31.3810' S 074° 40.0640' E	2 720 m	06/11/2011	14:10	48° 31.3810' S 074° 40.0640' E	2 706 m
F-L	GEL-TRAP-4	178	06/11/2011	14:30	48° 31.6350' S 074° 39.5300' E	2 689 m	06/11/2011	15:17	48° 31.6280' S 074° 39.1180' E	2 694 m
F-L	CTD-060	179	06/11/2011	16:00	48° 30.3135' S 074° 36.8180' E	2 679 m	06/11/2011	16:43	48° 30.3260' S 074° 36.8100' E	2 679 m
F-L	TURBOMAP-14	180	06/11/2011	17:02	48° 30.3570' S 074° 36.8270' E	2 680 m	06/11/2011	17:24	48° 30.6530' S 074° 37.2700' E	2 680 m
F-L	CTD-061	181	06/11/2011	18:05	48° 30.3550' S 074° 36.8540' E	2 670 m	06/11/2011	18:57	48° 30.3360' S 074° 36.8470' E	2 670 m
F-L	CTD-062	182	06/11/2011	20:34	48° 30.3369' S 074° 36.8514' E	2 675 m	06/11/2011	20:47	48° 30.3370' S 074° 36.8530' E	2 675 m
F-L	CTD-063	183	06/11/2011	21:49	48° 31.9460' S 074° 39.5210' E	2 695 m	06/11/2011	23:03	48° 31.9494' S 074° 39.5113' E	2 689 m
F-L	BONGO-31	184	06/11/2011	23:19	48° 31.9470' S 074° 39.5080' E	2 689 m	07/11/2011	00:19	48° 31.8500' S 074° 39.4680' E	2 687 m
F-L	TMR-PROD-12	185	07/11/2011	00:32	48° 31.8511' S 074° 39.4701' E	2 687 m	07/11/2011	01:43	48° 31.8428' S 074° 39.4691' E	2 685 m
F-L	CTD-064	186	07/11/2011	01:53	48° 31.8490' S 074° 39.4680' E	2 682 m	07/11/2011	02:14	48° 31.8505' S 074° 39.4703' E	2 691 m
F-L	ISP-QMA-SUPOR-09	187	07/11/2011	03:34	48° 31.8480' S 074° 39.4697' E	2 701 m	07/11/2011	11:10	48° 31.8250' S 074° 39.5000' E	2 700 m
F-L	GEL-TRAP-4	188	07/11/2011	12:37	48° 36.6000' S 074° 48.4000' E	2 700 m	07/11/2011	13:35	48° 31.1300' S 074° 39.2590' E	2 700 m
F-L	CTD-065	189	07/11/2011	13:54	48° 37.1290' S 074° 48.2600' E	2 700 m	07/11/2011	14:11	48° 37.1316' S 074° 48.2613' E	2 700 m
F-L	TMR-ISOTOPES-4	190	07/11/2011	14:30	48° 37.1300' S 074° 48.2600' E	2 700 m	07/11/2011	15:48	48° 37.1700' S 074° 48.3231' E	2 700 m
F-L	CTD-066	191	07/11/2011	16:05	48° 37.1740' S 074° 48.3251' E	2 700 m	07/11/2011	16:25	48° 37.1890' S 074° 48.3530' E	2 700 m

Table I **(continued)**

			start of station				end of station			
Station	**Code of opération**	**OP #**	**date**	**time**	**position**	**sounder**	**date**	**time**	**position**	**sounder**
F-L	CTD-067	192	07/11/2011	17:43	48° 37.1950' S 074° 48.4453' E	2 741 m	07/11/2011	18:24	48° 37.2650' S 074° 48.4480' E	2 690 m
F-L	MULTICORER-5	193	07/11/2011	18:56	48° 37.2622' S 074° 48.4453' E	2 741 m	07/11/2011	21:23	48° 37.2730' S 074° 48.4530' E	2 739 m
F-L	CTD-68	194	07/11/2011	21:58	48° 37.2740' S 074° 48.4460' E	2 739 m	08/11/2011	00:22	48° 37.2720' S 074° 48.4440' E	2 730 m
F-L	CLOSING-BONGO	195	08/11/2011	00:52	48° 37.2529' S 074° 48.3450' E	2 736 m	08/11/2011	01:00	48° 37.2425' S 074° 48.2950' E	2 736 m
F-S	CTD-069	196	08/11/2011	06:13	48° 30.0350' S 073° 59.9860' E	2 520 m	08/11/2011	08:28	48° 30.0590' S 074° 59.9820' E	2 520 m
G-1	CTD-070	197	09/11/2011	00:30	49° 54.0240' S 071° 53.9460' E	585 m	09/11/2011	01:08	49° 54.0102' S 071° 53.9842' E	582 m
G-1	BONGO-32	198	09/11/2011	01:28	49° 54.0070' S 071° 53.9878' E	588 m	09/11/2011	01:48	49° 54.0073' S 071° 53.9844' E	583 m
G-1	PHYTONET-19	199	09/11/2011	01:58	49° 54.0070' S 071° 53.9834' E	579 m	09/11/2011	02:16	49° 54.0064' S 071° 53.9804' E	590 m
G-1	CTD-071	200	09/11/2011	02:30	49° 54.0070' S 071° 53.9810' E	580 m	09/11/2011	03:01	49° 54.0110' S 071° 53.9770' E	580 m
G-1	CTD-072	201	09/11/2011	03:39	49° 54.0110' S 071° 53.9780' E	580 m	09/11/2011	04:20	49° 54.0140' S 071° 53.9740' E	580 m
G-1	TMR-PROD-13	202	09/11/2011	04:50	49° 53.9800' S 071° 53.9200' E	560 m	09/11/2011	05:23	49° 54.0100' S 071° 53.9700' E	589 m
G-1	CTD-073	203	09/11/2011	05:45	49° 54.0130' S 071° 53.9690' E	580 m	09/11/2011	06:29	49° 54.0170' S 071° 53.9600' E	580 m
G-1	CTD-074	204	09/11/2011	07:28	49° 54.0180' S 071° 53.9640' E	590 m	09/11/2011	08:08	49° 54.0200' S 071° 53.9110' E	580 m
G-1	CTD-075	205	09/11/2011	09:00	49° 54.0170' S 071° 53.9620' E	592 m	09/11/2011	09:42	49° 54.0170' S 071° 53.9620' E	582 m
G-1	CTD-076	206	09/11/2011	10:21	49° 54.0170' S 071° 53.9590' E	591 m	09/11/2011	10:30	49° 54.0170' S 071° 53.9590' E	591 m
G-2	CTD-077	207	09/11/2011	17:53	49° 07.9878' S 070° 38.9854' E	68 m	09/11/2011	18:08	49° 07.9000' S 070° 38.9900' E	68 m

Table I **(continued)**

			start of station				end of station			
Station	**Code of opération**	**OP #**	**date**	**time**	**position**	**sounder**	**date**	**time**	**position**	**sounder**
G-2	BONGO-33	208	09/11/2011	18:27	49° 07.9882' S 070° 38.9813' E	67 m	09/11/2011	18:36	49° 07.9841' S 070° 38.9913' E	66 m
G-2	PHYTONET-20	209	09/11/2011	18:46	49° 07.9864' S 070° 38.9754' E	67 m	09/11/2011	18:50	49° 07.9900' S 070° 38.9750' E	67 m
E-4 IODA	IODA-SED-TRAP-2	210	10/11/2011	10:37	48° 40.7730' S 072° 32.0791' E	2 201 m	10/11/2011	10:57	48° 40.6790' S 072° 31.8520' E	2 197 m
E-4 IODA	CTD-078	211	10/11/2011	11:26	48° 40.6807' S 072° 31.8535' E	2 200 m	10/11/2011	11:20	48° 40.6810' S 072° 31.8540' E	2 200 m
E-4W	CTD-079	212	11/11/2011	08:25	48° 46.0033' S 071° 25.7667' E	1 400 m	11/11/2011	09:20	48° 45.9981' S 071° 25.7575' E	1 390 m
E-4W	PHYTONET-21	213	11/11/2011	09:31	48° 45.9990' S 071° 25.7690' E	1 390 m	11/11/2011	09:42	48° 45.9980' S 071° 25.7570' E	1 390 m
E-4W	MULTINET-7	214	11/11/2011	10:05	48° 46.0130' S 071° 25.7760' E	1 400 m	11/11/2011	10:09	48° 45.9950' S 071° 25.7890' E	1 400 m
E-4W	CTD-080	215	11/11/2011	10:30	48° 45.9770' S 071° 25.7900' E	1 398 m	11/11/2011	10:50	48° 45.9905' S 071° 25.7990' E	1 398 m
E-4W	BONGO-34	216	11/11/2011	11:05	48° 45.9890' S 071° 25.7810' E	1 400 m	11/11/2011	12:11	48° 45.9595' S 071° 25.5800' E	1 400 m
E-4W	PHYTONET-22	217	11/11/2011	12:16	48° 45.9600' S 071° 25.5770' E	1 392 m	11/11/2011	12:26	48° 45.9410' S 071° 25.5310' E	1 388 m
E-4W	ISP-QMA-SUPOR-10	218	11/11/2011	12:49	48° 45.9270' S 071° 25.5100' E	1 388 m	11/11/2011	19:21	48° 45.9280' S 071° 25.5080' E	1 390 m
E-4W	TMR-PROD-14	219	11/11/2011	19:43	48° 45.9300' S 071° 25.5020' E	1 390 m	11/11/2011	20:53	48° 45.9250' S 071° 25.5060' E	1 390 m
E-4W	CTD-081	220	11/11/2011	21:07	48° 45.9254' S 071° 25.5059' E	1 400 m	11/11/2011	22:13	48° 45.9290' S 071° 25.5060' E	1 400 m
E-4W	BONGO-35	221	11/11/2011	22:32	48° 45.9290' S 071° 25.5120' E	1 400 m	11/11/2011	23:50	48° 45.9300' S 071° 25.5060' E	1 400 m
E-4W	CTD-082	222	12/11/2011	01:33	48° 45.9280' S 071° 25.5070' E	1 392 m	12/11/2011	01:59	48° 45.9280' S 071° 25.4980' E	1 392 m
E-4W	CTD-083	223	12/11/2011	03:00	48° 45.9280' S 071° 25.5050' E	1 392 m	12/11/2011	03:18	48° 45.9320' S 071° 25.5020' E	1 392 m

Table I **(continued)**

			start of station					end of station				
Station	**Code of opération**	**OP #**	**date**	**time**	**position**		**sounder**	**date**	**time**	**position**		**sounder**
E-4W	CTD-084	224	12/11/2011	04:13	48° 45.9320' S	071° 25.4990' E	1 385 m	12/11/2011	04:38	48° 45.9390' S	071° 25.4940' E	1 385 m
E-4W	CTD-085	225	12/11/2011	05:40	48° 45.9190' S	071° 25.5100' E	1 385 m	12/11/2011	06:15	48° 45.9310' S	071° 25.4990' E	1 385 m
E-4W	CTD-086	226	12/11/2011	07:25	48° 45.9310' S	071° 25.5000' E	1 385 m	12/11/2011	08:35	48° 45.9290' S	071° 25.5120' E	1 388 m
E-4W	CTD-087	227	12/11/2011	09:30	48° 45.9260' S	071° 25.5000' E	1 384 m	12/11/2011	10:52	48° 45.9259' S	071° 25.5038' E	1 382 m
E-4W	CTD-088	228	12/11/2011	12:50	48° 45.9280' S	071° 25.5050' E	1 384 m	12/11/2011	13:15	48° 45.9290' S	071° 25.5080' E	1 385 m
E-4W	CTD-089	229	12/11/2011	14:10	48° 48.8640' S	071° 25.3000' E	1 384 m	12/11/2011	14:37	48° 45.9100' S	071° 25.4900' E	1 385 m
IODA-DEP	IODA-DEP-2	230	12/11/2011	17:19	48° 41.6500' S	071° 57.6100' E	1 880 m	12/11/2011	18:04	48° 41.6983' S	071° 57.0920' E	1 885 m
E-4E	CTD-090	231	12/11/2011	20:52	48° 42.8450' S	072° 34.2490' E	2 060 m	12/11/2011	21:11	48° 42.8440' S	072° 34.2470' E	2 060 m
E-4E	BONGO-36	232	12/11/2011	21:45	48° 42.8400' S	072° 34.2330' E	2 060 m	12/11/2011	22:51	48° 42.8910' S	072° 34.1020' E	2 060 m
E-4E	CTD-091	233	13/11/2011	09:29	48° 43.0000' S	072° 34.0010' E	2 210 m	13/11/2011	09:53	48° 43.0090' S	072° 34.0070' E	2 210 m
E-4E	BONGO-37	234	13/11/2011	10:13	48° 43.0075' S	072° 33.9974' E	2 208 m	13/11/2011	11:14	48° 42.9470' S	072° 33.8730' E	2 210 m
E-4E	PHYTONET-23	235	13/11/2011	11:23	48° 42.9400' S	072° 33.8100' E	2 210 m	13/11/2011	11:39	48° 42.9230' S	072° 33.7750' E	2 210 m
E-4E	CTD-092	236	13/11/2011	11:53	48° 42.9290' S	072° 33.7720' E	2 208 m	13/11/2011	12:35	48° 42.9290' S	072° 33.7720' E	2 210 m
E-4E	CTD-093	237	13/11/2011	14:50	48° 42.9220' S	072° 33.7750' E	2 216 m	13/11/2011	16:17	48° 42.9200' S	072° 33.7690' E	2 213 m
E-4E	ISP-QMA-SUPOR-11	238	13/11/2011	16:54	48° 42.9218' S	072° 33.7792' E	2 210 m	13/11/2011	21:52	48° 42.9230' S	072° 33.7680' E	2 210 m
E-4E	CTD-094	239	13/11/2011	22:02	48° 42.9230' S	072° 33.7760' E	2 210 m	13/11/2011	23:15	48° 42.9240' S	072° 33.7760' E	2 210 m

Table I **(continued)**

			start of station				end of station			
Station	**Code of opération**	**OP #**	**date**	**time**	**position**	**sounder**	**date**	**time**	**position**	**sounder**
E-4E	TMR-PROD-15	240	13/11/2011	23:48	48° 42.9210' S 072° 33.7750' E	2 210 m	14/11/2011	01:06	48° 42.9283' S 072° 33.7711' E	2 211 m
E-4E	CTD-095	241	14/11/2011	01:30	48° 42.9260' S 072° 33.7730' E	2 212 m	14/11/2011	01:54	48° 42.9278' S 072° 33.7714' E	2 210 m
E-4E	TMR-PROCESS-08	242	14/11/2011	03:42	48° 42.9292' S 072° 33.7705' E	2 215 m	14/11/2011	04:00	48° 42.9200' S 072° 33.7600' E	2 210 m
E-4E	CTD-096	243	14/11/2011	04:26	48° 42.9260' S 072° 33.7640' E	2 210 m	14/11/2011	04:42	48° 42.9290' S 072° 33.7660' E	2 210 m
E-4E	TMR-ISOTOPES-5	244	14/11/2011	05:25	48° 42.9283' S 072° 33.7628' E	2 210 m	14/11/2011	06:40	48° 42.9301' S 072° 33.7313' E	2 210 m
E-4E	CTD-097	245	14/11/2011	07:07	48° 42.9310' S 072° 33.7620' E	2 210 m	14/11/2011	08:53	48° 42.9300' S 072° 33.7600' E	2 210 m
E-4E	CTD-098	246	14/11/2011	09:51	48° 42.9300' S 072° 33.7580' E	2 210 m	14/11/2011	10:24	48° 42.9290' S 072° 33.7580' E	2 210 m
A3-2	DRIFT-PART-TRAP-2	247	15/11/2011	21:28	50° 37.7973' S 072° 04.8100' E	520 m	15/11/2011	22:21	50° 38.2100' S 072° 03.3320' E	526 m
A3-2	CTD-099	248	15/11/2011	23:20	50° 37.4343' S 072° 03.3328' E	526 m	16/11/2011	00:07	50° 37.4300' S 072° 03.3320' E	526 m
A3-2	ISP-QMA-SUPOR-12	249	16/11/2011	01:35	50° 37.4306' S 072° 03.3366' E	526 m	16/11/2011	07:24	50° 37.4371' S 072° 03.3368' E	531 m
A3-2	CTD-100	250	16/11/2011	07:53	50° 37.4389' S 072° 03.3406' E	520 m	16/11/2011	08:44	50° 37.4406' S 072° 03.3368' E	520 m
A3-2	TMR-PROCESS-09	251	16/11/2011	09:20	50° 37.4394' S 072° 03.3365' E	527 m	16/11/2011	09:28	50° 37.4434' S 072° 03.3340' E	526 m
A3-2	CTD-101	252	16/11/2011	10:06	50° 37.4400' S 072° 03.3360' E	527 m	16/11/2011	10:43	50° 37.4410' S 072° 03.3380' E	527 m
A3-2	CTD-102	253	16/11/2011	11:26	50° 37.4460' S 072° 03.3360' E	527 m	16/11/2011	11:54	50° 37.4510' S 072° 03.3250' E	527 m
A3-2	BONGO-38	254	16/11/2011	12:14	50° 37.4550' S 072° 03.3261' E	527 m	16/11/2011	13:18	50° 37.4450' S 072° 03.3090' E	524 m
A3-2	PHYTONET-24	00:00	16/11/2011	13:27	50° 37.4500' S 072° 03.3123' E	532 m	16/11/2011	13:40	50° 37.4460' S 072° 03.3100' E	532 m

Table I **(continued)**

			start of station				end of station			
Station	**Code of opération**	**OP #**	**date**	**time**	**position**	**sounder**	**date**	**time**	**position**	**sounder**
A3-2	MULTINET-8	256	16/11/2011	13:50	50° 37.4490' S 072° 03.3156' E	532 m	16/11/2011	14:01	50° 37.4490' S 072° 03.3160' E	532 m
A3-2	CTD-103	257	16/11/2011	14:24	50° 37.4500' S 072° 03.3170' E	528 m	16/11/2011	14:55	50° 37.4480' S 072° 03.3110' E	532 m
A3-2	CTD-104	258	16/11/2011	16:40	50° 37.4492' S 072° 03.3055' E	528 m	16/11/2011	17:17	50° 37.4496' S 072° 03.2979' E	530 m
A3-2	TMR-ISOTOPES-6	259	16/11/2011	17:42	50° 37.4450' S 072° 03.2970' E	530 m	16/11/2011	18:09	50° 37.4467' S 072° 03.2991' E	530 m
A3-2	CTD-105	260	16/11/2011	19:15	50° 37.4660' S 072° 03.3340' E	525 m	16/11/2011	19:28	50° 37.4660' S 072° 03.3300' E	530 m
A3-2	CTD-106	261	16/11/2011	20:16	50° 37.4660' S 072° 03.3340' E	525 m	16/11/2011	20:48	50° 37.4700' S 072° 03.3350' E	528 m
A3-2	CTD-107	262	16/11/2011	21:34	50° 37.4650' S 072° 03.3400' E	527 m	16/11/2011	22:14	50° 37.4680' S 072° 03.3440' E	527 m
A3-2	BONGO-39	263	16/11/2011	22:30	50° 37.4660' S 072° 03.3470' E	527 m	16/11/2011	23:32	50° 37.4670' S 072° 03.3510' E	527 m
A3-2	TMR-PROD-16	264	17/11/2011	00:09	50° 37.4650' S 072° 03.3490' E	527 m	17/11/2011	00:37	50° 37.4630' S 072° 03.3470' E	527 m
A3-2	CTD-108	265	17/11/2011	01:08	50° 37.4680' S 072° 03.3520' E	532 m	17/11/2011	01:40	50° 37.4663' S 072° 03.3494' E	526 m
A3-2	CTD-109	266	17/11/2011	05:33	50° 37.4680' S 072° 03.3380' E	525 m	17/11/2011	06:11	50° 37.4672' S 072° 03.3363' E	521 m
A3-2	TURBOMAP-15	267	17/11/2011	06:35	50° 37.5515' S 072° 03.3193' E	525 m	17/11/2011	07:03	50° 38.0409' S 072° 03.5677' E	528 m
A3-2	TURBOMAP-16	268	17/11/2011	07:05	50° 38.0508' S 072° 03.5731' E	528 m	17/11/2011	07:16	50° 38.3174' S 072° 03.7296' E	527 m
A3-2	ISP-QMA-SUPOR-13	269	17/11/2011	08:08	50° 38.5025' S 072° 03.7833' E	533 m	17/11/2011	14:10	50° 38.4940' S 072° 03.7950' E	530 m
A3-2	CTD-110	270	17/11/2011	14:32	50° 38.4990' S 072° 03.7890' E	530 m	17/11/2011	15:22	50° 38.4560' S 072° 03.7780' E	530 m
A3-2	MULTICORER-6	271	17/11/2011	15:36	50° 38.4960' S 072° 03.7820' E	530 m	17/11/2011	16:45	50° 38.4990' S 072° 03.7830' E	530 m

Table I **(continued)**

			start of station				end of station			
Station	**Code of opération**	**OP #**	**date**	**time**	**position**	**sounder**	**date**	**time**	**position**	**sounder**
A3-2	DRIFT-PART-TRAP-2	272	17/11/2011	17:46	50° 42.5152' S 072° 09.6706' E	522 m	17/11/2011	19:00		
E-4W-2	TMR-PROD-17	273	18/11/2011	05:47	48° 45.9983' S 071° 28.7883' E	1 390 m	18/11/2011	07:00	48° 46.0016' S 071° 25.7814' E	1 394 m
E-4W-2	CTD-111	274	18/11/2011	07:20	48° 46.0030' S 071° 25.7810' E	1 390 m	18/11/2011	08:39	48° 46.0026' S 071° 25.7781' E	1 417 m
E-4W-2	MULTICORER-7	275	18/11/2011	08:50	48° 45.9980' S 071° 25.7880' E	1 410 m	18/11/2011	10:40	48° 45.9950' S 071° 25.7800' E	1 390 m
E-4W-2	PHYTONET-25	276	18/11/2011	10:40	48° 45.9990' S 071° 25.7870' E	1 390 m	18/11/2011	10:55	48° 45.9990' S 071° 25.7870' E	1 390 m
E-5	GEL-TRAP-5	277	18/11/2011	13:50	48° 25.0653' S 071° 59.8362' E	1 971 m	18/11/2011	14:33	48° 25.0463' S 071° 59.0178' E	1 966 m
E-5	DRIFT-PART-TRAP-3	278	18/11/2011	14:42	48° 25.0278' S 071° 58.1112' E	1 961 m	18/11/2011	15:16	48° 25.0361' S 071° 57.4632' E	1 960 m
E-5	CTD-112	279	18/11/2011	16:15	48° 24.7121' S 071° 54.1761' E	1 922 m	18/11/2011	17:25	48° 24.7134' S 071° 54.1853' E	1 920 m
E-5	PHYTONET-26	280	18/11/2011	17:36	48° 24.7131' S 071° 54.1780' E	1 921 m	18/11/2011	17:48	48° 24.7130' S 071° 54.1540' E	1 921 m
E-5	BONGO-40	281	18/11/2011	17:56	48° 24.7060' S 071° 54.1317' E	1 915 m	18/11/2011	19:00	48° 24.6935' S 071° 53.8998' E	1 922 m
E-5	CTD-113	282	18/11/2011	19:21	48° 24.6920' S 071° 53.9960' E	1 920 m	18/11/2011	20:58	48° 24.6950' S 071° 53.9960' E	1 920 m
E-5	TMR-PROCESS-10	283	18/11/2011	21:15	48° 24.6930' S 071° 53.9960' E	1 920 m	18/11/2011	21:26	48° 24.6920' S 071° 53.9950' E	1 920 m
E-5	CTD-114	284	18/11/2011	22:07	48° 24.6970' S 071° 53.9950' E	1 920 m	18/11/2011	23:08	48° 24.6970' S 071° 53.9940' E	1 920 m
E-5	TMR-PROD-18	285	18/11/2011	23:44	48° 24.6940' S 071° 53.9910' E	1 920 m	19/11/2011	01:15	48° 24.6960' S 071° 53.9940' E	1 920 m
E-5	CTD-115	286	19/11/2011	01:30	48° 24.6950' S 071° 53.9900' E	1 920 m	19/11/2011	01:49	48° 24.6570' S 071° 53.9930' E	1 920 m
E-5	BONGO-41	287	19/11/2011	01:59	48° 24.6947' S 071° 53.9903' E	1 914 m	19/11/2011	02:59	48° 24.6968' S 071° 53.9883' E	1 929 m

Table I **(end)**

			start of station				end of station			
Station	**Code of opération**	**OP #**	**date**	**time**	**position**	**sounder**	**date**	**time**	**position**	**sounder**
E-5	ISP-QMA-SUPOR-14	288	19/11/2011	03:09	48° 24.6980' S 071° 53.7894' E	1 915 m	19/11/2011	08:34	48° 24.7040' S 071° 53.9760' E	1 921 m
E-5	CTD-116	289	19/11/2011	08:53	48° 24.7040' S 071° 53.9770' E	1 921 m	19/11/2011	09:44	48° 24.7080' S 071° 53.9750' E	1 925 m
E-5	TMR-ISOTOPES-7	290	19/11/2011	09:58	48° 24.7030' S 071° 53.9730' E	1 921 m	19/11/2011	11:17	48° 24.7040' S 071° 53.9710' E	1 920 m
E-5	CTD-117	291	19/11/2011	11:36	48° 24.7060' S 071° 53.9690' E	1 921 m	19/11/2011	12:21	48° 24.7070' S 071° 53.9750' E	1 920 m
E-5	MULTINET-9	292	19/11/2011	12:37	48° 24.7040' S 071° 53.9710' E	1 920 m	19/11/2011	12:50	48° 24.7050' S 071° 53.9670' E	1 920 m
E-5	CTD-118	293	19/11/2011	13:24	48° 24.7060' S 071° 53.9680' E	1 920 m	19/11/2011	14:12	48° 24.7070' S 071° 53.9710' E	1 920 m
E-5	GEL-TRAP-5	294	19/11/2011	15:17	48° 30.2545' S 071° 57.4202' E	1 945 m	19/11/2011	16:12	48° 29.4928' S 071° 57.0778' E	1 943 m
E-5	CT-119	295	19/11/2011	17:16	48° 24.7252' S 071° 53.9841' E	1 915 m	19/11/2011	18:20	48° 24.7490' S 071° 53.9420' E	1 915 m
E-5	TMR-PROCESS-11	296	19/11/2011	18:39	48° 24.7501' S 071° 53.9379' E	1 921 m	19/11/2011	18:44	48° 24.7537' S 071° 53.9375' E	1 921 m
E-5	BONGO-42	297	19/11/2011	19:02	48° 24.7519' S 071° 53.9378' E	1 920 m	19/11/2011	19:32	48° 24.7504' S 071° 53.9398' E	1 920 m
E-5	ISP-QMA-SUPOR-15	298	19/11/2011	20:15	48° 24.7520' S 071° 53.9450' E	1 920 m	20/11/2011	02:53	48° 24.7503' S 071° 53.9466' E	1 920 m
E-5	DRIFT-PART-TRAP-3	299	20/11/2011	03:54	48° 33.1590' S 071° 56.8620' E		20/11/2011	05:00	48° 32.8010' S 071° 55.8490' E	
IODA-REC	IODA-REC-2	300	20/11/2011	08:16	48° 21.8300' S 072° 53.1860' E	2 300 m	20/11/2011	09:00	48° 21.6086' S 072° 53.1520' E	2 300 m
IODA-REC	CTD-120	301	20/11/2011	09:30	48° 21.6080' S 072° 53.1540' E	2 300 m	20/11/2011	11:26	48° 21.6040' S 072° 53.1540' E	2 300 m
IODA-REC	PHYTONET-27	302	20/11/2011	11:40	48° 21.6040' S 072° 53.1550' E	2 300 m	20/11/2011	11:53	48° 21.6050' S 072° 53.1570' E	2 300 m

Table II : Standard photometric depths for on-deck incubators (derived from PAR-sensor data)

station	# CTD	Date	Time of profile	75%	45%	25%	16%	4%	1%	0.3%	0.01%	k (m^{-1})
OISO–7	002	16/10/2011	12:08	4 m	12 m	20 m	27 m	47 m	67 m	84 m	134 m	0.069
A3–1	004	20/10/2011	5:32	6 m	18 m	31 m	41 m	71 m	102 m	128 m	204 m	0.045
TNS–10	006	21/10/2011	7:28	5 m	14 m	25 m	33 m	58 m	83 m	105 m	166 m	0.055
TNS–9	007	21/10/2011	13:40	4 m	12 m	21 m	27 m	48 m	69 m	87 m	137 m	0.067
TNS–2	014	23/10/2011	12:06	5 m	14 m	24 m	32 m	56 m	81 m	102 m	161 m	0.057
R–2 IODA	016	25/10/2011	14:58	6 m	15 m	27 m	35 m	62 m	89 m	112 m	178 m	0.052
R–2	019	26/10/2011	13:05	6 m	16 m	28 m	37 m	64 m	92 m	116 m	184 m	0.050
E–1	025	29/10/2011	11:53	4 m	11 m	19 m	25 m	43 m	62 m	78 m	124 m	0.074
E–1	026	29/10/2011	14:15	4 m	11 m	19 m	26 m	45 m	64 m	81 m	129 m	0.071
E–3	049	03/11/2011	11:57	4 m	12 m	21 m	27 m	48 m	68 m	86 m	137 m	0.067
F–L	057	06/11/2011	10:20	2 m	4 m	7 m	10 m	17 m	24 m	30 m	48 m	0.191
F–L	058	06/11/2011	11:59	2 m	5 m	8 m	10 m	18 m	26 m	33 m	52 m	0.175
F–L	059	06/11/2011	13:50	2 m	4 m	7 m	10 m	17 m	25 m	31 m	50 m	0.186
F–L	060	06/11/2011	16:00	2 m	4 m	8 m	10 m	18 m	25 m	32 m	50 m	0.183
F–L	061	06/11/2011	18:05	2 m	5 m	9 m	11 m	20 m	29 m	36 m	57 m	0.161
E–4W	079	11/11/2011	8:25	2 m	5 m	9 m	12 m	21 m	30 m	38 m	61 m	0.152
E–4W	080	11/11/2011	10:30	2 m	5 m	9 m	12 m	21 m	31 m	39 m	61 m	0.150

Table III : Standard photometric depths for on-deck incubators (derived from fluorescence profiles, using the empiric equation of Riley, 1956) – ATTENTION : These estimates will have to be refined after recalibration of the fluorescence signal by chlorophyll oncentrations measured by HLC.

station	# CTD	Date	Time of profile	75%	45%	25%	16%	4%	1%	0.3%	0.01%	k (m^{-1})
A3–2	099	15/11/2011	23:20	2 m	7 m	11 m	15 m	26 m	38 m	48 m	75 m	0.122
A3–2	100	16/11/2011	07:53	2 m	7 m	12 m	15 m	27 m	39 m	49 m	78 m	0.119
A3–2	101	16/11/2011	10:06	2 m	7 m	12 m	16 m	27 m	39 m	50 m	79 m	0.117
A3–2	102	16/11/2011	11:26	2 m	7 m	12 m	16 m	27 m	39 m	50 m	79 m	0.117
A3–2	103	16/11/2011	14:24	2 m	7 m	12 m	16 m	27 m	39 m	49 m	78 m	0.118
A3–2	104	16/11/2011	16:40	2 m	7 m	12 m	15 m	27 m	38 m	49 m	77 m	0.120
A3–2	105	16/11/2011	19:15	2 m	7 m	12 m	16 m	28 m	39 m	50 m	79 m	0.117
A3–2	106	16/11/2011	20:16	2 m	7 m	11 m	15 m	26 m	38 m	47 m	75 m	0.122
A3–2	107	16/11/2011	21:34	2 m	6 m	11 m	15 m	26 m	37 m	47 m	74 m	0.124
A3–2	108	17/11/2011	01:08	2 m	7 m	12 m	15 m	27 m	38 m	48 m	77 m	0.120
A3–2	109	17/11/2011	05:33	3 m	7 m	12 m	16 m	28 m	40 m	51 m	80 m	0.115
A3–2	110	17/11/2011	14:32	3 m	7 m	12 m	16 m	28 m	41 m	51 m	81 m	0.114
E-4W-2	111	18/11/2011	07:20	2 m	6 m	10 m	13 m	23 m	32 m	41 m	65 m	0.142
E-5	112	18/11/2011	16:15	3 m	9 m	16 m	21 m	37 m	54 m	68 m	107 m	0.086
E-5	113	18/11/2011	19:21	4 m	10 m	17 m	23 m	40 m	57 m	72 m	114 m	0.081
E-5	114	18/11/2011	22:07	3 m	9 m	16 m	21 m	38 m	54 m	68 m	107 m	0.086
E-5	115	19/11/2011	01:30	3 m	9 m	16 m	22 m	38 m	54 m	68 m	108 m	0.085
E-5	116	19/11/2011	08:53	3 m	9 m	15 m	20 m	35 m	50 m	64 m	101 m	0.091

Table III **(end)**

E-5	**117**	**19/11/2011**	**11:36**	**3 m**	**9 m**	**15 m**	**20 m**	**35 m**	**50 m**	**63 m**	**100 m**	**0.092**
E-5	**118**	**19/11/2011**	**13:24**	**3 m**	**9 m**	**16 m**	**21 m**	**37 m**	**53 m**	**67 m**	**106 m**	**0.087**
E-5	**119**	**19/11/2011**	**17:16**	**3 m**	**9 m**	**15 m**	**20 m**	**35 m**	**50 m**	**63 m**	**99 m**	**0.093**
IODA-REC	**120**	**20/11/2011**	**09:30**	**3 m**	**8 m**	**13 m**	**17 m**	**31 m**	**44 m**	**55 m**	**88 m**	**0.105**

2 Lagrangian analysis of Kerguelen bloom from multisatellite data

Principal investigator

Francesco d'Ovidio
LOCEAN-IPSL, 4, Place Jussieu, 75005, Paris
☎ +33 144277076
francesco.dovidio@locean-ipsl.upmc.fr

Other participants

- F. Nencioli (LOPB)
- A. Doglioli (LOPB)
- L. Resplandy (LOCEAN)

Abstract:
Multisatellite data (altimetry, sea surface temperature, surface chlorophyll) have been received daily from LOCEAN/LOPB and analyzed onboard. Data have been produced by CLS with support from CNES, as a standard global product and specifically for KEOPS2 as an optimized regional product. The Lagrangian analysis of these data allowed us to follow synoptically and in near real time the chlorophyll plume which developed during the cruise, and the possible mesoscale mechanisms capable of structuring it. The analysis guided the sampling strategy an the drifter release scheme. Preliminary comparisons with in situ data and drifter trajectories indicate that the chlorophyll plume developed at the end of the campaign was in an overall remarkable agreement with the shape predicted by the Lagrangian model, and that the regional altimetric product scored much better than the global one. The comparison with drifter trajectories obtained insofar revealed the presence of a surprisingly rich meso/submeso scale surface circulation around E1 station and not detected by altimetry.

2.1 Scientific context

Multisatellite data (notably altimetry, sea surface temperature and ocean color) can be combined together to provide physical and biogeochemical information like the position of fronts, water mass origin, chlorophyll concentration, stirring and mesoscale activity up to a spatial and temporal resolution of few tens of km and one day respectively. Previous studies [Mongin *et al.* 2007] have shown that horizontal stirring has a strong structuring effect on the extension of the chlorophyll rich plume which develops in spring east of Kerguelen islands. The impact of horizontal stirring on chlorophyll patchiness can be reconstructed from satellite-derived, surface geostrophic velocites through Lagrangian techniques [d'Ovidio *et al.* 2004; Lehahn *et al.* 2007; d'Ovidio *et al.* 2010], which estimate the origin and fate of a water parcel by analyzing its possible trajectories. In the context of the iron-limited ecosystems of the Southern ocean, such Lagrangian techniques provide key biogeochemical information, since they allow to test whether a water parcel has been in contact with a possible source of iron - like for instance the Kerguelen plateau – and hence predict whether a bloom will occur in a specific region.

2.2 Overview of the project and objectives

This project has some in-cruise and some post-cruise objectives.

In-cruise:

i. provide synoptic maps of the meso/submeso-scale features of the surface circulation and of the bloom which developed during the cruise.

ii. Guide the sampling strategy by identifying sites for fixed, Lagrangian and mooring stations representative of physical features of biogeochemical interest (eddies, filaments, jets, fronts, mixing regions..) present in the region, and by following their evolution in time (displacement, dispersion, lifecycle,..).

iii. Guide the drifter release scheme, by identifying from satellite data key water pathways inside and outside the plume which need to be validated or better located.

Post-cruise:

iv. Propose possible scenarios for the watermass origin of the sampling sites.

v. Try to link meso and submesoscale horizontal physical features to biogeochemical and ecological parameters.

vi. Identify the part of the plume of which the sampled stations are representative, so that the budget obtained at the sampled stations can be extended to wider regions.

vii. Contribute to explain the physical structure of the water column measured from CTD casts by describing the exchanges due to horizontal stirring.

2.3 Methodology and sampling strategy

Data were produced from CLS (Toulouse) with support from CNES. AMSRE satellite stopped functioning few days before the beginning of the cruise, allowing howeverto have at least some pre-bloom cloud-free SST images. One main site (LOPB in Marseille) and one redundant site (LOCEAN in Paris, to be used as a back up) were set up for collecting the data, preparing the files, and send them to the ship. Data anlaysis (eddy kinetic energy, Lagrangian calculations of water origins, Lyapunov exponents, Okubo-Weiss parameter, extension of the water dispersed from the plateau by the geostrophic velocities) was done on the ship. The same calculation was replicated on land, so that the main diagnostics could have been sent in case of a technical problem on the ship. The possibility of having raw satellite data on board allowed to perform several other ad hoc Lagrangian calculations, depending on the specific need of the sampling strategy (drifter or mooring trajectory prediction, higher resolution zoom on sampling areas, reconstruction of watermass origin for possible sampling sites,..).

Table IV : Exhaustive list of measured parameters

Parameter	code of operation	units
1.Altimetric geostrophic vel. (JASON-2, ENVISAT)	N/A (Remote sensing)	
2.Surface chlorophyll (MODIS, MERIS)	N/A (Remote sensing)	
3. Microwave surface temp. (AMSRE)	N/A (Remote sensing)	
4. Infrared surface temp. (MODIS)	N/A (Remote sensing)	

2.4 Preliminary results

Figure 2 shows the prediction of the plume extension (where the bloom was expected) from the Lagrangian model and which guided the identification of the sampling sites. Figure 2 shows the bloom which actually occurred at the end of the campaign. Note the remarkable agreement.

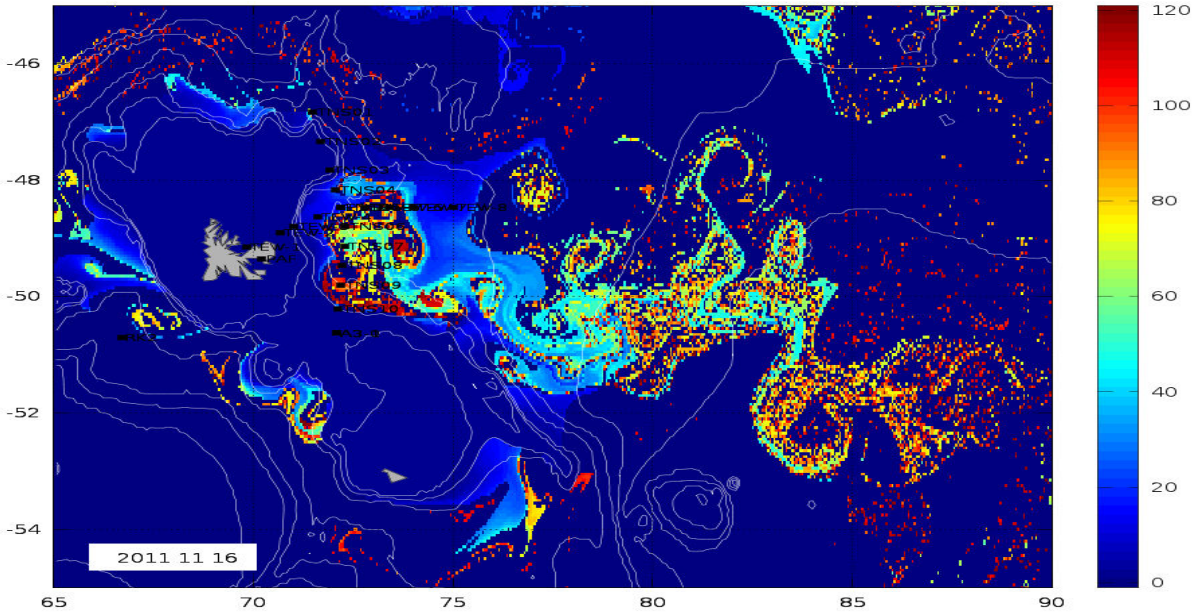

Figure 2 : Dispersion of water coming from the plateau from a Lagrangian model based on altimetry data.

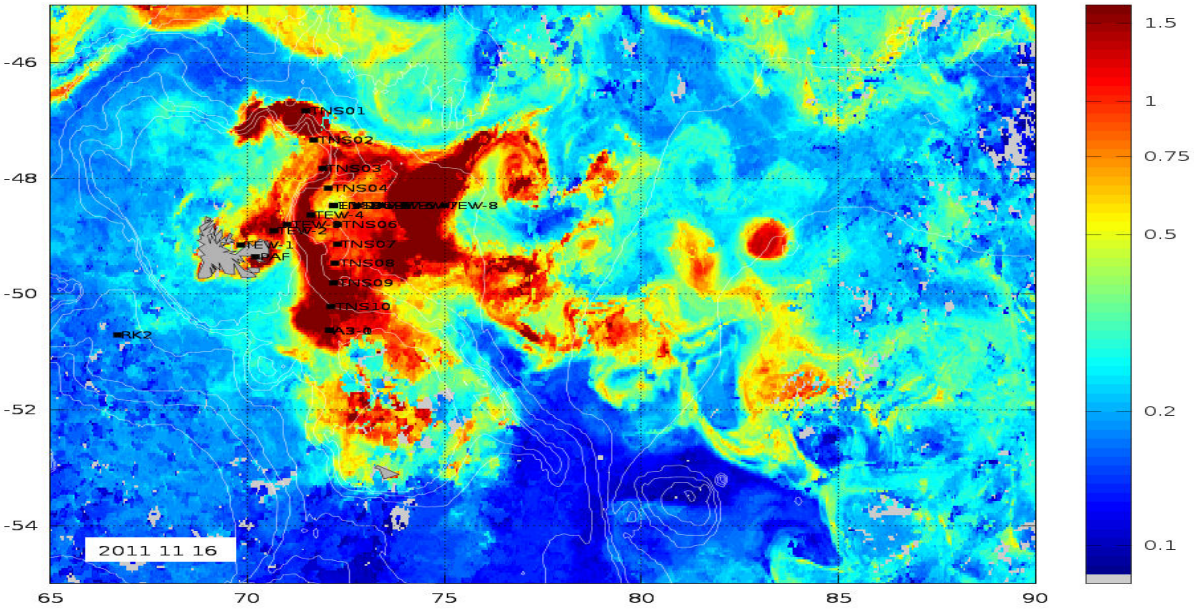

Figure 3 : Surface chlorophyll distribution.

2.5 Post-cruise sampling analyses and dead-lines

Delayed-trime altimetry data (of higher quality than near real-time) will be produced by CLS six months from the end of the cruise. They will be analyzed with the Lagrangian diagnostics and compared with the maps created at the time of the campaign from near real time data. Possibly, Synthetic Aperture Radar images will also integrate the satellite dataset in 4-6 months.

2.6 Data base organization

Most of the data will be available in the general cruise base. The other products will be available through the CLS AVISO website.

2.7 References of methods

d'Ovidio F., De Monte S., Alvain S., Dandonneau Y., and Lévy M. 2010. Fluid dynamical niches of phytoplankton types. Proceedings of the National Academy of Sciences 107: 18366-18370.

D'ovidio F., Fernández V., Hernández-García E., and López C. 2004. Mixing structures in the Mediterranean Sea from finite-size Lyapunov exponents. Geophysical Research Letters 31: doi:10.1029/2004GL020328.

Lehahn Y.F., D'ovidio F., Lévy M., and Heifetz E. 2007. Stirring of the northeast Atlantic spring bloom: A Lagrangian analysis based on multisatellite data. Journal of Geophysical Research 112: doi:10.1029/2006JC003927.

Mongin M., Molina E., and Trull T.W. 2008. Seasonality and scale of the Kerguelen plateau phytoplankton bloom: A remote sensing and modeling analysis of the influence of natural iron fertilization in the Southern Ocean. Deep Sea Research Part II: Topical Studies in Oceanography 55: 880.

3 Physics and dynamics of the Polar Front region east off the Kerguelen Islands

Principal investigator

Young-Hyang Park
LOCEAN/DMPA, Muséum National d'Histoire Naturelle, 45 rue Cuvier, 75005 Paris
☎ +33 1 4079 3170
🖷 +33 1 4079 5736
yhpark@mnhn.fr

Other participants

- Isabelle Durand (LOCEAN/MNHN): CTD data acquisition, analysis of salinity, analysis of different data sets in collaboration with Y.-H. Park
- Elodie Kestenare (LEGOS): Vertical velocity profiles from LADCP & SADCP, CTD data acquisition (coll. F. d'Ovidio, C. Cotté)
- Jae-Hak Lee (KORDI): Direct measurements of turbulent energy dissipation rate using a TurboMAP
- Francesco d'Ovidio (LOCEAN): Altimetry and surface chlorophyll data produced by CLS with support from CNES.
- Gilles Rougier (MIO): *In situ* surface and near-surface (100 to 200 m) velocity field using Iridum drifters and different floats, CTD data acquisition (coll. J.-H. Lee)
- Meng Zhou (U.Mass.): *In situ* surface velocity field using NOAA surface drifters

Abstract:

A large number of CTD profiles (a total of 120, of which 53 for a full depth) together with concomitant LADCP and SADCP profiles have been obtained mostly in a limited study area (4° x 4°) of the PF region east of the Kerguelen Islands. At 15 selected stations, we have sampled TurboMAP profiles down to a maximum depth of ~450 m. A salinity analysis using a Portasal salinometer for the water samples gathered at different depths and times have been made at a total of 24 stations. Although all these data sets should need a further post-cruise treatment and corrections, a preliminary analysis indicates an excellent quality of data, in general.

A quick inspection of CTD and LADCP data confirms the previous studies concerning the geographical location and intensity of the PF of the region, although a more detailed analysis is needed for a finer description. The vertical eddy mixing coefficients from both the Thorpe scale method using CTD data and direct TurboMAP measurements are of the same order of magnitudes (~10^{-4} m^{-2} s^{-1}) as those observed during the KEOPS 1 cruise.

Besides individual analysis by M. Zhou for drifters and by F. d'Ovidio for satellite data, which will be presented in separate reports, a synthesis of all available velocity data sets (drifters, floats, altimetric velocities) has been attempted by performing an optimal interpolation based on a stream-function method to simulate a nondivergent mean geostrophic velocity field of the study area, in comparison with satellite-derived quasi-real time Chl data. While the large scale feature is relatively well described by altimetry, the latter reveals an apparent shortcoming for the interior circulation of the retroflection, which has been rectified by combining with data from drifters and floats. The resultant optimal geostrophic circulation products have been usefully referenced in deciding the position of the "target" stations as well as for interpreting different parameters measured with the advent of the cruise. Finally, a Fourier analysis of the high-frequency undulations of the drifter and float trajectories indicates an equivalent contribution of tidal and inertial currents over

the shallow self, while in the deeper central part of the study area inertial currents appear as a dominant contributor. In short, the physical component of the cruise was very fruitful, with a number of new findings which wait for further confirmation and interpretations in a near future.

3.1 Scientific context

The region just east of the Kerguelen Islands, which is surrounded in the west and north by a steep escarpment of the Kerguelen Plateau at its northeastern corner, appears as a starting place of the annually recurrent phytoplankton bloom, which begins from late October, steadily developing through November and peaking in December, before fading out in January. This bloom area is surrounded at its outer boundary by topographically-steered, relatively strong flow whose hydrographic characteristics correspond to the Polar Front, although the exact pathway of which is still in debate. According to a number of previous studies, summarized in a synthetic paper by Park and Vivier (2011), the PF enters into the region from the west, flowing along the southern inner slope near 50°S immediately south of the Kerguelen Islands, turns to the north along the eastern inner slope along an isobath between 500 to 1000 m up to 47°30'S at 72°E, before retroflecting back southward to reach again a latitude of 50°S at 77°E. Compared to this quasi-permanent cyclonic circulation of the PF, the interior circulation of the retroflection has not been well documented, although it has been thought to be featureless or stagnant. The altimetry-derived circulation, unique means to infer quantitatively the pre-cruise circulation pattern, may be doubtful in this particular region due to its proximity to a prominent topographic obstacle such as the Kerguelen Islands and shallow shelf topography where time-mean geostrostrophic currents are ill-defined with the present knowledge of the geoid and insufficient in-situ velocity and hydrographic measurements. A detailed description of the regional circulation and the source tracking of water masses found within the region constitute thus our major challenge within the overall context of the KEOPS 2 cruise.

3.2 Objectives of the project

The rational and objectives of the present project are as followings:

1) Determine the geographical location of the PF and its transport as precise as possible. This is to definitely cease the long-lasting debate on the topic and to better interpret the spatial distribution of the recurrent bloom of the region in terms of the advective effect, among other factors.

2) Determine the pathways of different source waters found within the study area as well as their mixing ratios. There are at least two major sources of high iron or other terregeneous nutrient-rich waters that should critically affect the bloom: one is the southern source originating from the shallow plateau south of the PF, especially that from the Heard Island (van Beek, 2008); the other should come from the shallow shoal (<200 m) widely developed north of the Kerguelen Islands. These two sources are well separated by the presence of the PF where a band of a minimum in Chl concentration is consistently observed during the bloom period (Park *et al.*, 2008a). We also expect that a mixture of these two sources as well as with subantarctic waters originating from the north of the PF may be formed especially along the northern and eastern boundaries of the retroflection, before its possible injection into the interior of the retroflection.

3) Quantify the vertical mixing coefficients of the water column in the study area. There exist several empirical methods using CTD and LADCP data for estimating the intensity of vertical mixing, which is thought to form, besides horizontal advection, a major mechanism for pumping nutrient-rich waters below the thermocline into the eupotic layer, thus promoting the bloom (Park *et al.*, 2008b). However, the validation of these indirect methods against direct turbulence measurements has been very rare especially in the Southern Ocean. We will contribute to this important topic by deploying the TurboMAP at selected stations.

4) Document the relative importance of (semi-diurnal and diurnal) tidal currents versus inertial currents which form two major high-frequency (T<25h) energy sources for vertical mixing in the Southern Ocean.

5) Understand the underlying dynamics of the observed preferential development of the bloom in cyclonic rather than anticyclonic eddies or meanders.

3.3 Methodology and sampling strategy

3.3.1 CTD casts

Seabird SBE 911-plus CTD unit with a pair of S and T sensors, an O_2 sensor, and a pressure sensor have been mounted on a 22 bottles-rosette which was equipped with, among many other instruments of other teams, a pair of LADCP ("master" and "slave") and an altimeter for detecting the bottom within 35 m from the sea floor. After a first discover of ill-functioning of the altimeter due to the 15 m-long weight suspended below the rosette for the stabilizing purposes, the altimeter has been reinstalled with an angle of 15° from the vertical frame of the rosette to avoid the altimeter signals from hitting directly the weight, following a judicious advice of Xavier Morin of IPEV. That worked miraculously well, and most of the bottom reaching CTD casts were made within 20 to 15 m from the bottom. Other procedures concerning the preparation and acquisition of data are classic.

Most of bottom reaching stations have been planned to lie along two sections cutting the PF at a right angle: one in the N-S direction and the other in the E-W direction. This may permit to calculate efficiently the along-stream geostrophic velocity profiles and corresponding transport of the PF, in reference to the direct velocity measurements from the LADCP. Water mass analysis and the evaluation of mixing ratios between different source waters will be made with gathered hydrographic data in combination with available historical data.

3.3.2 LADCP and SADCP measurements (E. Kestenare)

LADCP: Two LADCP «Workhorse 300kHz» of the RD Instruments have been used: one is a so-called "master" installed at the base of the rosette for "down looking" measurements and the other called "slave" installed at the top of the rosette for "up looking" measurements. The parameters were recorded at intervals of 16 bins, corresponding to 16 m, with a nominal lowering speed of the rosette of 1 m/s. The profiles of each cast have been treated daily using a Matlab code adapted from the version v8b code of Martin Visbeck (http://www.ldeo.columbia.edu/~visbeck/ladcp/). A total of 102 casts have been recorded. The measurements are in excellent quality, however, a post-cruise validation in comparison with the SADCP data for the first hundreds meters is planned.

SADCP: The R/V Marion Dufresne II is equipped with two ship-mounted ADCP or SADCP: a 75 kHz narrow band model from "Ocean Surveyor" having a search range of 500 to 700 m, and the other is a 150 kHz model from RDI covering the first 200 to 400 m. These permit continuous measurements of currents of the surface layer, both underway and on station. The data treatment has been done using a code CODAS-3 (Common Oceanographic Data Access System, version 3) developed at the University of Hawaii (i.e., Bahr *et al.,* 1989). A preliminary treatment has been made regularly during the cruise.

Thermosalinograph (TSG): Although it is not part of the ADCP measurements, the TSG mounted on the ship at a 6 m depth permits to continuously record surface temperature and salinity along all ship tracks during the cruise, so may provide very useful information on the passage across a front. The TSG data quality has been controlled using CTD data at 6 m, which calls for a post-cruise calibration.

3.3.3 TurboMAP casts (J.-H. Lee, Y.-H. Park)

The microscale velocity shear has been measured by a TurboMAP immediately before or after CTD casts. The sampling frequency is 512 Hz and an optimal lowering speed of about 0.6 m s^{-1} is

recommended to obtain a good quality of data. The TurboMAP has been deployed at a total of 15 stations to a maximum depth of about 450 m using a portable winch installed on the starboard rear rack.

3.3.4 Iridium drifters for a Lagrangian sampling strategy (G. Rougier)

Three Iridium drifters developed at LOPB have been deployed during the cruise in order to follow water particles when revisiting a target station, such as station E1. The major advantage of these Iridium drifters compared to more conventional ones is that on can receive on board their GPS locations in real time, with a high precision, which is well adapted for a Lagrangian sampling strategy. A visualization software has been developed to monitor in quasi real-time the trajectories of these drifters, which has been efficiently used for planning or adjusting major stations (Fig. 3). These Iridum drifters are in compliment of 48 NOAA drifters deployed by M. Zhou (see his report). The combination of both kinds of drifters have been used for various analyses, such as the estimation of a mean geostrophic circulation field (Y.-H. Park and I. Durand) or a Fourier decomposition of high-frequency fluctuations of currents (Y.-H. Park and G. Rougier).

3.3.5 Salinity analysis (I. Durand, Y.-H. Park, G. Rougier)

Water samples obtained at selected depths at different times during the cruise have been analysed using a Portasal salinometer in a laboratory cabin where the room temperature was not well regulated. Therefore, a particular care was paid to check any abrupt rise in room temperature during the analysis. A total of 6 series of analyses, with a new standardization of the salinometer for each series, were carried out satisfactorily.

Table V : Exhaustive list of measured parameters

1. Temperature	CTD	°C
2. Conductivity	CTD	S/m
3. Oxygen	CTD	mL/l or µmol/kg
4. Pressure	CTD	db
5. LADCP velocity	CTD	m/s
6. Velocity shear	Turbo Map	1/s
7. Salinity	Analysis	PSU
8. SADCP velocity	Ship-born meas.	m/s
9. Thermosalinograph	Ship-born meas.	°C, PSU

3.4 Preliminary results

- Unsurprisingly, the study area is bounded by the cyclonically meandering PF which enters into the area from the west, hugging the Kerguelen Islands from the south and then east to flow northward up to the northeastern corner of the plateau, before retroflecting back to the south, which is a well-known general circulation pattern in this Kerguelen region (see Fig. 1). This pattern is well supported by across-section LADCP velocities (Fig.2), as well as by the water property distribution.
- What is unexpected and new is the inner circulation pattern within the retroflection area, which appears most clearly from a surface geostrophic velocity field obtained by an optimal interpola-

tion based on a nondivergent stream function method (Bretherton *et al.*, 1976) of all available in-situ data from drifters and floats as well altimetric velocity data, superimposed on a satellite Chl image (Fig. 4). In contrast to the altimetry-alone circulation (bottom panel), which shows an eastward branch of the PF at a latitude of 48°30'S, most of surface waters in the central part of the area largely originate from the further south, taking a further eastern pathway near 73°E (upper panel), instead of following the near-shore PF centered at 71°E. Also, there appears no concentric, isolated eddy-like circulation. Instead, the southern source waters flow directly northward to enter into the central region from about 50°S, 73°E, gradually peeling eastward while progressing northward. From drifter and float trajectories, we find no clear evidence for a westward branch flowing into the retroflection interior from the eastern boundary of the PF. The absence of this westward recirculation, which is rather seen in altimetric circulation at about 49°45'S, 74°E, may be real or could be related to the existence of widespread data-blank areas to the east of 73°E. Water mass analyses may provide more definite answer to this unclear feature.

- Among a total of 15 TurboMAP profiles, 4 are highly contaminated due to a rapid ship drift during strong wind conditions. For relatively good data sets, background values of the turbulent kinetic energy dissipation rate are: $\varepsilon = O(10^{-9}$ W/kg). Using a typical buoyancy frequency of the study area, $N = O(2*10^{-3}$ $s^{-1})$, a vertical eddy diffusivity ($K_v = 0.2\ \varepsilon/N^2$) of $5*10^{-5}$ m^2 s^{-1} is obtained, with a peak value of 10^{-4} m^2 s^{-1} in the thermocline developed below the surface mixed layer (Fig. 5). These values are of the same order of magnitude, albeit a little smaller, as those at A3 during the 2005 KEOPS 1 cruise (Park *et al.*, 2008b).
- A Fourier decomposition of high-frequency undulations in drifter (and float) trajectories (Fig. 6) shows that tidal currents (both semidiurnal and diurnal) are relatively strong (~10 to 15 cm s^{-1}) over the shallow plateau <1000 m, while they are very weak (a few cm s^{-1}) in the deep interior region. In contrast, inertial currents are strong in most places, except for the northern and western boundaries. This may suggest that the major impact of tidal currents on vertical mixing may be largely confined to a shallow topography while wind forcing exerts its influence regardless of bottom topography. A further comparison with historical velocity time series data from moored current meters as well as with a fine-resolution regional tide model is planned.

Post-cruise sampling analyses and dead-lines

- Post-cruise treatment of CTD data (correction of S, p, O_2; noise removal, vertical averaging, resampling at 1 m intervals): June 2012
- Post-cruise treatment of SADCP data and validation of LADCP data: August 2012
- Post-cruise treatment of TurboMAP data: March 2012.

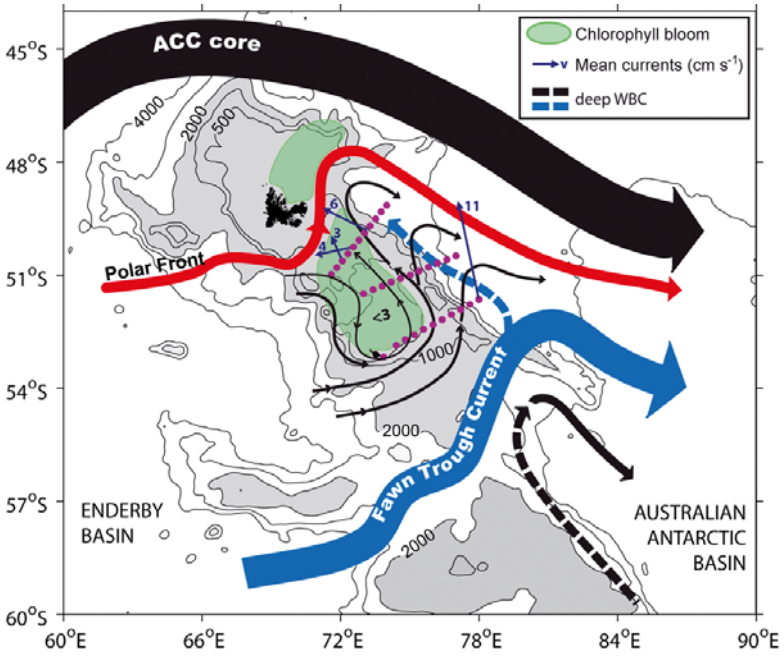

Figure 4 : A schematic of the large-scale circulation pattern around the northern Kerguelen Plateau. From Park *et al.* (2008c).

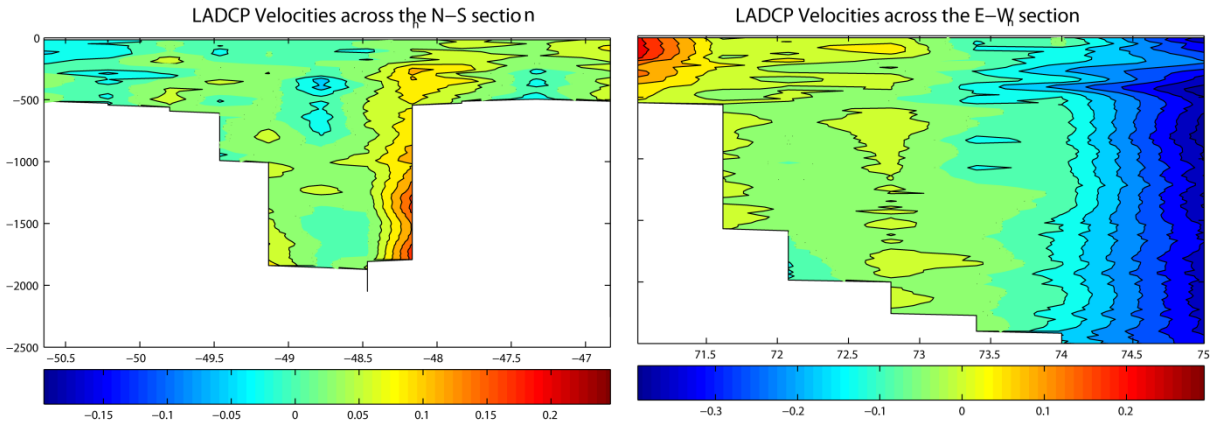

Figure 5 : LADCP velocities perpendicular to (left) the N-S section and (right) the E-W section. The cyclonic retroflection of the PF in the study area can be recognized by a strong northward flow at 71°E, a bottom-intensified eastward flow at 48°15'S, and a strong southward flow east of 74°30'S. LADCP data have been previously corrected for a global tide model-derived tidal currents.

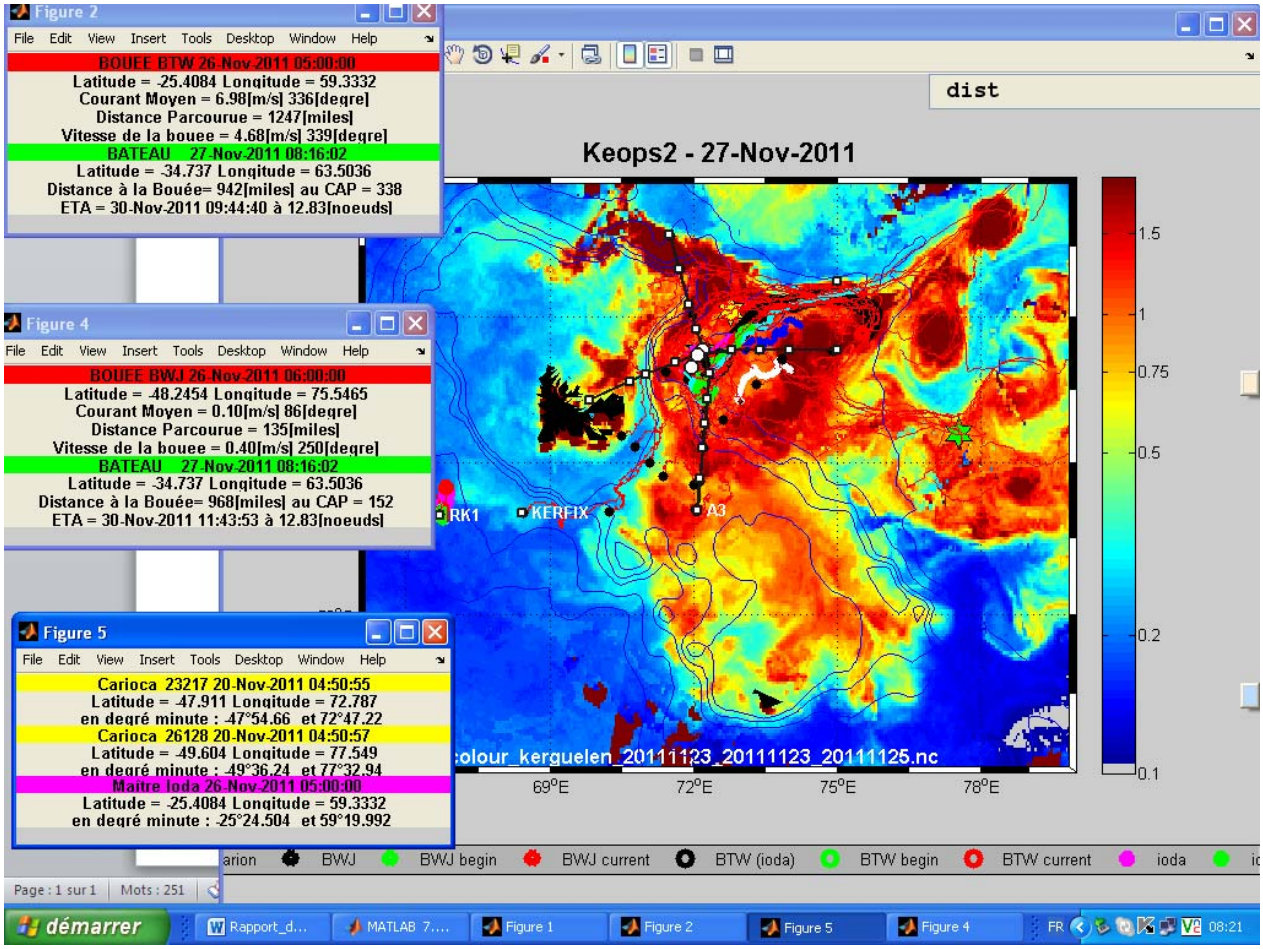

Figure 6 : An example of screen viewing of real-time monitoring of drifters superimposed on a satellite chlorophyll image on board the Marion Dufresne II.

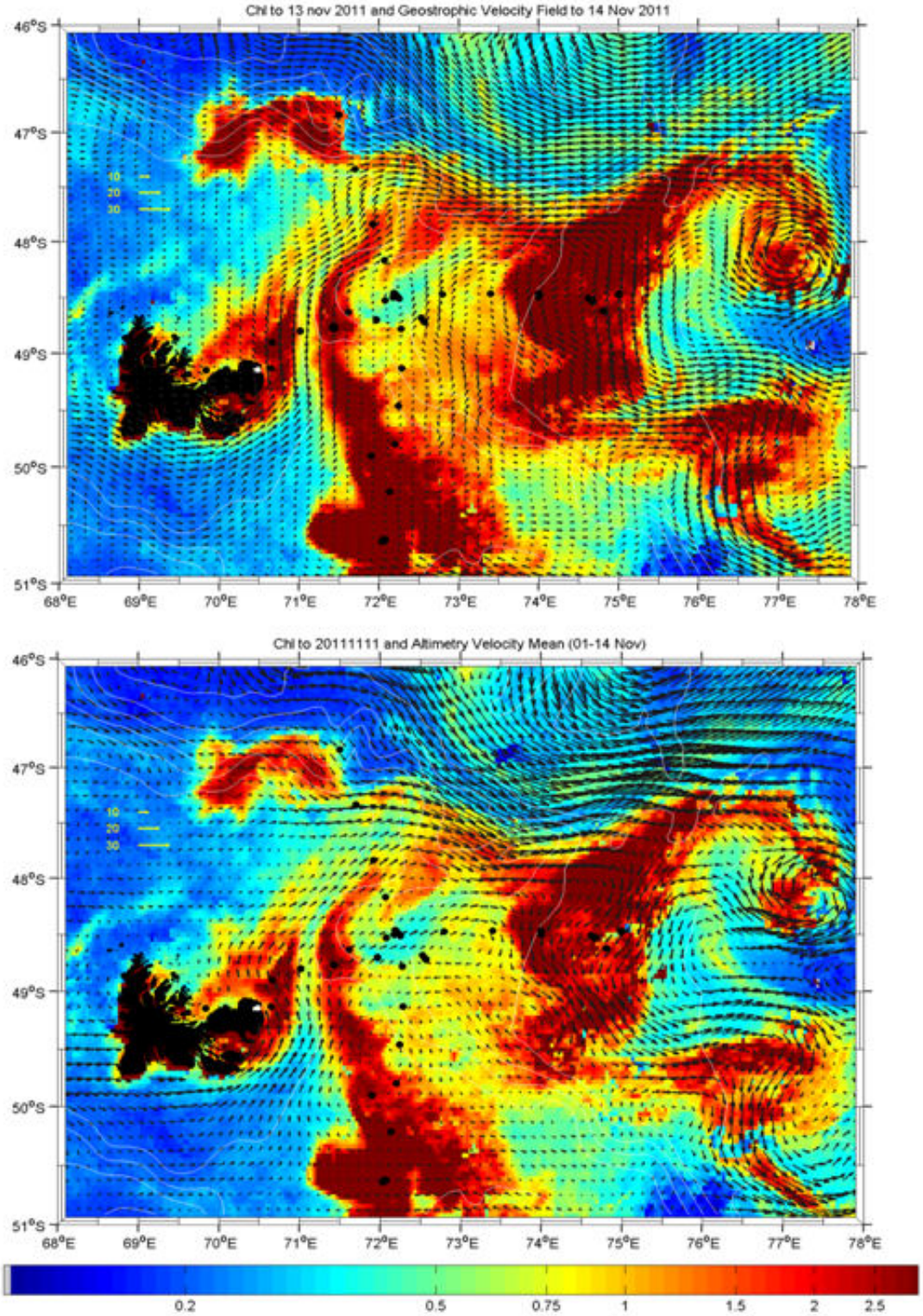

Figure 7 : Mean geostrophic velocity fields from (upper) combined (drifter+float+altimetry) velocity data and (lower) altimetry data only, superimposed on a composite satellite Chl image.

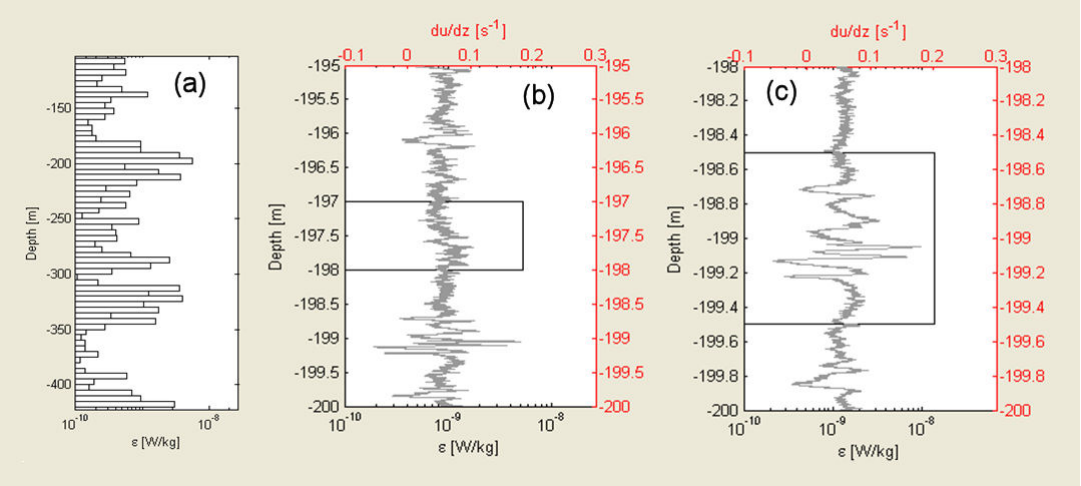

Figure 8 : (a) Turbulent energy dissipation rates (ε) computed at 5 m intervals at station TNS 2. (b) and (c) represent a zoom of velocity shears and corresponding ε in a depth range of 195-200 m and 198-200 m, respectively.

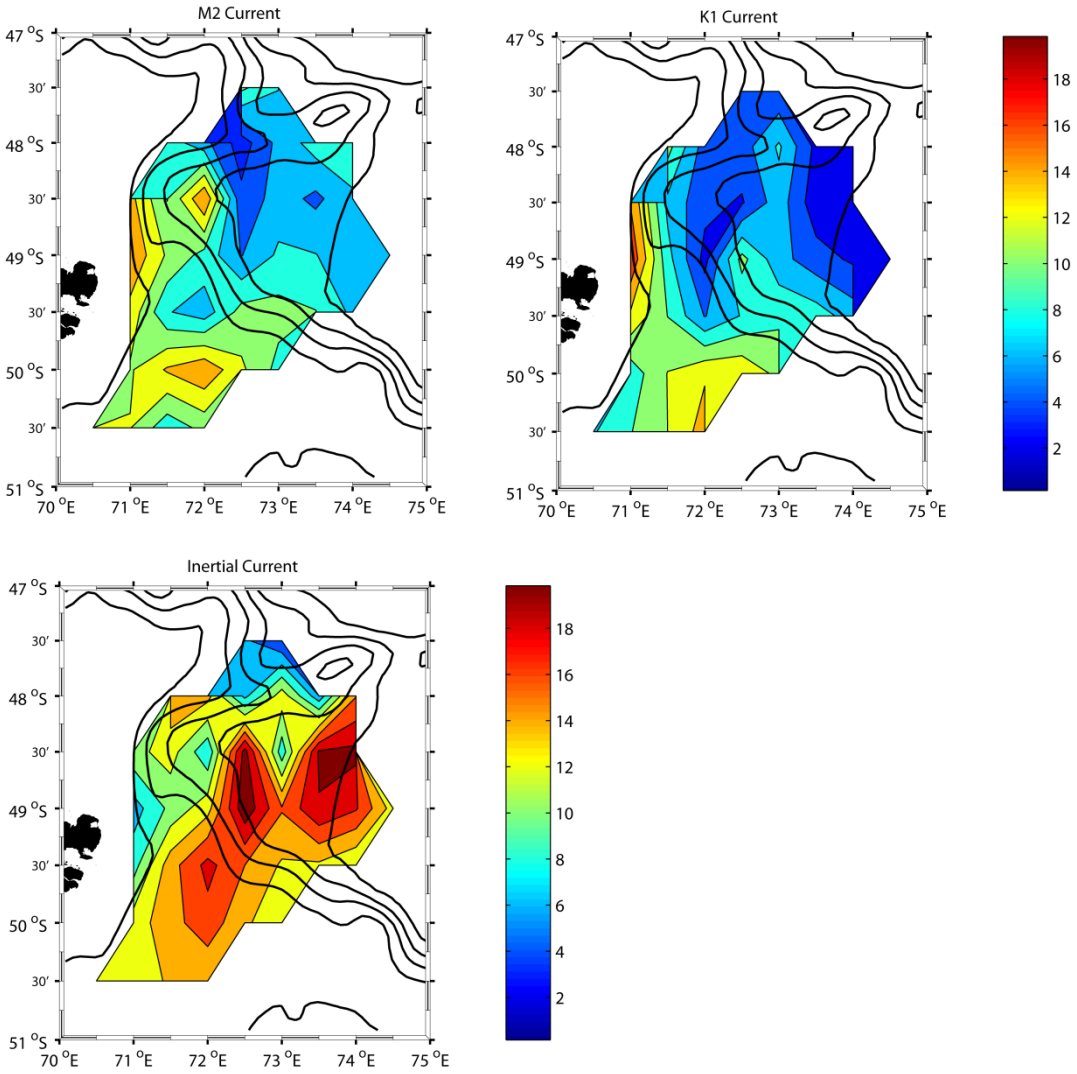

Figure 9 : Spatial distribution of the amplitude (in cm s-1) of M2 (12.4h) and K1 (24h) tidal currents, as compared to local inertial currents (Tf = 12h/sin□ ~15h at 49°S). These were obtained from a Fourier decomposition of high-frequency (<25 h) velocity fluctuations extracted from the trajectories of drifters and floats that have been deployed during the KEOPS 2 cruise.

References

Bahr, F., E. Firing and S. Jiang, 1989. Acoustic Doppler current profiling in the western Pacific during the US-PRC TOGA Cruises 5 and 6, JIMAR Contr. 90-0228, Univ. of Hawaii, 162 pp.

Bretherton, F., R. Davis and C. Fandry, 1976. A technique for objective analysis and design of oceanographic experiments applied to MODE-73. *Deep-Sea Res.*, 23, 559-582.

Fischer J. and M. Visbeck, 1993. Deep Velocity Profiling with self-contained ADCPs, *Journal of Atmospheric and Oceanic Technology,* 764-773.

Park, Y.-H. and F. Vivier, 2011. Circulation and hydrography over the Kerguelen Plateau, in *The Kerguelen Plateau: marine ecosystem and fisheries* (Eds. G. Duhamel *et al.*), 43-55.

Park Y.-H., N. Gasco and G. Duhamel, 2008a. Slope currents around the Kerguelen Islands from demersal longline fishing records. *Geophys. Res. Lett*., 35(9): L09604, doi:10.1029/2008GL033660.

Park Y.-H., J.L. Fuda, I. Durand and A.C. Naveira Garabato, 2008b. Internal tides and vertical mixing over the Kerguelen Plateau. *Deep-Sea Res. II*, 55, 582-593.

Park Y.-H., F. Roquet, I. Durand and J.L. Fuda, 2008c. Large-scale circulation over and around the Northern Kerguelen Plateau. *Deep-Sea Res. II*, 55: 566-581.

RD Instruments Acoustic Doppler Current Profilers Principles of Operation: A Practical Primer, 1989, RD Instruments, San Diego, CA 92131.

van Beek, P., M. Bourquin, J. L. Reyss, M. Souhaut, M. A. Charette, and C. Jeandel, 2008. Radium isotopes to investigate the water mass pathways on the Kerguelen Plateau (Southern Ocean), *Deep-Sea Res. II*, *55*, 622-637.

Visbeck M., 2002. Deep velocity profiling using Lowered Acoustic Doppler Current Profilers: bottom track and inverse solutions, *Journal of Atmospheric and Oceanic Technology*, 19(5), 794-807.

4 Surface circulation in the Kerguelen Plateau during the KEOPS2 study

Principal investigator

Meng Zhou
University of Massachusetts Boston/Universite de la Mediterranee
☎ 617-287-7419
🖷 617-287-7474
meng.zhou@umb.edu

Other participants

- Yiwu Zhu

University of Massachusetts Boston/Universite de la Mediterranee
☎ 617-287-7418
🖷 617-287-7474
yiwu.zhu@umb.edu

- Francesco d'Ovidio

LOCEAN - IPSL, Université Pierre et Marie Curie
☎ +33 1 44277076
francesco.dovidio@locean-ipsl.upmc.fr

Abstract

48 World Ocean Circulation Experiment (WOCE) Surface Velocity Program (SVP) drifters were released during the KEOPS-2 cruise supported by US National Ocean and Atmospheric Administration (NOAA), Global Drifter Program (GDP). The positions and times of deployments of these drifters were designed to map the Antarctic Circumpolar Current, circulation on the Kerguelen shelf, and interaction between them (Table 1). Two out of 48 drifters malfunctioned 1-2 days after their deployments. The remaining 46 drifters are currently working. Some of them have been advected out of our study area while most of them still remain in the study area. Each drifter received 30-40 positions per day. These positions were email to the RV Marion Dufresne 4 times a day during the study from NOAA GDP. The email of drifter positions was reduced to once per day till November 30, 2011, and then reduced to once per week till these drifters completely out of study area. In the original data processing, the time-irregular positions of a drifter is interpolated into a regular time step of 12 min, and then a low-pass filter of 48 hours applied to filter all tidal currents and inertial oscillations. The processed data have been provided to the group for scientific applications, and will be submitted to the KEOPS 2 data management.

4.1 Scientific context

Currents in the surface mixed layer play a critical role in transport of nutrients and biota. In the Kerguelen Plateau region, the current fields are primarily determined by Polar and shelf break fronts, tidal currents and wind-driven currents by strong cyclonic winds. A major feature is the existence of a strong jet as the shelf break current on the eastern shelf break flowing north- and north-easter-ward. The source and fate of waters in this jet are of interests in determining iron sources downstream. If the shelf break is a barrier for off-shelf transport of shelf waters, where and how shelf waters are transported off the shelf? The SVP drifters provide direct measurements of mean currents in the mixed layer, and dispersion of water masses due to small-mesoscale eddy activities

so that we can reveal these jets, eddies and offshelf transport and understand their roles in nature iron fertilization. These data can also be used to verify altimetry data in shelf regions and Lagrangian modeling results.

4.2 Overview of the project and objectives

48 WOCE SVP drifters were provided by US NOAA GDP. Their deployment positions were decided by the synthesis of satellite altimetry and chlorophyll data and Lagrangian modelling results from F. d'Ovidio (Figure 10). The primary objectives:

1) Large scale circulation patterns on the shelf and offshelf region of Kerguelen Island,
2) Mesoscale circulation patterns causing water mixing, convergence and cross-shelf break exchange,
3) Lagrangian coherent structure associated with mesoscale convergence and divergence patterns.

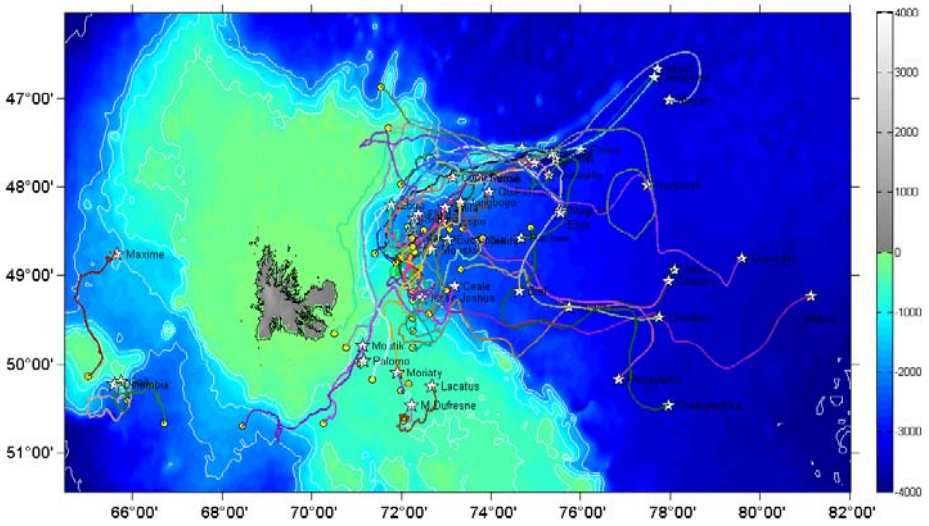

Figure 10 : Deployment positions (yellow dots), trajectories (color-coded solid lines) and their positions on Nov 23 2011. The background false color represents the bathymetry in meters.

4.3 Methodology and sampling strategy

All these SVP drifters have drogues centered at 30 m representing the mean currents in a mixed layer. Each drifter's position is sampled 30-40 times per day at irregular time intervals. The first data processing includes:

1) Interpolating original data into a regular time interval of 12 min using the "pchip" method which minimizes overshoots.
2) Applying a 48 hour low-pass filter to remove tidal and inertial oscillations.
3) Both original data and 48 hour filtered datasets will be provided to the community (Table VI).

Table VI : Exhaustive list of measured parameters

1. Date, time, latitude & longitude	Original SVP drifters	date, time, degree
2. Latitude, longitude, NE velocities	Processed drifter data	date, time, degree and cm/s

4.4 Preliminary results

Mean field: Drifter data can be binned into given latitude-longitude boxes for computing mean current fields (Figure 11). Though cares must be taken for deployment biases due to temporal and spatial variations of current fields and limited amount of drifters, drifters deployed on the shelf revealed a consistent flow pattern: 1) a jet starting from the offshelf region marked by drifter Moutik, intruding onto the shelf in the slope region, flowing along the shelfbreak forming a strong shelfbreak current of 30-40 cm/s, and exiting at the north-eastern corner of the shelfbreak, 2) weak current areas on and off the shelf such as Stations RK2 and A3. Drifters deployed at these 2 stations moved 60-90 km in 36 days equivalent to a mean current of 2-3 cm/s, 3) a strong horizontal mixing region mark by "M" in Fig. 2. Drifters in this area moved in cyclonic or anticyclonic patterns onto and off the shelf, and eventually exited either northeastern- or southeastern-ward, and 4) strong wind-dependent surface current in the deep bay marked by "E" in Fig. 2 where predominant westerly wind events produced a strong northeastward surface Ekman transport while a southwestward current occurred during weak wind periods.

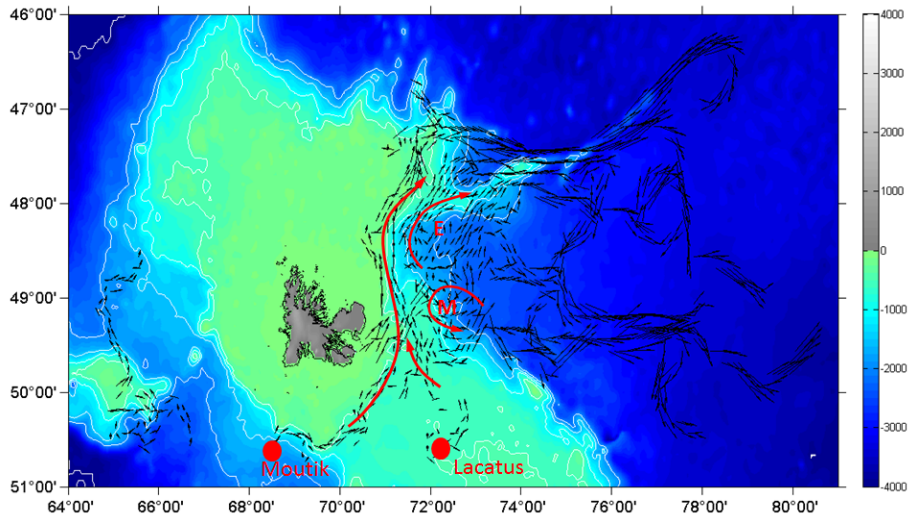

Figure 11 : Drifter velocities binned into 1/8x1/8 degree boxes. The red curved arrows on the shelf and shelfbreak represent the shelf break current and source waters. The offshelf red curved arrows represent areas of meso-large scale eddies. Note that these current fields have biased due to locations and times of drifter deployments.

Mesoscale activities: The mesoscale activities after removing the mean currents (Figure 11) contribute to horizontal dispersion of water masses. The mean autocorrelations of drifter velocities gives the decorrelation scale of motion approximately 3.5 days defined as the first zero crossing (Fig. 3). The time scale is consistent with the mesoscale features of a spatial scale at 20-40 km and a velocity of 20-30 cm/s. The horizontal mesoscale eddy diffusivity is proportional to

$$F_x \sim \left\{ K_{xx} \frac{\partial C}{\partial x}, K_{xy} \frac{\partial C}{\partial y} \right\} \qquad (1)$$

$$F_y \sim \left\{ K_{yx} \frac{\partial C}{\partial x}, K_{yy} \frac{\partial C}{\partial y} \right\} \qquad (2)$$

where F_x and F_y are the fluxes in the x and y directions, K_{xx}, K_{xy}, K_{yx} and K_{yy} are the horizontal eddy diffusivity coefficients, and c is the concentration of any scalar. We use the definition of eddy diffusivity defined (Davis, 1985; Zhou *et al.*, 2000), *i.e.* :

$$K_{ij}(x,\tau) = \langle u_i'(x|_t) d'(x|_{t+\tau}) \rangle \qquad (3)$$

where *i* and *j* represent indices of *x* and *y*, *u'* and *d'* represent the fluctuations of velocities and displacements of a Lagrangian drifter in a period of 2 times decorrelation time scale, and τ is the time lag. When τ reaches the decorrelation scale, the dispersion reaches the linear dispersion regime noted as K^{τ}_{xx}. The preliminary computations of these horizontal diffusivity coefficients are shown inFigure 13.

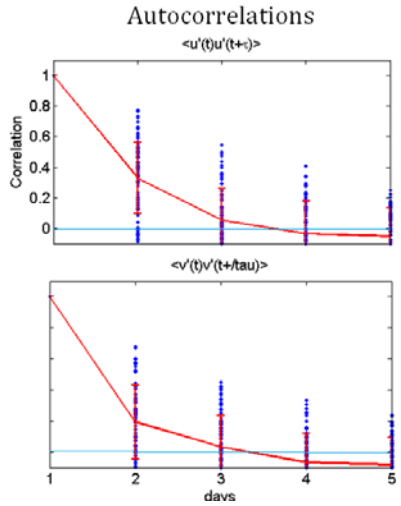

Figure 12 : Autocorrelations of drifter velocities in NS and EW directions. Blue dots are autocorrelations of individual 14 day-drifter time serious, red line is the mean and standard deviation.

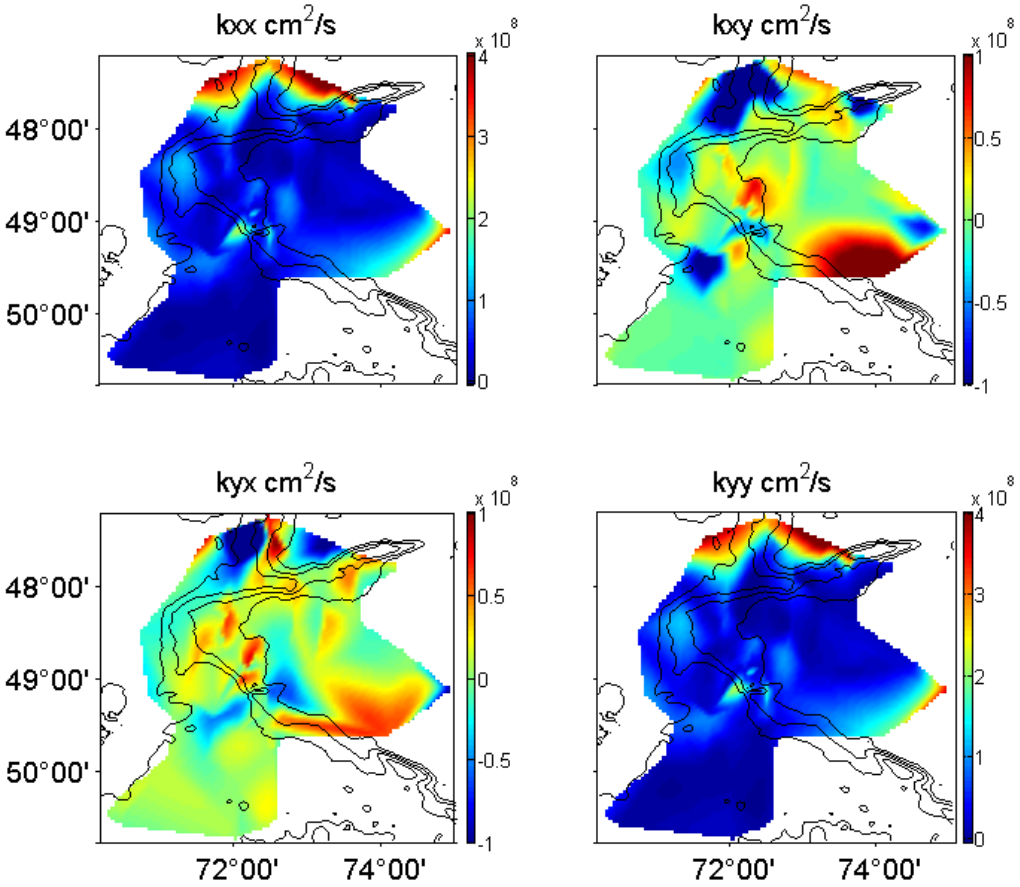

Figure 13 : Horizontal diffusivity coefficients based on Eq. 4 assuming a decorrelation scale of 3.5 days.

The magnitudes of estimated K_{xx}, K_{xy}, K_{yx} and K_{yy} are at the order of 1×10^8 cm^2/s similar to that of 6.3×10^8 cm^2/s in the southern Drake Passage (Dulaiova, *et al.* 2008).

4.5 Post-cruise sampling analyses and dead-lines

Table VII : Post-cruise analyses

Archiving and processing new drifter data including: a) Original drifter data in the study region b) 48 hour-filtered drifter data	Once every 1-2 weeks
Analyzing the mean current fields	Once every 1-2 weeks
Analyzing the mesoscale eddy fields as horizontal diffusivity coefficients	June 2012

4.6 Data base organization

Data will be submitted to the KEOPS database.

4.7 References of methods

Davis, R. (1985). Drifter observations of coastal surface currents during CODE: Statistical and dynamical views. Jour.nal of Geophysical Res, 90, 4756-4772.

Dulaiova, H., Henderson, P., Ardelan, M., & Charette, M. (2009). Shelf-derived iron inputs drive biological productivity in the Scotia Sea. Global Biogeochemical Cycles, 23, GB4014, doi:10.1029/2008GB003406.

Zhou, M., Paduan, J., & Niiler, P. P. (2000). The surface currents in the Canary Basin from drifter observations. Journal of Geophysical Research, 105, 893-21910.

5 Use of radium isotopes to investigate the age of the waters that have interacted with the shelf

Principal investigators

Pieter van Beek / Bruno Lansard
LEGOS, OMP, 14 av Edouard Belin 31400 Toulouse
☎ +33 1 561 333 051
🖷 +33 1 561 253 205
vanbeek@legos.obs-mip.fr / bruno.lansard@legos.obs-mip.fr

Other participants

- Marc Souhaut(LEGOS)
- Virginie Sanial (LEGOS)

Résumé :
Les isotopes du radium (^{223}Ra, ^{224}Ra, ^{226}Ra, ^{228}Ra) et l'actinium (^{227}Ac) sont apportés à l'océan principalement par diffusion depuis les sédiments des marges continentales et depuis les sédiments profonds. Les isotopes du radium permettent donc de tracer le contact d'une masse d'eau avec des sédiments marins et de caractériser un apport potentiel de fer d'origine sédimentaire. Les signatures ^{224}Ra/^{223}Ra et ^{223}Ra/^{228}Ra déterminées dans les eaux de surface et au niveau de quelques profils verticaux seront étudiées plus précisément pour estimer l'âge de ces eaux. Les âges déduits des isotopes du radium seront comparés aux âges obtenus d'après les cartes altimétriques (coll. F. d'Ovidio). Enfin, les isotopes du radium et l'^{227}Ac seront utilisés pour quantifier i) les coefficients de mélange horizontaux (K_h) au niveau de transects côte-large et ii) les coefficients de mélange verticaux (K_z) déduits des profils verticaux.

5.1 Scientific context

^{226}Ra ($T_{1/2}$ = 1602 yr) and ^{228}Ra ($T_{1/2}$ = 5.75 yr) have been widely used as tracers of water masses and to provide rates of mixing in the ocean. ^{228}Ra, ^{223}Ra and ^{224}Ra data are scarce in the Southern Ocean because the activities are close to detection limits in that region (several ag/kg). Ra isotopes have been recently used in the Southern Ocean as tracers of iron sources that fuel the phytoplankton blooms off Crozet Island (Charette *et al.*, 2007) and Kerguelen Island (van Beek *et al.*, 2008). These authors also report estimates of vertical eddy diffusivity (K_z) from the vertical profiles of ^{228}Ra that could be used to calculate vertical fluxes of Fe. With a shorter half life, ^{223}Ra ($T_{1/2}$ =11.4 d) and ^{224}Ra ($T_{1/2}$ = 3.7 d) are used for coastal studies. Moore (2000) thus proposed to use the ^{224}Ra/^{223}Ra and ^{223}Ra/^{228}Ra ratios to derive ages of continental shelf waters.

Overview of the project and objectives

One goal of the KEOPS 2 project is to understand the circulation and sources/ transport of chemical elements (including iron) that fertilize the waters off the Kerguelen Plateau. Because radium isotopes are delivered to the ocean by diffusion from the sediments, a water mass that interacts with the margins is thus enriched in radium. These Ra enrichments may then be transferred to offshore waters and would thus indicate that the water mass has interacted with the sediments (where it could also get enriched in Fe). The 4 radium isotopes that display various half-lives can also be used as chronometers to estimate the transit time of the waters since they detached from the margins. Ages may thus be determined for these waters. The age range covered by the method is sever-

al days to several years. Horizontal and vertical mixing will also be investigated using ^{228}Ra as well as ^{227}Ac, a radionuclide that is also rare in the ocean and that is, like Ra, delivered from bottom sediments.

5.2 Determination of the age of surface waters

Large volume underway samples (300-900 L) were collected in order to map the distribution of Ra isotopes in the surface waters of the investigated area. We will use the ^{224}Ra/^{223}Ra and ^{223}Ra/^{228}Ra ratios to discriminate the waters that interacted recently with the shelf ("young waters") from those that interacted some time ago ("old waters"). These ages will be compared to the ages derived from altimetric data and other physical observations, including drifters (F. d'Ovidio, Y-H. Park, M. Zhou).

5.3 Advection, Mixing

Vertical profiles of Ra isotopes will allow us to characterize advection - if any - of waters that have interacted with the shelf. In addition to Ra, waters advected from the shelf may transport Fe that could fertilize offshore waters. We will use the vertical profiles of Ra isotopes and ^{227}Ac to estimate vertical eddy diffusivity coefficients (K_z ; Charette *et al.*, 2007; van Beek *et al.*, 2008). 2 transects performed between Kerguelen Island and offshore waters will allow us to investigate horizontal mixing (K_h ; Moore, 2000b).

5.4 Methodology and sampling strategy

Large-volume samples were collected using either the ship seawater intake (surface samples) or Niskin bottles (vertical profiles). Up to 900 L could be collected for surface samples and circa 260 L (a full rosette for one single sample) were collected to build vertical profiles of Ra and ^{227}Ac. Seawater samples were then passed through acrylic fibers impregnated with MnO_2 (so-called, "Mn fibers") that retain Ra isotopes and Ac. Mn fibers were then analyzed on board using a Radium Delayed Coincidence Counter (RaDeCC; Moore and Arnold, 1996) to determine ^{223}Ra and ^{224}Ra activities. Mn fibers were analyzed again 3 weeks after sampling to determine the ^{224}Ra activities supported by ^{228}Th and 3 months after sampling to determine the ^{223}Ra activities supported by ^{227}Ac. Once back to the laboratory, Mn fibers will be analyzed using low background gamma spectrometers at the LAFARA underground laboratory located in the French Pyrénées (van Beek *et al.*, 2010). The latter analysis will give the ^{226}Ra and ^{228}Ra activities.

Table VIII : Exhaustiv list of measured parameters

1.^{223}Ra	CTD	dpm/ 100 kg
2.^{224}Ra	CTD	dpm/ 100 kg
3.^{226}Ra	CTD	dpm/ 100 kg
4.^{228}Ra	CTD	dpm/ 100 kg
5. ^{227}Ac	CTD	dpm/ m^{-3}

5.5 Preliminary results

The analysis of ^{223}Ra and ^{224}Ra activities was conducted on the ship using a RaDeCC. These activities still need to be corrected for the supported activities that will be determined from a second and third counting performed with the RaDeCC 3 weeks and 3 months after sampling. Then, the ^{226}Ra and ^{228}Ra activities will be determined using gamma spectrometry at the underground laboratory of Ferrières. Interpretation of the results will be possible once the entire dataset is available.

5.6 Post-cruise sampling analyses and dead-lines

Analyses conducted with the RaDeCC and with the low-background gamma spectrometers will be performed before beginning of September 2012 (target : post-cruise meeting in Banyuls)

5.7 Data base organization

No specific comment

5.8 References of methods

Charette, M.A., Gonneea., M.E., Morris, P., Statham, P., Fones, G., Planquette, H., Salter., I., Naveira Garabato, A., 2007. Radium isotopes as tracers of iron sources fueling a Southern Ocean phytoplankton bloom. Deep-Sea Res. II 54, 1989-1998.

Moore, W.S., Arnold, R., 1996. Measurement of ^{223}Ra and ^{224}Ra in coastal waters using a delayed coincidence counter, Journal Geophys. Res. 101, 1321-1329.

Moore, W., 2000a. Ages of continental shelf waters determined from ^{223}Ra and ^{224}Ra., Journal Geophys. Res. 105, 22117-22122.

Moore, W., 2000b. Determining coastal mixing rates using radium isotopes, cont. Shelf Res.

van Beek, P., Souhaut, M., Reyss J-L., 2010. Measuring the radium quartet (^{226}Ra, ^{228}Ra, ^{224}Ra, ^{223}Ra) in water samples using gamma spectrometry, Journal of Environmental Radioactivity, 101, 521–529.

van Beek, P., Bourquin, M., Reyss, J-L., Souhaut, M., Charrette, M., Jeandel, C., 2008. Radium isotopes to investigate the water mass pathways on the Kerguelen plateau, Southern Ocean, Deep-Sea Research Part II-Topical Studies in Oceanography, 55, 622-637.

6 Rare earth elements and Neodymium isotopes as tracers of sediment/water mass interactions over the Kerguelen Plateau (Southern Ocean)

Principal investigators

Ester Garcia Solsona / Catherine Jeandel
LEGOS, OMP, 14 av Edouard Belin 31400 Toulouse
☎ +33 1 561 332 847
🖷 +33 1 561 253 205
ester.garcia@legos.obs-mip.fr / catherine.jeandel@legos.obs-mip.fr

Abstract:
In order to better understand the sources and transport of geochemical tracers over the Kerguelen Plateau, what will help in the comprehension of iron fertilization mechanisms, Rare Earth Elements (REE) and Neodymium isotopes (Nd IC) will be measured from water (13 stations) and suspended particle (7 stations) samples collected during the Keops 2 cruise, including pre-bloom and bloom regions. Since dissolution of lithogenic material constitutes the main source for both dissolved Fe and REE/Nd in the ocean, this study proposes to use REE concentrations and the Nd IC to trace the origin and pathways of water masses as well as the exchanges between water masses and suspended lithogenic particles. The magnitude of the associated geochemical fluxes will be also estimated.

6.1 Scientific context

Rare Earth Elements (REEs: La, Ce, Pr, Nd, Sm, Eu, Gd, Tb, Dy, Ho, Er, Tm, Yb and Lu) present an extremely coherent chemical behaviour (Elderfield and Greaves, 1982) although several processes (e.g. scavenging) cause slight fractionations within them. In some cases, specific features of the lithogenic REE patterns allow tracing the lithogenic element origin in the ocean (Sholkovitz *et al.*, 1999). Thus, REE patterns in seawater are used to study the interactions between the lithogenic and sedimentary material and the water masses.

Given that the Nd IC distribution on the continents is heterogeneous, Nd ICs of marine lithogenic particles can be used to follow their pathways (Grousset *et al.*, 1988; Innocent *et al.* 1997). In the ocean, Nd is a (90-95% dissolved) trace element, with a heterogeneous isotopic distribution that, on first order, reflects the dominant imprint of the surrounding continent of each oceanic basin (Arsouze et al, 2008). In the absence of lithogenic input, Nd IC behaves conservatively in the ocean and it is used as a water mass tracer in order to reconstruct paleo or modern circulations (Piepgras and Jacobsen, 1988; Jeandel *et al.*, 1993, 1998). On the other hand, in the presence of lithogenic inputs (aeolian, riverine or derived from the sediments), this tracer is no more conservative. Several studies suggest that input from the margins resulting from sediment/water mass interactions (Tachikawa *et al.*, 2004; Lacan and Jeandel 2004) and remobilization of REE (including Nd) during early diagenesis (Sholkovitz *et al.*, 1992) may play a major role in determining water mass Nd signatures.

Therefore, the simultaneous measurement of REE concentrations and Nd IC will represent a valuable informant of external source terms to the ocean, of water mass pathways and a powerful tool for analyzing the dissolved/particulate exchanges in seawater (Tachikawa *et al.*, 1999).

6.2 Overview of the project and objectives (1/2 page max.)

The Southern Ocean is considered a key region in understanding the role of biogeochemical cycling on the global climate change (Marinov *et al.*, 2006). Even though this ocean is characterized by HNLC (high-nutrient low-chlorophyll) conditions, there exist regions of high biomass (De Baar *et al.*, 1995; Moore *et al.*, 2002) like the Kerguelen Plateau (Blain *et al.*, 2008). These bloom events are ascribed to natural fertilization due to iron inputs from the Kerguelen archipelago and Plateau (Blain *et al.*, 2001). In the context of progressing in the understanding of iron fertilization in the Kerguelen Plateau, one of the main objectives of Keops_2 cruise relies on the better comprehension of the circulation and the sources/transport of tracers in the studied area. With this in mind, and given that dissolution of lithogenic sediments deposited on continental shelves and slopes seems to constitute the main source for both dissolved iron (Johnson *et al.*, 1999; Elrod *et al.*, 2004) and REEs (Jeandel *et al.*, 1998b; Lacan and Jeandel, 2001, 2005; Arsouze *et al.*, 2007) in the ocean, this study proposes to use REE concentrations and the Nd IC in the Kerguelen Plateau waters to trace their origins and pathways, the particle/dissolved interactions in the water column, the magnitude of the associated geochemical fluxes and the potential implications for the iron sources.

6.3 Methodology and sampling strategy

Samples collected during the KEOPS_2 cruise for REE and Nd IC analysis were from (detailed list in the attached excel files):

- R2 station, regarded as an “open-ocean” reference (dissolved and particulated samples).
- A3 station, representative of water mass coming from the southern Kerguelen Plateau (dissolved and particulated samples), with a well developed bloom
- TNS4, to elucidate potential water mass influence coming from the north of the study area (only dissolved samples)
- E1, E3, E4_W and E5 stations (dissolved and particulate samples), to investigate the potential progression from non-bloom to bloom waters
- TEW1, TEW3, TEW7 and F_L (only dissolved samples, excepting F_L station), sampled to explore the potential plateau influence along an offshore transect from Kerguelen plateau (potential source, TEW1 and TEW3) eastwards and also the mixing of different water masses involved in the jet circulation.

Each station was sampled at several depths covering the whole water column (from 80 m to 2700 m), thus getting water from all the representative water masses. Water samples were collected using Niskin bottles mounted on a rosette frame with a CTD sensor. The samples were filtered on board through SARTOBRAN 150 0.45/0.2 μm pore size filters, cleaned up with 10L of Milli-Q water and preconditioned by 500 mL of the seawater sample. After filtering, an aliquot of 500 mL was collected for dissolved REE concentrations and the rest of the sample, about 10 L, was recovered in an acid-clean cubitainer for Nd IC analysis. All water samples were acidified to pH=2 with twice-distilled HCl and stored at room temperature. From the total 111 water samples, 97 Nd IC samples were also pre-concentrated on board. To do that, about 6 mL of suprapur ammoniac was added to each sample to obtain a pH of 3.8±0.2, necessary to quantitatively pre-concentrate all the REEs by slowly (max flow rate of 20 mL/min) passing the water sample through SEP-PAK C18 cartridges (2 per sample), previously impregnated (on board) with 300 mg de complexant HDEHP.H2.MEHP (Shabani *et al.*, 1992).

Concerning suspended particle samples (54 in total), large volumes (from 65 to 1200L) of seawater were pumped (Challenger and McLane InSitu Pumps) from different depths through SUPOR filters of 142 mm diameter and 0.8 μm pore size. After pumping, filters were dried in the clean lab with a vacuum pump. A ceramic blade was used to cut the filter in two portions, which will be devoted to 1) Nd isotopes, REE concentrations and Fe isotopes and 2) Si isotopes (D. Cardi-

nal team). Pictures from the filters were taken before and after cutting them to estimate the proportions of the sections by weigh. Each portion was kept in its corresponding, well labelled, recipient on the fridge until transportation to the lab.

Table IX : Exhaustiv list of measured parameters

1. La	CTD, ISP	pmol / kg
2. Ce	CTD, ISP	pmol / kg
3. Pr	CTD, ISP	pmol / kg
4. Nd	CTD, ISP	pmol / kg
5. Sm	CTD, ISP	pmol / kg
6. Eu	CTD, ISP	pmol / kg
7. Gd	CTD, ISP	pmol / kg
8. Tb	CTD, ISP	pmol / kg
9. Dy	CTD, ISP	pmol / kg
10. Ho	CTD, ISP	pmol / kg
11. Er	CTD, ISP	pmol / kg
12. Tm	CTD, ISP	pmol / kg
13. Yb	CTD, ISP	pmol / kg
14. Lu	CTD, ISP	pmol / kg
15. $^{143}Nd/^{144}Nd$	CTD, ISP	
16. Fe isotopes	CTD, ISP	

6.4 Preliminary results

No preliminary results are available. The collected samples need to be chemically treated and purified in the clean laboratory of Toulouse before analysis.

6.5 Post-cruise sampling analyses and dead-lines

Since all the samples need to be processed once in the clean laboratory of Toulouse, a minimum period of 9 months is estimated to carry out the required chemistry and analysis of 50% of the samples, while the other 50% will performed in 2013. The different steps will be:

Seawater

- REE samples (500 mL of seawater, filtered and acidified on board)

The purification and preconcentration of REEs will be performed following the method published by Tachikawa *et al.* (1999) and Lacan and Jeandel (2001). Briefly, the acidified seawater samples will be spiked with ^{150}Nd and ^{172}Yb. Then 2.5 mg Fe (dissolved $FeCl_3$) will be added. After isotopic equilibration for at least 24 h, the pH is increased to 7–8 by addition of NH_4OH, yielding REE–$Fe(OH)_3$ co-precipitation. The precipitate is then extracted by centrifugation and rinsed three times with deionized water. An anion exchange column (AG 1X8; 2 g) is used to purify the REE from the remaining matrix. REE concentrations will be then measured on a Inductively Coupled Plasma Mass Spectrometer (ICP-MS). All the REEs will be determined by the external standard

method, whereas Nd and Yb will be additionally determined by isotopic dilution. Comparison of these two methods allows us to determine the chemical procedure yields for Nd and Yb. A linear interpolation relative to mass is then used to estimate the yields for the other REE.

- Nd IC samples (~10L of seawater, only acidified)

The procedure of pre-concentration via C18 cartridges explained above will we performed in the clean laboratory before going on with the rest of the purification chemistry (described in next paragraph).

- Nd IC samples (~10L of seawater, pre-concentrated into C18 cartridges)

Nd isotopes will be determined using solid source thermo-ionization mass spectrometry (TIMS). The procedure that will be followed to analyze the Nd IC starts with the REEs elution from the C18 Cartridges. For that, we first pass 5 mL of HCl 0.01 M (20 mL/min) through the cartridge to eliminate the major fraction of barium. Then, 35 mL of HCl 6M (same flow rate) are required to elute the REE (and some remaining traces of other elements). The eluted sample is evaporated and 0.1 mL HNO_3 16 M is added to eliminate the organic matter by evaporation. Subsequently, the specific procedure to analyze the Nd IC has the following steps: i) chemical extraction using conventional anion-exchange resin (Dowex AG 1 X8; 4 mL) that allows separating the REE (including Nd) from Ra, Fe, Mn and Ba, ii) a second chromatographic extraction using cationic resin (Dowex AG 50WX8; 1 mL) to separates the REEs from the remaining ions (traces of Ca, Sr, Ba, Mg), and iii) a final purification extraction based on a reversed phase chromatography (anionic exchange with Ln resin; Jeandel, 1993).

Suspended particles

Filters containing the suspended particles will be digested in the laboratory. The particle leaching will be done using a mixture of HNO_3, HCl and HF. After digestion, a first aliquot will be taken to measure the REE concentrations, a second aliquot will be used to determine the Fe isotopic composition and the rest of the sample will be processed as described above to analyze the Nd IC.

6.6 Data base organization (general cruise base and/or specific data base(s))

The data will be posted in the national data base of Villefranche and in the International data base of the Geotraces Program (GEOTRACES International DATA Assembly CENTER at http://www.bodc.ac.uk/geotraces/

6.7 References of methods

Jeandel C. 1993. Concentration and isotopic composition of Nd in the South Atlantic Ocean. Earth and Planetary Science Letters 117: 581-591.

Lacan F., and Jeandel C. 2001. Tracing Papua New Guinea imprint on the central Equatorial Pacific Ocean using neodymium isotopic compositions and Rare Earth Element patterns. Earth and Planetary Science Letters 186: 497-512.

Shabani M.B., Akagi T., and Masuda A. 1992. Preconcentration of trace rare-earth elements in seawater by complexation with bis(2-ethylhexyl) hydrogen phosphate and 2-ethylhexyl dihydrogen phosphate adsorbed on a C18 cartridge and determination by inductively coupled plasma mass spectrometry. Analytical Chemistry 64 (7): 737–743.

Tachikawa K., Jeandel C., and Roy-Barman M. 1999. A new approach to the Nd residence time in the ocean: the role of atmospheric inputs. Earth and Planetary Science Letters 170: 433-446.

7 Size spectra of plankton during the KEOPS2 study

Principal investigators

Elodie Kestenare
LEGOS, OMP, 14 av Edouard Belin 31400 Toulouse
☎ +33 1 561 333 051
🖷 +33 1 561 253 205
vanbeek@legos.obs-mip.fr / bruno.lansard@legos.obs-mip.fr

Meng Zhou
University of Massachusetts Boston/Universite de la Mediterranee
☎ 617-287-7419/7418
🖷 617-287-7474
meng.zhou@umb.edu / yiwu.zhu@umb.edu

Names of other participants

Francois Carlotti (Université de la Mediterranée)

Abstract: Two acoustic Doppler current profilers were ship-mounted on the Marion Dufresne, a 153 kHz narrow band ADCP (153kHz ADCP) and a 75 kHz narrow band Ocean Survey ADCP (75kHz ADCP). 5-min ensembles of currents and volume backscattering (VBS) measurements from the 153kHz ADCP were recorded and single ping data and 5-min ensembles of current and VBS from the 75kHz ADCP were recorded for the entire KEOPS 2 cruise. The VBS data after corrections for range spreading and absorption can be used for studying mesozooplankton biomass distributions with the size and species information from net tow samples collected by a Bongo net during the cruise such as biomass distributions along the transects and time series stations, and diel vertical migration behavior of mesozooplankton and micronekton.

7.1 Scientific context

Mesozooplankton such as copepods and salps and micronekton such as krill are of major grazers on phytoplankton biomass which is an important pathway for primary production. Continuous measurements of VBS by 2 ship-mounted ADCPs provide measurements of mesozooplankton and micronekton at the high spatial and temporal resolutions which need for interpreting zooplankton distributions and migration behavior but cannot be provided by net tows. The size range measured by 75 and 153 kHz is above the sizes measured by the LISST and LOPC (Figure 14). The combination between the LISST (1-250 μm), LOPC (100μm – 35 mm), and ADCPs (10 mm -) provides a continuous size spectrum from primary producers to consumers.

7.2 Overview of the project and objectives

Volume acoustic backscattering become measureable integrating echos produced by all particles in a given water volume though a single zooplankter produces a very weak acoustic echo and sometimes immeasurable. The153 kHz ADCP was set at 8 m bins and 8 m pulse length with an effective measuring bin of 16 m, while the 75 kHz ADCP was set at 16 m bins and 16 m pulse length with an effective measuring bin of 32 m. The large measuring volumes of ADCPs provided strong echo returns.

The objectives of this acoustic study of mesozooplankton and micronekton are:

1) Spatial and temporal distributions of mesozooplankton and micronekton in the project,
2) Spatial and temporal distributions of specific size and species of them combining with analysis of net tow data,
3) Correlations of mesozooplankton and micronekton related to phytoplankton distributions and variations,
4) Feeding behavior and biomass demands of mesozooplankton and micronekton.

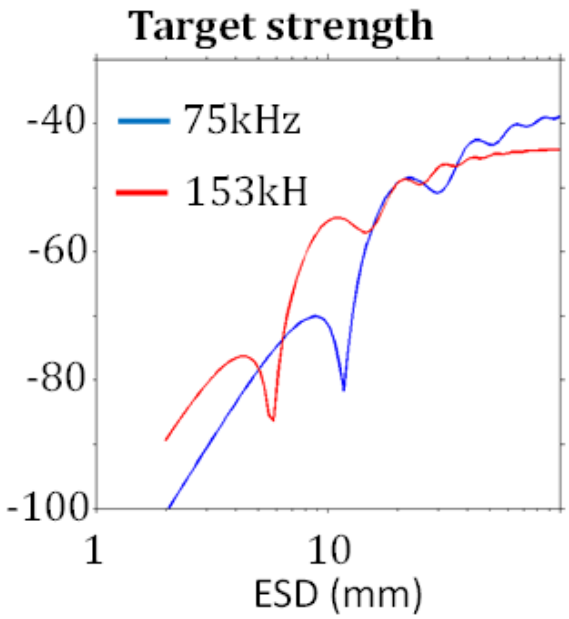

Figure 14 : Acoustic target strength of a marine organism as a function of size and acoustic frequencies (Foote & Stanton. 2000). The red line is the target strength (TS) of 153kHz as a function of equivalent spherical diameter, and the blue line is the TS for 75kHz. The TS of 75 kHz quickly decreases at the size of 10-20 mm in ESD and that of 153kHz decreases at the size of 4-10 mm to the noise level produced by electronics and a ship. Thus the 75 kHz system can provide measurements above 10 mm while the 153 system can provide measurements above 4-5 mm.

7.3 Overview of the project and objectives

Volume acoustic backscattering become measureable integrating echos produced by all particles in a given water volume though a single zooplankter produces a very weak acoustic echo and sometimes immeasurable. The153 kHz ADCP was set at 8 m bins and 8 m pulse length with an effective measuring bin of 16 m, while the 75 kHz ADCP was set at 16 m bins and 16 m pulse length with an effective measuring bin of 32 m. The large measuring volumes of ADCPs provided strong echo returns.

The objectives of this acoustic study of mesozooplankton and micronekton are:

5) Spatial and temporal distributions of mesozooplankton and micronekton in the project,
6) Spatial and temporal distributions of specific size and species of them combining with analysis of net tow data,
7) Correlations of mesozooplankton and micronekton related to phytoplankton distributions and variations,
8) Feeding behavior and biomass demands of mesozooplankton and micronekton.

7.4 Methodology and sampling strategy

Acoustic backscattering data were collected continuously during the entire cruise. The original data were quality-controlled by removing bad data based on a number of criteria such as noise levels, consistencies and spectrum width. These clean dataset are saved into matlab mat files as a standard ADCP data archive data format.

To obtain absolute VBS requires having exact information on power transmitted into water, transducer transmitting and receiving efficiencies, electronic noise and so on which we do not have due to the instrument design, and installations. An empirical method will be employed by sorting out size distributions of samples collected by the Bango net tows, and compute the mean target strength of a composed zooplankton assemblage. Using this empirical mean target strength to convert ADCP backscattering into biomass and match the estimate with the net tow biomass estimate by adjusting parameters for electronics in the sonar equation. After the instruments are empirically calibrated, ADCP VBS will be converted into biomass estimates.

Table X : Exhaustive list of measured parameters

5 min echo intensity measurements	153kHz ADCP	db
5 min echo intensity measuerments	75 kHz ADCP	db
Zooplankton size distributions	Bango	mm
Estimates of zooplankton biomass	ADCP	mm^3/m^3

7.5 Preliminary results

North-South transect: The transect revealed the layer structures of zooplankton. Relative large animals primarily measured by the 75 kHz ADCP show no significant difference between north and south stations. The high values in the offshelf regions were produced by zooplankton diel vertical migration. The relative small zooplankton measured by the 153 kHz ADCP show more zooplankton at the shelf stations in the south and offshelf stations, and less in the northern stations.

Time Series: The time series at Station E1-1 shows a clear diel vertical migration pattern. There were several zooplankton layers which might be formed by different species or sizes. Because the higher frequency acoustics measures smaller organisms, the difference in measurements of these two systems may provide the biomass estimate in the size range of 4 mm to 10 mm in ESD which is the size range of krill.

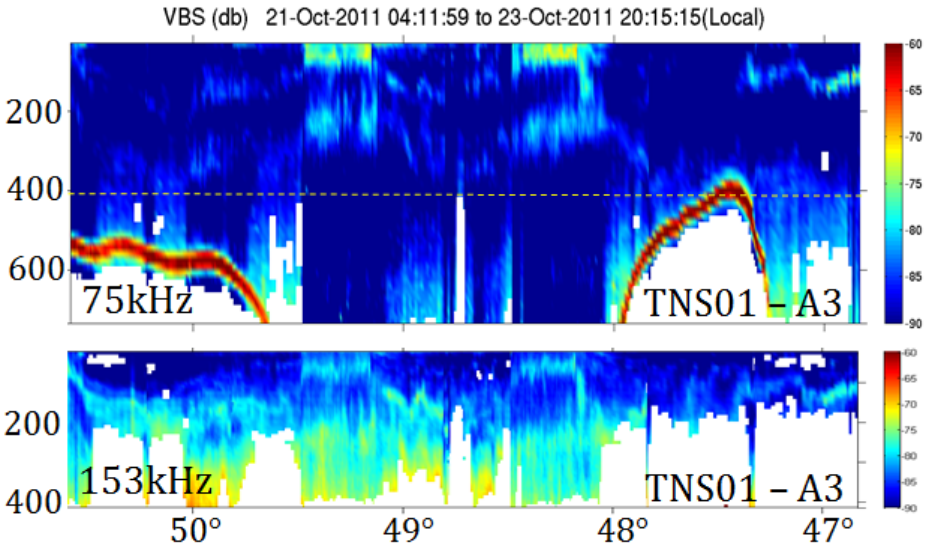

Figure 15 : Acoustic transects along the TNS01-A3 transect of both 75 and 153kHz ADCP. Note that the patchiness of zooplankton biomass in the upper layer along the TNS-A3 transect is primarily produced by zooplankton diel vertical migration, which is clearly elucidated in the time series measurement at E1-1 (Figure 16).

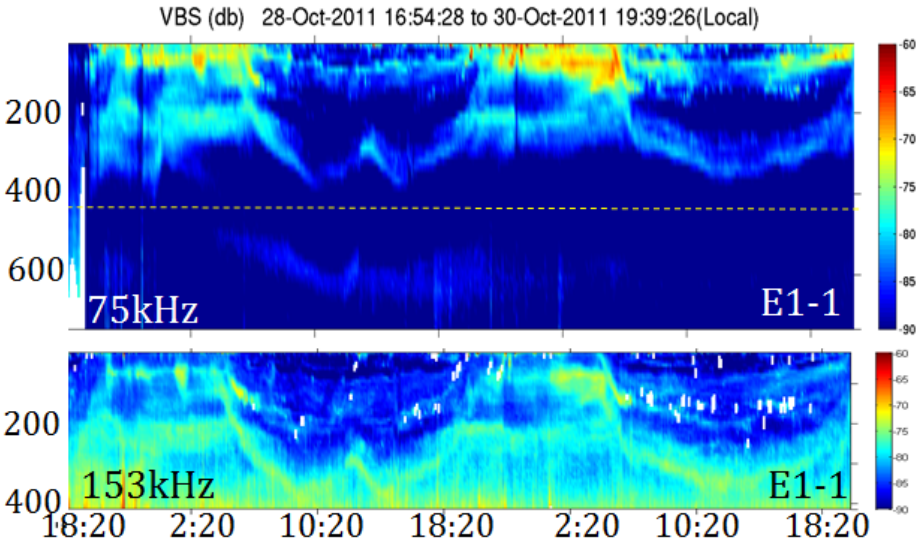

Figure 16 : Acoustic time series of 75 and 153kHz ADCP at Station E1-1. The diel vertical migration of zooplankton is clearly shown by the movement of acoustic backscattering layers between day and night. Notice the differences between these two ADCP system which is primarily produced by the frequency difference.

7.6 Post-cruise sampling analyses and dead-lines

Table XI : Post-cruise analyses

Analyzing zooplankton samples for sizes and species	June 2012
Analyzing ADCP VBS data for biomass estimate	June 2012

7.7 Data base organization (general cruise base and/or specific data base(s))

Data will be submitted to the KEOPS database.

7.8 References of methods

Foote, K., and T.K. Stanton. 2000. Acoustical methods, pp. 223-258. *In* R. Harris, P. H. Wiebe, J. Lenz, H.-R. Skjoldal and M. Huntley [eds.], ICES Zooplankton Methodology Manual. Academic Press, New York.

8 Temporal evolution of surface pCO_2 during the Kerguelen bloom as measured by CARIOCA buoys

Principal investigator

Jacqueline Boutin
LOCEAN-IPSL, 4, Place Jussieu, 75005, Paris
☎ +33 144277076
jacqueline.boutin@locean-ipsl.upmc.fr

Names of other participants

- L. Merlivat (LOCEAN)
- F. d'Ovidio (LOCEAN)
- L. Beaumont (LOCEAN)
- N. Martin (LOCEAN)
- S. Blain (LOMIC, Banyuls/mer)

Abstract:
CO_2 partial pressure (pCO_2) at the ocean surface is a key parameter for assessing air-sea CO_2 fluxes. In order to measure the temporal evolution of pCO_2 concentrations during the Kerguelen bloom two CARIOCA buoys have been released in the KEOPS2 study area (E1 station) and left drifting after the end of the cruise. The buoys are expected to remain in the Kerguelen region for several months, hence monitoring the evolution of pCO_2 along most of the bloom period and then integrating the global network of CARIOCA buoys. The buoys will also provide sea surface temperature and salinity, and will contribute to map the surface circulation.

8.1 Scientific context

The difference in CO_2 partial pressure (pCO_2) at the air-sea interface controls the CO_2 exchanges between the ocean and the atmosphere. Surface pCO_2 is therefore an important parameter for constraining the carbon cycle of the KEOPS2 region. As CO_2 is consumed by phytoplankton and produced by respiration, the evolution in time of pCO_2 is also an important indicator of the biological activity occuring in the mixed layer during the Kerguelen bloom.

8.2 Overview of the project and objectives

The main objective of this project is to monitor the temporal evolution of pCO_2 during the entire bloom period and contribute with this measurement to the quantification of the carbon cycle and biological activity in the KEOPS2 study region. The secondary objectives are (i) to provide other in situ physical parameters (sea surface temperature, salinity, dissolved oxygen) (ii) contribute to map the surface circulation around Kerguelen with the buoys' trajectories (iii) integrate the global network of drifting pCO_2 buoys in the relatively less sampled region of the Southern Ocean.

8.3 Methodology and sampling strategy

Two CARIOCA buoys, n. 26128 and 23217 have been released at the E1 station and left drifting after the end of the cruise. Buoy 23217 was recovered from a previous cruise. Both buoys

measure pCO_2, temperature and salinity at 2m depth, and wind at 2m above sea level. Buoy 26128 also measures dissolved oxygen. CO_2 partial pressure (pCO_2) and fugacity (fCO_2) is measured by colorimetry, dissolved oxygen by an optode. The buoys measure sea surface temperature, salinity, pH and pCO2 at 2m depth [Hood and Marlivat, 2001]. DIC concentrations can be retrieved fom these measurements by assuming a linear relation between salinity and alkalinity [Gonzales-Davila *et al.* 2005]. CARIOCA-derived pCO_2 and DIC can then be compared with shipboard measurements (OISO) as well as with the meso- and submeso-scale variability detected from multisatellite analysis [Resplandy *et al.* 2009]. The two CARIOCA buoys have been released at the same site (E1) on 29/10/2011 at short time interval (less than 1 hour) in order to allow intercalibration. Due to the presence of air bubbles in the colorimetry cell, the buoys started to record pCO_2 from 1/11/2011. Probably due to the presence of humidity, buoy 23217 recorded anomalous pCO_2 values from 3/11/2011. Positions of the buoys were received every four hours on the ship and integrated with the other Lagrangian drifters released, in order to follow in near real time stretching and advection associated to the surface waters of the sampling site.

Table XII : **Exhaustive** list of measured parameters

1. pCO_2 (2m)	N/A	
2. Temperature (2m)	N/A	
3. Salinity (2m)	N/A	
4. wind (2m above sea lev.)	N/A	
5. dissolved oxygen (26128 only)	N/A	

8.4 Preliminary results

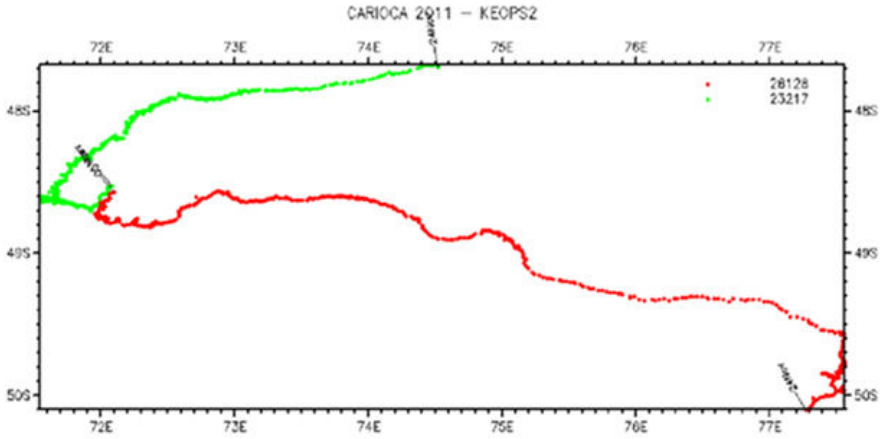

Figure 17 : Trajectories of the two drifters.

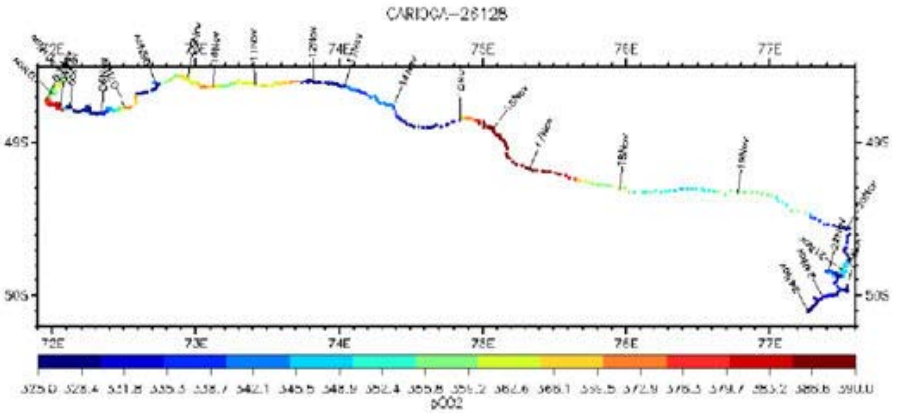

Figure 18 : Temperature of CO2 fugacity (fCO2) from buoy 26128.

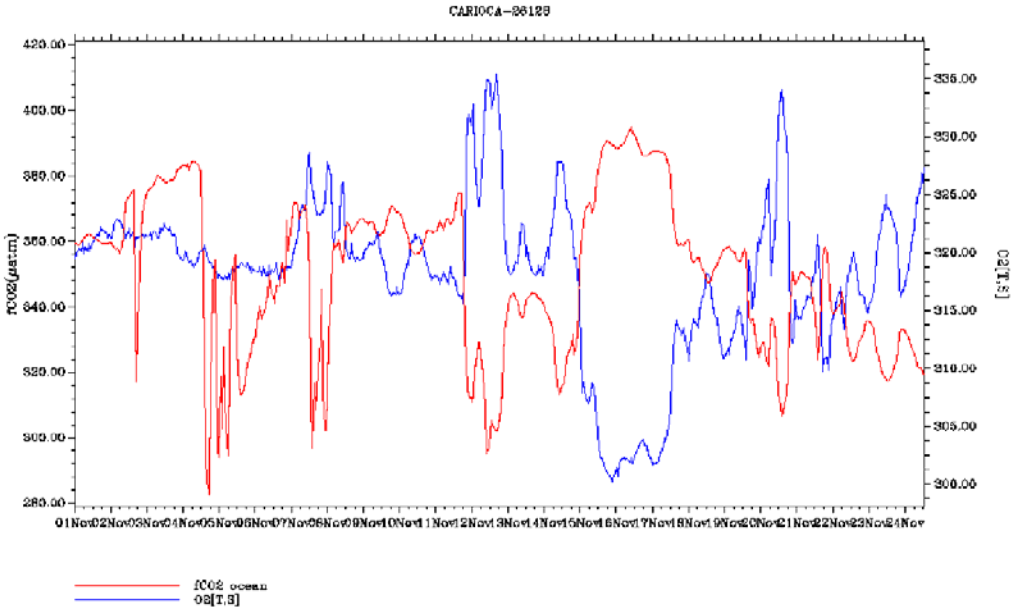

Figure 19 : CO_2 fugacity and dissolved oxygen.

8.5 References of methods

Hood, E., M. and Merlivat, L. (2001). Annual to interannual variations of fCO_2 in the northwestern Mediterranean Sea: Results from hourly measurements made by CARIOCA buoys, 1995-1997. J. Mar. Res., 59(1):113–131.

Gonzales-Davila, M., Santana-Casiano, J., M., Merlivat, L., Barbero-Munoz, L., and Dafner, V. (2005). Fluxes of CO_2 between the atmosphere and the ocean during the POMME project in the northeast Atlantic Ocean during 2001. J. Geophys. Res. , 110.

Resplendy L., Lévy M., d'Ovidio F., Merlivat L., "Evidence for intense submesoscale variability of pCO_2 in the northeast Atlantic Ocean", Global biogeochem. Cycles, 23, GB1017 (2009).

9 Net Community production – Biological CO_2 Fluxes

Principal investigator

Dominique Lefèvre
MIO, UMR Aix–Marseille Université CNRS 7294/UR IRD 235,
Campus de Luminy Case 901 F-13288 Marseille cedex 9
☎ + 33 (0)4 91 82 90 49
🖷 + 33 (0)4 91 82 90 51
dominique.lefevre@univ-amu.fr

Names of other participants

- Laure Chirurgien (MIO)

Résumé :

Le bilan de l'activité biologique des micro-organismes marins et représentatif de l'intensité de fonctionnement de la pompe biologique est appréhendé par les mesures de production communautaire nette (PCN). Les flux de PCN représente la balance entre les processus de photosynthèse et de respiration de la communauté microbienne et par conséquent permet de quantifier et de qualifier (autotrophie versus hétérotrophie) le rôle de la pompe biologique. La méthode d'étude est basée sur la mesure des variations de teneur en oxygène dissous ou de carbone inorganique dissous, dans des échantillons incubés pendant 24h à la lumière et à l'obscurité et lors de déploiement de systèmes IODA sur des mouillages dérivants. Les flux journaliers minimums détectés par ces approches sont de l'ordre de 0,2 µmol O_2 dm^{-3} (Williams & Jenkinson, 1982) ou de 1 µmol CO_2 dm^{-3} (Johnson *et al.*, 1985, Johnson, 1993 et Goyet & Hacker, 1992), Robert *et al.* Submitted.

Cette étude a été menée lors de la campagne océanographique « KErguelen :compared study of the Ocean and the Plateau in Surface water » (KEOPS) sur le plateau de Kerguelen, dans la région entre 49-54°S de latitude et 68-80°E de longitude : Rôle du plateau de Kerguelen dans la fertilisation naturelle en fer dans une région HLNC sur la pompe biologique de CO_2.

Abstract:

The assessment of the activity biological of the marine microorganisms and representative of the intensity of operation of the biological pump is apprehended by measurements of clear Community production (PCN). Fluxes of PCN represent the balance between the processes of photosynthesis and of respiration of the microbial community and consequently allow to quantify and qualify the role of the biological pump (autotrophy versus heterotrophy). The method of study is based on the measure of the variations of dissolved oxygen content or dissolved inorganic carbon content, in samples incubated during 24h in the light and in the dark and during the deployment of IODA systems on drifting mooring line. Minimum daily fluxes detected by this approach are about 0.2 µmol O_2 dm^{-3} (Williams & Jenkinson, 1982) or of 1 µmol CO_2 dm^{-3} (Johnson and Al, 1985, Johnson, 1993 and Goyet & Hacker, 1992), Robert *et al.* Submitted. This study has been carried out during the oceanographic cruise « KErguelen :compared study of the Ocean and the Plateau in Surface water » (KEOPS), on the Kerguelen plateau, located between the latitude 49-54°S and the longitude 68-80°E. The role of the Kerguelen plateau was investigated in term of natural iron fertilisation in an HNLC area on the CO_2 biological pump.

9.1 Scientific context, overview of the project and objectives

Cette étude a été menée lors de la campagne océanographique « KErguelen :compared study of the Ocean and the Plateau in Surface water » (KEOPS II) sur le plateau de Kerguelen, dans la région entre 49-54°S de latitude et 68-80°E de longitude : Rôle du plateau de Kerguelen dans la fertilisation naturelle en fer dans une région HLNC sur la pompe biologique de CO_2

Net community production is representative of the net storage of energy in the surface ecosystem (mixed or euphotic layer upon the ecosystem investigated). As such it is a proxy for determining the potential for export production to the ocean depth. In order to assess constrain NCP and export production it is necessary to investigate the ecosystem with a relevant spatio-temporal scale. The spatial scale could be investigated in relation to the mesoscale feature and knowledge of the "local" circulation dynamics. The temporal scale is dependant of the investigated processes, in our case photosynthesis and respiration, which are varying according to light, temperature, organic matter supply, nutritive resources, and trophic dynamics…For these reasons we have developed an in situ auto-sampler system for measuring at high frequency (3min) the dissolved oxygen in and out of an incubating chamber (IODA). This is providing us with day/light oxygen variation for determining GCP, NCP and DCR fluxes as well as the oxygen field variation integrating the physical processes as well as the biological ones. These approaches are complementary of other proxy for phytoplanktonic production based on carbon, nitrogen, silicon and oxygen units derived from deck or in situ incubation…

Mesopelagic remineralisation, proxy for the export production, including autochtonous and allochtonous inputs, is a key parameter for understanding the fate of organic carbon in pelagic ecosystem. This parameter could be assessed using the oxygen field dynamics in relation to water mass changes, or measuring short time scale processes through incubation or enzymatic activities. These approaches are not addressing the same scales, but provide complementary information of the ecosystem functioning. Even more relevant if complementary studies are carried out to determine particles export fluxes, particles remineralisation rates such as using sediment traps, geochemical approaches, and oxygen dynamics in sediment traps...

9.2 Methodology and sampling strategy

Oxygène dissous :

Détermination de la concentration en oxygène dissous par la méthode de Winkler et avec une détection photométrique du point final. Williams & Jenkinson (1982).

Carbone Total (CT) :

Détermination de la concentration en TCO_2 par la méthode coulométrique. Johnson *et al.* 1985, 1987, Goyet & Hackers (1992).

Activité ETS :

Détermination des flux de reminéralisation sur la colonne d'eau 0-900 m ont été effectués à partir des mesures d'activité enzymatiques ETS (Electron transport System). Packard 1971, Packard Williams 1981

IODA (In situ Oxygen Dynamic Auto-sampler)

Le $IODA_{6000}$ est un incubateur *in situ* qui permet de mesurer la dynamique de la concentration d'oxygène (Figure 20). La concentration d'oxygène est mesurée par une optode (principe de mesure optique de l'O_2, capable de mesurer de faibles variations de concentration).

Il se compose d'une cuve cylindrique d'incubation en verre borosilicaté et aux bords rodés dont l'étanchéité est faite par 2 plaques de verre borosilicaté. Deux optodes oxygène permettent de mesurer la concentration d'O_2 *in situ*, et la concentration d'O_2 à l'intérieur de la chambre d'incubation. Les mesures sont effectuées à une fréquence de 3minutes.

L'ensemble de l'appareil est entièrement automatisé ce qui le rend autonome et permet de modifier les paramètres d'incubation (temps d'incubation, fréquence de mesure d'oxygène et temps d'ouverture pour renouveler l'eau) en fonction de la profondeur d'immersion. Cet instrument peut être immergé jusqu'à 6000m de profondeur. Généralement, le temps d'incubation en surface (entre 0 et 200m) est de 24h. Cette durée de cycle suffit à mettre en évidence la dynamique de la concentration d'oxygène (production et consommation), tandis qu'au-delà de 200m, plusieurs jours peuvent être nécessaires (jusqu'à 5 jours à 2000m de profondeur).

Les systèmes IODA étant munis d'un capteur PAR, cela nous permet de discriminer entre les phases lumineuses et obscures. Ainsi comme pour les incubations décrites ci-dessus, les taux de GCP, NCP et DCR sont déduits pour chacun des cycles d'incubation lors des déploiements.

Flux biologique de CO_2.

Le dosage des concentrations en O_2 dissous et en TCO_2 réalisé permet de calculer les flux de production ou de consommation d'O_2 dissous et de TCO_2 intervenant dans le système : production communautaire brute, respiration communautaire à l'obscurité et production communautaire nette.

Les termes [zéro], [dark] et [light] représentent respectivement la moyenne des concentrations d'O_2 dissous ou de T_{CO2} des réplicats pour les séries "zéro", "dark" et "light". La production communautaire brute (GCP) correspond à une production d'O_2 dissous (flux positif), ou à une consommation de TCO_2 (flux négatif).

GCP= [light] – [dark]

La respiration communautaire à l'obscurité (RCO) correspond à une consommation d'O_2

dissous (flux négatif) ou à une production de TCO_2 (flux positif) :

DCR = [dark] – [zéro]

La production communautaire nette (NCP) représente la balance entre la production communautaire brute et la respiration à l'obscurité : NCP = GCP + DCR. Elle peut être

positive ou négative, aussi bien en terme d'O_2 dissous qu'en terme de TCO_2, suivant le

processus dominant :

NCP = [light] – [zéro]

L'ordre de grandeur du flux journalier d'oxygène est < 0,2 O_2 mmol m-3 et de 1 µmol TCO_2 $dm^{-3}d^{-1}$.

9.3 Stratégie d'échantillonnage

- Au total 96 analyses CT, et 2200 analyses d'oxygène dissous, calibrages inclus, ont été effectuées. Soit 48 heures d'analyse CT et 110 heures d'analyse O_2.
- Profils verticaux de Production en terme d'O_2, 7 profondeurs correspondant à 75%, 45%, 25%, 8%, 4% et 1% et 0.01% du PAR de surface à 8 stations (RK2, E1 1, E1 3, NPF L, E1 4 W, E1 4 E, A3 2, E1 5).
- Profils verticaux de Production en terme de CT, 2 profondeurs correspondant à 75% et 45% (E1 4 W, E1 4 E, A3 2, E1 5).
- Profils verticaux de distribution de l'oxygène dissous sur 26 CTD cast afin de d'étalonner le capteur SBE 43.
- Profils verticaux de respiration bactérienne (O_2) à 3 profondeurs dans la couche euphotique à 8 stations (RK2, E1 1, E1 3, NPF L, E1 4 W, E1 4 E, A3 2, E1 5). Eau de mer filtrée à 0.8µm par filtration inverse (Coll. Ingrid Obenosterer)

- Respiration de mesozoplancton (delta CT). 86 expériences menées sur un à plusieurs individus à plusieurs conditions de nutrition à plusieurs stations (Coll. François Carlotti, cf. Rapport F. Carlotti).
- Déploiement des systèmes IODA.

4 lignes de mouillages dérivantes ont été déployées à l'aide des collègues de la DT INSU (cf. Rapport de la DT INSU).

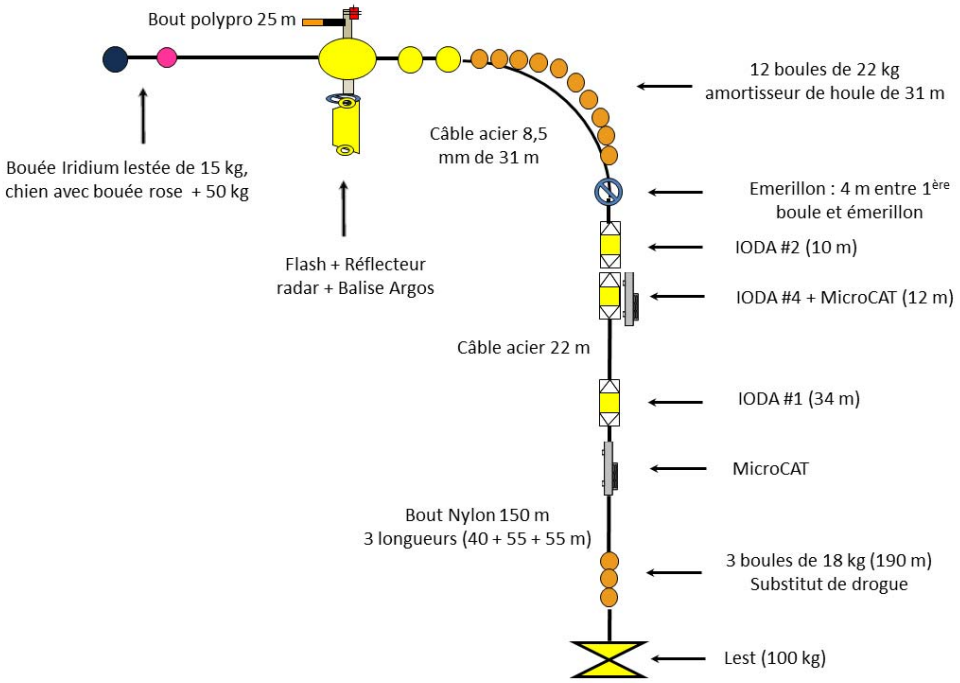

Figure 20 : schéma du mouillage "IODA"

Dépouillement des données brutes effectuées à bord, 6 mois pour le traitement primitif des données, étalonnage post cruise des capteurs ….

- Profils verticaux de reminéralisation : Activité ETS

Des volumes de 5 à 30 dm3 ont été filtré, selon la profondeur, afin de recueillir le matériel organique vivant.Les filtres sont fixés dans l'azote liquide et conservés à -80°C. Cet échantillonnage a été réalisé sur 8 sites (RK2, E1 1, E1 3, NPF L, E1 4 W, E1 4 E, A3 2, E1 5) et 13 profondeurs (Surface-900m). Les mesures d'activité ETS seront mesurées ultérieurement au laboratoire.

- Estimations des erreurs, précision, sensibilité des données.

Précision sur la détermination des concentrations en O_2 dissous sur les profils verticaux : 0.05 µmol dm^{-3}

Précision sur les flux biologiques d'O_2 dissous : 0.2 µmol O_2 dm^{-3} d^{-1}

Précision sur les flux biologiques de CT : 1 µmol O_2 dm^{-3} d^{-1}

Précision sur les flux biologiques d'O_2 à partir du IODA : 0.1 µmol O_2 dm^{-3} d^{-1}

Table XIII : Exhaustive list of measured parameters

Cf Excel file : Lefevre_Sampling_KeopsII

1. O_2 profiles	CTD	µmol dm^{-3}
2. ETS	CTD	µmol O_2 dm^{-3} d^{-1}
3. NCP	CTD	µmol O_2 dm^{-3} d^{-1}
4. IODA	drifting buoy	µmol O_2 dm^{-3}

9.4 Preliminary results (2 pages max.)

- Profiles oxygène dissous, étalonnage de la CTD SBE43

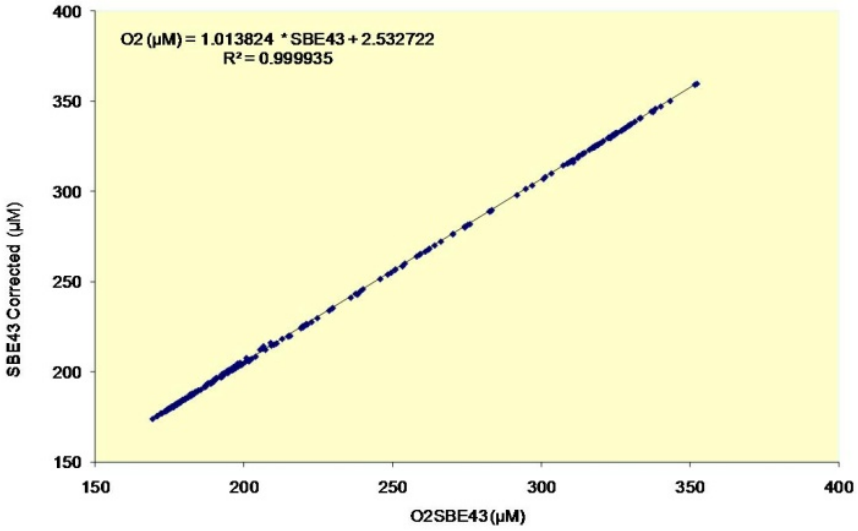

SOC_MD188	0.48807211
Offset_MD188	-0.494908785
E_MD188	3.69E-02

Figure 21 : Courbe de correction du capteur SBE43 après étalonnage avec les données discrètes « Winkler », nouveau jeu de coefficients pour rejouer les données en tenant compte de ce nouvel étalonnage. Données non validées post campagne !

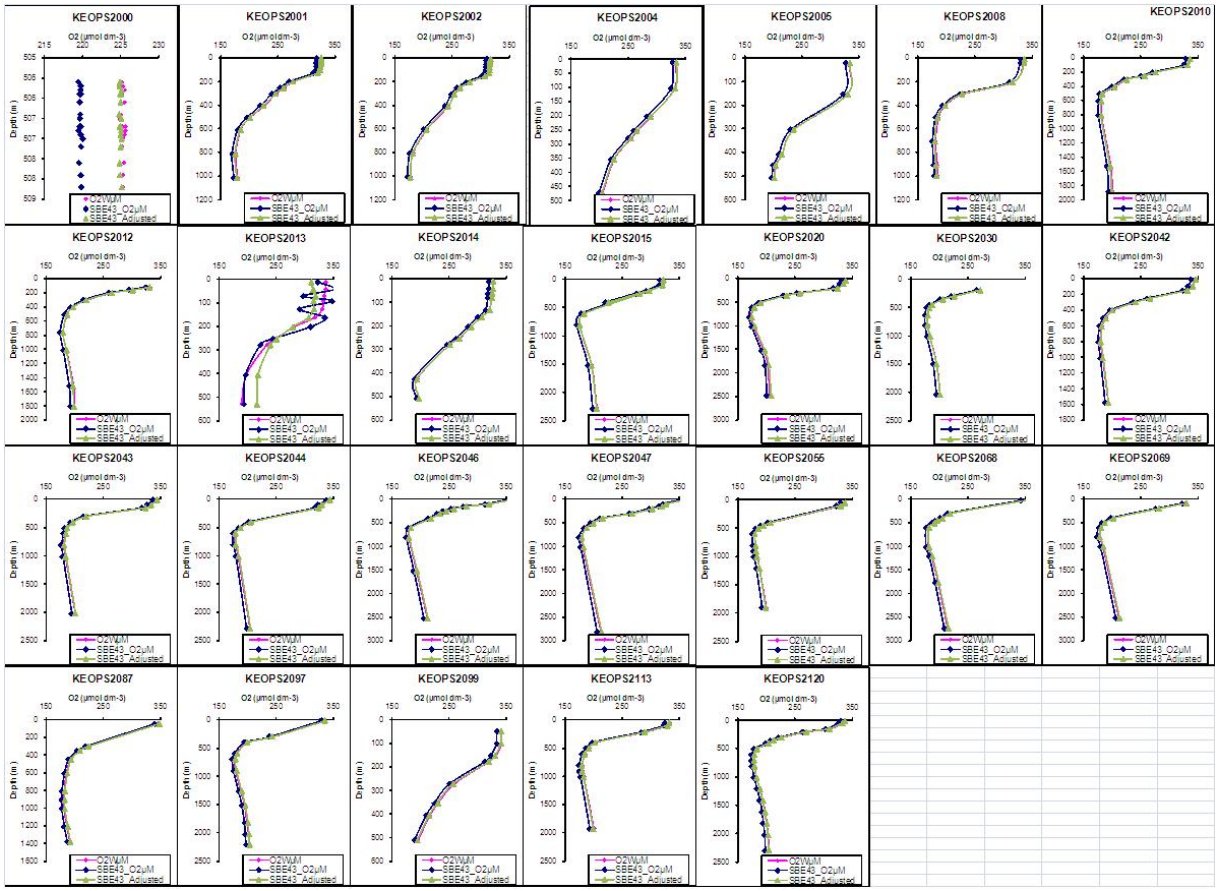

Figure 22 : 26 profils verticaux illustrant les données obtenues à partir du capteur SBE 43 avant et après correction et des profils obtenus à partir des analyses chimiques Winkler.

- NCP Bottle incubation: **Raw data !!!**

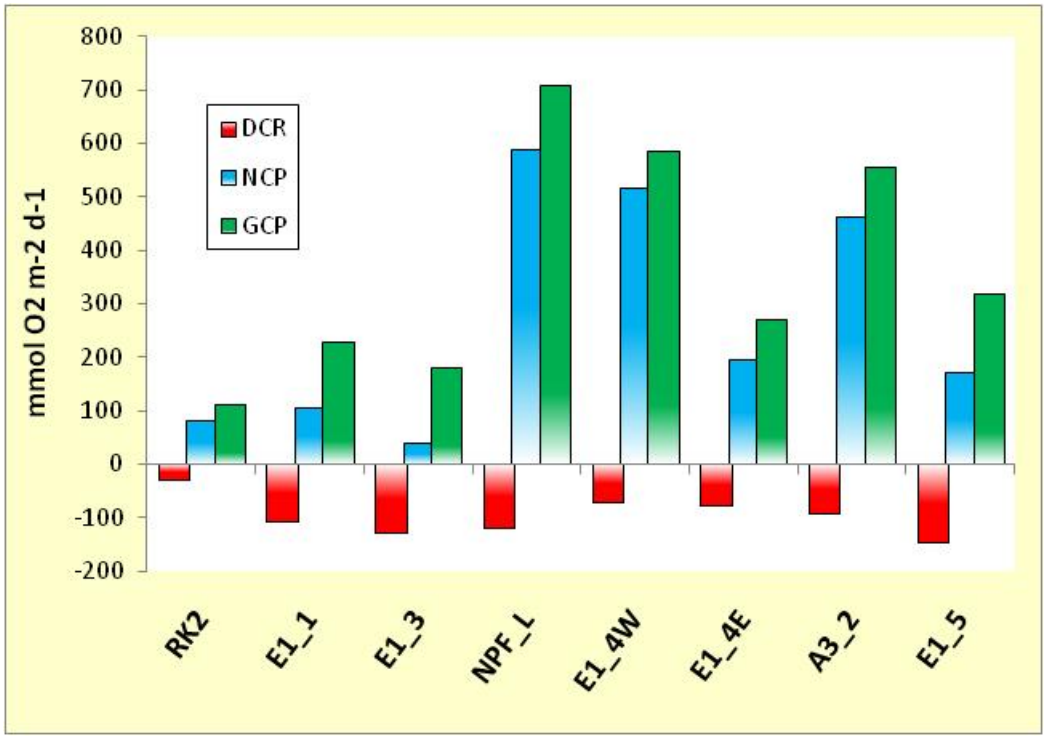

Figure 23 : Valeurs intégrées des DCR, GCP et NCP sur la couche euphotique aux différentes stations KEOPS II. Ces valeurs ne sont pas validées.

- IODA « mooring deployment » :

Figure 24 : IODA #1 / @DeepIodaV4 MSP version PP_2010_3_16 corr for 4330/ Optode Int 4330 373 / Optode ext 4330 120 / PAR # QSP 2200 – 50113 / QSL, SN:10434, microEinsteins/m2/s, dry calibration.

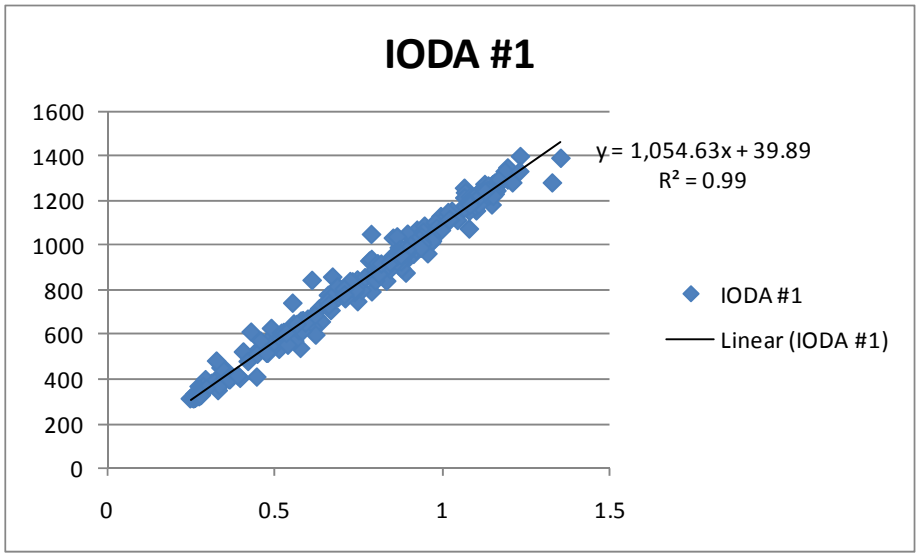

Figure 25 : IODA PAR # QSP 2200 – 50113 vs QSL, SN:10434, microEinsteins/m2/s, dry calibration / IODA #2 / DeepIodaV4 MSP version PP_2010_5_23 for 4330 / Optode Int 4330 121 / Optode ext 4330 273 / PAR # QSP 2100 50114.

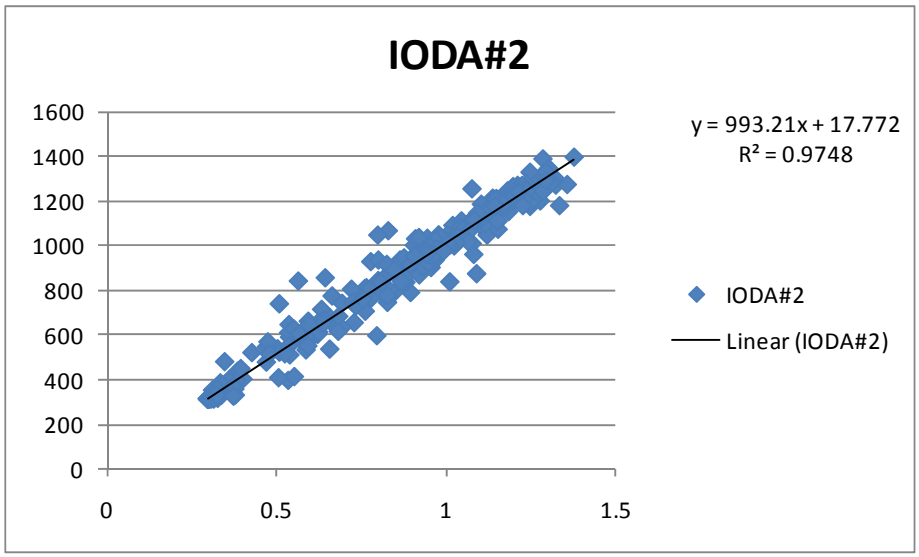

Figure 26 : IODA PAR # QSP 2100 50114. vs QSL, SN:10434, microEinsteins/m2/s, dry calibration / IODA #4 / Optode Int 4330 562 / Optode ext 3830 972 / No PAR.

Table XIV : Tableau des déploiements

Déploiement	Station	Depth 1	Depth 2	IODA ON TU +5	Mooring at Sea TU +5	Mooring Back TU +5	Comments
#1	RK2	IODA 1 25 m	IODA 2 235 m	17/10/2011 04:00 (#1) 04:05 (#2)	17/10/2011 22h00 à 23h2750°42,4528' S – 066°41,6945' E	25/10/2011 13h45 50°17,6586' S – 066°51,1489'	Cuves ouvertes sur IODA 1 & 2
#2	E1_1	IODA 1 25 m	IODA 2 75 m	29/10/2011 03:34 (#1) 03:38 (#2)	29/10/2011 10h35 à 11h33 48°30,0780' S – 072°14,6690' E	03/11/2011 18h14 à 19h10 48°38,4387'S – 071°48,9911' E	Cuve ouverte sur IODA 1
#3	E1_3	IODA 1&4 59 m	IODA 2 115 m	05/11/2011 03:30 (#1, #2 & #4)	05/11/2011 07h52 à 08h53 48°41,8005'S– 071°56,9667' E	10/11/2011 10h37 à 10h57 48°40,7730' S – 072°32,0791' E	OK…
#4	E1-3 bis	IODA 2&4 13 m	IODA 1 40 m	12/11/2011 03:30 (#1, #2 & #4)	12/11/2011 17h19 à 18h04 48°41,6983' S – 071°57,0920' E	20/11/2011 08h16 à 09h00 48°21,8300' S – 072°53,1860'	OK…

						E	

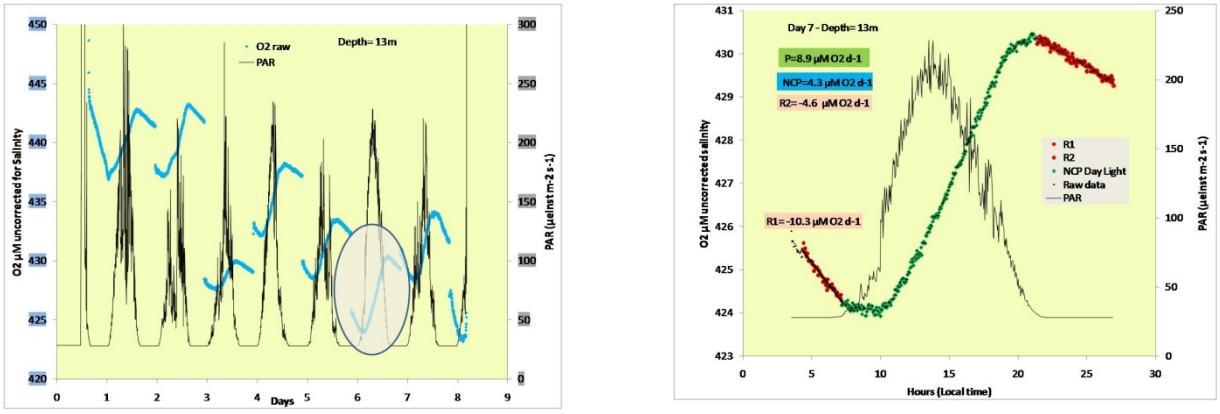

Figure 27 : Exemple du cycle 6 @ 13 m lors du 4eme déploiement.

9.5 Post-cruise sampling analyses and dead-lines

1) Traitement des données IODA, correction température, salinité et étalonnage post campagne des optodes. Juin 2012
2) Analyses des échantillons ETS : Juin 2012
3) Traitement des données NCP : Juin 2012

9.6 Data base organisation

cf. Sampling file

9.7 References of methods

GOYET C; HACKER S D 1992. Procedure for calibration of a coulometric system used for total inorganic carbon measurements of seawater. Marine Chemistry 38 (1-2) 1992. 37-51.

JOHNSON K.M., 1993. Operator's Manual. Single-Operator Multiparameter Metabolic Analyzer (SOMMA) for Total Carbon Dioxide (C_T) with Coulometric Detection. New York : 11

JOHNSON K.M., KING A.E., SIEBURTH J.MCN., 1985. Coulometric TCO_2 analysis for marine studies ; an introduction. *Marine chemistry,* 16 : 61.

WILLIAMS P.J. LEB. & N.W. JENKINSON (1982). A transportable microprocessor-controlled precise Winkler titration suitable for field station and shipboard use. Limnol. Oceanogr. 27, 576-585.

PACKARD, T.T. 1971. The measurement of respiratory electron-transport system in marine phytoplancton. Journal of Marine Research **39:** 235-244.

PACKARD, T.T., and P.J.L. WILLIAMS. 1981. Rates of Respiratory Oxygen Consumption and Electron Transport in Surface Seawater from the Northwest Atlantic. Oceanologica acta **4:** 351-358.

10 Analyse of size spectra of particles and macrozooplankton community based on Underwater Vision Profiler (UVP) data.

Principal investigator

Jouandet Marie-Paule
MIO, UMR Aix–Marseille Université CNRS 7294/UR IRD 235,
Campus de Luminy Case 901 F-13288 Marseille cedex 9
☎ + 33 (0)4 91 82 94 52
🖷 + 33 (0)4 91 82 90 51
jouandet@univ-amu.fr

Names of other participants (+affiliation)

- F. Carlotti (MIO),
- M. Picheral (LOV/UPMC)

Résumé

Le 'profiler de vision marine' (PVM) a été déployée au cours de la campagne KEOPS2 afin de quantifier la distribution verticale de la matière particulaire (allant de 0.052 mm à plusieurs mm) ainsi que la distribution du macro zooplankton (> 2 mm). L'analyse des données a pour objectif d'étudier l'effet d'une fertilisation naturelle en fer sur l'export de carbone en profondeur ainsi que la mise en évidence des mécanismes contrôlant l'export. Le rôle du fer sur la structure des communautés zooplanktoniques sera aussi exploré et comparé aux résultats provenant du LOPC et aux analyses taxonomiques dérivées des filets BONGO.

10.1 Scientific context

The effect of iron on biological carbon pump has been previously investigated during artificial and natural fertilisation experiments (Blain *et al.*, 2007; Boyd *et al.*, 2007). All experiments demonstrated an increase of the primary production in surface waters and a subsequent increase of carbon export until 400 m depth during KEOPS 1- a natural iron fertilisation study South East of Kerguelen Island (Jouandet *et al.*, 2010). The impact of iron on the carbon export in the ocean interior could not be estimated from these experiments.

Direct exports of diatoms have been pointed out as the main export pathway from microscopic analyse of the sediment trap whereas observations from the gel trap indicate an indirect export through fecal pellet excretion in KEOPS 1. Artificial iron fertilisations have also shown a dominance of sinking diatoms in the carbon flux exported. The mechanism responsible for carbon export still needs to be investigated in further details.

The quantification of mid water macrozooplankton community on temporal and spatial scales will help to predict vertical flux and describe processes involved in carbon export.

10.2 Overview of the project and objectives

The analyse of the vertical profiles of size distribution of particles recorded by the Underwater Video Profiler will allow to answer to the following issue:

What is the impact of iron on the particles abundance, biovolume according to their size in the water column?

viii. What is the magnitude of the increase of carbon export in deep water?

ix. What is the relationship between carbon export and zooplankton community structure?

x. What is the seasonal variability of particles dynamic at A3?

10.3 Methodology and sampling strategy

The Underwater Video Profiler 5 (UVP5) constructed in the Laboratoire d'Océanographie of Villefranche sur Mer was deployed during KEOPS 2 to study the dynamic of particles and the zooplankton community structure.

The UVP5 measured objects illuminated in a slab of water of known volume of 1.02 liters. An image provides information about the size and shape of particles in its field of vision which can be used to calculate particle size distributions (Gorsky *et al.*, 1992, 2000). Vignettes of objects larger than 2 mm are extracted from the images allowing to study the nature of large particles and the macrozooplankton community structure.

The number of pixels is converted to surface areas, using the results of size and volume calibrations conducted in a seawater tank using natural particles of different types to determine the conversion between pixels to metric units (Picheral *et al.*, 2010). The equivalent spherical diameter (ESD) of particles larger than 0.052 mm is calculated from the particle's projected area in the image, assuming spherical shape.

Vignettes are processed using zooprocess and Plankton Identifier (Gorsky *et al.* 2010) in order to detect, enumerate, measure and classify the digitized objects.

UVP5 was mounted on the 24 bottle rosette and deployed for each CTD casts. Images are recorded at a frequency up to 6 Hz

Table XV : Exhaustiv list of measured parameters

1.particles size	CTD	mm
2.particles abundance		#.m3
3.particles images		

10.4 Preliminary results

Figure 28 shows the vertical profiles of the total biovolume of particles with an equivalent spherical diameter ranging from 0.052 to 3.34 mm.

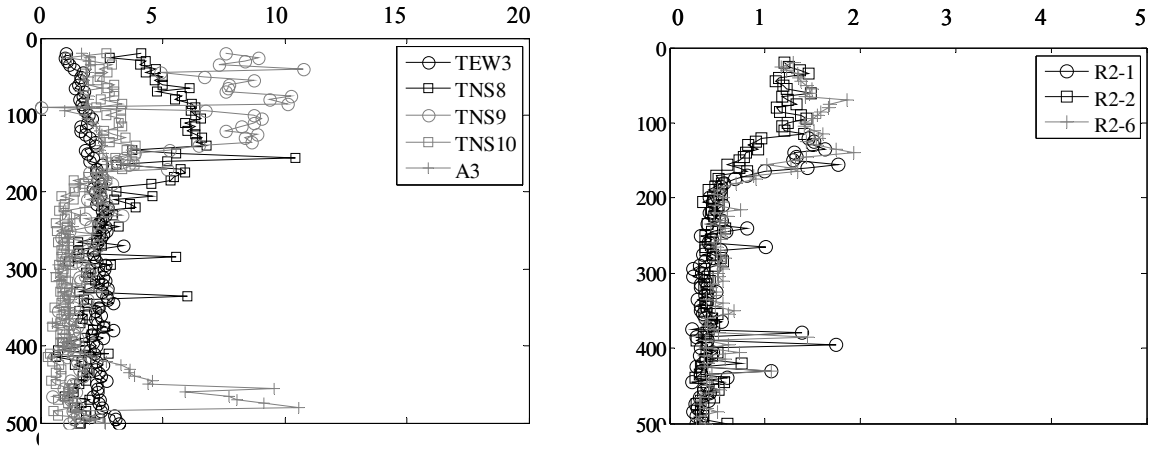

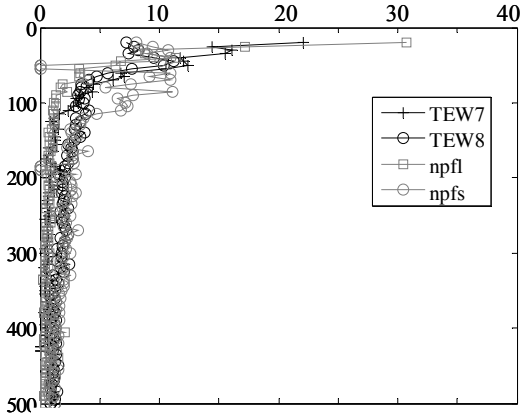

Figure 28 : : Vertical profiles of total (TPV) particle volumes in the water column (0–500 m) for stations of the cluster 1 (A) , cluster 2 (B) and cluster 3 (C).

10.5 Post-cruise sampling analyses and dead-lines

Vignettes will be post processed using zooprocess an Plankton identifier software by the end of January.

10.6 Data base organization

General cruise base

10.7 References of methods

GORSKY, G., M. PICHERAL, AND L. STEMMANN. 2000. Use of the underwater video profiler for the study of aggregate dynamics in the North Mediterranean. Estuar. Coast. Shelf Sci. 50: 121–128, doi:10.1006/ecss.1999.0539Gorsky

GORSKY, G., M. D. OHMAN, M.PICHERAL, S. GASPARINI, L. STEMMANN, J-B ROMAGNAN, A. CAWOOD, S.E PESANT, C. GARCIA-COMAS AND F. PREJGER, 2010. Digital zooplankton image analysis using the ZooScan integrated system. JOURNAL OF PLANKTON RESEARCH,VOLUME 32, NUMBER 3: 285–303;

PICHERAL, M., L. GUIDI, L. STEMMANN, D. M. KARL, G. IDDAOUD, and G. GORSKY. 2010. The Underwater Vision Profiler : An advanced instrument for high spatial resolution studies of particle size spectra and zooplankton. Limnology and oceanography: methods.

11 Size spectra of plankton during the KEOPS2 study

Principal investigator

Meng Zhou
University of Massachusetts Boston/Universite de la Mediterranee
617-287-7419
617-287-7474
meng.zhou@umb.edu

Names of other participants

- Yiwu Zhu (U. Mass. Boston)
- Bernard Queguiner (MIO)
- Francois Carlotti (MIO)

Abstract:
A Laser In-Situ Scattering and Transmissometry (LISST), which measures the size and volume concentration for particles from 1 to 250 μm, and a Laser Optical Plankton Counter (LOPC), which measures particle counts and their size distribution from 100 μm to 35 mm, were mounted on the CTD rosette during the KEOPS 2 cruise. Total 103 and 53 vertical profiles were taken by LISST and LOPC, respectively, during the cruise. Those measurements provided spatial and the temporal distributions of size structured plankton communities between 1 μm and 35 mm with high spatial and size resolutions. The analysis of the measurements will be closely linked to other biogeochemical, biological and physical measurements such as POC from net tow and water samples, the backscattering from ADCP, the fronts and blooms, to study the role of plankton in the bloom process and temporal evolution of plankton communities at time series stations.

11.1 Scientific context

Understanding plankton community structures responding to iron enrichment or depletion is of key questions in predicting effects of iron fertilization on primary production and carbon export. One of our approaches is to classify plankton community in their size classes. The advantages of using the LISST and LOPC are:

1) Providing in situ, no invasive contact measurements of size structured biovolume of POC,
2) Automated sampling at a high resolution (0.5 sec) in a broad size range (1μm – 35 mm),
3) Avoiding physical damage of POC during water sampling, filtration, or net tows,
4) Avoiding difficulties in identifying most of broken/partial parts of an organism which contribute a large percentage in net tow samples.

With such capability of automated sampling at high resolution, the LISST and LOPC mounted on a CTD rosette provided the measurements of biovolume betwee (1μm – 35 mm) along the transects and at the time series stations. The time series of size spectra can be further applied to study primary production, trophic interaction and carbon export.

11.2 Overview of the project and objectives

A LISST-DEEP (Sequoia Scientific, 3000 m) and a LOPC-DEEP (Brooke Ocean, 6000m) were mounted on the INSU 24 position water sampler (SeaBird) powered by a battery pack (Brooke

Ocean). Because of the short production time window (much less than 6 months required for production) for Brooke Ocean due to delayed purchase order issued by the Universite de la Mediterranee, both LOPC-DEEP and battery pack arrived one day before our departure for the cruise. The batter pack was malfunctioning at the first bench test. It had to be modified for a temporary solution which worked for the entire cruise. The LOPC worked in the first several weeks. But it started to work unstably and then failed eventually. LISST worked seamLessly.

Overall, 103 LISST profiles were recorded which are equivalent to all CTD casts except a few of shallow casts for water collections. Less than 53 LOPC profiles were recorded, of which some bad casts may be included due to difficulties to identify when the LOPC started to malfunction. All LISST data were processed though further quality control is needed. Processing LOPC data requires significant amount of efforts due to sort out good and bad data, and match depth and time for a number of LOPC casts deeper than 1000 m without a depth sensor.

11.3 Methodology and sampling strategy

The LISST is based on Mia theory using small forward angles determined almost entirely through light *diffracted* by a small particle (Agrawal & Pottsmith, 2000, Karp-Boss *et al.* 2007), while the LOPC measures relative shadow produced when a particle passing through a laser beam (Herman & Harvey 2006). The LISST measurements have 32 size classes in a $\log_{10}$ based increment from 1 to 250 μm while the LOPC measurements have 128 size classes for single element particles between 1 μm and 1 mm, and actual sizes for multiple element particles above 1 mm. During data processing, LISST original size classes are remained and LOPC sizes are regrouped into 50 size classes based on a $\log_{10}$ increment from 0.1 to 35 mm. Both instruments has a sampling rate of 2 Hz and were mounted on the Rosette which was deployed at a descending or ascending rate of approximately 1 m sec^{-1} giving a vertical resolution 0.5 m The measurements are converted into particle abundances based on their equivalent spherical diameter (ESD) sizes normalized by the water volume sampled into μL/L and integrated into 1 m depth bins for each down and up casts. For the bio-volume spectra analysis, the data is normalized by their size group interval to the unit of 1/L. These data will be made available to the community.

Table XVI : Exhaustive list of measured parameters

1. Bio-volume concentration in 32 sizes between 1 & 250 μm	Rosette-LISST	bio-volume concentration: (μL/L) Normalized size spectra: (1/L)
2. Biovolume in 50 sizes between 100 μm and 35 mm	Rosette-LOPC	bio-volume concentration: (μL/L) Normalized size spectra: (1/L)

11.4 Preliminary results

LISST-LOPC composed size spectra: The optical methods used to measure particle sizes and abundances are different for the LISST and LOPC. The bio-volume spectra obtained from these two instruments are shown in Figure 29Figure 2. If we assume the upward tail for sizes larger than 100 μm in the spectrum from LISST measurements is false due to the LISST limitation, the LISST and LOPC measurements form a linear size spectrum between 5 μm and 3 mm. The LOPC data become noisy for larger sizes than 3 mm due to small sampling volume. The continuity of the spectra confirms the reliability of the measurements.

North-South and West-East transect: The LISST measurements from north-south transect (TNS) shows a transition of bio-volume concentration in waters: lowest in the north, enhanced but patchy in the offshelf, and highest on the shelf (Figure 30). Similar shelf-offshelf transitions were also observed along the west-east transect (TEW) (Figure 31). With size specified particle distribu-

tions, specific features are shown: enhanced particle concentrations in all sizes along the shelf break regions, a pool of particles of 1 µm in the deep waters at the offshelf region, and deep export of particles in sizes 10-20 µm at Station TEW05.

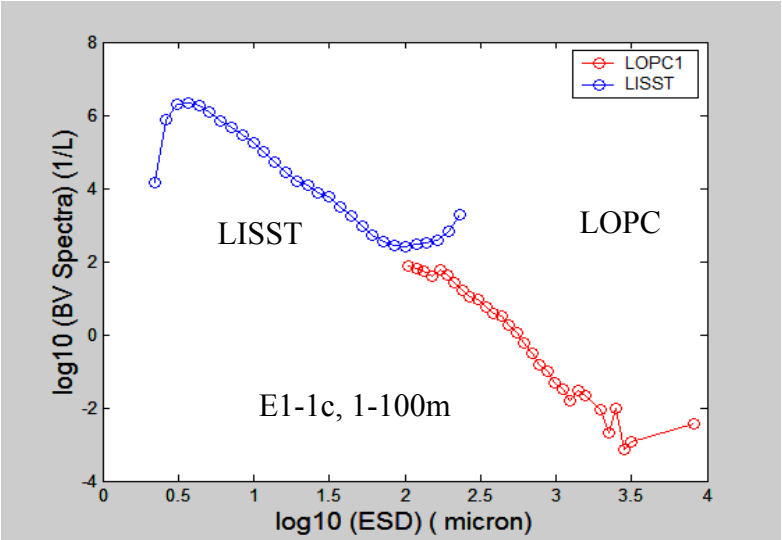

Figure 29 : A composed size spectrum from the LISST and LOPC taken at station E1-1. In the LISST measurements, the concentration increases from the lowest size class and peaks at 4-5 µm, decreases linearly between 5 and 100 µm, and increases exponentially after 100 µm. The LOPC measurements seem follow the trend of the linear decrease region of the LISST. We interpret the upward tail at the larger sizes than 100 µm may be caused by the limitation of the instrument.

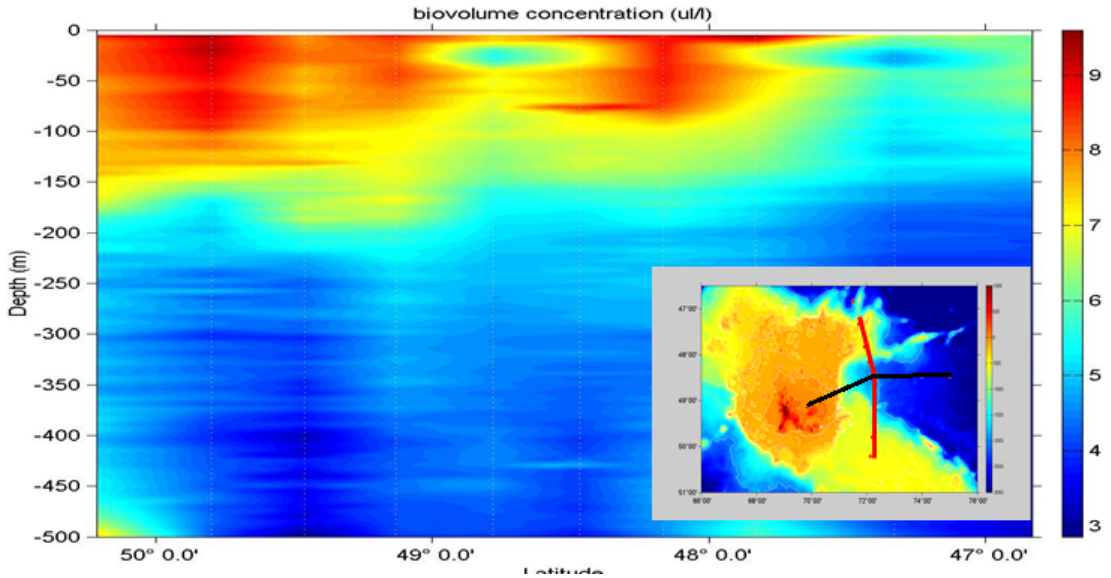

Figure 30 : Total bio-volume (µL/L) distribution from the LISST measurements along the TNS transect indicated by the red line in the inserted figure.

Vertical distribution of POC: The particles were mostly concentrated in the upper 200 m with a continuous size spectrum. Below the 200 m depth, size distributions were most abundant between sizes 4 and 10 mm forming a discontinuous size spectrum. At several thin layers, the spectra were more continuous. It is not known if these continuous spectrum layers mark the settling events of blooms or accumulation of particles at a density layer. Small particles between 1 and 4 µm appeared in the depth deeper than 500 m and increased as a function of depth that could be contributed by

resuspension of particles from the sediments or breakages from large POC by turbulence produced by the flow through the LILSST.

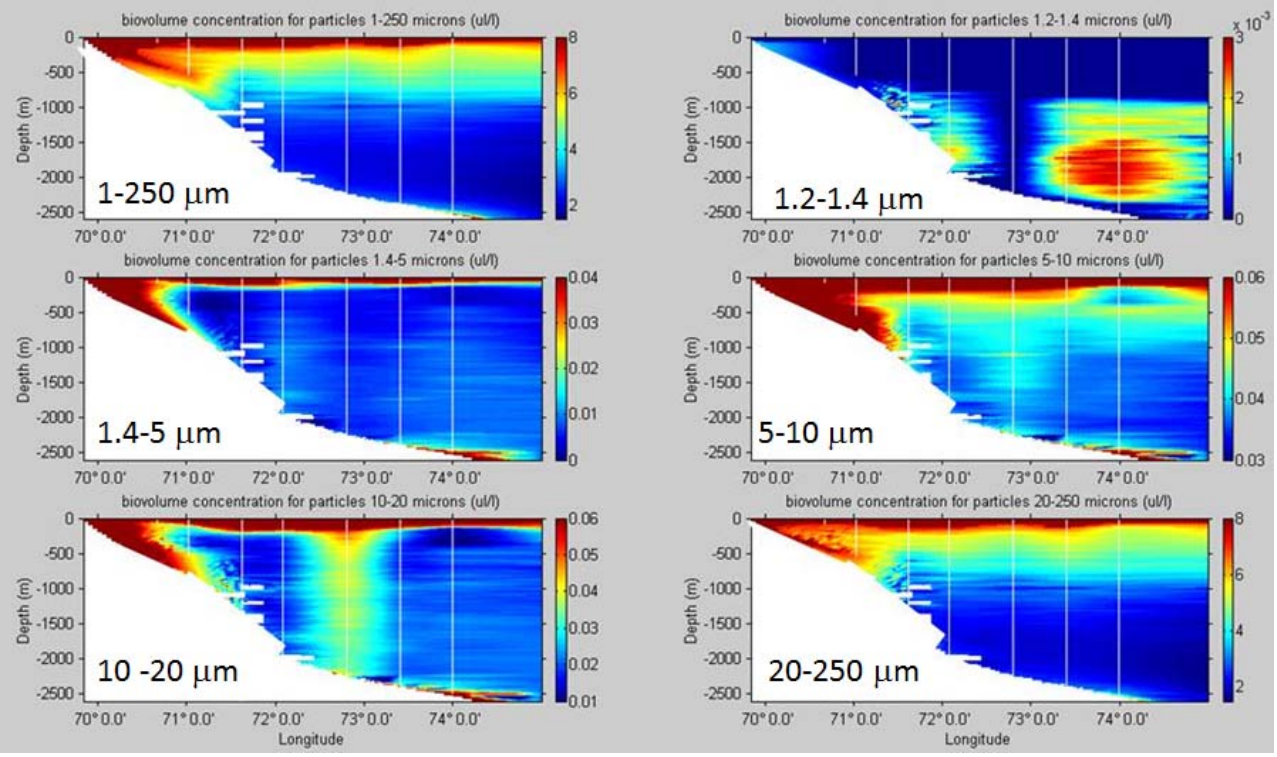

Figure 31 : Size separated biovolume (µL/L) distributions from the LISST measurements along the TEW transect indicated by the black line in the inserted figure inFigure 30.

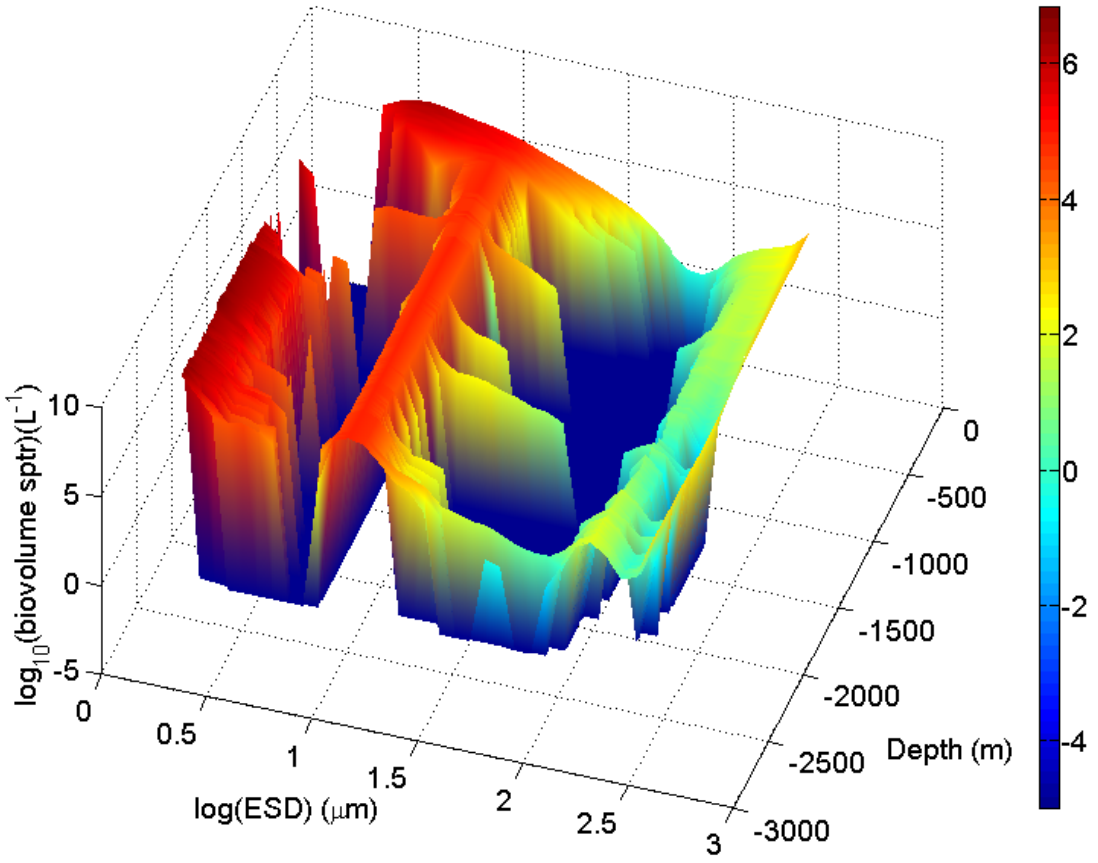

Figure 32 : The size spectrum of POC at Station TNS01.

11.5 Post-cruise sampling analyses and dead-lines

Table XVII : Post-cruise analyses

Task	Target date
Reprocessing LISST data into 32 size classes and 5 m depth bins	March 2012
Processing LOPC data into 50 m sizes classes and 5 m depth bins	June 2012

11.6 Data base organization

Data will be submitted to the KEOPS database.

11.7 References of methods

Agrawal, Y. C. and H. C. Pottsmith, 2000: Instruments for Particle Size and Settling Velocity Observations in Sediment Transport, Marine Geology, 168, pp 89-114.

Herman, A. W., & Harvey, M. (2006). Application of normalized biomass size spectra to laser optical plankton counter net intercomparisons of zooplankton distributions. Journal of Geophysical Res., 111, c05S05, doi:10.1029/2005JC002948.

Karp-Boss, L., Azevedo, L., & Boss, E. (2007). LISST-100 measurements of phytoplankton size distribution: evaluation of the effects of cell shape. Limn. and Oceanogr.: Method, 5, 396–406.

12 Dissolved inorganic and organic matter

Principal investigator

Blain Stéphane
LOMIC, Observatoire océanologique de Banyuls,avenue du Fontaulé,
66650 Banyuls sur mer. France
☎+33 468 887 343
stephane.blain@obs-banyuls.fr

Names of other participants (+affiliation)

- L. Oriol (LOMIC)
- A. Gueneuges (LOMIC)
- J. Capparos (LOMIC)
- I. Obernosterer (LOMIC)

Abstract:
Dans ce projet les concentrations en éléments nutritifs, nitrate, nitrite, ammonium, acide silicique, phosphate ont été déterminées à bord sur des échantillons prélevés dans la colonne d'eau ainsi que dans l'eau interstitielle du sédiment superficiel. Les formes organiques dissoutes de l'azote et du phosphore ont également été déterminées. Des échantillons ont été prélevés pour déterminer les concentrations en carbone organique dissous et en acides aminés totaux hydrolysables. Afin de caractériser plus finement la composition de la matière organique quelques échantillons de matière organique dissoute ont été préconcentrés.

12.1 Scientific context

The southern Ocean is characterized by high nutrient concentrations which could potentially support high level of primary of production. However iron limitation of phytoplankton growth leads to incomplete utilization of major nutrients (i.e. N and P) resulting in a low efficiency of the biological pump of CO_2. In iron fertilized regions higher utilization is expected, but complete utilization of nitrate was not observed so far. This contrasts with the depletion of silicic acid concentrations showing a strong decoupling between the N/P and Si cycling.

Iron fertilization of the Southern Ocean clearly enhances the activity of autotrophs, but the response of heterotrophic bacteria is still puzzling. Dissolved organic carbon (DOC), which is mainly produced by phytoplankton, is a major nutrient for heterotrophic bacteria. Therefore, following iron fertilization, it is always difficult to attribute any response of the bacterial community to the direct effect of iron addition or to the indirect effect resulting from increased supply of dissolved organic matter. In addition, the export of unused DOC in deep water can also contribute to carbon export.

12.2 Overview of the project and objectives

The aim of the project is to provide spatial and temporal distributions of the major dissolved nutrients in inorganic and organic forms, and dissolved organic carbon. The determination of total hydrolysable amino acid concentrations, and the qualitative analysis of DOM will provide a first insight into the bioavailability of DOM.

12.3 Methodology and sampling strategy

- **Dissolved Organic Carbon** (**DOC)**: Glass bottles used for sampling, GF/F filters and glass ampoules used for storage were combusted at 450°C for 24 hours. The seawater samples were taken from 10 liters clean Niskin bottles mounted on the trace metal clean rosette (TMR). After filtration through GF/F, subsamples of 20 mL (triplicates) were delivered in glass ampoules and acidified with 100 µL of 25 % H_3PO_4. Ampoules were sealed and stored at room temperature until analysis. Duplicates of unfiltered, acidified samples were also stored.
- **Total Hydrolysable Amino acids (THAA)** : Filtered (GF/F) and unfiltered seawater was stored frozen in 60 mL acid washed HDPE bottles. Analysis will be performed by HPLC as described in Davis and Benner (2005).
- **Qualitative determination of the composition of DOM** : Ten liters of 0.2 µm filtered seawater was collected by gravity filtration from a trace metal clean Niskin bottle. Following acidification to pH2, the DOM of the sample was retained on a SPE–PPL resin. The SPE-PPL cartridge was dried with ultra pure nitrogen, and the DOM was eluted with méthanol. The eluent was collected in glass ampoules, which were sealed and stored at -20°C until analysis. Analysis will be perfomed by Fourier-transform ion cyclotron resonance mass spectrometry as described in Kujawinski *et al.* (2004).
- **Major in organic nutrients (NO_2^-, NO_3^-, PO_4^{3-}, $Si(OH)_4$)** : Syringes of 50 mL were directly connected to the spigot of the Niskin bottles. The sample were drawn through a 0.45 µm Uptidisc adapted to the syringe. Duplicate samples were collected. One sample was immediately analyzed onboard using the continuous flow autoanalyser (Skalar) (Skalar). The second sample (25 mL) was poisoned with mercuric chloride ($HgCl_2$, 20 mg l^{-1}) and stored in the dark for later analysis.
- **Ammonium (NH_4^+)**. Samples were collected from Niskin bottles in two 50 mL Schott glass bottles. Following rinsing, the bottles were filled with 40 mL of seawater and closed immediately to avoid contamination by air. Back in the inboard laboratory the OPA reagent was added. Samples were incubated for et least 3 hours in the dark, at XX°C before fluorescence measurements.
- **Dissolved organic nitrogen and phosphorus (DON, DOP)**. Samples were collected from Niskin bottles in 100 mL calcinated Schott glass bottles. The samples were then filtered through 2 combusted GF/F filters. 20mL of the filtered samples were transferred to 20 mL teflon vials and poisoned with 100 µl of $HgCl_2$ (4g/L) before storage at 4°C. Following the addition of 2.5 mL of the oxidative reagent (boric acid + sodium hydroxide + potassium peroxodisulfate), samples were then heated at 120°C during 30 min. After cooling, the concentrations of nitrate and phosphate were determined using continuous flow analysis (Skalar).

Table XVIII : Exhaustiv list of measured parameters

Parameter	code of operation	units
1. COD	TMR	µM
2. Acides Aminés	TMR	nM
3. Matière organique dissoute	TMR	qualitative analysis
4. Phosphates	CTD, TMR, Corer, Go-Flow	µM
5. Silicates	CTD, TMR, Corer, Go-Flow	µM
6. Nitrites	CTD, TMR, Corer, Go-Flow	µM
7. Nitrates	CTD, TMR, Corer, Go-Flow	µM
8. Ammonium	CTD	µM

9. Azote organique dissous	CTD	µM
10. Phosphore organique dissous	CTD	µM

12.4 Preliminary results

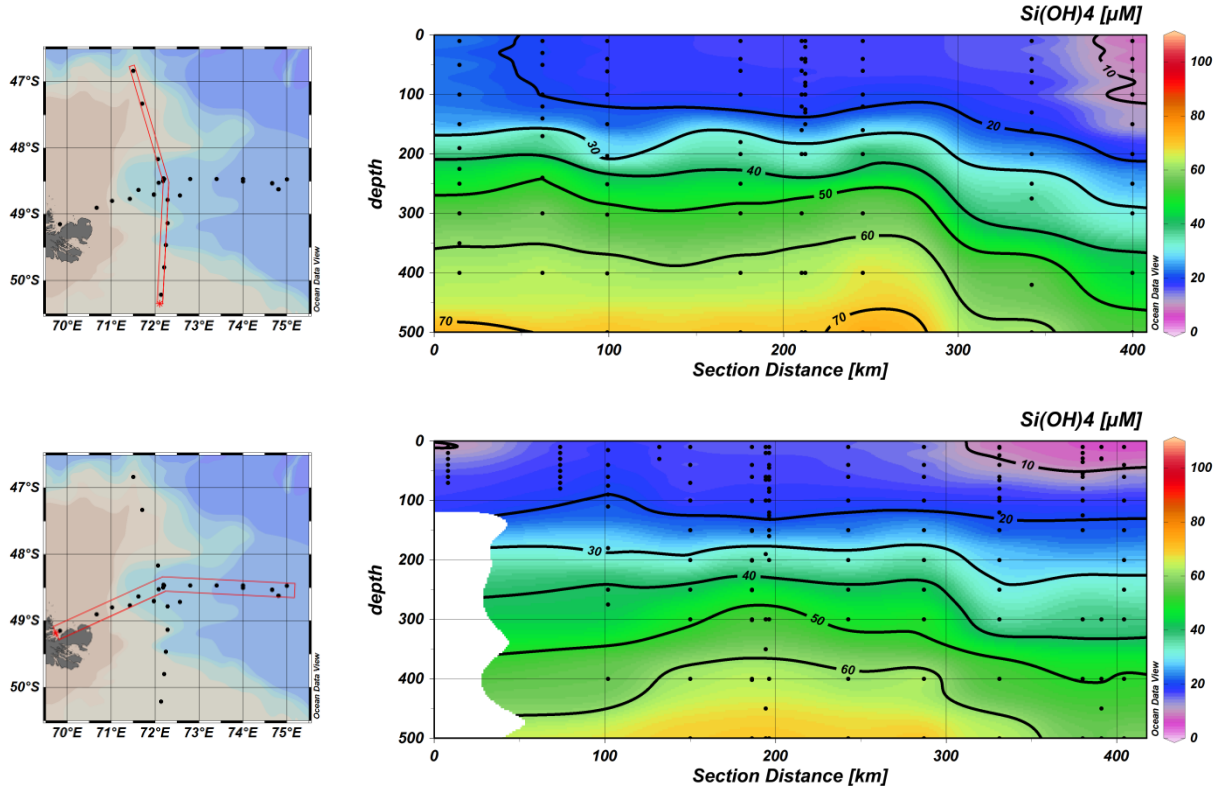

Figure 33 : distributions of silicic acid concentrations along the transects east -west and north-south

12.5 Post-cruise sampling analyses and dead-lines

Nutrients : A quality control protocol will be applied to all the measurements (PO_4^{3-}, $Si(OH)_4$, NO_2^-, NO_3^-, NH_4^+, DON and DOP) made onboard. It will include re-analysis of some poisoned samples, control of the low nutrient seawater used for the preparation of the standards and determination of base line. The validated data set will be available in March 2012 via the KEOPS2 general data base.

DOC samples will be analyzed within the two months following the arrival of the samples in Banyuls. Validated data will be available in April 2012.

THAA will be analyzed during 2012. Data should be available in January 2013

12.6 References of methods

Benner R., Strom M. (1993) A critical evaluation of the analytical blank associated with DOC measurements by high-temperature catalytic oxidation. Mar Chem 41: 153-160

Davis and Benner 2005. Seasonal trends in the abundance, composition and bioavailability of particulate and dissolved organic matter in the Chukchi/Beaufort Sea and western Canada Basin. DSRII 52 : 3396-3410.

Kujawinski E.B., Del Vecchio R., Blough N.V., Klein G.C., Marshall A.G. 2004. Probing molecular-level transfor- mations of dissolved organic matter: insights from electrospray ionization Fourier-transform ion cyclotron resonance mass spectrometry. Mar. Chem. 92:23–37

Aminot A., Kérouel R., 2007. Dosage automatique des nutriments dans les eaux marines : méthodes en flux continu. Ed. Ifremer.

Holmes R.M., Aminot A., Kérouel R., Hooker B.A., and Peterson B.J. 1999. A simple and precise method for measuring ammonium in marine and fresh water ecosystems. Can. J. Fish. Aquat. Sci. vol 56, 1801-1808 .

Pujo-Pay, M., Conan, P., and Raimbault, P.: Particulate and dissolved organic nitrogen and phosphorus in the north western Mediterranean Sea (EROS 2000 - Discovery cruise 1993), edited by: Martin, J. M., and Barth, H., 79-86, 1995.

Pujo-Pay, M., Conan, P., and Raimbault, P.: Excretion of dissolved organic nitrogen by phytoplankton assessed by wet oxidation and N-15 tracer procedures, Mar. Ecol. Prog. Ser., 153, 99-111, 1997

13 Isotopic composition of nitrate

Principal investigators:

Frank Dehairs
Vrije Universiteit Brussel
☎ +32-2-629 12 65 (VUB)
🖷 + 32-2-629 18 11 (VUB)
fdehairs@vub.ac.be

Thomas W. Trull
Tom.Trull@utas.edu.au

Camila Fernandez
LOMIC (UMR 7621), Banyuls sur Mer
fernandez@obs-banyuls.fr

Names of other participants

- D. Davies, ACE CRC
- L. Oriol, LOMIC- Banyuls s/Mer
- A.-J. Cavagna, VUB

Abstract:
To investigate whether processes other than nitrate uptake by phytoplankton are significant and show spatial variability possibly induced by varying availability of Fe in the region, seawater was collected from CTD casts jointly with the nutrient sampling, as well as by underway surface water pumping, for analysis of nitrate N, O isotopic composition.

To put the obtained data set into a biogeochemical context for the study area, parallel measurements of the main N cycling fluxes (uptake and regeneration) were performed at long stations (see cruise reports by A.-J. Cavagna *et al.* and C. Fernandez). Samples of N regeneration generated from these assays will be analyzed using the same denitrifying technique (see methods section).

13.1 Scientific context

The N, O isotopic composition of nitrate offers a means to investigate which processes affect the nitrate pool. Of these, nitrate uptake by the phytoplankton, ammonium oxidation by the chemolithotrophic nitrifying bacteria and archaea (nitrification) and N2-fixation are the most likely ones in well oxygenated environments, while denitrification represents an additional process under low oxygen conditions (Sigman *et al.*, 2009). These processes were studied directly via 15N tracer addition incubations (see C. Fernandez cruise report). The measurements of the natural abundance variations discussed here provide additional context for those studies. They also allow some of the same quantities to be estimated, in particular, assessment of the significance of euphotic layer nitrification, and the influence of iron on new production.

Recent studies in the Southern Ocean highlight that nitrification in the euphotic layer can be significant (DiFiore *et al.*, 2009; Sanders *et al.*, 2007). Yool *et al.* (2007) stress the possible impact that euphotic zone nitrification has on new production based on nitrate uptake. For the Kerguelen Plateau Trull *et al.* (2008) report significant nitrification rates reaching 10%, though mostly less

than 5% of ammonium uptake. It would appear, therefore, that calculations of new production (i.e. potential export production) based on nitrate uptake experiments need to take possible euphotic layer nitrification into account (Yool *et al.*, 2007; Cavagna *et al.*, 2011). Quantifying the extent of nitrification is also important to understand controls on ecosystem productivity and the Southern Ocean's role in the control of the regional nutrient stoichiometry in the Southern Ocean. Notably, KEOPS1 showed that surface waters were far more depleted in silicate than nitrate, so that "silica leakage" from the Southern Ocean to supply warmer waters is unlikely (Blain *et al.*, 2007; Mosseri *et al.*, 2008), and this may partly reflect rapid nitrification. Climatic implications of active nitrification in the mixed layer include the production and sea-atm exchange of nitrous oxide, a powerful greenhouse gas.

The influence of iron on new production, specifically by increasing the use of nitrate in comparison to ammonium, can be estimated by combining ^{15}N measurements for nitrate with those for phytoplankton (as determined on size-fractionated particulate matter samples – see the T. Trull cruise report). By estimating the isotopic fractionation associated with nitrate assimilation from the mixed layer $^{15}N\text{-}NO_3$ data, the expected phytoplankton ^{15}N composition can be determined, and lower values thus reflect ammonium uptake. This approach revealed and increase in f-ratio in iron fertilized waters over the Kerguelen plateau during KEOPS1 (Trull *et al.*, 2008).

13.2 Overview of the project and objectives

To investigate whether processes other than nitrate uptake by phytoplankton are significant and show spatial variability possibly induced by varying availability of Fe in the region, seawater was collected from CTD casts jointly with the nutrient sampling, as well as by underway surface water pumping, for analysis of nitrate N, O isotopic composition. Results will be interpreted in the light of prevailing nitrate-nutrient concentrations (nutrient team; L. Oriol) and N-uptake regimes (new vs. regenerated production and nitrification; A.-J. Cavagna *et al.* cruise report).

13.3 Methodology and sampling strategy

Samples for isotopic composition of nitrate were collected from the CTD rosette (whole water column) jointly with the nutrient sampling and also via continuous underway surface water sampling. All samples were filtered on 0.4 µm acrodiscs and kept at -20°C till analysis in the home-based laboratory. We will apply the denitrifier method elaborated by Sigman *et al.* (2001) and Casciotti *et al.* (2002). This method is based on the isotopic analysis of $\delta^{15}N$ and $\delta^{18}O$ of nitrous oxide (N_2O) generated from nitrate by denitrifying bacteria lacking N_2O-reductase activity. As a prerequisite the nitrate concentrations need to be known (data from the nutrient team; L. Oriol *et al.*) as this sets sample amount provided to the denitrifier community. Briefly, sample nitrate is reduced by a strain of denitrifying bacteria (*Pseudomonas aureofaciens*) which transform nitrate into N_2O, but lack the enzyme to produce N_2. N_2O is then analysed for N, O isotopic composition by IRMS (Delta V, Thermo) after elimination of CO_2, volatile organic carbon and further cryogenic focusing of N_2O (Mangion, 2011).

Table XIX : Exhaustive list of measured parameters

Parameter	code of operation	units
1. $\delta^{15}N$, $\delta^{18}O\text{-}NO_3$	CTD	‰
2. $\delta^{15}N$, $\delta^{18}O\text{-}NO_3$	Surface sampling from on-board pump at stations. See T. Trull Cruise Report	‰

13.4 Preliminary results

None for isotopic composition.

13.5 Post-cruise sampling analyses and dead-lines

Analysis for nitrate stable isotopic composition will start early in 2012 will last till autumn 2012. By then it is expected that most samples for natural isotopic composition of nitrate will have been processed.

13.6 Data base organization (general cruise base and/or specific data base(s))

General cruise base

13.7 References of methods

Casciotti K.L., D.M.Sigman, M.G. Hastings, J.K. Böhlke and A. Hilkert, 2002. Measurement of the oxygen isotopic composition of nitrate in seawater and freshwater using the denitrifier method, *Analytical Chemistry*, 74 (19): 4905-4912.

Mangion P., 2011. Biogeochemical consequences of sewage discharge on mangrove environments in East Africa, PhD Thesis, Vrije Universiteit Brussel, 208 pp.

Sigman D.M., Casciotti K.L., Andreani M., Barford C., Galanter M. and J.K. Böhlke, 2001. A bacterial method for the nitrogen isotopic analysis of nitrate in seawater and freshwater, *Analytical Chemistry*, 73: 4145-4153.

Sigman D. M., K. L. Karsh and K. L. Casciotti, 2009. Nitrogen isotopes in the ocean, *EOS*, Elsevier, 40-54.

Trull T.W., D. Davies and K. Casciotti, 2008. Insights into nutrient assimilation and export in naturally iron-fertilized waters of the Southern Ocean from nitrogen, carbon and oxygen isotopes, *Deep-Sea Research II*, 55, 820-840

14 Trace metal and isotope cycles during KEOPS 2

Principal investigator

Géraldine Sarthou
Technopôle Brest Iroise, Place Nicolas Copernic, F-29280 Plouzané
☎ 00- 33- 2 98 49 86 55
🖷 00- 33- 2 98 49 86 45
Geraldine.Sarthou@univ-brest.fr

Other participants

- Fabien Quéroué (LEMAR/UMR-CNRS6539/IUEM – ACE/CRC)
- Fanny Chever(LEMAR/UMR-CNRS6539/IUEM)
- Andy Bowie (ACE/CRC)
- Pier van der Merwe ((ACE/CRC)
- Marion Fourquez (LOMIC)
- Stéphane Blain (LOMIC)
- François Lacan (LEGOS)
- Derek Vance (School of Earth Sciences, University of Bristol)
- Eva Bucciarelli (LEMAR/UMR-CNRS6539)

Résumé :
Les métaux traces jouent un rôle majeur dans l'océan. Pendant KEOPS 2, nous étudions les distributions, sources et cycles internes des métaux traces (principalement Fe, Mn, Cu, Co, Ni, Zn, Cd et Pb), y compris leur spéciation physique et chimique et leur composition isotopique. Au total, 18 stations ont été échantillonnées, incluant 4 déploiements de bouteilles Go-Flo et 34 déploiements de la rosette propre. Seul le fer dissous a été mesuré à bord. Les autres paramètres seront analysés dans les différents laboratoires. Les concentrations les plus élevées de fer ont été observées au dessus du plateau. Elles sont minimales au niveau de l'eddy puis augmentent à nouveau au niveau du front et au nord de celui-ci.

Abstract:
Trace metals play a crucial role in the ocean. During KEOPS 2, we studied the distributions, sources and internal cycle of trace metals (mainly Fe, Mn, Cu, Co, Ni, Zn, Cd and Pb), including their physical and chemical speciation, and their isotopic composition. A total of 18 stations were sampled, with the deployments of 4 Go-Flo casts and 32 TMR casts. Only dissolved Fe was analysed on board. The other parameters will be analysed in the shore-based laboratories. The highest concentrations of Fe were observed above the plateau. Then concentrations were minimal in the eddy area and increased again when reaching the polar region and north of it.

14.1 Scientific context

Trace elements and their isotopes (TEIs) play a crucial role in the ocean. Some of them (e.g., Fe, Cu, Mn, Co, Zn) serve as essential micronutrients, being involved in many metabolic processes

of marine organisms (e.g., Sunda, 1994; Morel and Price, 2003). Some of these micro-nutrients are thought to control the structure of ocean ecosystems and their biological productivity (de Baar et al., 2005; Peers and Price, 2006; Boyd et al., 2007; Blain et al., 2007; Pollard et al., 2007; Middag et al., 2011), both of which are key factors regulating the ocean carbon cycle and hence have effects throughout the Earth system, responding to and influencing global change. A better knowledge of the distributions and internal cycling of such important micro-nutrients is thus crucial in the context of global change. Some of these elements are also contaminants of the environment. They are either toxic at high concentration but essential at low concentration, or only toxic (eg Pb). The poor knowledge of their cycles is a major drawback for the understanding of their biogeochemical impact on the food web. For some trace metals, more than 90% of their dissolved fraction is complexed by organic ligands (Rue and Bruland, 1995, Moffett and Dupont, 2007), preventing precipitation and removal by scavenging or regulating their bioavailability. Moreover, recent studies have shown that a significant fraction of the dissolved Fe pool exists as colloidal Fe species (Bergquist et al., 2007, Schlosser and Croot, 2009, Chever et al., 2010a). Only a few studies have examined the soluble fraction of Fe, although it may strongly control its bioavalability (Wu et al., 2001; Bergquist et al., 2007; Chever et al., 2010a).

KEOPS-1 highlighted the interest of natural laboratories in the context of iron fertilization of the ocean (Blain et al., 2007), as well as the use of a multi-proxy approach to better quantify and study the impact of Fe fertilization on food web structure and functioning (Chever et al., 2010b, van Beek et al., 2008; Zhang et al., 2008).

In the context of a multi-proxy approach, the isotopic composition of some trace metals, such as Fe, Zn, Cd, and Ni, have been shown to be useful tools to better quantify the iron sources to the ocean (Lacan et al., 2008).

14.2 Overview of the project and objectives

In this project, our main objective is to study the distributions, sources and internal cycle of trace metals (mainly Fe, Mn, Cu, Co, Ni, Zn, Cd and Pb), including their physical and chemical speciation, and their isotopic composition.

14.3 Methodology and sampling strategy

At the first station (A3-1), seawater samples were collected using acid-cleaned Go-Flo bottles mounted on a 6 mm Kevlar hydrowire. For the other stations, seawater was collected using a Trace Metal Clean Rosette (TMR, General Oceanics Inc. Model 1018 Intelligent Rosette), attached to a 6 mm Kevlar line. Immediately after collection, Go-Flo or Niskin bottles were transferred into a clean container for sampling, and processed under a laminar flow unit.

In total 4 Go-Flo casts and 32 TMR casts were performed, including all the long stations and the East-West transect (18 stations in total).

14.3.1 Physical speciation

Total dissolvable Fe and Cu were collected without any filtration. Dissolved trace metals were filtered on-line through 0.2 µm filter cartridges (SARTOBRAN® 300, Sartorius or Pall Supor membrane, Acropak 200). Soluble samples were obtained by immediate ultrafiltration of dissolved Fe on 0.02 µm filters (ANOTOP 25®). All samples were acidified within 24 h of collection with ultrapure hydrochloric acid (HCl, Merck, 250 µL, final pH 1.7).

Dissolved Fe was analysed on board by flow injection analysis following the method by Obata et al. (1993) modified by Sarthou et al. (2003). The other physical fractions of Fe will be analysed in the shore-based laboratory (LEMAR, Brest, France).

Dissolved trace metals (Mn, Fe, Co, Ni, Cu, Zn, Cd and Pb) will be analysed using an isotope dilution high resolution magnetic sector inductively coupled mass spectrometry (HR-ICP-MS)

method following Milne et al. (2010), in the shore-based laboratory at the University of Tasmania (Hobart, Australia). 6 stations were pre-concentrated on board.

Fe solubility will be assessed on 0.2 µm filtered samples following the method by Schlosser and Croot (2008), combining the addition of ^{55}Fe and ultrafiltration (0.025 µm Nuclepore Nitrate cellulose filters). Most of the 0.2 µm filtered samples collected for Fe solubility were not processed on board and were stored frozen at -20°C. They will be analysed in the shore-based laboratory (LOMIC, Banyuls/mer, France).

14.3.2 - Organic speciation

Samples for organic speciation of Fe were filtered on-line through 0.2 µm filter cartridges (SARTOBRAN® 300, Sartorius or Pall Supor membrane, Acropak 200) and were immediately frozen. They will be analysed in the shore-based laboratory (LEMAR, Brest, France) by cathodic stripping voltammetry (Croot and Johanson, 2000, Leal et al., 1999 for Fe and Cu speciation respectively).

On the TMR deployments, samples were also taken for dissolved inorganic carbon, Fe uptake, Fe/Cu/Mn incubations, Bacteria/Fe incubations, Fe solubility incubations, and Fe isotope incubations. The experiments are described in related reports.

14.3.3 - Trace metal isotopic composition

Samples for Fe, Zn, Cd, and Ni IC were filtered on-line through 0.2 µm filter cartridges (SARTOBRAN® 300, Sartorius or Pall Supor membrane, Acropak 200).

Fe IC will be analysed in the shore-based laboratory (LEGOS, Toulouse, France), with a multicollector-inductively coupled plasma mass spectrometer (MC-ICPMS) Neptune, coupled with a desolvator (Aridus II or Apex-Q), using a ^{57}Fe-^{58}Fe double spike mass bias correction following Lacan et al. (2010).

Zn, Cd, and Ni IC will at the University of Bristol (UK), with a multicollector-inductively coupled plasma mass spectrometer (MC-ICPMS).

Table XX : Exhaustive list of measured parameters

Parameter	code of operation	units
1. Dissolved Fe	TMR	nM
2. Total dissolvable Fe	TMR	nM
3. Dissolved Cu	TMR	nM
4. Total dissolvable Cu	TMR	nM
5. Soluble Fe	TMR	nM
6. Organic Fe	TMR	nM
7. Organic Cu	TMR	nM
8. Trace Metals (Mn, Fe, Co, Ni, Cu, Zn, Cd and Pb)	TMR	nM
9. Fe solubility	TMR	nM
10. Fe isotopes	TMR	%
11. Zn, Cu, and Ni isotopes	TMR	%

14.4 Preliminary results

Dissolved Fe concentrations were measured on board. The other parameters will be analysed back in the shore-based laboratories.

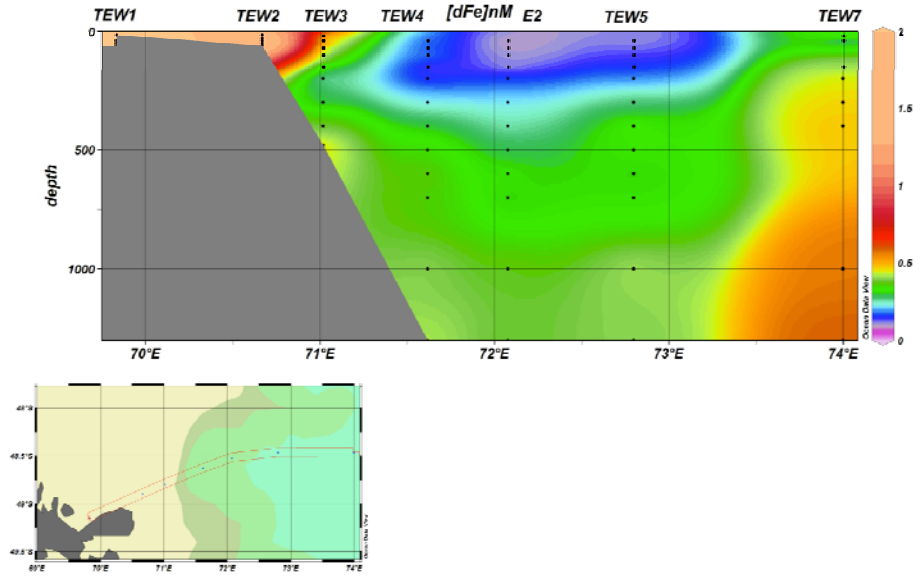

Figure 34 : East-West transect of dissolved Fe concentrations (in nM)

In the surface mixed layer, dissolved Fe concentrations varied from very low values (0.06 nM) at station E5 to values as high as 0.5 nM north of the polar front (station F). In the deep waters, concentrations varied between 0.3 nM (R station) and 1.3 nM (A3-2 station). A clear enrichment was observed above the plateau at depth. Figure 1 shows that the highest concentrations were observed above the plateau. Then concentrations were minimal in the eddy area and increased again when reaching the polar region and north of it.

14.5 Post-cruise sampling analyses and dead-lines

The analyses of all the parameters should be completed in the next 12-18 months.

14.6 Data base organization

Data will be posted on the KEOPS-2 database in a timely manner after analysis and processing.

14.7 References of methods

Bergquist, B.A., Wu, J. and Boyle, E.A.: Variability in oceanic dissolved iron is dominated by the colloidal fraction, Geochim. Cosmochim. Acta, 71 2960–2974, 2007.

Blain, S., Quéguiner, B., Armand, L., Belviso, S., Bombled, B., Bopp, L., Bowie, A., Brunet, C., Brussaard, C., Carlotti, F., Christaki, U., Corbière, A., Durand, I., Ebersbach, F., Fuda, J.-L., Garcia, N., Gerringa, L., Griffiths, B., Guigue, C., Guillerm, C., Jacquet, S., Jeandel, C., Laan, P., Lefèvre, D., Lomonaco, C., Malits, A., Mosseri, J., Obernosterer, I., Park, Y.-H., Picheral, M., Pondaven, P., Remenyi, T., Sandroni, V., Sarthou, G., Savoye, N., Scouarnec, L., Souhaut, M., Thuiller, D., Timmermans, K., Trull, T., Uitz, J., van-Beek, P., Veldhuis, M., Vincent, D., Viollier, E., Vong, L. and Wagener, T.: Impact of natural iron fertilization on carbon sequestration in the Southern Ocean, Nature, 7139, 1070-1074, 2007.

Boyd, P.W., Jickells, T., Law, C.S., Blain, S., Boyle, E.A., Buesseler, K.O., Coale, K.H., Cullen, J.J., Baar, H.J.W.d., Follows, M., Harvey, M., Lancelot, C., Levasseur, M., Owens,

N.P.J., Pollard, R., Rivkin, R.B., Sarmiento, J., Schoemann, V., Smetacek, V., Takeda, S., Tsuda, A., Turner, S. and Watson, A.J.: Mesoscale Iron Enrichment Experiments 1993–2005: Synthesis and Future Directions, Science, 315, 612-617, 2007.

Chever, F., Bucciarelli, E., Sarthou, G., Speich, S., Arhan, M., Penven, P. and Tagliabue, A.: Physical speciation of iron in the Atlantic sector of the Southern Ocean, along a transect from the subtropical domain to the Weddell Sea Gyre, J. Geophys. Res. Ocean, 115, C10059, doi: 10.1029/2009JC005880, 2010a.

Chever, F., Sarthou, G., Bucciarelli, E., Blain, S. and Bowie, A.R.: An iron budget during the natural iron fertilisation experiment KEOPS (Kerguelen Islands, Southern Ocean), Biogeosciences, 7, 455-468, 2010b.

Croot, P. and Johanson, M.: Determination of iron speciation by cathodic stripping voltammetry using the competing lignad 2-(2-Thiazolylazo)-p-cresol (TAC), Electroanalysis, 12(8), 565-576, 2000.

de Baar, H.J.W., Boyd, P.X., Coale, K.H., Landry, M.R., Tsuda, A., Assmy, P., Bakker, D.C.E., Bozec, Y., Barber, R.T., Brzezinski, M.A., Buesseler, K.O., Boye, M., Croot, P.L., Gervais, F., Gorbunov, M.Y., Harrison, P.J., Hiscock, W.T., Laan, P., Lancelot, C., Law, C.S., Levasseur, M., Marchetti, A., Millero, F., Nishioka, J., Nojiri, Y., van Oijen, T., Riebesell, U., Rijkenberg, M.J.A., Saito, H., Takeda, S., Timmermans, K.R., Veldhuis, M.J.W., Waite, A.M. and Wong, C.-S.: Synthesis of iron fertilization experiments: From the Iron Age in the Age of Enlightenment, J. Geophys. Res., 110, C09S16, doi:10.1029/2004JC002601, 2005.

Lacan, F., Radic, A., Jeandel, C., Poitrasson, F., Sarthou, G., Pradoux, C. and Freydier, R.: Isotopic Composition of dissolved Iron in the Ocean, Geophys. Res. Lett., 35, L24610, doi:10.1029/2008GL035841, 2008.

Lacan, F., Radic, A., Labatut, M., Jeandel, C., Poitrasson, F., Sarthou, G., Pradoux, C., Chmeleff, J. and Freydier, R.: High-Precision Determination of the Isotopic Composition of Dissolved Iron in Iron Depleted Seawater by Double Spike Multicollector-ICPMS, Anal. Chem., 82, 7103–7111, 2010.

Leal, M.F.C., Vasconcelos, M.T.S.D. and van den Berg, C.M.G.: Copper-induced release of complexing ligands similar to thiols by *Emiliania huxleyi* in seawater culutres, Limnol. Oceanogr., 44(7), 1750-1762, 1999.

Middag, R., de Baar, H.J.W., Laan, P., Cai, P.H. and van Ooijen, J.C.: Dissolved manganese in the atlantic sector of the Southern Ocean, Deep Sea Res. II, doi:10.1016/j.dsr2.2010.10.043, in press, 2011.

Milne, A., Landing, W., Bizimis, M. and Mortona, P.: Determination of Mn, Fe, Co, Ni, Cu, Zn, Cd and Pb in seawater using high resolution magnetic sector inductively coupled mass spectrometry (HR-ICP-MS), Anal. Chim. Acta, 665, 200–207, 2010.

Moffett, J.W. and Dupont, C.: Cu complexation by organic ligands in the sub-arctic NW Pacific and Bering Sea, Deep-Sea Res. I, 54, 586–595, 2007.

Morel, F.M.M. and Price, N.M.: The biogeochemical cycles of trace metals in the Oceans, Science, 300(5621), 944 - 947, DOI: 10.1126/science.1083545, 2003.

Obata, H., Karatani, H. and Nakayama, E.: Automated determination of iron in seawater by chelating resin concentration and chemiluminescence, Anal. Chem., 65, 1524-1528, 1993.

Peers, G. and Price, N.M.: Copper-containing plastocyanin used for electron transport by an oceanic diatom, Nature, 441, 341-344, 2006.

Pollard, R., Sanders, R., Lucasa, M. and Statham, P.: The Crozet Natural Iron Bloom and Export Experiment (CROZEX), Deep Sea Res. II, 54(18-20), 1905–1914, 2007.

Rue, E.L. and Bruland, K.W.: Complexation of iron(III) by natural organic ligands in the Central North Pacific as determined by a new competitive ligand equilibration/adsorptive cathodic stripping voltammetric method, Mar. Chem., 50(1-4), 117-138, 1995.

Sarthou, G., Baker, A.R., Blain, S., Achterberg, E.P., Boye, M., Bowie, A.R., Croot, P.L., Laan, P., de Baar, H.J.W., Jickells, T.D. and Worsfold, P.J.: Atmospheric iron deposition and sea-

surface dissolved iron concentrations in the eastern Atlantic Ocean, Deep Sea Res. I, 50(10-11), 1339-1352, 2003.

Schlosser, C. and Croot, P.L.: Application of cross-flow filtration for determining the solubility of iron species in open ocean seawater, Limnol. Oceanogr.: Methods, 6, 630–642, 2008.

Schlosser, C. and Croot, P.L.: Controls on seawater Fe(III) solubility in the Mauritanian upwelling zone, Geophys. Res. Lett., 36, L18606, doi:10.1029/2009GL038963,, 2009.

Sunda, W.G.: Trace metal/phytoplankton interactions in the sea, In: G.B.a.W. Stumm (Editor), Chemistry of Aquatic systems: Local and Global Perspectives. ECSC, EEC, EAEC, Brussels and Luxembourg, pp. 213-247, 1994.

van Beek, P., Bourquin, M., J.-L., R., Souhaut, M., Charrette, M.A. and Jeandel, C.: Radium isotopes to investigate the water mass pathways on the Kerguelen Plateau (Southern Ocean), Deep Sea Res. II, 55(5-7), 622-637, 2008.

Wu, J., Boyle, E., Sunda, W. and Wen, L.-S.: Soluble and colloidal iron in the oligotrophic North Atlantic and North Pacific, Science, 293, 847-849, 2001.

Zhang, Y., Lacan, F. and Jeandel, C.: Dissolved rare earth elements tracing lithogenic inputs over the Kerguelen Plateau (Southern Ocean), Deep Sea Res. II, 55(5-7), 638-652, 2008.

Acknowledgements

We would like to thank the crew of the R.V. Marion-Dufresne, for all their efforts in helping us during the TMR and Go-Flo operations and on-board incubations. We also acknowledge the Chief Scientist Bernard Quéguiner. We would also like to thank Michael Ellwood from the Australian National University for the loan of the TMR for KEOPS-2.

15 Particulate iron dynamics and related projects

Principal investigator

Andrew R. Bowie
Antarctic Climate & Ecosystems CRC, University of Tasmania,
Private Bag 80, Hobart, TAS 7001, Australia
☎ +61 3 6226 2509
🖷 +61 3 6226 2440
Andrew.Bowie@utas.edu.au

Names of other participants

- Pier van der Merwe (ACE CRC)
- G. Sarthou (LEMAR/IUEM)
- F. Quéroué (LEMAR/IUEM)

Abstract:
Dominant 'new' iron fluxes for iron biogeochemical budgets may be associated with particulate phases. This KEOPS-2 project will measure iron and other geochemical 'fingerprint' trace elements in the particulate phase in both suspended and sinking particles. In collaboration, we will also constrain iron-to-carbon (Fe/C) ratios through the water column and in exported particles. Measurement of dissolved trace elements will be achieved through collaboration with the group of Geraldine Sarthou.

15.1 Scientific context

KEOPS-1 demonstrated that the natural fertilisation of the Southern Ocean resulted in dramatic changes in the functioning of the ecosystem with large impacts on the biogeochemical cycles. A study of waters downstream of island land masses such as Kerguelen represents an excellent approach to examine biogeochemical cycling in the Southern Ocean, because it can address the effects of persistent, varying and multiple iron sources that are not accessible through deliberate mesoscale fertilisation experiments. The interaction of the waters and plateau in the Kerguelen- Heard Island region with several circumpolar fronts of the broader Southern Ocean also allows us to place our regional observations within a global context. KEOPS-1 highlighted the interest of natural laboratories in the context of iron fertilisation of the ocean, but they could cover only a small part of the potential new findings in the region (Blain *et al.*, 2007).

The formation, consumption, sinking and remineralisation of organic matter dominate the biogeochemistry of iron in the ocean. The particulate phase thus represents an important transport vector for trace metals in the marine ecosystem. Since iron is actively taken up into phytoplankton, and transferred throughout the food-web, including removal by particle settling and remineralisation in deep waters, the assessment of its availability is quite complex and cannot be judged from dissolved iron levels in surface waters alone. A simple one dimensional vertical model that correctly represented the input of dissolved iron to surface waters during KEOPS-1 did not accurately represent the supply of other geochemical tracers or particulate iron. Few previous studies have concurrently measured iron associated with different phases (dissolved and particulate), or quantified by observation iron export losses from surface waters. The results from earlier work during FeCycle (Boyd *et al.*, 2005; Frew *et al.*, 2006), KEOPS-1 (Blain *et al.*, 2007; Chever *et al.*, 2009), Crozex (Planquette *et al.*, 2007, 2009) and SAZ-Sense (Bowie *et al.*, 2009) have highlighted that the dominant 'new'

iron fluxes for iron biogeochemical budgets are associated with the particulate phase. Suspended particles have been shown to be important aspects of sedimentary, boundary layer iron sources and export processes. Results from these projects also indicate that biological iron 'demand' cannot be satisfied by the 'new' iron supply. The biological cycling of particulate iron may therefore be the most important aspect of the complete iron biogeochemical cycle, although it's role earlier in the season (winter stock) has yet to be ascertained.

15.2 Overview of the project and objectives

This project will address important uncertainties through the measurement of iron and other geochemical 'fingerprint' tracers (such as aluminium and manganese that confirm the provenance of iron supplied from shelf sediments) in the particulate phase in both suspended and sinking particles. In collaboration with other KEOPS-2 projects, we will also constrain iron-to-carbon (Fe/C) ratios through the water column and in exported particles. The program of research links closely with other planned KEOPS-2 science, in particular projects led by Tom Trull (carbon export), Géraldine Sarthou and Fabien Queroue (dissolved iron), Frank Dehairs and Frederick Planchon (234Th based export production, remineralisation), and Pieter van Beek, Catherine Jeandel, Francois Lacan and Ester Garcia (iron isotopes, radionuclides and geochemical tracers).

15.3 Methodology and sampling strategy

All sampling and analytical methods were performed following recommended international GEOTRACES guidelines. All methods have been successfully used during the SAZ-Sense project (Bowie *et al.*, 2009).

- In situ pumps (ISPs): Suspended particulate trace metal samples were collected in situ using a 142 mm diameter stack consisting of a 53 µm nylon screen (filter SEFAR-PETEX®; polyester) and a QM-A quartz fibre filter (~1 µm porosity, Pall Life) supported by a 350 µm polyester screen. Prior to use PETEX screens were conditioned by soaking in HCl 5 %, rinsed with Milli-Q grade water, dried at ambient temperature under a laminar flow hood and were stored in clean plastic zip-loc bags. QMA filters were conditioned for trace-metal analysis (pre-combustion and acid bath; Bowie *et al.*, 2010). Filter stacks were housed in large volume McLane WTS6-1-142LV and Challenger Oceanics pumps (ISPs) suspended on hydrowire. Sub-samples for trace metals were taken from the QM-A filters using a circular plastic punch (13 mm diameter), and by cutting the nylon mesh using ceramic scissors. Sub-samples were also taken for 234Th activity (see report by Planchon *et al.*) and Chl-*a* (report by V. Cornet). Aliquots dedicated to compound specific isotope analysis (CSIA) were packed in cryotubes and stored at -80°C till processing in the home-laboratory (see report of Cavagna *et al.*).
- Sediment traps: Sinking particulate trace metal samples were collected in separate cups using a PPS3/3 free-floating sediment trap (full details in report of Trull *et al.*), and filtered off-line onto a 47 mm diameter, 2 µm porosity polycarbonate filter (using a 350 µm porosity Teflon PFA pre-screen to exclude zooplankton 'swimmers'). Sampled particles will be acid digested and analysed by magnetic sector inductively coupled plasma mass spectrometry (Bowie *et al.*, 2010).
- Trace metal rosette (TMR): Methods for sampling and processing from the trace metal rosette (TMR) will be included in the cruise report of Sarthou *et al.* Dissolved samples will be analysed for a series of trace elements (Mn, Fe, Co, Ni, Cu, Zn, Cd and Pb) using an isotope dilution high resolution magnetic sector inductively coupled mass spectrometry (HR-ICP-MS) method following Milne *et al.*, (2010).

Table XXI : Exhaustiv list of measured parameters

Parameter	code of operation	units
1. Dissolved iron[1]	TMR	nmol l^{-1}

2. Dissolved trace elements (Mn, Fe, Co, Ni, Cu, Zn, Cd and Pb)[1]	TMR	nmol l^{-1}
3. Particulate iron (suspended)	ISP	nmol l^{-1}
4. Particulate trace elements (suspended)[2]	ISP	nmol l^{-1}
5. Particulate iron (sinking)	PPS3/3 trap	nmol l^{-1}
6. Particulate trace elements (sinking)[2]	PPS3/3 trap	nmol l^{-1}

1 Collaboration with Géraldine Sarthou and Fabien Quéroué

2 Up to 17 trace elements will be analysed by ICP-MS (Mo, Cd, Ba, Pb, U, Al, P, Ti, V, Cr, Mn, Fe, Co, Ni, Cu, Zn, Ga)

15.4 Preliminary results

Analysis of samples for particulate trace elements will take place in the home laboratory at the University of Tasmania in 2012. Shipboard data for dissolved iron will be included in the cruise report of Geraldine Sarthou and Fabien Queroue.

15.5 Post-cruise sampling analyses and dead-lines

Analysis of samples for particulate trace elements will take place in the home laboratory at the University of Tasmania in 2012. Data will be ready to be presented at the KEOPS-2 workshop in September 2012.

15.6 Data base organization (general cruise base and/or specific data base(s))

Data will be posted on the KEOPS-2 database in a timely manner after analysis and processing.

15.7 References of methods

Blain S. *et al.*, 2007. Effect of natural iron fertilization on carbon sequestration in the Southern Ocean. Nature 446, 1070-1074

Boyd P.W. *et al.*, 2005. FeCycle: Attempting an iron biogeochemical budget from a mesoscale SF6 tracer experiment in unperturbed low iron waters. Global Biogeochemical Cycles 19, GB4S20, doi:10.1029/2005GB002494

Bowie A.R., Townsend A.T., Lannuzel D., Remenyi T., van der Merwe P., 2010. Modern sampling and analytical methods for the determination of trace elements in marine particulate material using magnetic sector ICP-MS. Analytica Chimica Acta, 676 (1-2) 15-27, doi: 10.1016/j.aca.2010.07.037

Bowie A. R., Lannuzel D., Remenyi T.A., Wagener T., Lam P.J., Boyd P.W., Guieu C., Townsend A.T., Trull T.W., 2009. Biogeochemical iron budgets of the Southern Ocean south of Australia: Decoupling of iron and nutrient cycles in the subantarctic zone by the summertime supply. Global Biogeochemical Cycles 23, GB4034, doi: 10.1029/2009GB003500

Chever F., Sarthou G., Bucciarelli E., Blain S., Bowie A.R., 2009. An iron budget during the natural iron fertilization experiment KEOPS (Kerguelen Island, Southern Ocean). Biogeosciences 7, 455–468

Frew, R.D., Hutchins D.A., Nodder S., Sanudo-Wilhelmy S., Tovar-Sanchez A., Leblanc K., Hare C.E., Boyd P.W.,2006. Particulate iron dynamics during FeCycle in subantarctic waters southeast of New Zealand. Global Biogeochemical Cycles 20, GB1S93, doi:10.1029/2005GB002558.

Milne A., Landing W., Bizimis M, Morton P., 2010. Determination of Mn, Fe, Co, Ni, Cu, Zn, Cd and Pb in seawater using high resolution magnetic sector inductively coupled mass spectrometry (HR-ICP-MS). Analytica Chimica Acta 665, 200–207

Planquette H. *et al.*, 2007. Dissolved iron in the vicinity of the Crozet Islands, Southern Ocean.

Deep-Sea Research II 54(18-20), 1999-2019
Planquette H., Fones G.R., Statham P.J., Morris P.J., 2009. Origin of iron and aluminium in large particles (>53 μm) in the Crozet region, Southern Ocean. Marine Chemistry 115 (2009) 31–42

16 On-board Fe-Cu and Fe-Mn incubations

Principal investigator

Géraldine Sarthou
Technopôle Brest Iroise, Place Nicolas Copernic, F-29280 Plouzané
☎ 00- 33- 2 98 49 86 55
🖷 00- 33- 2 98 49 86 45
Geraldine.Sarthou@univ-brest.fr

Other participants

- Fanny Chever(LEMAR/UMR-CNRS6539/IUEM)
- Fabien Quéroué (LEMAR/UMR-CNRS6539/IUEM – ACE/CRC)
- Andy Bowie (ACE/CRC)
- Pier van der Merwe ((ACE/CRC)
- Eva Bucciarelli (LEMAR/UMR-CNRS6539)

Résumé :

Notre objectif au cours de la campagne KEOPS 2 était d'étudier les co-impacts Fe-Cu et Fe-Mn sur les paramètres physiologiques du plancton, ainsi que sur les liens entre ces co-limitations potentielles et la spéciation physique et organique de ces différents métaux. Pour cela, des incubations ont été réalisées à bord avec des ajouts combinés de Fe, Cu et Mn à quatre stations (A3-1, R, E3 et E4-E). La plupart des paramètres sera analysée au retour au laboratoire. Les résultats préliminaires obtenus à partir des mesures de nutriments et de Chla, réalisées à bord suggèrent qu'une addition en fer stimule la croissance, alors que les additions de Cu et Mn semblent avoir des effets contrastés.

Abstract:

During KEOPS 2, our objective was to study the co-impact Fe/Cu and Fe/Mn on plankton physiology, as well as the link between these potential co-limitations and the physical and organic speciation of these trace metals. We carried out on-board incubations at four different stations (A3-1, R, E3 and E4-E). Most of the parameters will be analysed back to the Laboratory. However, preliminary results from on-board measurements of Chla and nutrients suggest that Fe additions enhanced chlorophyll levels and nutrient depletion at all stations, while Cu and Mn appeared to have contrasting effects.

16.1 Scientific context

The limiting role of trace metals and particularly iron (Fe) in controlling phytoplanktonic production and the structure of the planktonic community has now been largely admitted in the Southern Ocean (Boyd et al., 2007, Blain et al., 2007). Other metals, such as copper (Cu) and manganese (Mn), also play a key role in the biological pump of carbon. Recent studies showed that the biological demand for iron might be linked to Cu (Peers et al., 2005). Our own studies, conducted during the international Bonus-Goodhope cruise in the Southern Atlantic Ocean (Feb.-March 2008), clearly indicate that Cu not only partly controls the intensity of the Fe impact, but may even control pri-

mary production by itself (Sarthou et al., 2009). Mn is also an essential element for algal growth, being a key component of carbon fixation processes (Sunda, 1988-1989). Moreover there is increasing evidence that Fe/Mn co-limitations impact Fe acquisition by marine phytoplankton (Peers and Price, 2004). Recent studies also suggest that Mn may disrupt Fe uptake through reactions with microbial siderophores (Duckworth et al., 2009).

16.2 Overview of the project and objectives

During the KEOPS 2 cruise, we aimed at better determine the effect of Fe, Fe-Cu and Fe-Mn additions on the growth parameters of the phytoplanktonic community in on-deck incubations, and the bioavailable form of Fe in these incubations.

16.3 Methodology and sampling strategy

On-board Fe-Cu and Fe-Mn incubations were performed at four stations (A3-1, R, E3 and E4-E). At station A3, seawater for incubations was collected between 40 and 80 m, using acid-cleaned Go-Flo bottles mounted on a 6 mm Kevlar hydrowire. The bottles were individually attached to the synthetic line and triggered at depth using Teflon messengers. For the three other stations, seawater was collected using a Trace Metal Clean Rosette (General Oceanics Inc. Model 1018 Intelligent Rosette), attached to a 6 mm Kevlar hydrowire.

Seawater was gently mixed in acid-cleaned 30-l Nalgene polyethylene carboys, then immediately transferred into acid-cleaned 2.4-l Nalgene polycarbonate bottles.

The 2.4-l experimental containers were immediately amended with Fe and/or Cu, and/or Mn as described below, then set in circulating surface seawater inside Plexiglas incubators located on deck. Each incubator was individually covered with LEE Filters (Pale Blue 063) to mimic a 50% of incident light.

Table XXII : Stations, with latitude, longitude, starting and ending dates, and experimental treatments at which incubations were performed.

Station	Latitude	Longitude	Starting date	Ending date	Experimental treatment
A3-1	50°38.7257' S	72°1.839'E	20/10/2011	29/10/2011	Control + Fe (1 nM) + Cu (0.5 nM) + Mn (1 nM)
R	50°23.37'S	66°41.57'E	27/10/2011	10/11/2011	Control + Fe (1 nM) + Cu (0.5 nM) + Mn (1 nM)
E3	48°42.0686'S	71°58.0193'E	04/11/2011	17/11/2011	Control + Fe (1 nM) + Cu (0.5 nM) + Mn (1 nM)
E4E	48°42.9292'S	72°33.7705'S	114/11/2011	22/11/2011	Control + Fe (1 nM) + Cu (0.5 nM) + Mn (1 nM)

Table XXIII : Exhaustive list of measured parameters

Parameter	code of operation	units
1. Fe physical speciation (TdFe - unfiltered, dFe – filtrered through 0.2 µm, sFe – filtered through 0.02 µm)	TMR	nM
2. Other Trace Metal physical speciation (unfiltered and filtered through 0.2 µm)	TMR	nM
3. Fe and Cu organic speciation	TMR	nM
4. pH	TMR	
5. Nutrients	TMR	µM
6. Bacterial counting	TMR	Cells/ml
7. Domoic acid	TMR	µM
8. Biogenic silica	TMR	µM
9. POC/PON	TMR	µM
10. Chla	TMR	µg/L
11. Taxonomy	TMR	Cells/ml
12. Enzymatic activity	TMR	
13. Proteomic/transcriptomic	TMR	

16.4 Preliminary results

Most of the parameters will be analysed at the laboratory. The physical speciation of Fe will be analysed by flow injection analysis following the method by Obata et al., (1993), modified by Sarthou et al. (2003). Dissolved trace metals (Mn, Fe, Co, Ni, Cu, Zn, Cd and Pb) will be analysed using an isotope dilution high resolution magnetic sector inductively coupled mass spectrometry (HR-ICP-MS) method following Milne et al., (2010). Fe and Cu organic speciation will be analysed by cathodic stripping voltammetry (Croot and Johanson, 2000, Leal et al., 1999). Nutrients and some samples for Chla were analysed on board. Preliminary results confirm that Fe additions enhanced chlorophyll levels and nutrient depletion at all stations, while Cu and Mn appeared to have contrasting effects.

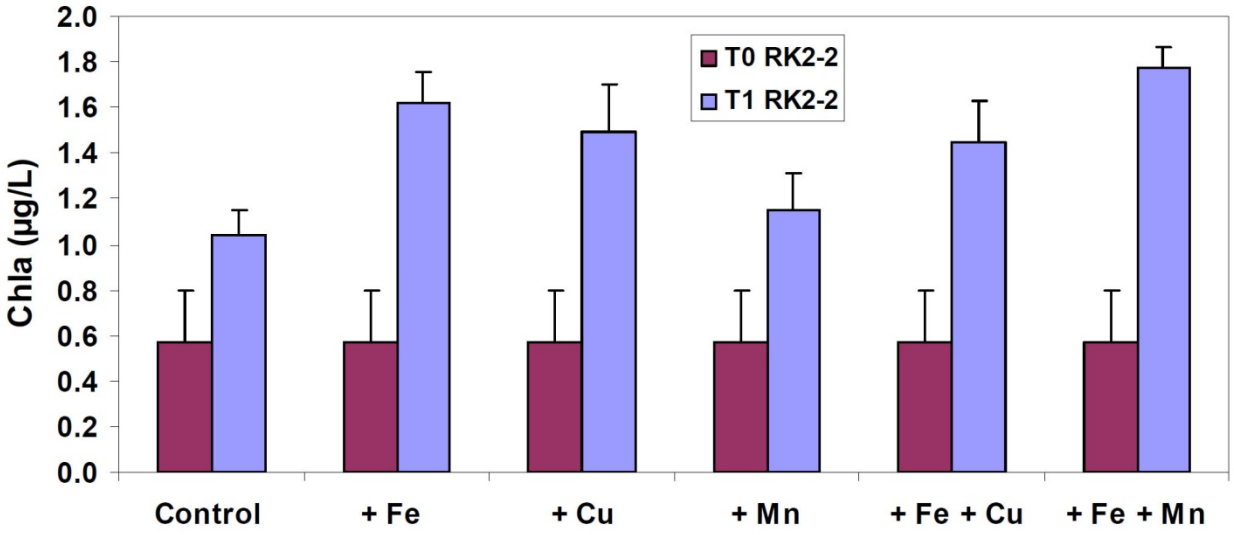

Figure 1: Example of the evolution of Chla between T0 and T1 (4 days) at station R2 for the different treatments.

16.5 Post-cruise sampling analyses and dead-lines

The analyses of all the parameters should be completed in the next 12-18 months.

16.6 Data base organization

Data will be posted on the KEOPS-2 database in a timely manner after analysis and processing.

16.7 References

Blain, S., Quéguiner, B., Armand, L., Belviso, S., Bombled, B., Bopp, L., Bowie, A., Brunet, C., Brussaard, C., Carlotti, F., Christaki, U., Corbière, A., Durand, I., Ebersbach, F., Fuda, J.-L., Garcia, N., Gerringa, L., Griffiths, B., Guigue, C., Guillerm, C., Jacquet, S., Jeandel, C., Laan, P., Lefèvre, D., Lomonaco, C., Malits, A., Mosseri, J., Obernosterer, I., Park, Y.-H., Picheral, M., Pondaven, P., Remenyi, T., Sandroni, V., Sarthou, G., Savoye, N., Scouarnec, L., Souhaut, M., Thuiller, D., Timmermans, K., Trull, T., Uitz, J., van-Beek, P., Veldhuis, M., Vincent, D., Viollier, E., Vong, L. and Wagener, T.: Impact of natural iron fertilization on carbon sequestration in the Southern Ocean, Nature, 7139, 1070-1074, 2007.

Boyd, P.W., Jickells, T., Law, C.S., Blain, S., Boyle, E.A., Buesseler, K.O., Coale, K.H., Cullen, J.J., Baar, H.J.W.d., Follows, M., Harvey, M., Lancelot, C., Levasseur, M., Owens,

N.P.J., Pollard, R., Rivkin, R.B., Sarmiento, J., Schoemann, V., Smetacek, V., Takeda, S., Tsuda, A., Turner, S. and Watson, A.J.: Mesoscale Iron Enrichment Experiments 1993–2005: Synthesis and Future Directions, Science, 315, 612-617, 2007.

Croot, P. and Johanson, M.: Determination of iron speciation by cathodic stripping voltammetry using the competing lignad 2-(2-Thiazolylazo)-p-cresol (TAC), Electroanalysis, 12(8), 565-576, 2000.

Duckworth, O.W., Bargar, J.R. and Sposito, G.: Coupled biogeochemical cycling of iron and manganese as mediated by microbial siderophores, BioMetals, 22, 602-613, 2009.

Leal, M.F.C., Vasconcelos, M.T.S.D. and van den Berg, C.M.G.: Copper-induced release of complexing ligands similar to thiols by *Emiliania huxleyi* in seawater culutres, Limnol. Oceanogr., 44(7), 1750-1762, 1999.

Milne, A., Landing, W., Bizimis, M. and Mortona, P.: Determination of Mn, Fe, Co, Ni, Cu, Zn, Cd and Pb in seawater using high resolution magnetic sector inductively coupled mass spectrometry (HR-ICP-MS), Anal. Chim. Acta, 665, 200–207, 2010.

Obata, H., Karatani, H. and Nakayama, E.: Automated determination of iron in seawater by chelating resin concentration and chemiluminescence, Anal. Chem., 65, 1524-1528, 1993.

Peers, G. and Price, N.M.: A role for manganese in superoxide dismutases and growth of iron-deficient diatoms, Limnol. Oceanogr., 49(5), 1774–1783, 2004.

Sarthou, G., Baker, A.R., Blain, S., Achterberg, E.P., Boye, M., Bowie, A.R., Croot, P.L., Laan, P., de Baar, H.J.W., Jickells, T.D. and Worsfold, P.J.: Atmospheric iron deposition and sea-surface dissolved iron concentrations in the eastern Atlantic Ocean, Deep Sea Res. I, 50(10-11), 1339-1352, 2003.

Sarthou, G., Bucciarelli, E. and Chever, F.: The co-impact of iron and copper on phytoplankton growth in the South Atlantic and the Southern Ocean, ASLO, Ocean Sciences Meeting 2009, , Nice, France, 2009.

Sunda, W.G.: Trace metal interactions with marine phytoplankton, Biol. Oceanogr., 6(5-6), 411-442, 1988-1989.

Acknowledgement

We greatly acknowledge Louise Oriol, Jocelyne Caparro and Audrey Gueguenes for nutrient analyses. We would also like to thank the crew of the R.V. Marion-Dufresne, for all their efforts in helping us during the TMR and Go-Flo operations and on-board incubations. We also acknowledge the Chief Scientist Bernard Quéguiner and the project PI Stéphane Blain. We thank S.B. and Marion Fourquez, for their help during the TMR deployment. We would also like to thank Michael Ellwood from the Australian National University for the loan of the TMR for KEOPS-2.

17 Iron-limitation and heterotrophic bacteria: Insights from experimental studies

Principal investigator

Ingrid Obernosterer
LOMIC, 66650 Banyuls sur mer, France
☎ +33 468 887 353
🖷 +33 468 887 398
Ingrid.obernosterer@obs-banyuls.fr

Names of other participants

- Stéphane Blain (LOMIC)

Résumé :
Durant KEOPS1, la demande à court terme du fer dissous par le phytoplancton n'était pas couverte par les apports de fer nouveau. La biodisponibilité d'une partie du fer lithogénique pourrait constituer une autre source de fer nouveau. C'est cette hypothèse qui a été expérimentalement testée dans ce projet. En parallèle des expériences ont également été réalisées pour mieux comprendre le rôle potentiellement limitant de la matière organique dissoute et du fer sur l'activité bactérienne.

17.1 Scientific context

During KEOPS 1, a surprising finding was that the short term (day) balance between the net biological iron demand and the iron supply required the use of a missing term that accounted for 70% of the iron supply. Remineralisation of iron was already considered in this budget, thus the missing flux had to be provided by new sources of iron, that are the winter stock and the use of part of the lithogenic particulate iron stock. However, none of these hypotheses could be confirmed or refuted on the basis of the KEOPS 1 data set. The biological availability of lithogenic particulate or colloidal iron is also largely unknown due to experimental difficulties. However, the results of KEOPS 1 strongly suggest that part of these fractions are available as new sources of iron. Biologically-mediated dissolution of particulate lithogenic iron most likely occurred, probably related to bacteria-mediated siderophore production. Whether iron is a limiting factor for bacterial growth will determine the extent to which heterotrophic bacteria apply strategies to access non-bioavailble iron sources. The question whether carbon or iron represent the first limiting nutrient in the Kerguelen study region has not been extensively addressed thus far.

17.2 Overview of the project and objectives

The two questions we wanted to address during KEOPS2 are:

1) Are heterotrophic bacteria C or Fe limited in the study region?
2) What is the role of the bacterial community in making particulate iron bioavailable?

We adressed these questions by experimental approaches as detailed below.

17.3 Methodology and sampling strategy

To better understand the role of heterotrophic bacteria in the iron cycle, we performed two types of experiments.

1) Enrichment Experiments : At 4 Stations (R, E3, E4_W, E5) seawater was sampled in the

surface mixed layer, using the trace métal clean rosette. Incubations were done with raw seawater (300mL) amended with glucose (10 µM final conc.), Fe (1 nM final conc.) or a combination of both. Unamended seawater incubations served as control. Incubations were performed in the dark, at 4°C. The bacterial response to C-or Fe-additions were followed by measurements of bacterial abundance and leucine incorporation over time.

2) Fe-particle experiment : At Station A3, Particles (< 53 µm) were collected on a 0.8 µm SUPOR filter using the challenger ISP. The particles were recovered from the filter and one part of the particles was killed by microwaving for 5 min. The killed and live particles were subsequently resuspended in 0.2 µm filtered seawater and 1 mL was transferred to dialysis bags. Twelve batch cultures (4 treatments in triplicates) were prepared containing 1) a dialysis bag with live particles 2) a dialysis bag with killed particles, 3) dialysis bag with 0.2 µm filtered seawater and 4) 1mL of particle suspension. Incubations were performed in the dark for 3 weeks. Samples for bacterial abundance and activity, dissolved iron concentration and iron solubility were collected every 3 days. At the end of the experiment, additional samples were collected for bacterial diversity and concentration of iron ligands. The content of the dialysis bags was filtered on a 0.2 µm PC filter, PFA-fixed and stored at -20°C.

Table XXIV : Exhaustiv list of measured parameters

Parameter	code of operation	units
1. Fe vs C limitation experiment	TMR followed by Process Experiment	
2. Fe-Particle experiment	TMR, ISP followed by Process Experiment	

17.4 Preliminary results

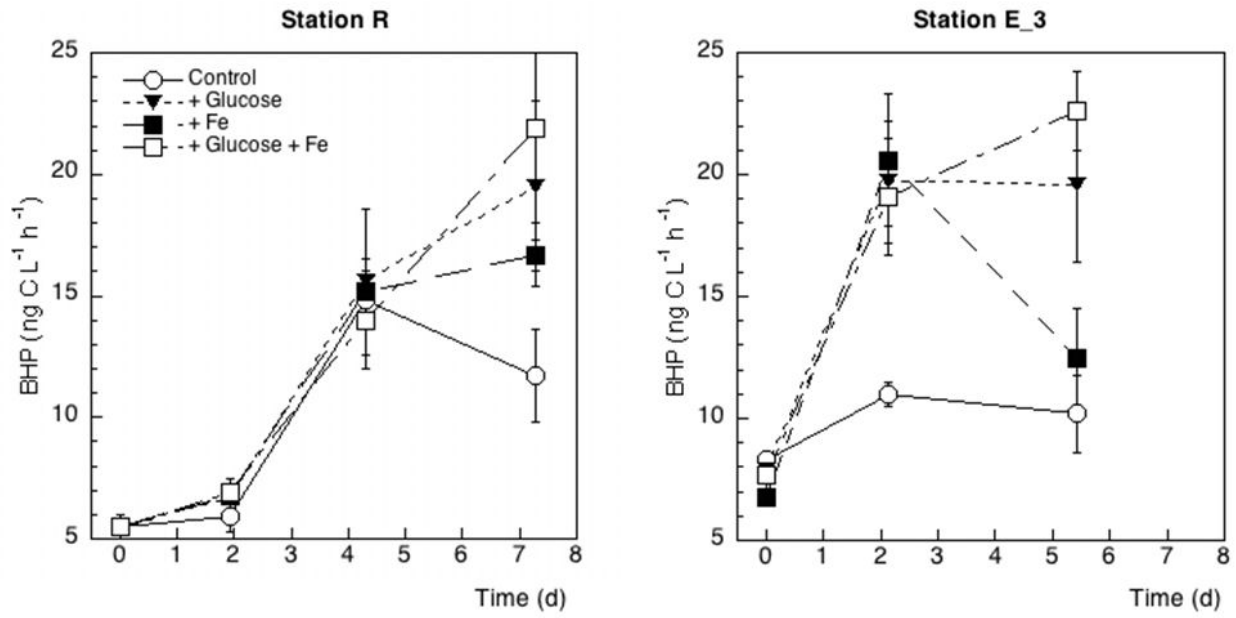

Figure 35 : Bacterial heterotrophic production (BHP) over time in bottle enrichment experiments. Each data point reflects the mean and standard deviation of triplicate biological incubations.

17.5 Post-cruise sampling analyses and dead-lines:

The flow cytometric analyses will be finished by June 2012. The molecular and analyses will take approximately 2-3 years. Chemical analyses will be done in 2012.

17.6 Data base organization

17.7 Reference of method

Lebaron, P., Servais, P., Agogue, H., Courties, C., Joux, F., 2001a. Does the high nucleic acid content of individual bacterial cells allow us to discriminate between active cells and inactive cells in aquatic systems? Appl. Environ. Microbiol. 67, 1775-1782.

18 Iron uptake and cellular iron contents of phytoplankton and microbial communities

Principal investigator

Marion Fourquez
LOMIC UMR7621, 1 avenue du Fontaulé 66650 Banyuls-sur-mer
☎ (+33) 4 68 88 73 54
e-mail: marion.fourquez@obs-banyuls.fr

Names of other participants

- Stéphane Blain (LOMIC UMR7621)

Résumé :
L'objectif de ce projet est d'étudier la compétition pour l'accès à la ressource en fer entre bactéries hétérotrophes et phytoplancton. Les vitesses d'assimilation du fer ont été déterminées en utilisant le radioisotope ^{55}Fe lors d'incubations d'échantillons prélevés dans des conditions « trace metal clean ». L'influence de la lumière sur l'assimilation a aussi été étudiée. Par ailleurs afin de mieux comprendre quels sont les acteurs principaux de la communauté bactérienne hétérotrophe qui contribuent à l'assimilation du fer, des échantillons ont été incubés et traités pour une analyse ultérieure par la méthode MAR-FISH.

18.1 Scientific context

Iron is a crucial element for several metabolic processes such as photosynthesis or respiration. However, its low bioavailability in seawater leads to limit the primary production and the CO_2 drawdown associated in large regions of the global ocean as the Southern Ocean. Bacteria also require iron for their growth and consequently they can compete with phytoplankton for the resource of iron. However, the iron content cell of natural plankton and bacterial cells remains less investigated in these regions. To improve our understanding on the role played by phytoplankton and microbial communities in the biogeochemical cycle of iron, we assessed the iron uptake rate by incubation with ^{55}Fe and size fractioning.

Several studies have reported the importance of microbial bacterial communities in the biogeochemical cycle of iron, however the capability of different bacterial groups to access various chemical forms of iron is, ignored thus far.

18.2 Overview of the project and objectives

The aim of the study was to investigate the competition between heterotrophic bacteria and phytoplankton for iron resource in contrasted environment (fertilized and non fertilized sites). Our goal was to quantify the uptake rates of Fe and possibly to derive iron content of cells. The competition for iron is also very likely a function of light and of the community composition of phytoplanktonic and heterotrophic bacterial community. Both factors were investigated.

18.3 Methodology and sampling strategy

Seawater from the mixed layer was collected using trace metal clean rosette. Subsequently, subsamples (300 mL) of filtered (<25µm) and unfiltered seawater were spiked with ^{55}Fe at a final concentration of 0.2 nM. Samples were incubated in incubator on the deck at *in situ* temperature for

different level of light: 75%; 45%; 16%; 4% and 1% of the PAR. All incubations started at the sunrise. After 24h of incubation with ^{55}Fe, subsamples were filtered on 0.8 µm and 0.2µm respectively. The size fraction >0.8 µm was dominated by phytoplankton, and the size fraction <0.2 µm was dominated by heterotrophic bacteria. Filters were rinsed with a washing solution to remove extracellular iron. The intracellular ^{55}Fe was determined by counting radioactivity with a scintillation counter. Iron cell content of the cells can then be calculated when the in situ iron concentration is known. Moreover subsamples for flow cytometry were preserved for further analysis.

For microFISH analyses, seawater was filtered on 0.8 µm before ^{55}Fe was added. Incubations were performed in darkness at different amounts of ^{55}Fe (0.2-1-5 and 15 nM of ^{55}Fe added) and several time of incubations (1 to 5 days). Then, cells were collected on filters and conditioned for further analysis in laboratory.

Tableau 1 : Exhaustiv list of measured parameters

Parameter	code of operation	units
Iron uptake rate	TMR	nmol Fe h^{-1}
2. MAR FISH 55Fe	TMR	Cells mL^{-1}

18.4 Preliminary results

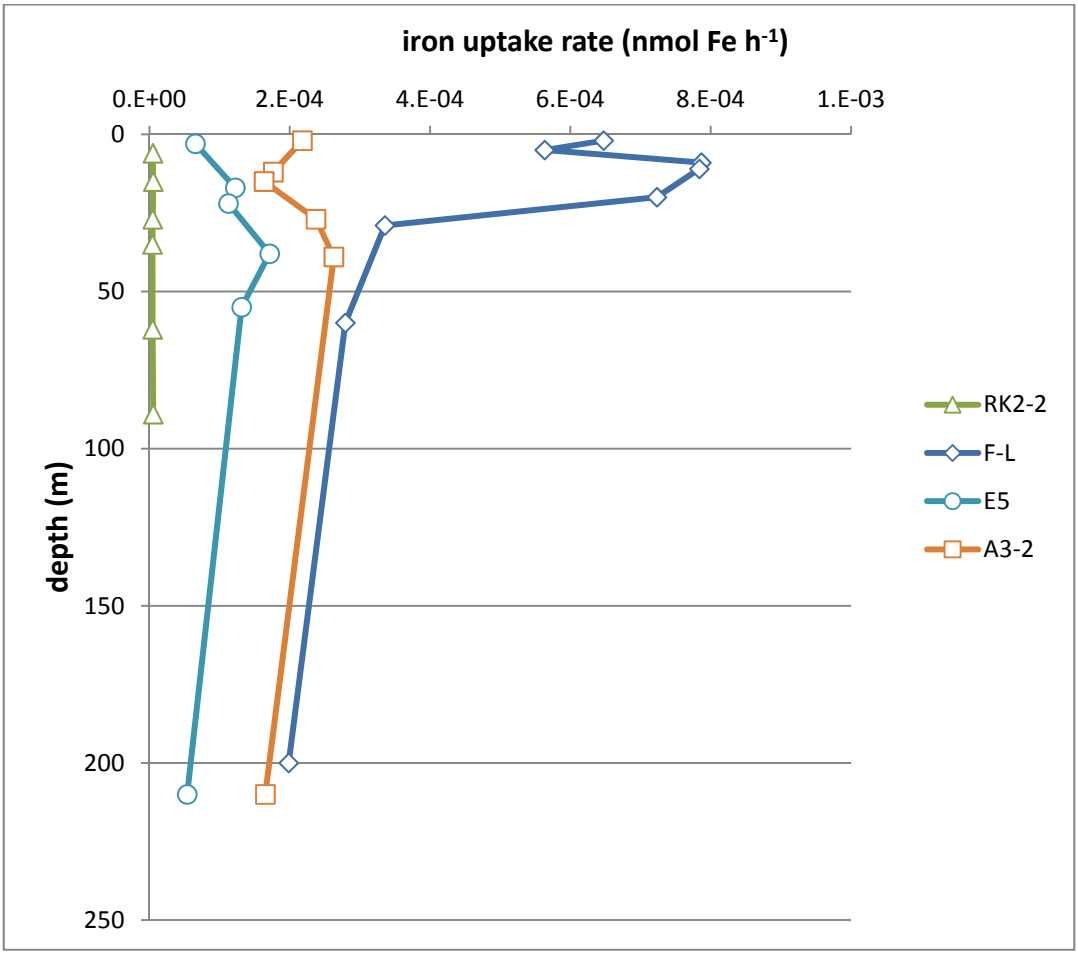

Figure 36 : iron uptake rate of the size fraction 25-0.8 µm (volume of the sample 300 mL) incubated at different light levels. The vertical profile was obtained by placing the iron uptake value at the depth corresponding to the light level of incubation.

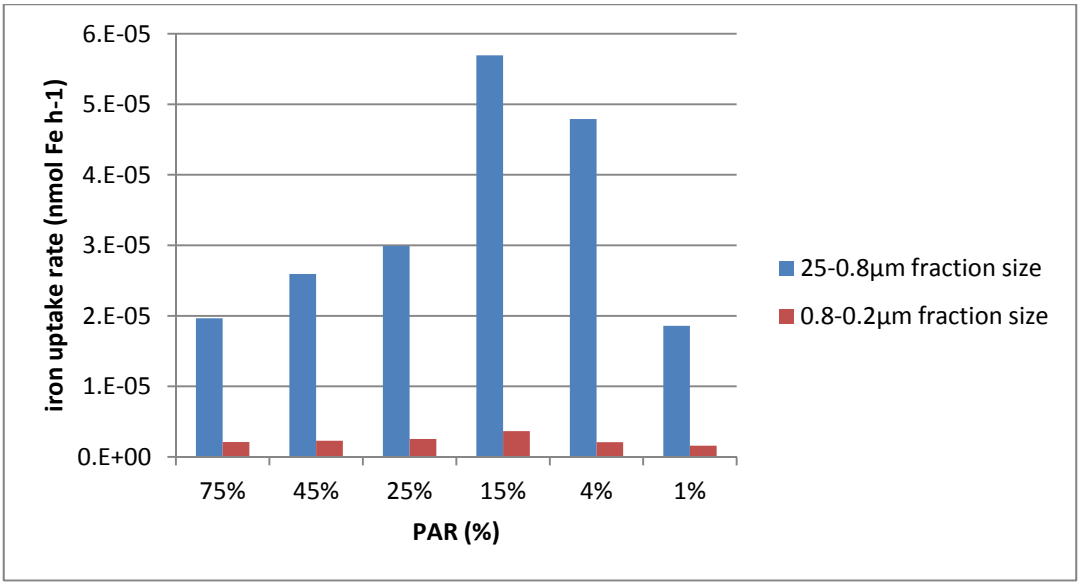

Figure 37 : iron uptake rates for different level of PAR at E1 station. Blue and red bars show the 25-0.8µm and 0.8-0.2µm size fraction, respectively.

18.5 Post-cruise sampling analyses and dead-lines

Samples collected for flow cytometry will be analysed during December 2011. Analysis of the data set will be done for July 2012.

18.6 Data base organization (general cruise base and/or specific data base(s))

General data base

18.7 References of methods

Strepzek R F, Maldonado M T, Higgins J L, Hall J, Safi K, Wilhem S W and Boyd P W. Spinning the ‘‘Ferrous Wheel’’: The importance of the microbial community in an iron budget during the FeCycle experiment (2005) GLOBAL BIOGEOCHEMICAL CYCLES, VOL. 19.

19 Biomolecular and genomic characterization of the microbial community

Principal investigator

Ingrid Obernosterer
LOMIC, 66650 Banyuls sur mer, France
☎ +33 468 887 353
🖷 +33 468 887 398
Ingrid.obernosterer@obs-banyuls.fr

Names of other participants

- Urania Christaki (LOG)
- Marine Landa (LOMIC)
- Nyree West (OOB, Banyuls sur mer, France)

Résumé :
Les résultats obtenus lors de la campagne KEOPS1 ont montré une réponse prononcée de la communauté bactérienne à la fertilisation en fer, en termes d'activité et de diversité. Notre objectif pour la campagne KEOPS2 est d'approfondir notre connaissance du rôle de la communauté bactérienne suite à une fertilisation naturelle, en prenant compte plus d'aspects spatiaux et temporels. Nos objectifs sont d'étudier 1) l'évolution temporelle de l'activité et de la diversité bactérienne face à une effluorescence phytoplanctonique induite par le fer et 2) la diversité bactérienne associée à des communautés phytoplanctoniques différentes. Pour atteindre ces objectifs, l'échantillonnage des communautés bactériennes et phytoplanctoniques *in situ* a été réalisé à des stations contrastées. Ces échantillons seront analysés par des approches moléculaires, qui nous permettront de décrire les changements temporels et spatiaux de la structure de la communauté bactérienne et de suivre l'abondance et l'activité des groupes bactériens d'intérêt. Les analyses métagénomiques et métatranscriptomiques nous permettront de décrire la présence et l'expression des gènes de la communauté microbienne dans des conditions contrastées d'apport en fer et de biomasse phytoplanctonique.

19.1 Scientific context

The previous KEOPS cruise results showed a pronounced response of the bacterial community to the phytoplankton bloom induced by natural iron fertilization. Measurements of bacterial production and respiration indicated that the bacterial community processed a high proportion of primary production. Further, the diversity of the heterotrophic bacterial community associated with the Kerguelen bloom was different from that in HNLC waters. These results relate to the third month of an intense phytoplankton bloom studied during KEOPS1. Based on these results, we hypothesize that the duration of the Kerguelen bloom allowed the microbial community to adapt and eventually to select for the most efficient bacterial groups. KEOPS2 offers an excellent opportunity to address the question of how rapidly heterotrophic bacteria respond to phytoplankton blooms induced by natural iron fertilization in the Southern Ocean, and whether this response is linked to changes in the bacterial diversity. This is important for understanding the contribution of different members of the microbial food web to the cycling of organic carbon and possibly iron, and for identifying the seasonal scenario by combining KEOPS 1 and KEOPS 2 results.

19.2 Overview of the project and objectives

Our main objective is to better understand the response of the bacterial community to natural iron fertilization in the Southern Ocean. We will address the following 3 questions :

1) Which bacterial groups are present and active in the early stages of the Kerguelen bloom? Are they the same bacterial groups which showed high activity and suggested high processing of organic matter at the later stages of the bloom ? Or is there a lag in the establishment of these specific bacterial groups ?
2) Is the bacterial diversity specific to a given water mass with its proper biogeochemical and bloom characteristics ? Can we link phytoplankton and bacterial diversity ?
3) Can gene expression patterns of the microbial community provide insights into key biocheochemical pathways linked to the Fe- and C- cycle ?

19.3 Methodology and sampling strategy

- To determine bacterial and phytoplankton abundance, seawater samples were collected at each station throughout the water column. Raw seawater was fixed with 2% formaldehyde (final conc.) for bacterial abundance, and with 1% glutaraldehyde (final conc.) for phytoplankton abundance. Samples were incubated for 30min at 4°C and subsequently quick-frozen in liquid nitrogen. Samples are stored in a -80°C until analyses on a flow cytometer.
- Samples for bacterial and phytoplankton diversity analyses were collected at each main station at 4 depth layers in the upper 300m water column. For bacterial diversity analyses, small (500ml) and large volumes (5-8 L) of 25 µm prefiltered seawater were sequentially filtered through 3µm, 0.8µm and 0.2µm. For phytoplankton diversity, 9L of 65µm prefiltered seawater was filtered through a 10µm filter. All filters were stored at -80°C. Following extraction and PCR, 16S RNA genes and transcripts will be analysed by fingerprinting methods and/or 454 pyrosequencing.
- MICRO-CARD-FISH samples were collected at each main station at 4 depth layers in the upper 300m water column. Raw seawater samples (10ml, in duplicate) were incubated with radiolabelled leucine for 7-8 hours in the dark, then filtered on a 0.2 µm Polycarbonate filter. The filteres were rinsed with Milli-Q water and are stored at -20°C. MICRO-CARD-FISH analyses will be performed with specifically-designed probes targeting bacterial groups at a narrow phylogenetic level.
- Samples for quantitative PCR (qPCR) were collected at each main station at 4 depth layers in the upper 300m water column. Seawater (25 µm prefiltered) samples (1 L, in triplicate) were rapidly filtered through 3µm, 0.8µm and 0.2µm. All filters were stored in RNA-later at -80°C. Primer sets will be designed for specific bacterial groups or genes of interest and applied to the in situ samples of interest.
- Samples for metagenomic and metatranscriptomic analyses were collected at all main stations at 2 depth layers in the upper 150m water column. For metatranscriptomic analyses, 20L of seawater was prefiltered through 200 µm, then sequently through 5 µm (PC) and 0.2 µm (Supor plus membranes) in less than 10 min. Both filters were stored in RNA-later at -80°C. For metagenomic analyses, 60L of 200µm prefiltered seawater was filtered through 5 µm and 0.2 µm, and the filters were stored at -80°C. For metatranscriptomic analyses of phytoplankton collected with net tows, the cell suspension was diluted in approximately 5L of seawater, and then filtered on 5 µm and 0.2 µm filters. Up to date sequencing techniques will be applied to analyze DNA and mRNA extracts from these filters.

Table XXV : Exhaustiv list of measured parameters

Parameter	code of operation	units
1. Bacterial Abundance	CTD	Cells per ml
2. Phytoplankton Abundance	CTD	Cells per ml
3. 16S RNA gene and transcripts	CTD	Non quantitative (Diversity of total and active bacteria)
4. 18S RNA gene	CTD	Non quantitative (Phyto-plankton diversity)
4.MICRO-CARD-FISH	CTD	Cells per ml (Abundance and activity of bacterial groups)
5. quantitative PCR	CTD	Abundance and expression of genes of interest
6. Metagenomic analyses	CTD, Phytonet	Gene sequences
7. Metatranscriptomic analyses	CTD, Phytonet	Gene sequences

19.4 Preliminary results

At this stage, no results are available.

19.5 Post-cruise sampling analyses and dead-lines:

The flow cytometric analyses will be finished by June 2012. The molecular and genomic analyses will take approximately 3-4 years. The analyses of the MICRO-CARD-FISH samples will take 1-2 years.

19.6 Data base organization

19.7 References of methods

Lebaron, P., Servais, P., Agogue, H., Courties, C., Joux, F., 2001a. Does the high nucleic acid content of individual bacterial cells allow us to discriminate between active cells and inactive cells in aquatic systems? Appl. Environ. Microbiol. 67, 1775-1782.

Marie D, Simon N, Guillou L, Partensky F, Vaulot D (2000) Flow cytometry analysis of marine picoplankton In: De Maggio (ed) In Living Color: Protocols in flow cytometry and cell sorting. Springer Verlag, p 421-454.

20 Linking dissolved organic matter and bacterial diversity: Insights from continuous cultures

Principal investigator

Marine Landa-Bezwierchy (Ph.D. student)
Laboratoire d'Océanographie Microbienne (LOMIC), avenue Fontaulé 66650 Banyuls/mer
☎ +33 4 68 88 73 54
🖷 + 33 4 68 88 73 95
marine.landa@obs-banyuls.fr

Names of other participants

- I. Obernosterer, supervisor (LOMIC, Banyuls)
  ingrid.obernosterer@obs-banyuls.fr
- S. Blain, supervisor (LOMIC, Banyuls)
  stephane.blain@obs-banyuls.fr

Abstract:

Phytoplanktonic and bacterial communities are closely linked in the ocean in terms of presence and activity. Phytoplankton blooms have been known to be associated with bacterial diversity shifts, which is often interpreted as a response of bacteria to the dissolved organic matter (DOM) produced by the blooming phytoplanktonic species. During KEOPS1, the bacterial communities associated with the Kerguelen bloom revealed striking differences to the communities in HNLC waters. KEOPS2 offered us the possibility to address the hypothesis of the phytoplankton-DOM-bacteria relationship, using continuous cultures. Our experiment consisted of two treatments: In one treatment a natural bacterial community was supplied with seawater containing in situ concentrations of DOC, in one treatment the bacterial community was supplied with seawater containing in situ concentrations of DOC amended with roughly 10 µM of DOC produced by a culture of *Chaetoceros* spp. Triplicate cultures for each treatment were carried out for three weeks with frequent sampling for several parameters such as bacterial abundance, DOC and nutrient concentrations, and bacterial diversity. Molecular biology will be the main tool used to investigate the diversity of the bacterial community grown in the two treatments.

Résumé :

Les communautés phytoplanctoniques et bactériennes sont étroitement liées dans l'océan en termes de présence et d'activité. Les blooms phytoplanctoniques sont classiquement associés à des modifications de structure des communautés bactériennes, ce qui est interprété comme une réponse des bactéries à la production de matière organique dissoute (MOD) par les espèces phytoplanctoniques en efflorescence. Pendant KEOPS1, les communautés bactériennes associées au bloom de Kerguelen étaient très différentes des communautés observées en milieu HNLC. Nous avons eu l'opportunité, pendant KEOPS2, de tester l'hypothèse de la relation entre la MOD phytoplanctonique et les bactéries à l'aide de cultures continues. Notre système expérimental était constitué de trois traitements : dans le premier traitement une communauté naturelle de bactéries était alimentée en eau de mer contenant des concentrations de DOC *in situ*, dans le second traitement la communauté bactérienne était alimentée en eau de mer à laquelle environ 10 µM de DOC provenant d'une culture de *Chaetoceros* spp. ont été ajoutés. Les cultures, réalisées en triplicats, ont été maintenues pendant trois semaines et régulièrement échantillonnées de manière à déterminer par la suite divers paramètres tels que l'abondance bactérienne, les concentrations en carbone organique dissous et en nutriments, ainsi que la diversité bactérienne. La biologie moléculaire sera l'outil de référence pour analyser la diversité des communautés bactériennes s'étant développées dans les deux traitements.

20.1 Scientific context

Dissolved organic matter (DOM) is the major source of organic carbon and nutrients for heterotrophic bacteria in the ocean. This DOM is a result of phytoplankton growth and metabolism. As a consequence, bacteria and phytoplankton are tightly linked, since bacteria feed on phytoplankton products and contribute to the remineralization of carbon and nutrients. Many studies show a significant shift in bacterial community structures following a phytoplankton bloom. The hypothesis has been proposed that bacteria present in a given environment respond differently to an input of bioavailable carbon, some bacterial groups being more adapted or faster to degrade the organic compounds than others. It has been suggested that the increase in bioavailable DOC associated with phytoplankton blooms could drive changes in the bacterial community structures observed during and after a bloom event. The question whether the diverse bacterial community equally degrades bioavailable DOC or if there are specialist species with preferences and adaptations to specific compounds remains unresolved.

20.2 Overview of the project and objectives

Continuous cultures were used to test the response of a bacterial community to an increase in bioavailable DOM. The objective was to grow an initial bacterial community under two different culture conditions, that are a seawater only treatment and a seawater + phytoplankton derived DOM treatment. The aim was to maintain the cultures under stable conditions over several generation times to follow the changes in the bacterial community composition induced by the organic compounds available in the two treatments.

20.3 Methodology and sampling strategy

The initial bacterial community (< 0.8 µm fraction) was sampled at Station A3-1 during winter conditions. The 0.2 µm-filtered seawater used to prepare the cultures and the media for the two treatments was also collected at Station A3-1. The bioavailable DOM was produced in the lab before the cruise. A diatom typical of the Kerguelen site (*Chaetoceros debilis*) was cultivated in artificial seawater containing very low carbon concentrations (around 15 µM). After a few weeks of culture the DOM was collected by filtering the culture on a 0.2 µm filter. The DOC concentration wasaround100 µM, corresponding to the bioavailable DOM produced by the phytoplankton culture.

The continuous cultures were carried out in six polycarbonate carboys, three for each treatment, at stable temperature (around 6°C) in the dark. Every two days the six carboys were sampled for DOC and nutrient concentrations, as well as bacterial abundance, and diversity. Some incubations were also conducted to measure enzymatic activities (alpha- and beta-glycosidase, and leucine aminopeptidase).

Table XXVI : Exhaustive list of measured parameters

Parameter	code of operation	units
Chemostat Experiment	TMR followed by process experiment	

20.4 Preliminary results

Most of the analyses will be conducted back in Banyuls. Nutrient concentrations determined on board indicate very stable media and cultures over time. Enzymatic activities profiles are already available and seem to indicate higher glucosidase activity in the DOM-amended treatments.

20.5 Post-cruise sampling analyses and dead-lines

The type of molecular analyses to be done will be determined once the basic parameters such as DOC concentration and abundance of heterotrophic bacteria are finalized. All analyses should be done by September 2013.

20.6 Data base organization

20.7 References of methods

Aminot A., Kérouel R. 1997. Dosage automatique des nutriments dans les eaux marines : méthodes en flux continu. Ed. Ifremer.

Benner R, Strom M (1993) A critical evaluation of the analytical blank associated with DOC measurements by high-temperature catalytic oxidation. Mar Chem 41: 153-160

Lebaron, P., Servais, P., Agogue, H., Courties, C., Joux, F., 2001. Does the high nucleic acid content of individual bacterial cells allow us to discriminate between active cells and inactive cells in aquatic systems? Appl. Environ. Microbiol. 67, 1775-1782.

21 Phytoplankton composition, distribution, biomass in the Kerguelen region and short palaeontological records from the underlying sediments

Principal investigator

Dr Leanne Armand
Dept. of Biological Sciences, Macquarie University, North Ryde,
2109, N.S.W., Australia.
☎ +61 2 9850 8351
leanne.armand@mq.edu.au

Names of other participants.

Net Hauls:

- B. Quéguiner (MIO)
- V. Cornet (MIO)
- K. Leblanc (MIO)
- O. Sackett (University of Technology, Australia)
- I. Obernosterer (LOMIC)
- P.Van Beek (LEGOS)

CTD:

- V. Peralta (Volunteer technical assistant, Macquarie University)
- B. Quéguiner (MIO)
- V. Cornet (MIO)
- K. Leblanc (MIO)

Sediments:

- M.-L. Delgard (University of Bordeaux)
- B. Quéguiner (MIO)
- A.-J. Cavagna (University of Brusells)

Abstract:
Phytoplankton occurrences in the water column and from the sea floor sediment were sampled during KEOPS2 by Phytoplankton nets, CTD and Multicorer instrument deployments. Water samples and Net samples have been poisioned with Lugols and will be returned for microscopic analyses at Macquarie University, Sydney and additional samples were poisoned with either Formol (CTD), Lugols (net), filtered (net) or unposioned (net) to be processed for other studies on the plankton composition or products related to the breakdown of material or genetic composition in France (Marseille, Banyuls, Toulouse). Net samples were also sampled and reserve material preserved (formol) for an experimental analysis of macromolecular composition of individual diatom cell protein, lipid and carbohydrate content (Student at UTS Australia in collaboration with L. Armand).

Preliminary data on the net hauled diatom qualitative abundance from 27 stations has been made available and mapped, along with presence-absence of major zooplankton groups encountered. Approximately 2000 photographs of the phytoplankton net samples, some Bongo samples and P-trap samples will be made available per station in the near future.

Future analysis will be focused on the taxonomic and morphological variation in two diatoms (*Odontella weissfloggii* and *Eucampia antarctica* v. *antarctica*) followed by seafloor sediment absolute diatom abundances and then a prioritised CTD analysis of the diatoms, biometrics and biomass contribution to the Kerguelen ecosystem. Additional sediment analyses will be on-going until 2014/15 as student projects.

21.1 Scientific context

KEOPS-1 confirmed the importance of diatoms in the bloom region accounting for the majority of carbon biomass in the photic zone (Blain *et al.* 2007, Armand *et al.* 2008a). Shifts in the community structure were observed with bloom evolution, degradation and silicic acid limitation on the plateau (Armand *et al.* 2008a, Mosseri *et al.* 2008). Exterior to the bloom zone, species were largely representative of normal, less diverse, open-ocean communities. Species from the genus *Pseudo-nitzschia*, previously identified as an iron-fertilization responsive taxon (summarized by de Baar *et al.* 2005), were poorly represented in the bloom region. This discrepancy is thought related to the age of the bloom, with *Pseudo-nitzschia* species observed as dominant after experimental iron fertilized blooms; KEOPS-I was surveyed at the demise of the bloom. The sea-floor study of diatom remains identified signature species across the plateau and open-ocean sea floor when placed in comparison to previous datasets (Crosta *et al.* 1998, Armand *et al.* 2008b). Evidence for iron-enhanced/bloom conditions were exemplified by elevated abundances of *Chaetoceros* spp. resting spores, *Thalassionema nitz*. f. *nitzschioides*, *Eucampia antarctica* v. *antarctica* and *Thalassiosira antarctica* in the sediments (Armand *et al.* 2008b). These occurrences being clearly differentiated to the dominating abundances of *Fragilariopsis kerguelensis, Thalassiosira lentiginosa* and *Thalassiothrix antarctica* in the surrounding sediments of the open ocean region. The sea floor diatom distributions could not always be linked to the bloom abundances in the overlying water column. In some cases the affect of deep and bottom water currents and silica dissolution were at the root of the digressions preserved in the sediments. Some of these biological observations were backed by the findings from oceanographic pathway proxies and rare earth element distributions that also invoked the influence of currents originating west of Heard Island and heading northeastward across the plateau particularly through the Heard- McDonald Trough (Van Beek *et al.* 2008, Zhang *et al.* 2008).

Although KEOPS-1 provided evidence of nature's own iron and nutrient fertilization project by revealing the effect produced on the ecosystem at the lower tropic levels and its value in drawing down CO_2, it left many questions unanswered. None more so, than on the mode and degree of export of carbon. Identifying the components of particle export and the degree that remineralization within the twilight zone remains an important issue in the continuation of KEOPS-2 and also in the global interest of CO_2 mitigation measures. Other examples of unanswered questions from the biogeo perspective included:

- Was there a differentiated vertical distribution of the phytoplankton in the top 100m of the bloom where KEOPS-1 transiometer and fluorescence readings suggest a secondary peak of diatoms at the thermocline. Does a secondary community exist?
- What was the original phytoplankton community at the bloom commencement (i.e. composition of microflora/biota and bacteria) and which species represented the ramp up and bloom peak phases?
- What was the magnitude of the bloom?

- Which of the responsive diatom species in the bloom evolution sequence represented the preserved sea-floor signals?
- Would the pattern of diatom distributions continue to the east of Kerguelen concomitant with satellite observations of the bloom extent?

21.2 Overview of the project and objectives

The KEOPS-2 objectives remain largely focused on the biochemical and ocean hydrodynamics and will attempt to meld the observations into the models from both lagrangian (eddy following stations) and eulerien (fixed stations). Dr Armand's contribution to KEOPS-2 is through her Australian-funded SPEAK programme (Sediment Parameters, Export Analysis and 'K'omposition)

The Australian SPEAK contribution aims to provide biological information at the base of the food chain to aid in solving the questions put forward under the KEOPS-2 objectives 3-5, *"3) can we characterize the pathways that lead to the export and the fate of material exported to the deep water? 4) how is the biological diversity of the microbial and classical food web impacted? 5) can we understand the seasonal and inter-annual variability of 5.1 the size of the bloom?"* through the following aims:

1) enumeration, identification and biomass calculations for the diatom component of the KEOPS-2 survey,
2) enumeration and identification of sediment trapped material, and
3) enumeration, identification and transfer function development of diatoms from seafloor surface sediments.

These project aims and objectives are relevant to the contribution of diatoms to the dominant algal bloom, their export, attenuation and relationship to bacteria through the water column, and their sea-floor contributions, whereby:

- The enumeration and identification of major contributor species is expected to change with depth from the epipelagic zone to the sub-littoral to bathyal environment sea floor.
- Assessment of diatom biomass from morphometric measurements from surface and short-term drifting traps will contribute the carbon contribution of diatoms to the complete carbon cycle assessment.
- As in KEOPS-1 the role of species community shifts can be directly related to nutrient availability in the oceans, providing a biological response link to the chemical changes particularly with the response to silicic acid (link to KEOPS-2 objective no. 2).
- A comparison with bacterial community dominances through the water column.
- Annual cycle composition from moored sediment traps will be worked on to provide the annual context from which the diatom bloom rises and falls annually (Post-2012 project).

21.3 Methodology and sampling strategy

For KEOPS-2 objectives: Phytoplankton samples from net hauls provide a preliminary indication of the major species composition of the studied region. Additional samples taken from CTD casts will be used in laboratory studies to determine biomass and quantitative community composition. Sea floor samples will be used to determine the distribution of iron-related bloom indicator species against the open ocean iron deplete flora and also the influence of sea-floor currents in that composition.

21.3.1 Net Hauls (taken in conjunction with Zooplankton sampling programme of KEOPS-II).

A 35µm meshed phytoplakton net was deployed to sample the top 100m of the surface waters at most stations. Hauling speed was minimised to around 5m/minute. Incomplete sampling of the N-S transect (TNS) occurred due to the planning of the station activities (an oversight on my part). In general 2 to 4, 100ml archive samples were taken from each station haul (2 Armand - lugols/formol, 1 Leblanc lugols, 1 Van Beek no preservative). Additional set of subsampling direct from the hauled material was taken and filtered by Obernosterer for genomic analysis (see Obenosterer for precise sample details).

Net hauls were taken at 27 stations (Table 1) with an additional net filtered CTD cast station (=12 bottles filtered) at one of the IODA deployment stations (CTD078). I also made photographic observations from the 120µm mesh fraction of the zooplankton bongo nets (see Carlotti report for details on Bongo net deployments). This bongo net related data is not included in Table 1, but will be made available in 2012 along with the photographic material.

On board a fresh 1ml aliquot of the net sample was placed in Sedgewick Rafter 1mm x 1mm gridded cell and observed Under a Nikon TS100 inverted microscope. Preliminary taxonomic identification occurred at x10 and then x40 magnification. All diatoms and major zooplankton groups observed were photographed with the attached D5000 Nikon digital camera. Forty to 90 photographs were taken per station. The images were saved into the photographic database iPhoto™. A scale bar was added to all images using Adobe Illustrator™ CS4 after having taken photos of a scale graticule under the same magnifications used to take the images. SEM imagery may be undertaken on some samples.

Twenty-one phytoplankton net stations (Pnet stations 7 to 27, excluding stn 23) were subsampled for an experimental study of the macromolecular composition of individual diatom cells through Fourier Transformed Infrared (FTIR) spectroscopy. Approximately 6 x 25µl individual drops of fresh sample were pipetted onto Low-e microscope slides, air dried in a laminar flow cabinet and stored with silica pellets to be returned to the laboratory for spectroscopic analysis. Additional sample as back up (1x~100ml Armand-formol) was preserved to return to the lab. Ms Olivia Sackett, a PhD student at the University of Technology in Sydney, in collaboration with Dr Leanne Armand will complete this macromolecular study that may prove useful for understanding the carbon composition and variability of certain diatom species that could link into other studies of carbon composition and transfer through the system.

21.3.2 CTD Phytoplankton biomass (taken in conjunction with K. Leblanc and B. Quéguiner, MIO).

652 x 200 ml CTD samples were taken during the voyage (Table XXVII) for phytoplankton analysis from various biological related CTD deployments. Samples were poisoned with Lugols. Continued assessment by Leanne Armand for specific biomass and taxonomic studies is planned through 2012 on these preserved samples. Additional sampling from the same rosette was undertaken for B. Quéguiner. These samples are preserved with Formol and will return to the University of Marseille for analysis of the non-diatom component of the plankton in the CTD samples. Procedures and analysis will follow those successfully employed during KEOPS-1 and developed and published in Armand *et al.* (2008a) and Cornet-Barthaux *et al.* (2007). The data complied will be used to assess species community/composition, abundance and carbon biomass of the assemblage at different depths and stations. These latter values will be employed in the carbon budget of the main KEOPS-2 outcomes. SEM imagery may be undertaken on some samples.

Table XXVII : CTD Samples taken for further analyses by L. Armand.

CTD Type	Station	Sample Depths (m) (200ml taken per depth)												
none specified	OISO-6	1	20	40	50	75	100	150	200	300	400	600	800	1000
none specified	OISO-7	20	50	75	100	200	300	400	500	600	800	1000		
BioGeoShort Shallow	A3-1	20	80	100	125	150	200							
BioGeoShort Shallow	TNS10	12	148	189	226	249	250							
BioGeoShort Shallow	TNS9	31	100	123	141	171	241							
BioGeoShort Shallow	TNS3	11	91	126	161	200								
BioGeoShort Shallow	TNS2	12	81	132	162	202	252							
BioGeoShort Shallow	TEW1	10	20	30	41									
BioGeoShort Shallow	TEW2	31	40	49	80									
BioGeoShort Shallow	TEW3	16	75	90	110	181	252							
BioGeoShort Shallow	G1	10	51	76	100	181	250							
BioGeoShort Shallow	A3-2	10	125	150	174	200	275							
BioGeoShort Deep	TNS8	41	61	100	150	203	401	500	701	988				
BioGeoShort Deep	TNS7	11	41	82	101	152	202	403	503	1006	1846			
BioGeoShort Deep	TNS6	12	41	61	101	182	202	403	503	805	1861			
BioGeoShort Deep	TNS5	10	40	60	102	120	161	402	503	1000	2036			
BioGeoShort Deep	TNS4	10	40	60	100	121	159	402	502	1001	1780			
BioGeoShort Deep	TNS1	11	41	61	101	150	201	400	501	801	2242			
BioGeoShort Deep	TEW4	10	40	60	100	150	200	400	600	800	1559			
BioGeoShort Deep	E1-2	10	40	60	101	151	201	402	502	803	1993			
BioGeoShort Deep	TEW5	10	40	60	100	150	200	400	600	800	2250			
BioGeoShort Deep	TEW6	10	40	60	100	150	200	400	500	800	2390			
BioGeoShort Deep	TEW7	10	40	60	100	150	200	400	500	800	2486			
BioGeoShort Deep	TEW8	10	40	60	100	150	200	401	501	800	2768			
BioGeoShort Deep	NPF-L	11	24	40	67	79	95	402	500	800				
BioGeoShort Deep	NPF-S	11	24	40	67	79	95	402	500	800	2487			
BioGeo 900	RK-2	401	601	701	901									
BioGeo 900	E1	400	599	700	903									
BioGeo 900	E1-3	400	600	700	900									
BioGeo 900	NPF-L	301	501	700	901									
BioGeo 900	E1-5	400	601	700	900									
BioGeo 900	E1-4W	401	602	702	900									
BioGeo 900	E1-4E	400	600	700	901									
BioGeo 200	RK-2	12	32	62	92	112								
BioGeo 200	E1	10	19	45	65	86	130							
BioGeo 200	E1-3	11	22	27	48	68	86	138						

Table XXVII (continued)

BioGeo 200	NPF-L	9	20	29	36									
BioGeo 200	E1-5	10	17	22	37	55	69	110						
BioGeo 200	E1-4W	10	13	25	34	42	67							
BioGeo 200	E1-4E	10	14	19	32	47	61	94						
BioGeo 200	A3-2	10	15	27	39	49	78							
BioGeo Process	RK-2	11	31	91										
BioDivRoll	E1	20	80	150	300									
BioDivRoll	E1-3	20	70	80										
BioDivRoll	NPF-L	20	65	180										
BioDivRoll	E1-5	20	80	150										
BioDivRoll	E1-4W	30	80	150										
BioDivRoll	E1-4E	30	80	160										
BioDivRoll	A3-2	20	80	160										

21.3.3 Seafloor and water interface sampling program (taken in conjunction with M.-L. Delgard, (EPOC, B. Quéguiner, MIO, and A.-J Cavagna, University of Brusells)

Seven multicore stations were sampled (see detailed report by M.-L. Delgard). At each station 3-4 multitubes were sampled for the top surface layer (0-0.5cm) to enable a statistical analysis of diatom variability in replicate material. This work is envisioned as student projects at Macquarie University for 2012 and 2013. At each station one multicore was fully subsampled to depth for various analyses (see Table 3 for Armand sample list). The palaeontological diatom analysis will follow standard silica-selective methods (Rathburn *et al.* 1997) and refer directly to the work in Armand *et al.* (2008b). Water samples will be microscopically analysed and then be processed to a permanent slide using the same method as for sediment samples. Where warranted after microscopic observation they may undergo SEM analysis.

Table XXVIII : Sediment samples taken for further analyses by L. Armand.

CORE #	E1-4W-2	A3-2	NPF-L	E1-3	TEW-1	RK2	A3-1
1		1 samples: 0-0.5 cm			1 sample: 0-0.5 cm	1 sample: 0-0.5 cm	1 sample: 0-0.5 cm
2	1 sample: 0-0.5 cm		18 samples: 0-24 cm		1 sample: 0-0.5 cm	16 samples: 0-20 cm	
3	11 samples: 0-10 cm		1 sample: 0-0.5 cm		13 Samples: 0-13 cm		1 sample: 0-0.5 cm
4	1 sample: 0-0.5 cm	1 samples: 0-0.5 cm	1 sample: 0-0.5 cm		no sediment		
5	1 sample: 0-0.5 cm		1 sample: 0-0.5 cm				20 samples: 0-30cm
6		1 samples: 0-0.5 cm	1 sample: 0-0.5 cm	1 sample: 0-0.5 cm			
7	1 sample: 0-0.5 cm	20 Samples: 0-30 cm	1 sample: 0-0.5 cm	18 samples: 0-24 cm		1 sample: 0-0.5 cm	unused core: suspended particles
8		1 samples: 0-0.5 cm		1 sample: 0-0.5 cm	1 sample: 0-0.5 cm	1 sample: 0-0.5 cm	1 sample: 0-0.5cm

Table XXIX : Exhaustive list of measured parameters

Parameter	code of operation	units
1. Net hauls: Diatom taxonomy	Phytonet	Genera and species identification, qualitative abundance estimate (absent, rare, minor, common, dominant), photographs for biometrics, morphological change and taxonomic purposes.
2. Macromolecular composition	Phytonet	Protein, lipid and carbohydrate content.
3. Scanning Electron microscopy	Phytonet	Taxonomic description and measurements.
4. CTD: Diatom taxonomy	CTD	Genera and species identification
5. CTD: Diatom Abundance	CTD	Cells/L
6. CTD: Diatom Biometrics and Biomass	CTD	• Biometrics (transapical, apical pervalvar and diameter means and ranges in µm) • species-specific biovolume (mean μm^3), • biomass (mean pg C.$Cell^{-1}$) • surface (mean μm^2) • surface to volume ratio
7. sediments: Diatom taxonomy	CORER	Genera and species identification
8. sediments: Diatom abundance	CORER	• Absolute Diatom Abundance (Frustules per gramme dry weight), • No. species (S) • Shannon's diversity (H) • Evenness (EH)
9. sediments: Diatom distribution	CORER	Maps of species-specific diatom distribution in units of Absolute Diatom Abundance
10. sediments: Replication study	CORER	• Absolute Diatom Abundance (Frustules per gramme dry weight), • No. species (S) • Shannon's diversity (H) • Evenness (EH) • ANOVA result
11. sediments: Palaeo down-core record	CORER	• Absolute Diatom Abundance (Frustules per gramme dry weight), • Possibly ^{14}C data • Transfer function derived SST (°C) Palaeo-record.

21.4 Preliminary results

Preliminary results are only available for the section: 3.1 Net Hauls.

A summary of the diatoms encountered and their qualitative abundance from Phytonet sampling is provided in Table 5 (Refer to separate Excel file attachment). A diatom taxonomic guide to the species or genera encountered and featured in Table 5 has been provided in the pdf and word files: Table1 Phytoplankton Summary.

Summary maps of the 5 principal diatoms qualitative diatom distributions were presented during one of the last scientific meetings on board the ship and have been provided in the pdf file: Diatom Quick Summary 24Nov.pdf

Summary maps of the major zooplankton presence-absence distributions have been provided in the pdf and word files: KEOPS2 ARMAND Zooplankton obs Phytonet.pdf

Around 2000 photographs have been taken during the voyage covering the following sampled stations: 27 Phytonet stations, 1 CTD-Phytonet station, 4 Bongo 120 µm net stations on the NS transect and 8 P-trap samples from 4 deployments of T. Trull/D. Davies. The P-trap diatom occurrence data has been supplied to T. Trull for integration in his report.

21.5 Post-cruise sampling analyses and dead-lines.

Analyses will be undertaken principally over 2012-2013. Priority will be taxonomic description of *Odontella weissflogii* initial cell and auxospore formation, and *Eucampia antarctica* v. *antartica* seasonal morphological changes, followed by surface seafloor sample analysis and plotting and then a prioritised list of CTD sample analyses after discussion with B. Quéguiner and K. Leblanc. Student projects on sediments may start in 2012 and continue through to 2015 depending on the number of students selecting diatom projects. The macromolecular experimental study of Sacket and Armand should be completed by Sept 2012. Will do my best to have sediment and some preliminary CTD results ready for first meeting in Sept 2012.

21.6 Data base organization

I will generate a diatom taxonomic database and related biometric and biovolume data as in KEOPS-1. Additional dataset will be the Palaeo record that will contain depth, age and SST parameters and diatom absolute abundances by species. I am uncertain what sort of data will be forthcoming out of the macromolecular study.

21.7 References of methods.

Armand, L.K., Cornet-Barthaux, V., Mosseri, J., Quéguiner, B., (2008a). Late summer diatom biomass and community structure on and around the naturally iron-fertilised Kerguelen Plateau in the Southern Ocean. Deep Sea Research Part II: Topical Studies in Oceanography, 55 (5-7): 653-676.

Armand, L.K., Crosta, X., Quéguiner, B. Mosseri, J. Garcia, N. (2008b) Diatoms preserved in surface sediments of the northeastern Kerguelen Plateau. Deep-Sea Research II: Topical Studies in Oceanography, 55(5-7): 677-692.

Cornet-Barthaux, V., Armand, L., Quéguiner, B., 2007. Biovolume and biomass measurements of key Southern Ocean diatoms. Aquatic Microbial Ecology, 48 (3): 295-308.

Rathburn, A.E., Pichon, J.-J., Ayress, M.A., DeDeckker, P., 1997. Microfossil and stable-isotope evidence for changes in Late Holocene paleoproductivity and paleoceanographic conditions in the Prydz Bay region of Antarctica. Palaeogeography, Palaeoclimatology, Palaeoecology 131, 485-510.

22 Phytoplankton communities study from HPLC pigment analysis

Principal investigator

Hervé Claustre and Julia Uitz
Laboratoire d'Océanographie de Villefranche
CNRS, BP08 Quai de la Darse, 06238 Villefranche sur mer, France
☎ +33 493 763 729
🖷 +33 493 763 739
claustre@obs-vlfr.fr

Names of other participants (+affiliation)

- M. Ouhssain (OOV-CNRS, France)
- J. Ras (LOV-CNRS, France)

Abstract:
During the KEOPS2 cruise, seawater was collected, filtered and the filters stored in liquid nitrogen until HPLC analysis by the SAPIGH team of the Observatoire Oceanologique de Villefranche sur mer (OOV), France. The SAPIGH platform is dedicated to the analysis of marine phytoplankton pigments which are important organic bioindicators of phytoplankton biomass and population composition. A recognized and validated HPLC methodology will be used for these analyses and the pigment dataset will finally contribute to a global pigment database. The data from this cruise, and its comparison with satellite data and with a global parameterization should help to better understand and characterize the distribution and composition of the phytoplankton communities the Southern Ocean.

22.1 Scientific context

Phytoplankton pigments (chlorophylls and carotenoids) are important organic bioindicators of phytoplankton population distribution in the frame of research studies in marine biogeochemical cycling and in marine optics. The HPLC technique not only provides a proxy for phytoplankton biomass (Chlorophyll *a*), but it also has the advantage of being able to characterize, from a single sample, a large range of phytoplankton populations from the very small (less than 2µm) picophytoplankton cells to the very large (greater than 20µm) microphytoplankton cells. This type of measurement has been classified as an important core parameter for projects in oceanography and marine biogeochemistry.

At the LOV, we have, over the years, assembled a global pigment database comprising pigment profiles across the world ocean. Work on this database has revealed very unique features associated to the Southern Ocean in comparison to the lower latitudes. The pigment data from the KEOPS2 cruise should therefore contribute to a better understanding and characterization of the biology of phytoplankton in this area.

22.2 Overview of the project and objectives

The KEOPS2 cruise offers, once more, the opportunity to improve our knowledge of the phytoplankton community composition and distribution in Southern Ocean waters which tend to favour particular assemblages with respect to those of temperate regions, and in contrasting trophic conditions such as encountered in the HNLC zone and during the early-bloom periodin the deep waters off the Kerguelen Plateau.

The HPLC (High Performance Liquid Chromatography) technique allows the determination of the chlorophyll *a* (universal indicator of the phytoplankton biomass), and of a suite of accessory pigments (carotenoids and chlorophylls) used as biomarkers of diverse phytoplankton taxa or groups. Indeed, phytoplankton pigments are specific to phytoplankton groups, and can also be assigned to size classes, such as micro- (> 20 µm) nano- (2-20 µm), and pico-phytoplankton (< 2 µm).

Our first objective is therefore to determine the phytoplankton community biomass and composition using HPLC-determined pigments.

Our second objective is to compare the in situ surface measurements with coinciding Chl*a* concentrations obtained from satellite data.

We finally plan to investigate whether the in situ distributions of pigment-based size classes conform with the predicted distributions derived from the application of a global pigment parametrization(Uitz *et al.*; 2006)to remotely sensed TChl*a* concentrations. In this way, any difference between measured and predicted distributions could be scrutinized and further interpreted in terms of regional particularities of the Southern Ocean relative to the mean (global ocean) trend.

22.3 Methodology and sampling strategy

22.3.1 Sampling strategy:

- Sampling of seawater samples varying between 2.23 L and 1 L according to the charge in particles. This water is collected from the niskin bottles on the CTD rosette.
- Filtration is carried out on GF/F Whatmanfilters(25 mm diameter) by vacuum.
- Once the filtration ended, the filters are stored in cryotubes and placed in liquid nitrogen is made available. They will be sent to Villefranchesurmer in dry shippers and stored in a -80°C freezer.

22.3.2 Methodology: HPLC (High Performance Liquid Chromatography)

- Extraction of the samples: in 100% methanol containing a Vitamin E acetate internal standard. Filters are disrupted by sonication. After 2 hours at -20°C, the extracts are clarified by filtration.
- Extracts are injected into an Agilent Technologies 1200 series HPLC system. Separation takes place within 28 minutes on a reversed phase Zorbax Eclipse XDB C8 column (3x150 mm; 3.5µm). The pigments are then detected by a diode array detector, at 4 detection wavelengths: 450nm (for carotenoids, chlorophylls *c* and *b*), 676nm (for Chlorophyll a and derived pigments), 770nm (for bacteriochlorophyll *a*) and 222nm (for internal standard).
- Calibration of the HPLC system is carried out with pigment standards from *DHI Water and Environment* (Denmark) and *Sigma*.
- As part of the data validation phase, the Total Chl *a* data will be compared with the CTD bottle fluorescence data.

The analytical procedure is described in more detail in Ras *et al.* (2008)

Table XXX : Exhaustive list of measured parameters

Parameter	code of operation	units
1. Chlorophyll *c3*	CTD	$mg.m^{-3}$
2. Chlorophyll *c2+c1*	CTD	$mg.m^{-3}$
3. Chlorophyllide *a*	CTD	$mg.m^{-3}$
4. Peridinin	CTD	$mg.m^{-3}$
5. Phaeophorbide *a*	CTD	$mg.m^{-3}$
6. 19'Butanoyloxyfucoxanthin	CTD	$mg.m^{-3}$
7. Fucoxanthin	CTD	$mg.m^{-3}$
8. Neoxanthin	CTD	$mg.m^{-3}$
9. Prasinoxanthin	CTD	$mg.m^{-3}$
10. Violaxanthin	CTD	$mg.m^{-3}$
11. 19'-Hexanoyloxyfucoxanthin	CTD	$mg.m^{-3}$
12. Diadinoxanthin	CTD	$mg.m^{-3}$
13. Alloxanthin	CTD	$mg.m^{-3}$
14. Diatoxanthin	CTD	$mg.m^{-3}$
15. Zeaxanthin	CTD	$mg.m^{-3}$
16. Lutein	CTD	$mg.m^{-3}$
17. Bacteriochlorophyll *a*	CTD	$mg.m^{-3}$
18. Divinyl Chlorophyll *b*	CTD	$mg.m^{-3}$
19. Chlorophyll *b*	CTD	$mg.m^{-3}$
20. Divinyl Chlorophyll *a*	CTD	$mg.m^{-3}$
21. Chorophyll *a*	CTD	$mg.m^{-3}$
22. Total Chlorophyll *b* (18+19)	CTD	$mg.m^{-3}$
23. Total Chlorophyll *a* (20+21)	CTD	$mg.m^{-3}$
24. Phaeophytin *a*	CTD	$mg.m^{-3}$
25. alpha+beta Carotene	CTD	$mg.m^{-3}$

22.4 Preliminary results

231 samples, corresponding to 31 vertical profiles, were collected during the cruise. Additionally, 59 filters from the in situ pumps were also collected.

In the frame of a French intercomparison exercise of pigment analysis by HPLC (FIPIG-1), 6 batches of 12 replicates (*i.e.* 72 filters) have also been sampled at various stations and depths.

Samples will be analysed at the laboratory in Villefranche sur mer. Until then there will be no preliminary results.

22.5 Post-cruise sampling analyses and dead-lines

Samples should be analysed during the months of December 2011 and January 2012. Data processing and final data checks and validation should bring the deadline for submission of the data to end of February 2012.

22.6 Data base organization

The phytoplankton pigment database is described inTable XXXI.

Table XXXI : Pigment database line of titles, description, units, pigment detection wavelengths and limits of detection.

Titles	Description	Units	Detection wawelength	LOD ng/inj	LOD for 1L filtered in $mg.m^{-3}$
Sampling date	UTC	dd/mm/yy			
Sampling time	UTC	hh:mm			
Date of analysis	UTC	dd/mm/yy			
Cruise or project					
Ship					
Latitude	Latitude	decimal degrees			
Longitude	Longitude	decimal degrees			
Sample code	HPLC file name				
Station					
CTD	CTD number				
Depth (m)	Sampling depth	metres			
Bottle #	Rosette bottle number				
Fileterd vol. (L)	Filtered volume	Litres			
Chlorophyll *c3*		$mg\ m^{-3}$	450	0.017	0.0004
Sum chl *c2*+*c1*	Sum chlorophyll *c2* and *c1* + MgDVP	$mg\ m^{-3}$	450	0.021	0.0005
Sum chlorophyllide *a*	Chld *a* + Chld *a*–like	$mg\ m^{-3}$	667	0.045	0.0012
Peridinin		$mg\ m^{-3}$	450	0.008	0.0002
Sum phaeophorbide *a*		$mg\ m^{-3}$	667	0.053	0.0013
19'Butanoyloxyfucoxanthin		$mg\ m^{-3}$	450	0.011	0.0003
Fucoxanthin		$mg\ m^{-3}$	450	0.011	0.0003
Neoxanthin		$mg\ m^{-3}$	450	0.011	0.0003
Prasinoxanthin		$mg\ m^{-3}$	450	0.011	0.0003
Violaxanthin		$mg\ m^{-3}$	450	0.014	0.0003
19'-Hexanoyloxyfucoxanthin		$mg\ m^{-3}$	450	0.011	0.0003
Diadinoxanthin		$mg\ m^{-3}$	450	0.017	0.0004
Alloxanthin		$mg\ m^{-3}$	450	0.017	0.0004
Diatoxanthin		$mg\ m^{-3}$	450	0.016	0.0004
Zeaxanthin		$mg\ m^{-3}$	450	0.016	0.0004
Lutein		$mg\ m^{-3}$	450	0.016	0.0004
Bacteriochlorophyll *a*		$mg\ m^{-3}$	770	0.018	0.0005
Divinyl Chlorophyll *b*		$mg\ m^{-3}$	450	0.005	0.0001
Chlorophyll *b*		$mg\ m^{-3}$	450	0.005	0.0001
Total Chlorophyll *b*	DV Chl *b* + Chl *b*	$mg\ m^{-3}$	450	0.005	0.0001
Divinyl Chlorophyll *a*		$mg\ m^{-3}$	667	0.031	0.0008
Chorophyll *a*		$mg\ m^{-3}$	667	0.033	0.0008
Total Chlorophyll *a*	DV Chl a + Chl *a* + chlorophyllid *a*	$mg\ m^{-3}$	667	0.033	0.0008
Sum phaeophytin *a*	Phytn *a* + Phytn *a*–like	$mg\ m^{-3}$	667	0.0359	0.0009
Sum alpha+beta carotene	alpha carotene + beta carotene	$mg\ m^{-3}$	450	0.016	0.0004
Observations					

A “readme” file will be provided with the database. This will comprise the above Table XXXI, a summary of the analytical procedure, the limits of detection for each measured pigment and a summary of the performance metrics of the method at the time of the analysis of the KEOPS2 samples.

22.7 References of methods

Ras, J, Uitz, J, and H. Claustre (2008). Spatial variability of phytoplankton pigment distributions in the Subtropical South Pacific Ocean: comparison between in situ and modelled data. *Biogeosciences*, 5, 353-369.

Uitz, J., Claustre, H., Morel, A., Hooker, S. (2006). Vertical distribution of phytoplankton communities in open ocean: an assessment based on surface chlorophyll .*Journal of GeophysicalResearch*, **111**, (C08005, doi:10.1029/2005JC003207).

23 Dissolved inorganic carbon, nitrate and ammonium uptake rate measurements

Principal investigator

Anne-Julie Cavagna
ANCH & ESS depts. – Vrije Universiteit Brussel – Pleinlaan 2 – Brussels, Belgium
☎ +32-2 629 39 71
🖷 +32-2 629 18 11
acavagna@vub.ac.be

Bernard Quéguiner
Institut Méditerranéen d'Océanographie,Campus de Luminy, case 901
F-13288 Marseille Cedex 09
☎ +33 491 829 105
🖷 +33 491 821 991
bernard.queguiner@univ-amu.fr

Names of other participants

- Camila Fernandez (LOMIC)
- Frank Dehairs (ANCH & ESS dept. – VUB)

Abstract:
Using ^{13}C and ^{15}N labeling experiments we measured net primary production and nitrogen uptake along the light attenuation profile in the mixed layer to assess depth integrated net primary production. From nitrate and ammonium uptake rates the relative importance of new vs. regenerated production was assessed (*f*-ratio). Furthermore, 2 experiments were conducted to study: (1) ammonium concentration kinetics to assess Vmax and Ks values of ammonium uptake and inhibition of nitrate uptake by ammonium; (2) the time course over 24h of C-assimilation and nitrate, and ammonium uptake.

Résumé :
Ce projet vise à mesurer la production primaire nette de carbone et d'azote dans la couche de mélange afin d'obtenir la production primaire nette intégrée sur la colonne d'eau. L'outil utilisé pour cela est l'utilisation des traceurs isotopes stables ^{13}C et ^{15}N au cours d'expériences d'incubation. De plus la comparaison entre vitesse d'incorporation des nitrates vs. de l'ammonium (*f*-ratio) permet de caractériser le régime de production du système étudié (production nouvelles vs. production régénérée).
En parrallèle, 2 expériences de cinétique ont été conduites : (1) une cinétique étudiant l'effet de la concentration en ammonium du milieu sur l'incorporation de différents substrat azoté (ammonium ou nitrate); (2) une cinétique temporelle pour étudier le comportement circadien d'incorporation du carbone, des nitrates et de l'ammonium.

23.1 Scientific context

Assessing the contribution of the different N substrates to the primary production process provides a means to assess the potential of the biological pump for carbon export. In a steady state system, primary production sustained by the nitrate from deep waters (where it is formed via nitrification) and by fixation of atmospheric N2 is considered to represent the potentially exportable fraction of primary production, called new production (Dugdale and Goering, 1967; Eppley and Peterson, 1979; Falkowski, 1997). Primary production sustained by N-nutrients such as ammonium, amino acids and urea resulting from shallow, local release and remineralization is called regenerated production. The exportable fraction of primary production is represented by the ''f-ratio'' (i.e., the ratio of new over total primary production; Eppley and Peterson, 1979). Recently, work in the Southern Ocean revealed that nitrification in the euphotic layer (EZ) could be significant (DiFiore *et al.*, 2009; Sanders *et al.*, 2007) and Yool *et al.* (2007) highlighted the possible impact of EZ nitrification on new production estimates. For the Kerguelen Plateau, Trull *et al.* (2008) report nitrification rates reaching up to 10% of ammonium uptake.

Another issue investigated using kinetic experiments concerns the impact of Fe availability on *f*-ratio. Cavagna *et al.* (2011) report that under conditions of Fe and nitrate repleteness, and sufficient ammonium, *f*-ratio is possibly decreased, mainly due to nitrate uptake inhibition (Southern Ocean; SAZ-Sense expedition, Jan.-Feb. 2007), in agreement with conclusions formulated by Dortch (1990) and Elskens *et al.* (2002).

23.2 Overview of the project and objectives

This work aims at assessing the impact of environmental conditions (light, temperature, stratification, etc.) and availability of macro and micro-nutrient (Fe) on primary production and N-uptake regime. Sites with contrasting conditions above the Kerguelen Plateau and the basin east of Kerguelen were investigated. Our experiments were designed to focus in particular on (i) significance of ammonium uptake (reflecting regenerated production) under conditions of nitrate repleteness (mostly 20 µM and more) and the impact of Fe on this process and (ii) significance of regenerated nitrate in the euphotic layer, that is impact of euphotic layer nitrification on new production, and the possible impact of Fe on this process.

Following the scientific context, the classical experimental design for biogenic carbon and nitrogen production measurements is also constrained in terms of nitrification rates using the denitrifier method (Mangion, 2011; Casciotti *et al.*, 2002, Sigman *et al.*, 2001). Likewise, for the temporal kinetic experiment intended to describe the time course of nitrate and ammonium uptake over 24H, we also will analyze for possible nitrification. Finally, the concentration kinetic experiments are designed to investigate the possible inhibition of nitrate uptake by ammonium under Fe-replete conditions.

23.3 Methodology and sampling strategy

Uptake rates of C and N were assessed during incubation experiments enriched with $^{15}N\text{-}NO_3^-$, $^{15}N\text{-}NH_4^+$ and $^{13}C\text{-}HCO_3^-$ tracers.

- Production measurements (8 stations)

We sampled CTD casts dedicated to C, N, Si biogenic production (see also K. Leblanc and C. Fernandez cruise reports). Seawater is sampled at 7 PAR levels (75, 25, 16, 4, 1, 0.3 and 0 % PAR). Two sets are studied here which are (1) nitrate uptake rate + C-assimilation, and (2) ammonium uptake rate + C-assimilation. Set 1 is sampled for nitrate concentration (nutrient team support) and $\delta^{15}N$-nitrate at t initial and t + 24h (samples are filtered on 0.2µm acrodiscs and stored at -20°C for later analysis). Set 2 is sampled for ammonium concentration (fluorescence method – see nutrient

team & C. Fernandez reports) at t initial and t + 24h. At t + 24h, samples are filtered on precombusted glass fiber filters (Sartorius MGF; 0.7 µm nominal pore size; Ø 25mm) which are dried at 50°C and stored at ambient temperature for analysis later.

At every level, samples were taken for natural abundance and isotopic composition of PON and POC (see C. Fernandez report). This data will be used for production rate calculations.

- Kinetic experiments (7 stations for concentration kinetics – 3 stations for temporal kinetics)

A CTD cast was especially dedicated to C, N and Si process experiments (K. Leblanc and C. Fernandez reports). Concentration kinetics were based on PAR level 25% which was close to the average condition in the mixed layer and avoided possible bias due to light inhibition. Two sets of parameters were studied: (1) nitrate uptake rate vs. ammonium concentration and (2) ammonium uptake rate vs. ammonium concentration. Kinetics are based on 8 levels of increasing ammonium concentration, including the initial condition. Each sample is then spiked with stable isotope tracers (^{13}C-HCO_3 and (1) ^{15}N-NO_3^- / (2) ^{15}N-NH_4) and aliquots taken for initial ammonium concentration. Incubation bottles (1L polycarbonate Nalgene bottles) were then incubated on deck at 25% PAR during 6h. After 6h, an aliquot for final ammonium is taken and samples filtered on precombusted MGF filters. Filters are dried at 50°C and stored in the dark at ambient temperature till processing in the home laboratory. For the temporal kinetics, 8 time steps were defined over 24h (initial time, t+2h, t+4h, t+6h, t+8h, t+12h, t+18h and t+24h), at three PAR levels (75, 25 and 1%). Again, two incubation experiments were run: (1) nitrate uptake rate + C-assimilation, (2) ammonium uptake rate + C-assimilation.

At the home laboratory particulate organic nitrogen and carbon are processed as follows: particulate nitrogen (PN) and particulate organic carbon (POC) concentrations along with their ^{15}N and ^{13}C abundances are analyzed via elemental analyzer—isotope ratio mass spectrometer (EA-IRMS) using a method described by Savoye *et al.* (2004). Briefly, inorganic carbon (carbonate) is removed from the filters by exposing these for 24 h to concentrated HCl vapor inside a closed-glass container. After drying the samples at 50 °C they are packed in silver cups and analyzed with a Carlo Erba NA 2100 elemental analyzer configured for C and N analysis and coupled on-line via a Con-Flo III interface to a Thermo-Finnigan Delta V isotope ratio mass spectrometer.

- Euphotic zone nitrification

To assess possible nitrification during the incubation experiments we analyze the ^{15}N-dilution of the nitrate pool in the ^{15}N-NO_3^- spiked incubation bottles. This is more accurate than measuring the ^{15}N-enrichment of the nitrate pool from the ^{15}N-NH_4^+ spiked bottles. Indeed, in the second case, possible ammonium release could bias results. δ^{15}N-nitrate is analyzed via the denitrifier method (Mangion, 2011; Casciotti *et al.*, 2002, Sigman *et al.*, 2001; see also report on nitrate isotopic composition, F. Dehairs *et al.*): briefly, NO_3 and NO_2 are converted quantitatively to N_2O by a strain of bacterial denitrifier that lacks nitrous oxide reductase activity, and the product N_2O is extracted, purified, and analyzed by continuous flow isotope ratio mass spectrometry.

Table XXXII : Exhaustive list of measured parameters

Parameter	code of operation	units
1. nitrate concentration	CTD	µmol L^{-1}
2. ammonium concentration	CTD	µmol L^{-1}
3. C fixation rate	CTD	mmol m^{-2} d^{-1}
4. Nitrate uptake rate	CTD	mmol m^{-2} d^{-1}
5. Ammonium uptake rate	CTD	mmol m^{-2} d^{-1}

6. δ15N Nitrate from incubations	CTD	‰

23.4 Post-cruise sampling analyses and dead-lines

Production and uptake kinetic data are expected to be available for the first post-cruise meeting (early September 2012).

Data will be included in the general data base of the KEOPS-2 project.

23.5 References of methods

Casciotti, K.L., Sigman, D.M., Hastings, M.G., Böhlke, J.K., Hilkert, A., 2002. Measurement of the oxygen isotopic composition of nitrate in seawater and freshwater using the denitrifier method. Analytical Chemistry, 74, 4905-4912.

Cavagna A-J., M. Elskens, F. B. Griffiths, S.H.M. Jacquet and F. Dehairs, 2011. Contrasting regimes of productivity and potential for carbon export in the SAZ and PFZ south of Tasmania, *Deep-Sea Research II*, 58, 2235-2247.

DiFiore, P.J., Sigman, D.M., Dunbar, R.B., 2009. Upper ocean nitrogen fluxes in the Polar Antarctic Zone: constraints from the nitrogen and oxygen isotopes of nitrate. Geochemistry Geophysics Geosystems, 10. doi:10.1029/2009GC002468.

Dortch, Q., 1990. The interaction between ammonium and nitrate uptake in phytoplankton. Marine Ecology-Progress Series 61, 183–201.

Dugdale, R.C., Goering, J.J., 1967. Uptake of new and regenerated form of nitrogen in primary productivity. Limnology and Oceanography 12, 196–206.

Elskens, M., Baeyens, W., Cattaldo, T., Dehairs, F., 2002. N uptake conditions during summer in the Subantarctic and Polar Frontal Zones of the Australian sector of the Southern Ocean. Journal of Geophysical Research 107, 3182–3193.

Eppley, R.W., Peterson, B.J., 1979. Particulate organic matter flux and planktonic new production in the deep ocean. Nature 282, 677–680.

Falkowski, P.G., 1997. Evolution of the nitrogen cycle and its influence on the biological sequestration of CO2 in the ocean. Nature 387, 272–275.

Mangion P., 2011. Biogeochemical consequences of sewage discharge on mangrove environments in East Africa, PhD Thesis, Vrije Universiteit Brussel, 208 pp.

Trull, T.W., Davies, D., Casciotti, K., 2008. Insights into nutrient assimilation and export in naturally iron-fertilized waters of the Southern Ocean from nitrogen, carbon and oxygen isotopes. Deep-Sea Research II 55, 820–840.Trull *et al.* (2008)

Sanders, R., Morris, P.J., Stinchcombe, M., Seeyave, S., Venables, H., Lucas, M., 2007. New production and the f-ratio around the Crozet Plateau in austral summer 2004–2005 diagnosed from seasonal changes in inorganic nutrient levels. Deep-Sea Research II 54, 2191–2207.

Savoye, N., Dehairs, F., Elskens, M., Cardinal, D., Kopczyńska, E.E., Trull, T.W., Wright, S., Baeyens, W., Griffiths, B.F., 2004. Regional variation of spring N-uptake and new production in the Southern Ocean. Geophysical Research Letters 31, L03301.

Sigman, D.M., Casciotti, K.L, Andreani, M., Barford, C., Galanter, M., Böhlke, J.K., 2001. A bacterial method for the nitrogen isotopic analysis of nitrate in seawater and freshwater. Analytical Chemistry, 73, 4145-4153.

Yool, A., Martin, A.P., Fernandez, C., Clark, D.R., 2007. The significance of nitrification for oceanic new production. Nature 447, 999–1002. doi:10.1038/nature05885.

24 Nitrogen cycle and greenhouse gases during KEOPS2

Principal investigator

Camila Fernandez
LOMIC (UMR 7621), Banyuls sur Mer
fernandez@obs-banyuls.fr

Names of other participants

- L.-F. Lennis (PROFC Laboratory, University of Concepcion, Chile)
- F. Dehairs (ANCH & ESS dept. – VUB)
- A.J Cavagna (ANCH & ESS dept. – VUB)
- S. Blain (LOMIC)
- L. Oriol (LOMIC)

Résumé :

L'objectif de ce projet est d'évaluer les sources d'azote dans la couche euphotique venant de la fixation d'azote moléculaire, et de la régénération de N via nitrification. En particulier, des expériences ont été menées pour évaluer le couplage des deux étapes de la nitrification (ammonium et nitrite oxydation), et les effets de la disponibilité en fer sur la production d'oxyde nitreux (N_2O) par les communautés oxydatrices de NH_4 (archées et bactéries).

Pour atteindre les objectifs de ce projet, les techniques isotopiques de l'azote-15 en phase liquide et gazeuse ont été appliquées.

L'effet climatique de la fertilisation naturelle en fer du plateau de Kerguelen a été également évalué à travers la distribution de deux gazes à effet de serre dans la colonne d'eau, l'oxyde nitreux et le méthane (N_2O et CH_4).

Abstract:

The objective of this project is to evaluate possible N sources in the mixed layer coming from either nitrogen fixation or in situ nitrification. In particular, experiments were carried out for evaluating the coupling between ammonium and nitrite oxidation as well as the effects that iron availability can have on nitrous oxide production via nitrification.

For doing so, ^{15}N tracer techniques were applied in both liquid and gas faces.

The climatic relevance of natural iron fertilization over the Kerguelen plateau was also approached via the distribution of two biologically mediated green house gases, nitrous oxide and methane.

24.1 Scientific context

The biological production observed over the Kerguelen Plateau during the annual austral spring and summer bloom is enhanced by natural iron fertilization (Blain *et al.* 2001). Interestingly, the presence of high macronutrients concentrations in the surface euphotic layer (mainly NO_3 and PO_4) after the macrophytoplankton-dominated bloom suggests an important role of remineralization and other fixation processes (e.g. diazotrophic) in nutrient cycling. This is supported by the idea that around 30% of primary production might be fuelled and maintained in time by in situ microbial nitrification (Yool *et al.* 2007). Also, naturally iron-fertilized areas should be prime candidates for

nitrogen fixation activity, due to the high iron demand of the nitrogenase enzymatic complex (Zehr & Turner 2001).

The role of N regeneration processes in nutrient production needs to be assessed from an integrative point of view, taking into account the interaction among other limiting nutrients (Si, P for instance), trace metal availability, light limitation and microbial community structure. Also, it is important to assess the dynamics within nitrifying communities since uncoupled nitrification might result in increased N_2O production, a biologically-mediated greenhouse gas with well-known radiadive effects.

1. Overview of the project and objectives

This project is a contribution to the following questions of KEOPS2:

- What is the degree of coupling/decoupling between the C, N, P, Si cycles in the fertilized region?
- Why is there an excess of nutrients at the end of the productive season (following observations during KEOPS1)?

It will also contribute to the specific questions identified during the cruise.

The main objectives of this project are:

1) To characterize the air-sea exchange and concentration within the water column of nitrous oxide (N_2O) and methane (CH_4) in the study area.

2) To estimate nitrogen fixation fluxes via ^{15}N isotope enrichment experiments and to evaluate the dynamics between N_2, NH_4 and NO_3 utilisation in the context of new and regenerated production. This work is a collaborative effort with measurements made onboard by VUB (see report by A.-J. Cavagna and F. Dehairs).

3) To estimate rates of net nitrification in the water column and explore the variability of ammonium and nitrite oxidation as well as their role as N_2O mediating pathways.

4) To explore the shifts in community structure and functional genes responsible for nitrification during the onset of the bloom in Kerguelen in order to asses the impact of environmental conditions on N regeneration.

24.2 Methodology and sampling strategy

- Objective 1 – N_2O and CH_4 in the water column.

Samples for N_2O and CH_4 were taken at 25 and 6 stations, respectively. All depth levels between the surface and 500 m were sampled. Particular sampling effort was put in transects TNS and TEW in order to cover the spatial variability of the study area.

Samples were taken in triplicate in 20 mL glass vials, poisoned with saturated $HgCl_2$ and stored at room temperature until laboratory analyses at Universidad de Concepcion, Chile. Samples will be analyzed through gas chromatography according to existing protocols (Cornejo *et al.* 2006, Cornejo *et al.* 2007, Karl *et al.* 2008).

- Objectives 2 and 3 – N_2 fixation and nitrification

Nitrogen fixation through diazotrophy and nitrification by ammonium and nitrite oxidizing microorganisms were assessed through isotope tracer techniques (^{15}N) and the use of specific process-targeted experiments (Montoya *et al.* 1996, Ginestet *et al.* 1998). Incubations were done on deck using solar incubators at different incident light levels (ranging between 75 and 0.01% PAR).

Profiles of nitrogen fixation were obtained at all process-stations, covering 7 depth levels between the surface and the base of the euphotic zone. Samples (1L) were amended with 2 mL of $^{15}N_2$ gas and incubated for 24 h. Additionally, size fraction-time series incubations (4 stations) were done in surface waters (incubated at 75% of incident light) in order to estimate the kinetic of ^{15}N during the solar cycle for potential diazotrophic groups below 5 μm. In order to avoid cell stress after sampling from the rosette, the fraction below 5 μm was simultaneously retrieved from the underwater sampling system (see report by Tom Trull).

Incubations were ended by filtration through 0.7 μm GFF filters (previously treated at 450ºC for 12h). Filters were recovered and dried at 60ºC for 24 h, then stored in dry conditions until laboratory analysis through continuous flow Isotope Ratio Mass Spectrometry (IRMS).

At process stations, profiles of nitrogen fixation were coordinated with experiments targeting uptake of C, N and Si as well as net community production and respiration (see reports by K. Leblanc, A. Cavagna and D. Lefèvre).

In order to estimate nitrogen fluxes, it is crucial to know the natural isotopic composition of organic matter ($\delta^{15}N/\delta^{13}C$ in POM) as well as its carbon and nitrogen content. Samples were taken at 22 stations (depth levels between surface and 200 m depth). This will allow characterizing accurately the $\delta^{15}N/\delta^{13}C$ signature and composition of organic matter. As described for N_2 fixation experiments, filters were recovered and dried at 60ºC for 24 h, then stored in dry conditions until laboratory analysis.

Nitrification was assessed as net nitrate regeneration as well as specific rates of ammonium and nitrite oxidation. Experiments were performed using ^{15}N techniques and specific inhibitors such as Allylthiourea (inhibiting ammonium oxidation), azide (inhibiting nitrite oxidation) and GC7 (inhibiting archaeal protein synthesis). This will allow evaluating both nitrification steps and the archaeal contribution to this process (Ginestet *et al.* 1998).

Overall 13 experiments were performed at long or lagrangian stations. Experiments were performed at long stations in surface as well as mid and base of the euphotic layer in order to test the role of light in the regulation of this process. Rates and fluxes of ammonium and nitrite oxidation will be obtained by analysing the following parameters: the isotopic composition of dissolved inorganic nitrogen (^{15}DIN) at the beginning and end of the incubation experiment, the inorganic nitrogen evolution (as nitrate, nitrite and ammonium), cell abundance and functional gene activity. In this context, ammonium concentrations were measured onboard through the fluorimetric technique(Holmes *et al.* 1999). Nitrite and nitrate concentrations were also followed through the experiments by the colorimetric method (Aminot & Kérouel 2007) (see L. Oriol's report for nitrate and nitrite analysis on board). Isotopic analyses will be performed using the denitrifying method (see report by AJ Cavagna) and liquid face mass spectrometry for the isotopic composition of $^{15}NO_2$ and $^{15}NO_3$.

Two experiments (at RK-2 and A3-2 stations) were designed in order to evaluate the response of nitrification to iron addition in terms of N_2O production. Samples were taken from the Trace Metal Rosette at depths within the mixed layer (70 and 29 m for RK2 and A3-2, respectively) and amended with $^{15}NH_4$, $^{15}NO_2$ and specific inhibitors in order to assess ammonium, nitrite and net nitrification fluxes. Dissolved iron was added to duplicate samples at a final concentration of 1 nM per sample. Incubations were performed at 4ºC during 8 to 10 h then ended by recovery of the following parameters: RNA, cell abundance (flux cytometry), isotopic composition of dissolved inorganic nitrogen (^{15}DIN), evolution of DIN concentrations, isotopic composition of N_2O (which will be analyzed by continuous flow mass spectrometry coupled with a gas bench at Universidad de Concepcion, Chile).

The natural isotopic composition of nitrate ($\delta^{15}N$, $\delta^{18}O$ in NO_3) will provide crucial information for the interpretation of tracer-amended experiments carried out onboard and to accurately estimate the role of N regeneration during pre-bloom conditions (see report by F. Dehairs).

- Objective 4 – Nitrifying community structure and activity

Seawater samples were taken during the underway sampling crossing the Crozet bloom as well as in 17 stations of the KEOPS sampling track (this includes stations from TNS and TWE transects as well as long stations). Seawater was filtered through 0.2 µm, and filters were preserved with RNA later (Qiagen ®) at -80ºC until laboratory analysis.

Molecular tools will be applied in order to evaluate the activity if the main nitrifying groups, ammonium oxidizing archaea, bacteria and nitrite oxidizing bacteria (Molina *et al.* 2010).

Table XXXIII : Exhaustive list of measured parameters

Parameter	code of operation	Units
1. Nitrous oxide (N_2O)	CTD	nM and % saturation
2. Methane (CH_4)	CTD	nM and % saturation
3.N_2 fixation	CTD and underway sampling at long stations	nM d^{-1}
4.Nitrification	CTD, TMR and underway sampling at long stations	nM d^{-1}
5.PON/POC	CTD	µg
6.δ15N in PON / δ13C in POC	CTD	‰
7.RNA (amoA and NOB)	CTD / subsamples	
8. Cell abundance (CMF)	CTD / subsamples	Cell L^{-1}

24.3 Preliminary results

Preliminary results obtained from nutrient evolution during nitrification experiments show a highly dynamic microbial community, in which archaea and bacteria ammonia oxidizers can actively produce nitrite in the water column. However, ammonium and nitrite oxidation seem to be occasionally uncoupled, therefore suggesting the possibility of biological N_2O production in the study area.

24.4 Post-cruise sampling analyses and dead-lines

Greenhouse gases samples are expected to be analysed within the next 7 months (L. Farias, Universidad de Concepcion, Chile).

Isotopic analysis in PON and POC samples as well as the isotopic analysis of N_2 fixation samples should be completed before September 2012.

Timelines for molecular analysis still need to be defined but should not exceed the end of 2012.

24.5 Data base organization (general cruise base and/or specific data base(s))

General cruise data base.

Gene expression results can be included in a specific molecular data base.

24.6 References of methods

Aminot A, Kérouel R (2007) Dosage automatique des nutriments dans les eaux marines, Vol. Editions Quae

Blain S, Tréguer P, Belviso S, Bucciarelli E, Denis M, Desabre S, Fiala M, Jézéquel VM, Fèvre JL, Mayzaud P, Marty JC, Pazouls S (2001) A biogeochemical study of the island mass effect in the context of the iron hypothesis: Kerguelen Islands, Southern ocean. Deep Sea research I 48:163-187

Cornejo M, Farias L, Gallegos M (2007) Seasonal cycle of N2O vertical distribution and air-sea fluxes over the continental shelf waters off central Chile (~36°S). Progress in Oceanography 75:383-395

Cornejo M, Farias L, Paulmier A (2006) Temporal variability in N20 water content and its air-sea exchange in an upwelling area off central Chile (36ºS). Marine Chemistry 101:85-94

Ginestet P, Audic J, Urbain V, Block J (1998) Estimation of nitrifying bacterial activities by measuring oxygen uptake in the presence of the metabolic inhibitors Allylthiourea and Azide. Applied and Environmental Microbiology 64:2266-2268

Holmes RH, Aminot A, Kérouel R, Hooker BA, Peterson BJ (1999) A simple and precise method for measuring ammonium in marine and freshwater ecosystems. Canadian Fisheries and Aquatic Sciences 56:1801-1808

Karl DM, Beversdorf L, Bjorkman KM, Church MJ, Martinez A, Delong EF (2008) Aerobic production of methane in the sea. Nature Geosci 1:473-478

Molina V, Belmar L, Ulloa O (2010) High diversity of ammonia-oxidizing archaea in permanent and seasonal oxygen-deficient waters of the eastern South Pacific. Environmental Microbiology

Montoya J, Voss M, Kähler P, Capone D (1996) A simple, high-sensitivity tracer assay for N_2 Fixation. Applied and environmental microbiology 62:986 - 993

Yool A, Martin A, Fernández C, Clark D (2007) The significance of nitrification for oceanic new production. Nature 447:999-1002

Zehr JP, Turner PJ (2001) Nitrogen fixation: Nitrogenase genes and gene expression. Methods in microbiology 30:271-286

25 Si, C and N cycling and diatom community structure during KEOPS2

Principal investigator

Leblanc Karine
MIO, Campus de Luminy, 163 av de Luminy Case 901 – 13288 Marseille
+33 491 829 109
karine.leblanc@univmed.fr

Names of other participants

- B. Quéguiner (MIO)
- M. Lasbleiz (MIO)
- V. Cornet (MIO)
- S. Bonnet (MIO)
- I. Closset (LOCEAN)
- D. Cardinal (LOCEAN)
- Franck Dehairs (VUB)
- A.-J. Cavagna (VUB)
- M. Ouhssain (LOV)
- H. Claustre (LOV)
- C. Fernandez (OOB)
- L. Armand (Macquarie University)

Résumé :

Le LOPB a pris en charge la description des stocks et des flux d'éléments biogènes (Si,C,N) en collaboration avec plusieurs autres laboratoires (LOCEAN, VUB, OOB, Macquarie) dans la zone d'étude de KEOPS 2. Nous aurons pour but d'élucider la dynamique du bloom printannier de diatomées dans les eaux naturellement fertilisées en fer du plateau de Kerguelen et de détailler la réponse de ces organismes en terme d'assimilation des éléments biogènes et d'exportation de matière particulaire vers le sédiment avec un focus particulier sur le silicium. Une étude taxonomique complète des espèces constitutives du bloom printannier, combinée à des mesures d'assimilation d'éléments à l'échelle de la cellule et de l'espèce (marqueur fluorescent, nanosims) devraient nous permettre d'appréhender le cycle des élements biogènes en lien avec l'activité des organismes phytoplanctoniques à un niveau de détails rarement documenté.

25.1 Scientific context

An extensive diatom bloom is observed every year around Kerguelen Island in the Southern Ocean in the middle of otherwise high nutrients low chlorophyll (HNLC) waters. It is known that natural fertilization by islands, bringing trace elements such as Fe to surrounding waters is the main cause for these important blooms. The KEOPS program is dedicated to understanding how this Fe supply affects the spring bloom occurring East of the plateau in the wake of the main currents paths, and how planktonic community, namely diatoms, respond to this natural iron fertilization. Diatoms

are known to form dense aggregates and to sediment en masse at the end of their blooming period, and are also heavily grazed on by zooplankton, resulting in both case in a potential large C export to depth. The different response of the plankton community at various sites impacted differently by the Fe supply will help us understand if natural iron fertilization is an efficient mechanisms increasing nutrient drawdown and C export efficiency in this coastal region of the Southern Ocean.

25.2 Overview of the project and objectives

Our group at LOPB (B.Quéguiner, K.Leblanc, M.Lasbleiz & V. Cornet) was in charge of particulate stock sampling at all sites (35 stations sampled), and will document the vertical distribution of particulate Si, C, N and P in the KEOPS study area. We were also interested in measuring TEP (Transparent Exopolymer Particles) in the surface layer, as it is a powerful vector to start aggregate formation which may result in increased sinking velocity of particulate matter. We focused on the Si cycle in particular, with a complete study of Si production and dissolution rates (using ^{30}Si and a fluorescent probe), complemented by the study of the natural distribution of particulate and dissolved ^{30}Si in seawater in collaboration with LOCEAN (D.Cardinal & I.Closset). Vertical production/dissolution profiles were carried out in on deck incubators together with the VUB group (F.Dehairs & A.J. Cavagna) as well as Banyuls laboratory (C.Fernandez) for C and N. Parallel Fe uptake experiments were carried out by M.Fourquez & S.Blain (OOB). Process studies were also carried out at selected sites, to determine Si, C, and N uptake kinetics, temporal incorporation of biogenic elements, as well as species specific elemental uptake. Incorporation rates of Si, C and N will be determined in each individual diatom species as well as other groups, thanks to the use of innovative techniques such as PDMPO staining and Nanosims analyses in collaboration with S.Bonnet at LOPB. A particular effort will be made on the taxonomic determination of diatom species at all sites (gathered from plankton nets and CTD casts) with the help of Leanne Armand at Macquarie University. Together, these results should bring unprecedented description of biogenic element cycling in the surface layer linked to community structure and to single species dynamics regarding nutrient uptake.

25.3 Methodology and sampling strategy

Table XXXIV : Exhaustive list of measured parameters

Parameter	code of operation	units
1. PIC, POC, PON, POP	CTD	µmol L^{-1}
2. BSi/LSi/Al	CTD	µmol L^{-1}
3. TEP (alcian blue)	CTD	µg eq. xanthan gum L^{-1}
4. ^{30}Si production/dissolution fluxes	CTD	µmol L^{-1} d^{-1}
5. ^{30}Si uptake kinetics	CTD	µmol L^{-1} d^{-1}
6. Temporal kinetic ^{30}Si uptake	CTD	µmol L^{-1} d^{-1}
7. Natural abundance of ^{30}Si	CTD/ISP	$\Delta^{30}Si$
8. PDMPO uptake	CTD	nmol PDMPO L^{-1} d^{-1}
9. PDMPO uptake per species	CTD	nmol PDMPO L^{-1} d^{-1}
10. Kinetic uptake parameters for Si	CTD	V_{max} and K_S
11. Species list database in the form of diatom image bank	CTD and NET	species1-2-3...jpg database
12. ^{30}Si, $^{15}NO_3$, $^{15}NH_4$ and ^{13}C labelling for NanoSIMS	CTD	% enrichment per species + image bank

- **Parameter 1** – TPC, POC, PON, POP : 0,5 to 1L seawater were sampled on each BIOGEO CTD cast at 35 different stations at 6 to 13 depths for total particulate carbon (TPC), particulate organic carbon (POC), nitrogen (PON) and phosphorus (POP). Pre-combusted GFF filters were used and stored in precombusted glass vial upon filtration. They were dried several days at 60° C, then sealed with an aluminium cap and stored at room temperature until analyses. TPC will be analyzed on CHN, POC/PON filters will first be acidified to remove any PIC, and analyzed on a CHN. PIC will be deduced from the two previous measurements. POP filters will be digested following the wet oxydation method (Pujo-Pay and Raimbault, 1994) and analyzed on a spectrophotometer.
- **Parameter 2** – BSi, LSi, particulate Al : 2 L seawater were sampled at each BIOGEO CTD cast and filtered onto 20 and 0,8 µm polycarbonate filters simultaneously. Samples were stored folded in 4 in eppendorf vials and dried overnight at 60°C. Closed eppendorfs were stored at room temperature. Filters will be analyzed for biogenic and lithogenic silica following the triple extraction procedure described in Ragueneau *et al.* (2005). Particulate aluminium will be measured in parallel to correct for LSi contamination.
- **Parameter 3 –** TEP : 2 replicate of 0,25 L were filtered onto 0,4 µm polycarbonate filters, stained with 1 ml Alcian blue, rinsed, and frozen immediately at -20°C. Samples were digested on board in 80% H_2SO_4 and analyzed on as spectrophotometer according to Passow and Alldredge (1995). Calibration curve with Gum Xanthan will be done in the laboratory with the remaining Alcian Blue stock .
- **Parameter 4** – ^{30}Si production and dissolution fluxes : On all BIOGEO200 casts, 1 L seawater samples were incubated with 30Si following the method described in Corvaisier *et al.* (2005) modified by Fripiat *et al.* (2010). Samples for production were spiked at 10% of initial SiOH4 concentration and incubated for 24h whereas dissolution samples were incubated at 100 % for 48h to increase sensibility of the method. Samples were incubated in on deck incubators at 7 different light levels from dawn to dawn. For each time point (T0, T24, and T48), samples for natural dissolved $^{30}SiOH_4/^{28}SiOH_4$, spiked $^{30}SiOH_4/^{28}SiOH_4$, natural $^{30}SiO_2/^{28}SiO_2$ and spiked $^{30}SiO_2/^{28}SiO_2$ were collected. The filtrates at T0, T24 and T48 were preconcentrated using the MAGIC method.
- **Parameter 5** – ^{30}Si uptake kinetics : Following the BIOGEO cast, samples were collected on the PROCESS CTDs at each long station to do kinetic uptake experiments. 8 samples were spiked with 10% ^{30}Si, then with increasing concentrations of Na_2SiO_3 (up to 160 µM) and incubated for 24h, at 3 different light levels (75, 25 and 1 %). Same treatment as for parameter 4.
- **Parameter 6** – Temporal kinetic of ^{30}Si uptake : At 4 contrasted sites, 12 X 0,5 L were collected on the PROCESS CTDs at 25% light level, spiked with 10% ^{30}Si and incubated on deck. Samples were filtered every 2 h to follow the sequential uptake of Si over the light and dark periods. Samples will be analyzed as described in the parameter 4 section.
- **Parameter 7** – Natural 30Si particulate and dissolved distribution : Seawater was collected using Niskin bottles at 15 stations (2 transects both with 3 stations, 5 visits at the Lagrangian station E, 2 visits at the plateau station A3, the reference station R and the front F). The entire water column is sampled with a higher resolution through the first 1000m, and the volume of water collected decreases with depth. Water samples were filtered under pressure through 0.4µm polycarbonate filters to collect $Si(OH)_4$. Filters containing $bSiO_2$ were stored in Petri dishes and dried at 50°C during 24h. Support filters come from in situ pump casts which were not deployed at all stations and all depths sampled by CTD casts (only 8 stations : A3_2, E1, E3, E4_E, E4_W, E5, F, and R). Filters were dried at 50°C during 24h, shared between different parameter analyses. Only 12% of them will be used for silicon isotopes analyses. All of these samples will be analyzed at the LOCEAN laboratory (Paris) by MultiCollector Inductively Coupled Plasma Mass

Spectrometer (MC-ICP-MS ; Cardinal *et al.* 2003) after digestion (for filter samples, Ragueneau *et al.*, 2005), concentration and purification (De la Rocha *et al.* 1996 ; Brzezinski *et al.* 2003 ; Reynolds *et al.* 2006).

- **Parameter 8** – PDMPO uptake : On the production CTDs, 165 ml samples were incubated with 0,125 µM PDMPO to trace Si production rate. After 24h, samples were filtered onto 0,8 µm polycarbonate filters and digested immediately in hot NaOH. The samples were analyzed for both BSi and PMDPO uptake on a spectrophometer according to Strickland and Parsons (1972) and on a spectrofluorometer according to Leblanc and Hutchins (2005).
- **Parameter 9** – PDMPO uptake per species : From the same water sample as before, a subsample was filtered onto a black polycarbonate filter and mounted on a glass slide, stored at -20°C. At the laboratory, samples will be analyzed on the microscope using image analyses and dedicated macros allowing to quantify the mean fluorescence per cell. This will allow to estimate the % contribution of each species present to the total silicification rate. Coupling this information with the 30Si production fluxes will allow to attribute an absolute Si production flux to each species. PDMPO and BSi measurements were done on board, microscopic slides remain to be analyzed.
- **Parameter 10 –** Species specific kinetic uptake parameters for Si : In parallel to 30Si incubations, the same experiment was duplicated with PDMPO, and will allow to determine kinetic parameters for individual species within a mixed assemblage. PDMPO and BSi measurements were done on board, microscopic slides remain to be analyzed.
- **Parameter 11** - Species list database from nets and water samples and diatom image bank : will be obtained from observation and counts of the lugol preserved samples as well as from the PDMPO slides in epifluorescence. Samples were collected using either the plankton nets or the CTD water samples incubated with PDMPO for 24h. Samples are preserved with Lugol (0,4 ml per 125 ml) and stored at 4°C until analysis. PDMPO slides are stored at -20°C.
- **Parameter 12** – Triple labelling of ^{30}Si, $^{15}NO_3$, $^{15}NH_4$ et ^{13}C for nanosims analysis (for S.Bonnet). 4 contrasted sites (E1, E5, A3-2 and F) were chosen to perform triple labelling of cells with stable isotopes. At 3 depths on the PROCESS CTD, 2 samples were spiked with ^{30}Si, $^{15}NH_4$, $^{13}HCO_3$, or ^{30}Si, $^{15}NO_3$, $^{13}HCO_3$. After 24h incubation, samples were fixed in formalin and stored at 4°C. At the laboratory, an adequate volume of samples will be filtered onto special filters and analyzed on a Nanosims in Paris. This will allow to quantify the isotopic uptake of each element within the cells, and help determine which species preferentially take up NO_3 or NH_4, as well as C and Si. Data will be in the form of images showing the isotopic enrichment of each cell for each element in a coloured scale.

25.4 Preliminary results

Samples stained with PDMPO and mounted on glass slides were observed on board and an extensive image bank was already collected for each visited site (Figure 38).

Samples for PDMPO uptake and BSi were analyzed on board directly after incubation. Vertical profiles of BSi and PDMPO were obtained at 8 long study sites (Figure 39). They evidence low biomass and Si production at the reference station, the highest siliceous biomass at the A3-2 station, and the highest Si production rates were observed at the first visit of E1.

Average PDMPO uptake normalized to biomass evidenced some differences in productivity between stations (Figure 40 and Figure 41). Station E1 was clearly more productive than any other stations.

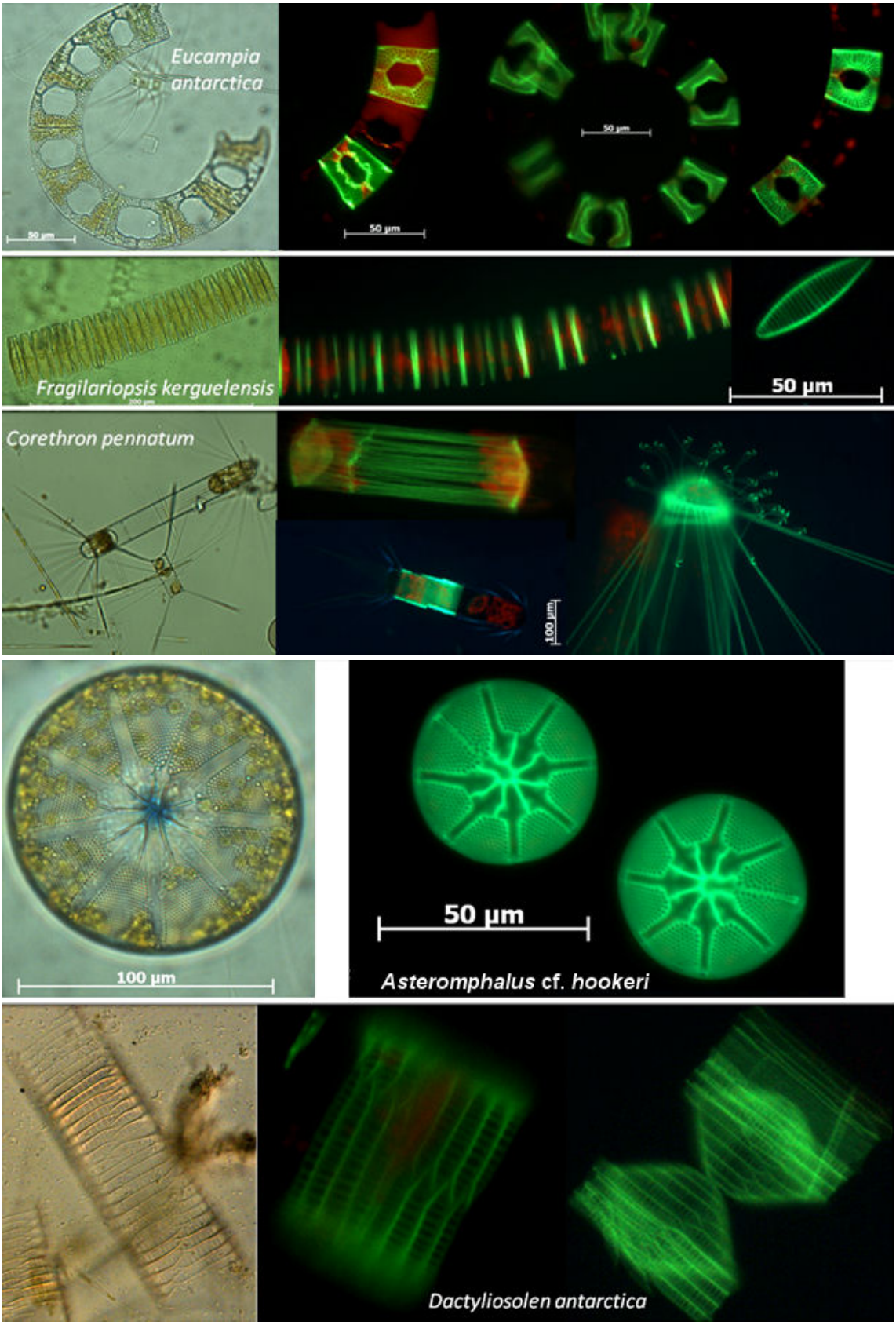

Figure 38 : Diatom cells observed in light microscopy (left panels) and in epifluorescence microscopy after staining with PDMPO. The green fluorescence indicates where new BSi has been produced by the cells, while red fluorescence shows the Chl *a* in chloroplasts.

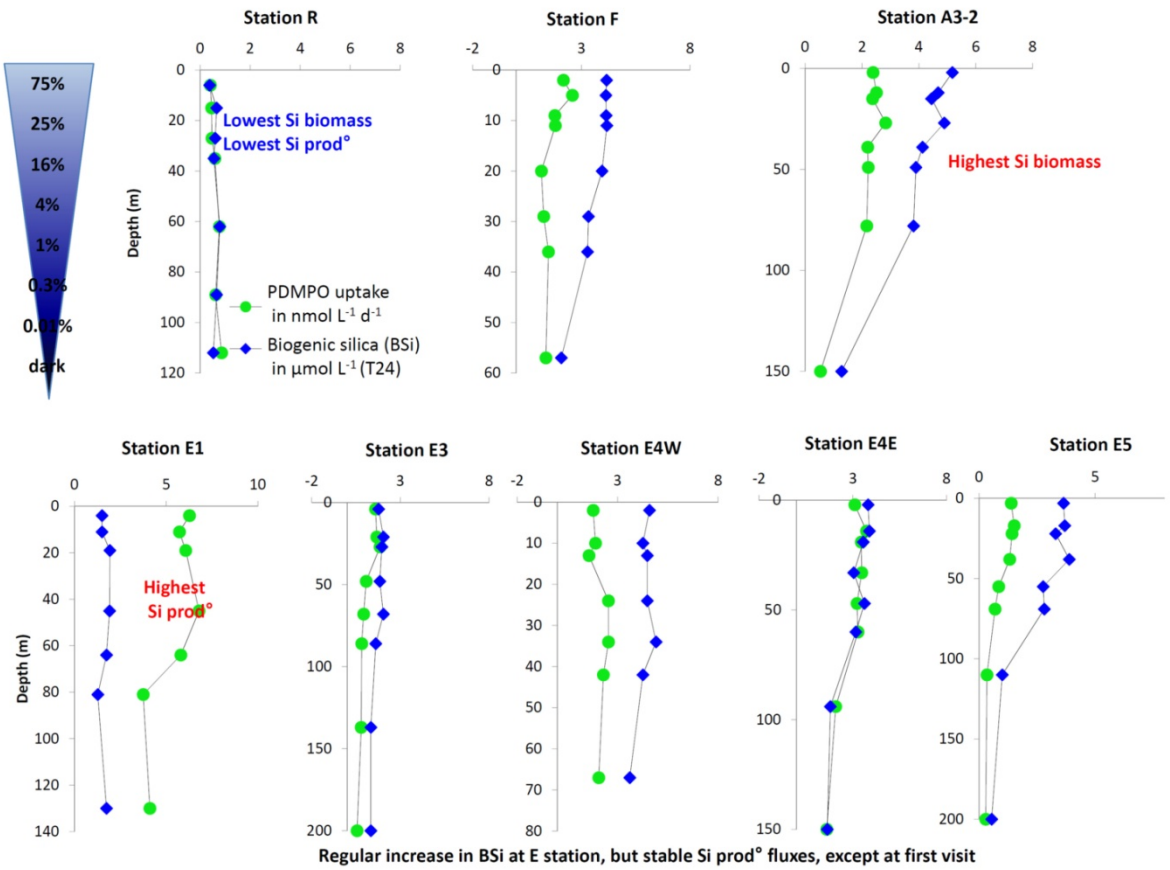

Figure 39 : Vertical profiles of BSi (in µmol L^{-1}) and PDMPO uptake rate (in nmol L^{-1} d^{-1}) after 24h incubation in on deck incubators.

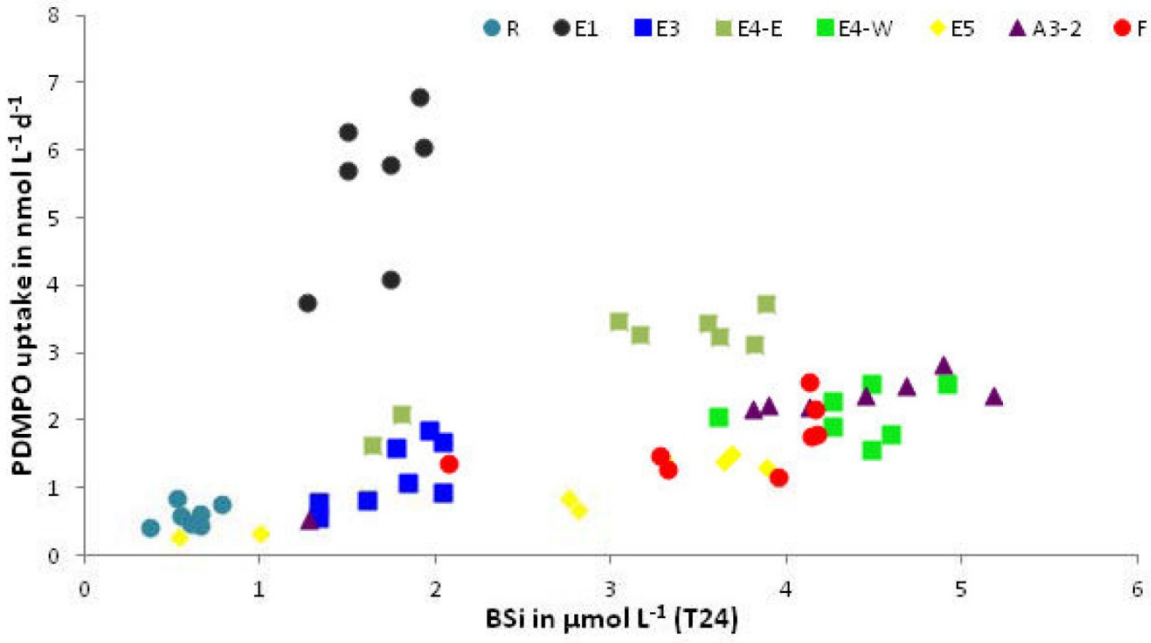

Figure 40 : PDMPO uptake rates vs BSi standing stock for each site at 8 incubation levels.

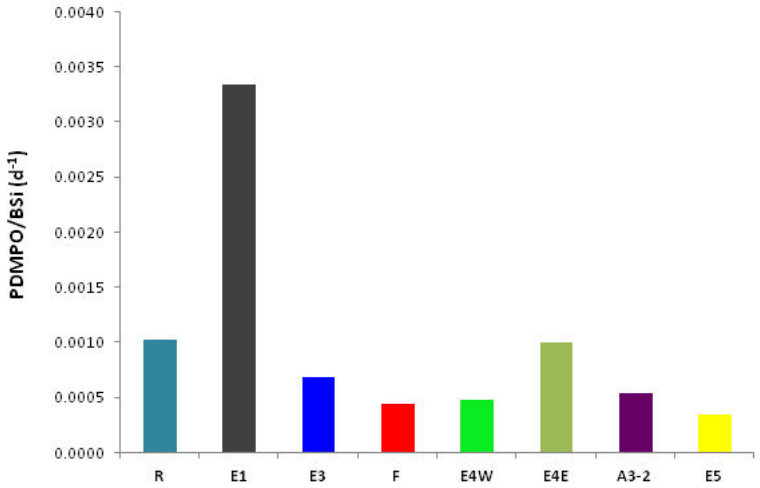

Figure 41 : Average PDMPO/BSi specific uptake rates, showing and index of productivity for each station. Right pannel : detail of the PDMPO uptake rates vs BSi standing stock for each site at 8 incubation levels.

25.5 Post-cruise sampling analyses and dead-line

Table XXXV : Post-cruise analyses

Parameter	Number of samples	Analyses schedule
1. PIC, POC, PON, POP	745	July 2013
2. BSi/LSi/Al	738	December 2013
3. TEP (alcian blue)	110	DONE
4. ^{30}Si production/dissolution fluxes	152 DSi 248 BSi (^{30}Si/^{28}Si) 248 filtrats (^{30}Si/^{28}Si)	July 2013 December 2013 December 2013
5. ^{30}Si uptake kinetics	280 DSi 280 BSi (^{30}Si/^{28}Si) 132 filtrats (^{30}Si/^{28}Si)	July 2013 December 2013 December 2013
6. Temporal kinetic ^{30}Si uptake	60 BSi (^{30}Si/^{28}Si)	December 2013
7. Natural abundance of ^{30}Si	276 filtrats (^{30}Si/^{28}Si) 276 BSi (^{30}Si/^{28}Si) 54 BSi from ISP (^{30}Si/^{28}Si)	December 2013
8. PDMPO uptake	64	DONE
9. PDMPO uptake per species	256 microscopic slides	July 2014
10. Kinetic uptake parameters for Si	192 PDMPO 192 BSi 192 DSi	DONE DONE DONE
11. Species list database in the form of diatom image bank	~ 370 lugol samples ~ 100 formol samples	July 2014
12. ^{30}Si, $^{15}NO_3$, $^{15}NH_4$ and ^{13}C labelling for NanoSIMS	24	December 2013

25.6 Data base organization

Most of the data will be included in the CTD database according to station and sampling depth (stocks and fluxes - Si production and dissolution rates, PDMPO uptake rates). Other data regarding kinetic experiments and temporal uptake kinetics with both 30Si and PDMPO will be in a different file format. Finally, all taxonomic data from microscopic observations, PDMPO measurements per cell, and nanosims analyses will be in included in a third type of files compiling taxonomic lists vs measured parameters (abundance, fluorescence per cell, cell sizes and biovolumes, calculated C content, average isotopic enrichment % per cell).

25.7 References of methods

Brzezinski M. A., Jones J. L., Bidle K. D. and Azam F.: The balance between silica production and silica dissolution in the sea: Insights from Monteray Bay, California, applied to the global data set, Limnol. Oceanogr., 48, 1846-1854, 2003.

Cardinal D., Alleman L. Y., De Jong J., Ziegler K., and Andre L.: Isotopic composition of silicon measured by multicollector plasma source mass spectrometry in dry plasma mode, J. Anal. Atom. Spectrom., 18, 213-218, 2003.

Corvaisier, R., Treguer, P., Beucher, C., and Elskens, M.: Determination of the rate of production and dissolution of biosilica in marine waters by thermal ionisation mass spectrometry, Analytica Chimica Acta, 534, 149-155, 2005.

De la Rocha C. L., Brzezinski M. A. and DeNiro M. J.: Purification, recovery and laser-driven fluorination of silicon from dissolved and particulate silica for the measurement of natural stable isotope abundances, Anal. Chem., 68, 3746-3750.

Fripiat, F., Corvaisier, R., Navez, J., Elskens, M., Schoemann, V., Leblanc, K., André, L., and Cardinal, D.: Measuring production–dissolution rates of marine biogenic silica by ^{30}si-isotope dilution using a high-resolution sector field inductively coupled plasma mass spectrometer L&O Methods, 7, 470-478, 2009.

Leblanc, K., and Hutchins, D. A.: New applications of a biogenic silica deposition fluorophore in the study of oceanic diatoms, Limnology and Oceanography-Methods, 3, 462-476, 2005.

Passow, U., and Alldredge, A. L.: A dye-binding assay for the spectrophotometric measurement of transparent exopolymer particles (tep). Limnol. Oceanogr., 40, 1326-1335, 1995

Pujo-Pay, M., and Raimbault, P.: Improvement of the wet-oxidation procedure for simultaneous determination of particulate organic nitrogen and phosphorus collected on filters, Mar. Ecol. Prog. Ser, 105, 203-207, 1994.

Ragueneau, O., Savoye, N., Del Amo, Y., Cotten, J., Tardiveau, B., and Leynaert, A.: A new method for the measurement of biogenic silica in suspended matter of coastal waters: Using si:Al ratios to correct for the mineral interference, Cont. Shelf Res., 25, 697-710, 2005.

Reynolds B. C., Frank M., and Halliday A. N.: Silicon isotope fractionation during nutrient utilization in the North Pacific, Earth Planet. Sci. Lett., 244, 431-443, 2006.

26 Microbial food web: from virus to protist

Principal investigator

Urania Christaki
Laboratoire d'Océanologie et des Geosciences – LOG UMR 8187
Université du Littoral Côte d'Opale
32 Ave. FOCH, 62930 Wimereux
☎ +33 321 912 864
🖷 +33 321 912 800
urania.christaki@univ-littoral.fr

e-mail: M.Hartmann@noc.ac.uk

Names of other participants

- C. Georges (LOG)
- S. Monchy (LOG)
- M. Hartmann (NOC)
- M.V. Zubkov (NERC)
- J. Dolan (LOV)
- T. Sime-Ngando (LMGE – UMR 6023)
- J. Colombet (LMGE – UMR 6023)
- E. Viscoliosi (Institut Pasteur of Lille)

Résumé :

Notre travail porte sur le réseau trophique planctonique (Fig. 1) et plus particulièrement sa partie hétérotrophe. Ce travail donc, inclut aussi bien des ***aspects dynamiques*** (mesure de la production bactérienne hétérotrophe, taux d'infection virale sur les bactéries, taux de broutage), et des aspects de la ***distribution spatiale et temporelle*** des différents organismes (virus, bactéries, nanoflagellés hétérotrophes, ciliés et dinoflagellés). Enfin une grande partie de ce travail portera sur la ***biodiversité micro- et nanoplaktonique*** qui sera abordé par des analyses microscopiques détaillées sur des échantillons de petits et grands volumes obtenus à bord et des analyses moléculaires (pyrosequençage) sur des stations clés de la campagne.

26.1 Scientific context:

Viruses (1) can be a major source of mortality and influence the community composition of prokaryotes (Figure 42). Different aspects of viral community were studied during KEOPS I and some important but preliminary conclusions were drawn. Although viral production (studied with the dilution approach) was 7 times higher in the bloom than in the HNLC environments the fraction of infected cells showed no significant differences between environments (Malits *et al.* 2009 ASLO and unpublished data).

Bacterial Production (2): Bacterial numbers and production were studied in the upper 200 m layer and were 2-3 fold and 10 fold higher in the bloom relative to the HNLC area, respectively.

Microzooplankton and Relations with Lower and Higher trophic levels (3,4,5) Together, nanoflagellates and ciliates play a key role in the transfer of bacterial and phytoplankton biomass to higher trophic levels (Figure 42). Low ciliate concentrations during KEOPS 1, implied a low microzooplankton grazing pressure on phytoplankton (Christaki *et al.* 2008). A possible role of copepod grazing in shifting ciliate community composition was also suggested by the high proportion of relatively grazing-resistant ciliate taxa, the tintinnids (Christaki *et al.* 2008).

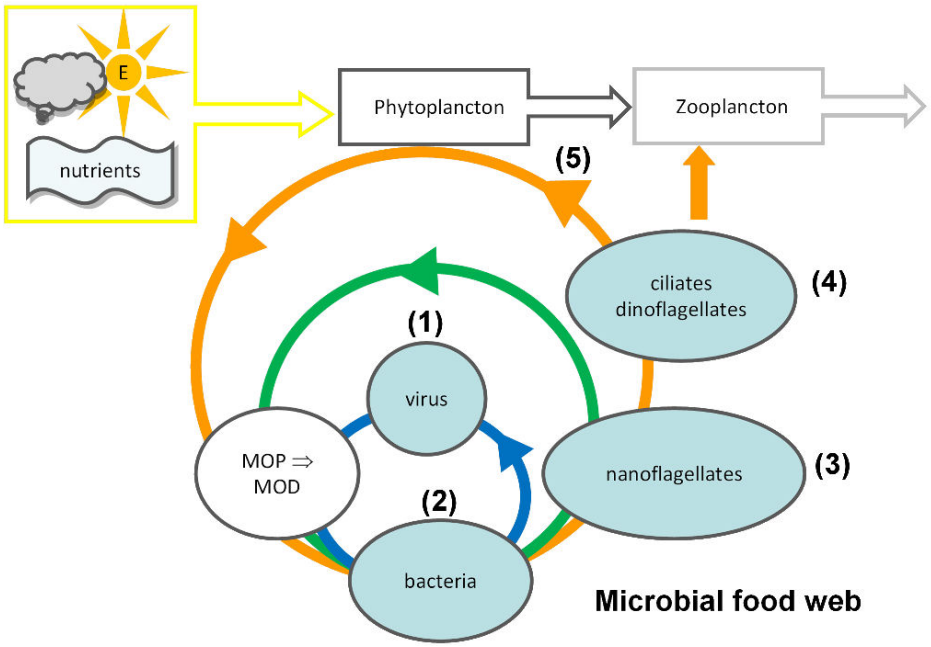

Figure 42 : Simplified planctonic food web

26.2 Overview of the project and objectives

This work aims to expand and complete the information obtained during KEOPS 1 in the new context of winter-spring transition. This overall objective translates into the following specific tasks:

Virus (1) Viral abundance and temporal changes are to be considered as core parameters. Viral infection of bacteria intends to complete the image of bacterial mortality (see below "Trophic Transfers")

Bacterial production (2) During KEOPS 1, bacterial production was measured in the 0-200 layer only, however there was indication of high efficiency of fertilisation below 200 m (e.g. Jacquet *et al.* 2008), for this reason the measurements of BP were expanded to the mesopelagic (down to 900 m).

Nanozooplankton function (3) Grazing activity of heterotrophic nanoflagellates plays an important part in the control of bacterial production. During KEOPS 1 it was shown that in HNLC region, heterotrophic nanoflagellates can control up to 98% of the bacterial production, while there role is less pronounced in the bloom region (~35%). Using a novel pulse-chase labelling approach we expanded measurement of KEOPS 1 to include *mixotrophic nanoflagellates* in the picture and to exactly measure the assimilation of bacterial prey into predator cells.

Microzooplankton numbers and biomass (4a) Three aspects were added relative to the microzooplankton stocks. (a) Dinoflagellates are known to be very important grazers of diatoms, thus their counts and biomass were included during KEOPS 2 (b) Sampling in the water column was expanded down to 300-400 m (c) Twelve L samples were concentrated on 10µm mesh, these samples (besides diversity studies) will permit to count the copepod nauplii and copepodites which escape the zooplankton net sampling.

Nano- and microzooplankton diversity (4b) Many challenging and up-to-date questions remain open for nano- and microzooplankton: What is their diversity? Do temporal shifts occur? Is it possible to track less abundant species? Are there major differences between the HNLC relative to the high biomass region studied during KEOPS 2 and what could be the ecological implications and consequences on biogeochemical fluxes? Are observations from tag pyrosequencing data and microscope comparable?

Microzooplankton and Relations between Lower and Higher trophic levels (5) The crucial aspect of the trophic transfer in the microbial food web was assessed with an original an innovative approach. The main objective was to assess carbon channelling from large, dominant phytoplankton groups (e.g. diatoms) to microzooplankton through grazing activity. Single cell grazing rates will be determined using radiolabelling of prey cells in combination with laser dissecting microscopy to precisely excise cells of interest and measure the transfer of carbon from prey to predator. In parallel single-cell carbon uptake rates of phytoplankton will be determined with a similar approach.

26.3 Methodology and sampling strategy

- Stock Parameters: **Virus** and **HNF**: Samples were taken at all stations (long and transect stations) at the whole water comumn and will be analysed by flow-cytometry (Brussaard 2004; Christaki *et al.* 2011) Samples for **Ciliates** and **Dinoflagellates** were taken at all "E" , NPF, A3 stations and R station.
- Bacterial production, was measured by the 3H-leucine incorporation method (Kirchman, 1993) on board at all "E" , NPF, A3 stations, R station, and a couple of other station on the SN transect.
- Microzooplankton diversity: Samples for **454 tag pyrosequencing** were taken at all long stations (8 stations) at 4 depths (mixed layer, base of the mixed layer, pycnocline and deeper layer 300 m). Five to seven L of sea-water were filtered with a size fractionation system (10, 3 and 0.6µm). Additionally 500 ml lugol fixed samples (duplicate) were teken for **microscopical analysis.** Also, 12 L samples were concentrated on 10µm mesh, these samples were fixed with lugol (microscopy) and ethanol (single cell PCR). During the cruise **live microplankton observation** was preformed at each station with an inversed microscope on board. Several hundreds pictures (≈800) and videos (≈300) of ciliates, dinoflagellates and other microzooplankton (foraminifera, etc) were registered which will help identify and illustrate microzooplankton diversity (example of these pictures at the end of this document, plate I)
- Nanozooplankton function was assessed by measuring grazing activity of smallest picoeukaryotic organisms on bacterioplankton. We used a pulse-chase dual-labelling approach (^{3}H leucine and ^{35}S methionine) to estimate assimilation of prey into the predator cell (Zubkov and Tarran, 2008). Samples were fixed with 1% paraformaldehyde for 1h at 4°C, subsequently flash frozen with liquid nitrogen and stored at -80°C for later flow cytometric cell sorting at the National Oceanography Centre. Grazing was measured at "E", F, A3 and R stations as well as three additional stations along the NS and EW transect. In addition, ambient concentrations and uptake rates of the organic nutrients by total bacterioplankton were measured using isotopic dilution time-series incubations (Zubkov *et al.*, 2004). Microbial organic nutrient dynamics were determined to estimate ambient concentrations and turnover rates of the bioavailable fraction of these nutrients to complement grazing rate measurements. All seawater samples were processed within an hour of collection.
- Microzooplankton and Relations between Lower and Higher trophic levels For sample collection a specially constructed size fractionating plankton net was used. Collected size fractions were between 40-100µm and 100-180µm. Sodium ^{14}C-bicarbonate was used in a series of experiments to trace carbon fixation rates by large phytoplankton groups and grazing rates of microzooplankton on the phytoplankton. Plankton net concentrated and size-fractionated samples were incubated for up to 6h in an incubator at ambient temperature (±2°C) and 150µmol m^{2-}

$^{1}s^{-1}$ light, subsequently fixed with 1% glutaraldehyde and filtered on 20µm pore size nylon membranes by gravity filtration. To determine grazing rates, experiments incubated in the light for 6h were further incubated in the dark for 8h and 10h. Microzooplankton grazing and carbon uptake of phytoplankton were measured at the "E", F, A3 and R stations.

Table XXXVI : List of measured parameters

Parameter	code of operation	units
1. Bacterial production (BP)	CTD	ng C L^{-1} h^{-1}
2. viral abundance (VLP)	CTD	VLPml^{-1}
3. Virus visibly infected bacterial cells (*FVIC*) + burst size (*BS*)	CTD	
2. Heterotrrophic flagellate numbers + biomass (HNF)	CTD	HNF ml^{-1}, µg C L^{-1}
3. Ciliates (CIL) number + biomass	CTD	CIL ml^{-1}, µg C L^{-1}
4. Dinoflagellate (DIN) number + biomass	CTD	DIN ml^{-1}, µg C L^{-1}
5. Micro- and nanoplankton diversity	CTD	pyrosequencing of hypervariable small subunit ribosomal RNA (SSU rRNA) tag region
6. Leucine uptake rates	CTD	nM d^{-1}
7. Leucine concentration	CTD	nM
8. Leucine turnover time	CTD	h
9. Methionine uptake rates	CTD	nM d^{-1}
10. Methionine concentration	CTD	nM
11. Methionine turnover time	CTD	h
12. Grazing rates of eukaryotes (<10µm)	CTD	Bacterial cells h^{-1}
13. Grazing rates of eukaryotes (>40µm)	NET	Phytoplankton cells h^{-1}
14. Carbon fixation rates of phytoplankton (>40µm)	NET	mg C $m^{3\ -1}$ d^{-1}

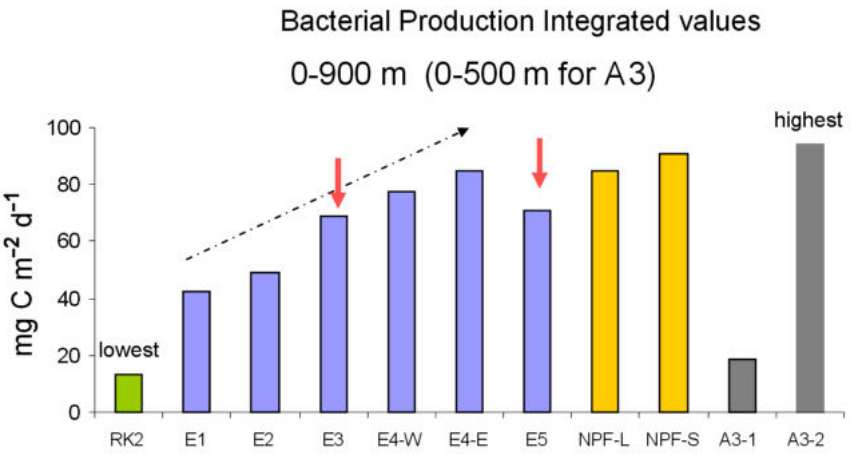

Figure 43 : Integrated bacterial production (preliminary results, samples to be recounted in the labo-

ratory).

26.4 Preliminary results

Bacterial production measured on board varied from <1 (below 500 m) to ≈ 50 ng C L^{-1} h^{-1} (in the mixed layer). Lowest integrated production was measured at the Reference station (RK2) and highest during the second visit at A3 (Figure 43).

Nanozooplankton function The bioavailable, organic amino acid concentrations ranged between 0.08-2 nM for leucine and 0.2-0.8 nM for methionine. The estimated turnover time varied between 21-239 hours for leucine and 37-412 hours for methionine. Moreover, daily uptake rates of amino acids by total bacterioplankton were determined as 0.03-0.65 nM/day for leucine and 0.03-0.35 for methionine.

26.5 Post-cruise sampling analyses and dead-lines

- Stocks Will be completed by the end of 2012
- Molecular analysis DNA extraction and pyrosequencing will be preformed by the end of February. Data analysis will be completed by 2013.
- Nanozooplankton function Specific single cell grazing activity of mixotrophic and heterotrophic nanoflagellates as well as uptake of organic matter by specific bacterioplankton groups will be determined at the National Oceanography Centre by Dr. Manuela Hartmann using a flow cytometric cell sorting approach in combination with ultra-low level scintillation counting of radiolabelled samples. Dead-line: End of 2012
- Microzooplankton and Relations between Lower and Higher trophic levels
- Single cell carbon fixation rates of phytoplankton rates and microzooplankton grazing on these phytoplankton cells will be measured by Dr. Manuela Hartmann using laser dissecting microscopy in collaboration with Dr. Bernhard Fuchs (Max-Planck-Institute, Bremen, Germany). Due to the large amount of samples this work will finalise beginning 2014.

26.6 References

Brussaard, C. P. D. 2004. Optimization of procedures for counting viruses by flow cytometry. Appl. Environ. Microbiol.70:1506-1513

Christaki U, C Courties, R. Massana, P. Catala, P. Lebaron, P. Gasol, MV Zubkov. (2011). Optimized routine flow cytometric enumeration of heterotrophic flagellates using SYBR Green I. Limnology and Oceanography Methods, 9, 2011, 329–339.

Christaki, U., Obernosterer, I., Van Wambeke, F., Veldhuis, M., Garcia, N., Catala, P. 2008. Microbial food web structure in a naturally iron fertilized area in the Southern Ocean (Kerguelen Plateau)., doi:10.101/j.dsr2.2007/12.009, 55:706-719

Jacquet, S., D. Cardinal, N. Savoye, I. Obernosterer, **U. Christaki,** C. Monnin, F. Dehairs, 2008. Mesopelagic organic carbon mineralisation in the Kerguelen Plateau region tracked by biogenic particulate Ba. Deep Sea Research doi:10.1016/j.dsr2.2007.12.038, 55:868-879

Kirchman, D.L. (1993) Leucine incorporation as a measure of biomass production by heterotrophic bacteria. In: Kemp, P.F., Sherr, B.F., Sherr, E.B., Cole, J.J. (Eds.), Handbook of Methods in Aquatic Microbial Ecology. Lewis Publishers, Boca Raton, pp. 509 – 512.

Zubkov MV & Tarran GA (2008) High bacterivory by the smallest phytoplankton in the North Atlantic Ocean. *Nature* 455(7210):224-226

Zubkov MV, Tarran GA, & Fuchs BM (2004) Depth related amino acid uptake by Prochlorococcus cyanobacteria in the Southern Atlantic tropical gyre. *Fems Microbiology Ecology* 50(3):153-161.

Plate A : Some Tintinnids (ciliates) and Dinoflagellates in live samples during KEOPS II

27 Zooplankton and fish biomass/distribution using echosounding during the Kerguelen bloom

Principal investigator

Cédric Cotté
LOCEAN-IPSL, 4, Place Jussieu, 75005, Paris
CEBC, Villiers en Bois, 79360 Beauvoir sur Niort
cecotte@cebc.cnrs.fr, cedric.cotte@locean-ipsl.upmc.fr

Names of other participants

- E. Josse (IRD-LEMAR)
- F. d'Ovidio (LOCEAN-IPSL)
- Y. Cherel (CEBC)
- C. Guinet (CEBC)

Abstract:
During the Keops-2 cruise, the Simrad EK60 scientific echosounder system was mounted on board to estimate biomasses of mid-trophic level organisms, i.e. macrozooplankton and small pelagic fish. The single frequency- 70kHz was used to detect organisms bigger than 5-10mm. Despite the presence of parasites from ADCP and a strong background noise, the vertical and horizontal distribution of integrated biomasses will be especially linked to the dynamic landscape of the plume. Preliminary results show spatial and temporal variability (nychtemeral migration for instance) of acoustic detections, with different shape and amplitude.

27.1 Scientific context

While the Kerguelen plume is known to correspond to a high chlorophyll area in the Southern Indian Ocean, very few information is available on mid-trophic levels in this region. Several studies showed that this area is important for numerous top predators from Kerguelen since they used it intensively to forage (Guinet *et al.* 1996, Cherel *et al.* 2010). Most of these predators, seals and penguins, presented the same prey preference and they mostly feed on myctophids which are small pelagic lantern fish. It is thus important to elucidate the spatial and temporal distribution of zooplankton and fish and to understand the link with lower trophic level to better understand biogeochemical fluxes across trophic network. Active acoustic techniques have proved useful in studying the spatial distribution and behaviour of pelagic fish (Fréon and Misund 1999), and the echo-integration of data delivered by the scientific echosounders is nowadays a standard method to estimate pelagic fish abundance, (Simmonds and MacLennan 2005, Kloser *et al.* 2009). Importantly, acoustics is the best way among the available techniques to look continuously at fine-scale spatio-temporal variations of the deep-scattering layers. This work is also a preliminary study in the framework of the ANR "MYCTO" that will also use the same acoustic system with 3 frequencies (38kHz, 120kHz and 200kHz)

27.2 Overview of the project and objectives

The main objective of the project is thus to study the spatial and temporal distribution of mid-trophic organisms in the Kerguelen plume, especially regarding the influence of the circulation and water masses on this distribution. More specific approaches will be (i) to validate the detected echos with samplings from Bongo net (collaboration with F. Carlotti et M.P. Juandet), and (ii) to

complement our high-resolution measurement with backscaterring information from ADCP giving global pattern (of nychtemeral migration for instance)

27.3 Methodology and sampling strategy

The echosounder system consists of one transducer hull-mounted in a sink and connected to the General Purpose Transceiver (GPT). The system was in active mode during the whole cruise and record continuously during both transit and stations. The pulse duration was 512 microseconds with a sample interval of 128 microseconds at a bandwidth of 4687. The power used by the system was 600 W and the emission interval was 1s. The environmental parameters (temperature and salinity) were adjusted at the different encountered water masses to calibrate the sound speed.

Table XXXVII : Exhaustiv list of measured parameters

Parameter	code of operation	units
1. Echosounding Backscaterring	N/A	DB (decibel) = amplitude of signal

27.4 Preliminary results

We firstly observe in our data the presence of parasites from ADCP and a strong background noise (Figure 1). Nevertheless, we obtained clear signal of organisms through the shape of layers (probably zooplankton) or schools (fish).

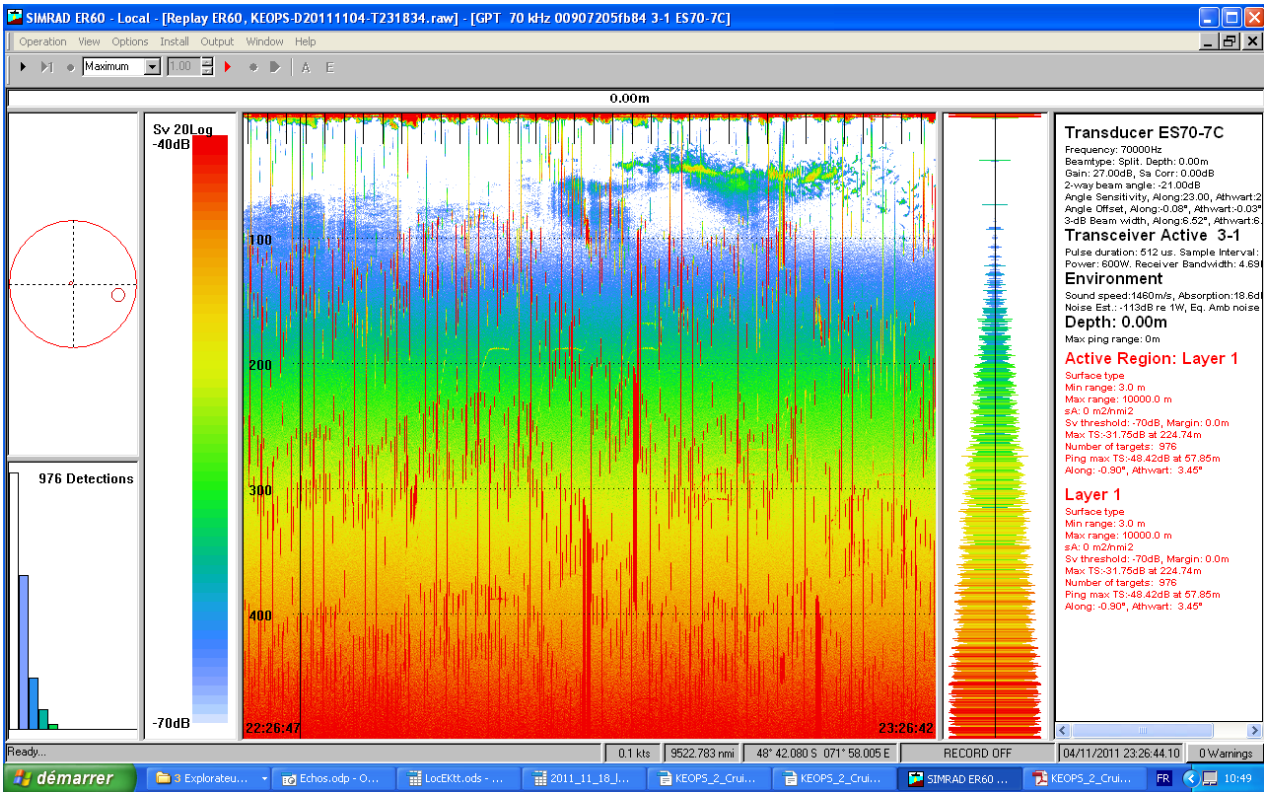

Figure 44 : Example of an Echogram. The amplitude of the backscaterring is in colour (indicating decibels)

27.5 Post-cruise sampling analyses and dead-lines

Data will be processed after the cruise in the framework of the ANR “MYCTO”

27.6 Data base organization (general cruise base and/or specific data base(s))

A specific database will be organized by the team of LEMAR and LOCEAN

27.7 References of methods

Cherel Y, Fontaine C, Richard P, Labat JP (2010) Isotopic niches and trophic levels of myctophid fishes and their predators in the Southern Ocean. Limnol Oceanogr 55: 324-332

Fréon P, Misund OA (1999) Dynamics of pelagic fish distribution and behaviour: effects on fisheries and stock assessment. Fishing new books. Oxford

Guinet C, Cherel Y, Ridoux V, Jouventin P (1996) Consumption of marine resources by seabirds and seals in Crozet and Kerguelen waters: changes in relation to consumer biomass 1962-85. Antarct Sci 8:23-30

Simmonds EJ, MacLennan DN (2005) Fisheries acoustics: theory and practice. 2nd edition, Fish and Fisheries Series, Blackwell, Oxford

28 Intake of oceanographic measurements from elephant seals to KEOPS 2 cruise

Principal investigator

Christophe Guinet
CEBC, Villiers en Bois, 79360, Beauvoir sur Niort
guinet@cebc.cnrs.fr

Names of other participants

- C. Cotté (LOCEAN-IPSL, CEBC)
- F. d'Ovidio (LOCEAN-IPSL)
- M. Lévy (LOCEAN-IPSL)
- F. Bailleul (CEBC)
- J. Vacque-Garcia (CEBC)

Abstract:

The aim of this project was to equip elephants seals from Kerguelen with CTD tag to obtain complementary data to the KEOPS2 cruise. Post breeding seals are known to prospect the region east of Kerguelen. Along their path, the devices fitted on 18 seals have measured profiles of temperature and salinity during their deep and regular dives; 5 devices included a fluorometry sensor and 4 devices included a oxygen sensor. Because of the large area prospected by seals in only several days/weeks, a synoptic view of the plume could be obtained. For the same reason, seals could also help to extrapolate the observations of KEOPS2 to the entire plume, especially in other mesoscale eddies of the plume

28.1 Scientific context (1/2 page max.)

Elephant seals has proven to be very useful in collecting environmental data together with location and behaviour of animals. Because they perform long-distance trips over the Southern Indian Ocean and they dive at a mean depth of 600m (maximum over 2000m), seal allowed to improve our knowledge on the oceanic circulation (Boehme *et al.* 2007, Roquet *et al.* 2009) and the origin of deep Antarctic water (Charrassin *et al.* 2008). Moreover, since 2008, the classical CTD-Argos satellite tag fitted to the seals has included new sensors measuring the fluorometry or the oxygen. Previous study showed that female elephant seals from Kerguelen travel and forage preferentially in the frontal systems of the Antarctic Circumpolar Current in the eastern area of Kerguelen (Bailleul *et al.* 2010a), and adjust their behaviour to mesoscale eddies (Bailleul *et al.* 2010a).

28.2 Overview of the project and objectives

The objective of the project is to equipped elephant seals with CTD-Argos tag, some including also fluo/oxygen sensor, to collect additional and original data to the KEOPS2 cruise. More specifically, (i) we expected to obtain a large and synoptic view of the area from seals which is difficult using sampling from the ship, and (ii) seals could be very helpful to extrapolate the observations of KEOPS2 to the entire plume

28.3 Methodology and sampling strategy

A total of 18 devices (designed by the Sea Mammal Research Unit, University of Saint Andrews) were fitted on elephant seals in Kerguelen Island. 9 tags recorded Conductivity Temperature Depth data, 5 others included the Fluorescence sensor, and 4 others included the Oxygen sensor. Each profile correspond to a dive of seals, explaining the variable maximum depth of profiles. Both locations and profiles are transmitted using Argos system allowing a near-real time acquisition of data.

Table XXXVIII : Exhaustiv list of measured parameters

Parameter	code of operation	units
1. Temperature	N/A	°C
2. Salinity	N/A	
3. Fluorescence	N/A	
4.Oxygen	N/A	mL/L

28.4 Preliminary results

Data were transmitted in near-real time on board. Figure 45 reports the tracking of all seals in the area around Kerguelen during one month after seal equipment. Thus we obtain in-situ measurements from elephant seal. Figure 46 shows a synoptic horizontal view of several parameters during the first week of data collection. However, data from the different tags need to be calibrated in order to pool them and before interpreting the maps

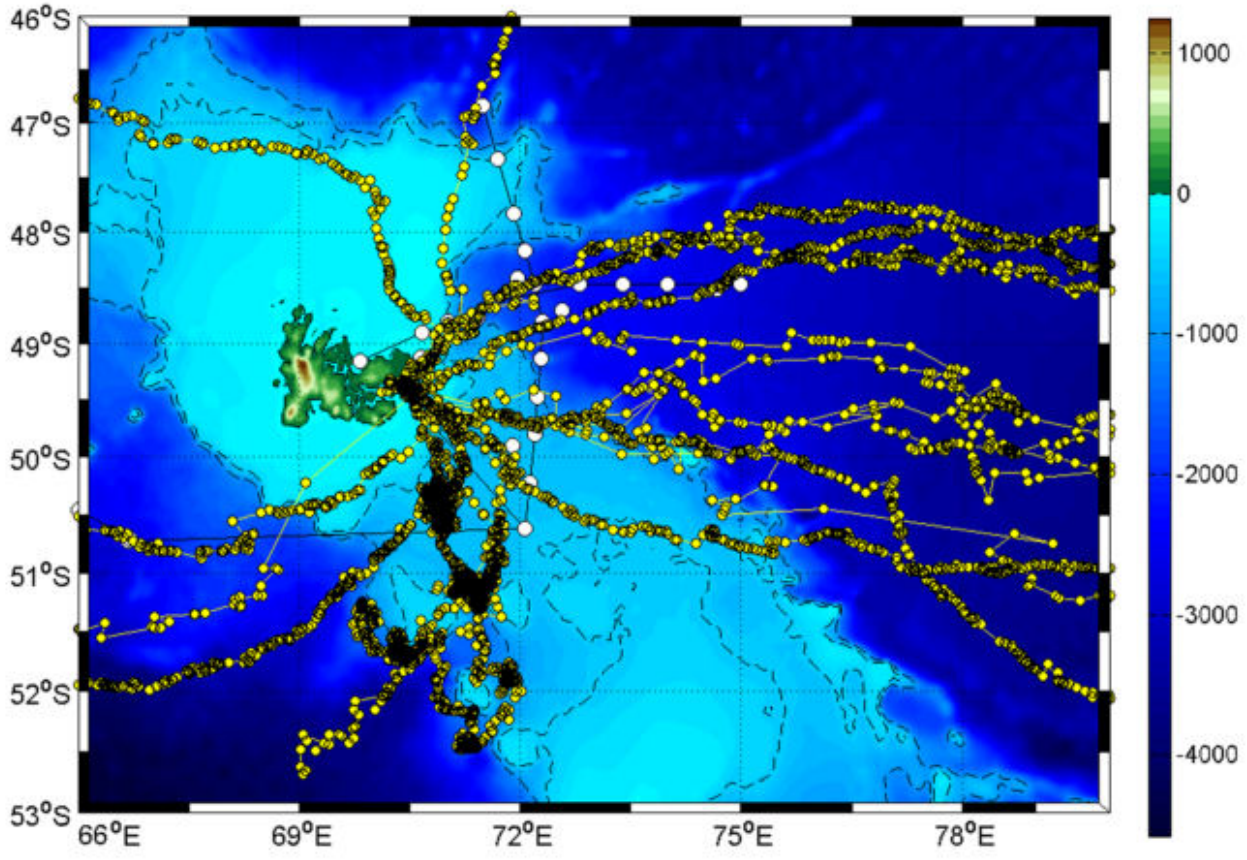

Figure 45 : Seal tracking (18 individuals) from 24/11/2011 to 25/11/2011 overlayed to bathymetry of the Kerguelen plateau. Stations carried out during Keops 2 are white dot.

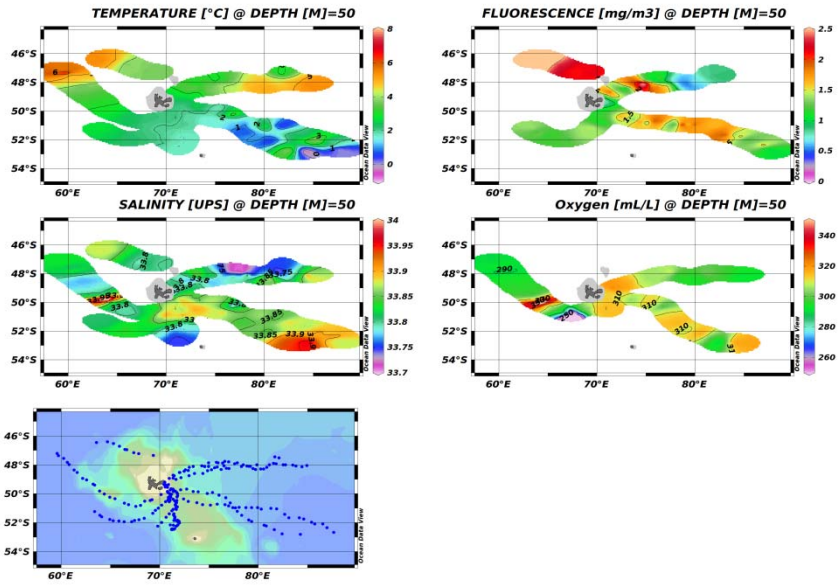

Figure 46 : Horizontal sections of parameters measured by devices fitted on elephant seals during the first week of deployment (from 24/10/2011 to 01/11/2011).

We also drawn section from the different profils obtained from the same individual. An example is given in Figure 47.

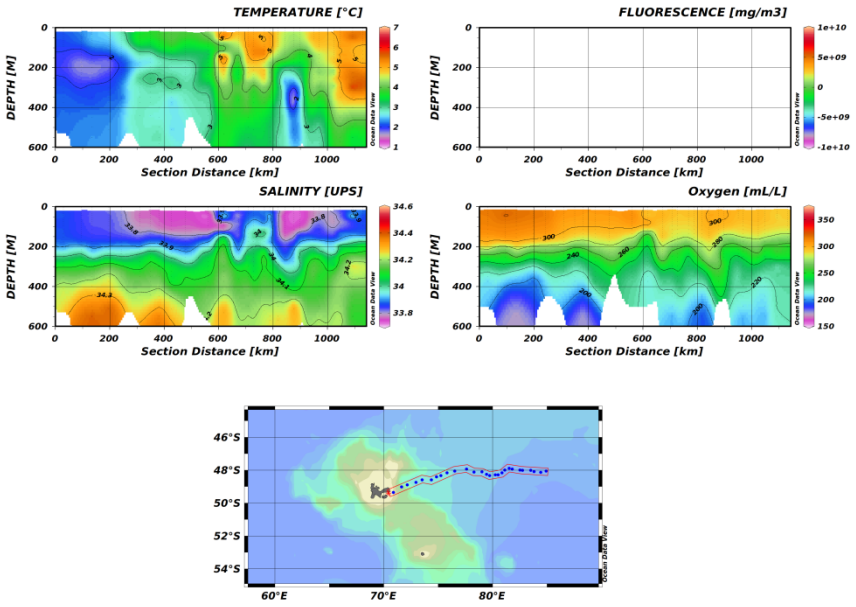

Figure 47 : Vertical sections of parameters mesured by the device of a single individual.

28.5 Post-cruise sampling analyses and dead-lines

Data will be processed (filtered and calibrated) after the cruise

28.6 Data base organization (general cruise base and/or specific data base(s))

Specific database on elephant seals organized at the CEBC, and inclusion of temperature and salinity in the Coriolis database.

28.7 References of methods

Bailleul F, Authier M, Ducatez S, Roquet F, Charrassin JB, Cherel Y, Guinet C (2010a) Looking at the unseen: combining animal bio-logging and stable isotopes to reveal a shift in the ecological niche of a deep-diving predator. Ecography 33:709-719

Bailleul F, Cotté C, Guinet C (2010b) Mesoscale eddies as foraging area of a deep-diving predator, the southern elephant seal. Mar Ecol Prog Ser 408:251-264

Boehme L, Thorpe S.E., Biuw M., Fedak M., & Meredith M.P. 2008. Monitoring Drake Passage with elephant seals: Frontal structures and snapshots of transport. Limnol. Oceanogr. 53: 2350–2360.

Charrassin J.B, Hindell M., Rintoul S.R., Roquet F., Sokolov S., Biuw M., Costa D., Boehme L., Lovell P., Coleman R., Timmermann R., Meijers A.J., Meredith M., Park Y.H., Bailleul F., Goebel M., Tremblay Y., Bost C.A., McMahon C.R., Field I.C., Fedak M.A. & Guinet C. 2008. Southern Ocean frontal structure and sea-ice formation rates revealed by elephant seals. Proc. Nat. Acad. Sci. 105: 11634-11639

Roquet F, Park YH, Guinet C, Bailleul F, Charrassin JB (2009) Observations of the Fawn Trough Current over the Kerguelen Plateau from instrumented elephant seals. J Mar Syst 78:377-393

29 Influence of physical aggregation in the removal of carbon from a Southern Ocean naturally iron-fertilized phytoplankton bloom as quantified by in-situ and roller tank observations.

Principal investigator

Emmanuel Laurenceau
Antarctic Climate and Ecosystems Cooperative Research Center, Hobart, Australia.
and
Institute of Marine Antarctic Studies, University of Tasmania, Hobart, Australia
☎ +33 617 085 456
emmanuel_laurenceau@hotmail.com

Names of other participants

- T.W. Trull (ACE–CRC, Institute of Marine Antarctic Studies, and CSIRO)
- D. Davies ACE–CRC, Institute of Marine Antarctic Studies)
- C. De La Rocha (LEMAR)

Résumé :

Au cours de la campagne KEOPS2 Kerguelen Ocean and Plateau compared Study, de l'eau de mer a été prélevée au-dessus et au large du plateau des Kerguelen, à deux profondeur dans la couche de mélange. L'incubation de cette eau durant 1 à 3 jours a permis d'obtenir des agrégats composés majoritairement de phytoplankton. Des mesures individuelles de paramètres physiques (ex : la porosité) et chimiques (POC, BSi, TEP) ont été réalisées sur chaque agrégat dans le but de préciser les paramètres les plus influents sur leur vitesse de chute. Des observations miroscopiques seront également mise en œuvre afin d'identifier les composants de chaque agrégat (ex : espèces de diatomées majoritaires). Les premiers résultats montrent des vitesses de chute qui s'étendent de 10 à 140 m.jour-1 ce qui est en accord avec les vitesses d'agrégats de Diatomées rencontrées dans la littérature (Alldredge & Gotschalk 1989). De plus, les vitesses de chute des agrégats semblent être une fonction du lieu de prélèvement des particules primaires puisque des différences significatives d'une station à l'autre sont observées. La porosité des agrégats s'étend de 20 à 67% et une faible relation avec la vitesse de chute observée sur les premiers résultats nécessite d'être précisée.

Abstract : During the Kerguelen Ocean and Plateau compared Study KEOPS2, natural seawater has been sampled at several stations above and off-shore the Kerguelen Plateau at two different depths in the mixed layer. The incubation of this water during 1 to 3 days in rolling tanks permited to obtain aggregates mainly composed of phytoplankton. Individual measurements of physical (e.g. porosity) and chemical parameters (POC, BSi, TEP) have been done on each aggregates in order to investigate the critical parameters influencing their sinking velocity. Microscopic observations will also been carried to identify the components of each aggregate (e.g. major diatoms species). The first results display sinking velocities values between 10 and 140 m.day-1 which is in the range of sinking velocities of natural diatoms aggregates observed in the litterature (Alldredge & Gotschalk 1989). Moreover, sinking velocities of aggregates seem to be a function of the locations of primary particles since significative differences between stations are observed. The porosity of aggregates ranges between 20 and 67% and a slight relation with the sinking velocity from the preliminary results needs to be precised.

29.1 Scientific context

The findings from the Kerguelen Ocean and Plateau compared Study (KEOPS) demonstrate that the impact of natural iron fertilization in the Southern ocean is significantly different from those observed in artificial iron fertilization experiments (Boyd & Trull 2007). These results shed light on the implication of deep water iron supply on seasonal high biomass production accompanied by high carbon sequestration efficiency over the natural iron fertilized Kerguelen plateau (Blain *et al.* 2007). The downward flux of carbon processed mainly by biological aggregation through the heterotrophic food web was conducted by the settling of three major types of particles: the oval fecal pellets, the cylindrical fecal pellets and aggregates which mainly consisted of agglomerations of the cylindrical pellets (Ebersbach & Trull 2008). Particles sinking speed, estimated from comparison between particle abundance size spectra and those observed previously in polyacrylamide gel-filled sediment traps displayed higher values in High Nutrient Low Chlorophyll (HNLC) waters than beneath the bloom, supporting that the sinking speed was not as a simple monotonic function of the size and varied spatially (Jouandet *et al.* 2011).

KEOPS confirmed the effect of natural iron fertilization on the primary production above the plateau and brought quantitative results of the flux of carbon exported in the ocean interior. However the processes implied in the efficiency of this export are still unclear and need to be investigated. The part of exported particles formed by physical aggregation, the efficiency of this export and the possible links between the composition and the settling velocity of these particles are particularly big issues.

29.2 Overview of the project and objectives

KEOPS2 represents a big opportunity to carry aggregation experiments onboard in order to study the characteristics of aggregates obtained from natural primary particles sampled in the Southern Ocean. The study of the physical parameters and composition of aggregates in term of particles and chemical components could bring very interesting informations about the crucial parameters influencing the sinking velocity of aggregates and thus the efficiency of the carbon export. The major objective of the study is to link the composition and properties of aggregates formed in roller tanks to their sinking velocity and to assess the reliability of these results using other measurements done on naturally formed particles. Then, the comparison of the aggregates formed in roller tanks to the particles collected in gel traps deployed at several stations and with the images from the Underwater Video Profiler (UVP) is likely to permit to extend the results to the mechanism occuring in the open ocean.

29.3 Methodology and sampling strategy

29.3.1 Overview of the experiment

The experiments were carried out in cylindrical tanks rotating on rolling table to simulate the sinking of particles through a water column (Shanks and Edmondson, 1989). Four transparent cylindrical 10L tanks, designed especially for this experiment were used. Natural seawater from 12 L niskin bottles sampled in duplicate at two depths in the mixed layer chosen in accordance with the CTD profile locating the maximum of chlorophyll. The water was stored several days before to be incubated in the roller tanks in the dark, during 1 to 3 days. At the end of each experiment 3 selected aggregates in each duplicate were photographied, sized and their sinking velocity measured in situ with a serological pipet. The aggregates were then collected. A set was used to measure crucial parameters like TEP, BSi and POC and the other set put in lugol for microscopic observations. The sampling of the background water was also done to measure TEP, BSi and POC in order to correct the aggregates values from it.

29.3.2 Chemical measurements

TEP were measured onboard using a spectrophotometric method from Passow and Alldredge (1995). BSi will be determined using a variation of the method of Ragueneau and Tréguer (1994).

29.3.3 Sampling strategy

The sampling strategy was based on the objective to form aggregates from different locations and on time series from a same station. The stations sampled were: E3, E-4W, E-4E, F-L, A3-2, and E5.

Table XXXIX : Exhaustiv list of measured parameters

Parameter	code of operation	units
1. POC in aggregates and background water	CTD Biodiv. Roll.	µmol.L^{-1}
2. BSi in aggregates and background water	CTD Biodiv. Roll.	µmol.L^{-1}
3. TEP in aggregates and background water	CTD Biodiv. Roll.	µg eq. xanthan gum · mL agg^{-1}
4. Sinking velocity of aggregates	CTD Biodiv. Roll.	m.day^{-1}
5. Porosity of aggregates	CTD Biodiv. Roll.	%
6. Size (ESD) of aggregates	CTD Biodiv. Roll.	mm
7. Volume of aggregates	CTD Biodiv. Roll.	mm^3

29.4 Preliminary results

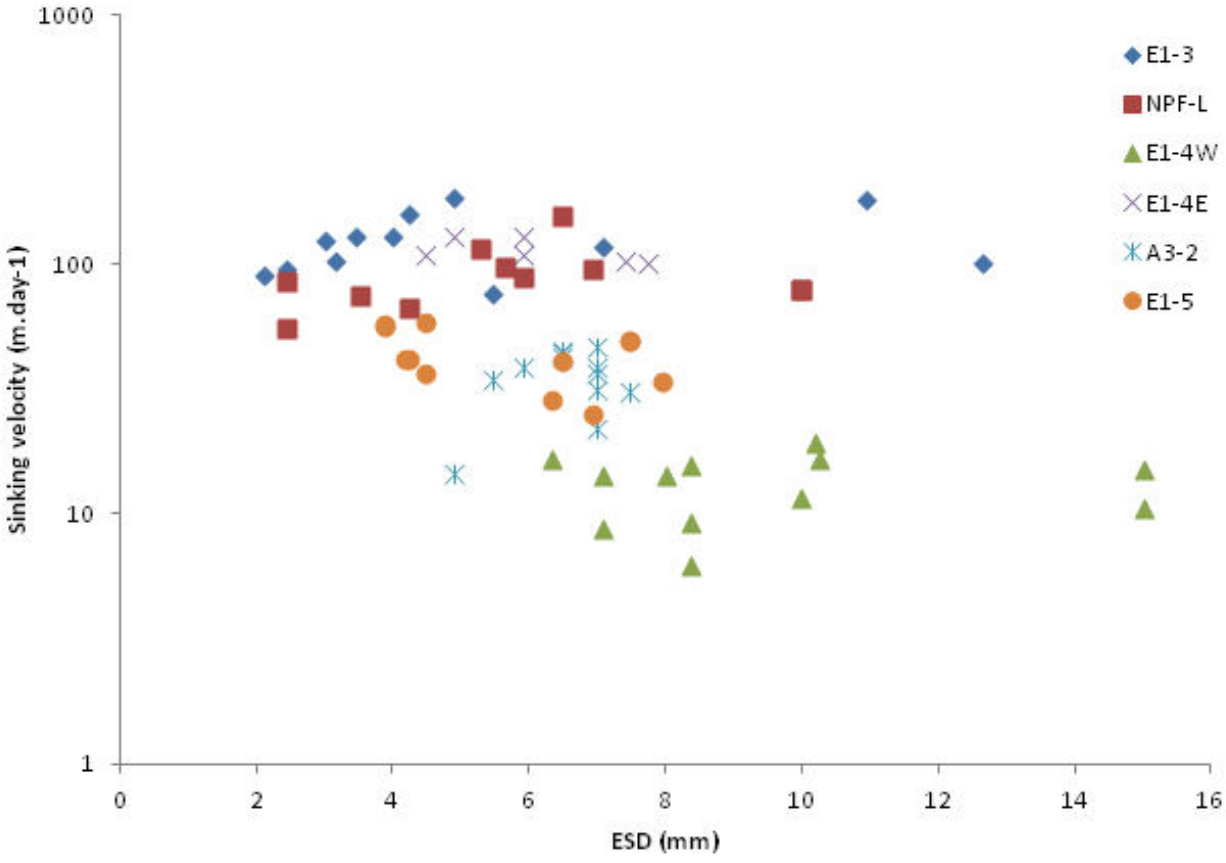

Figure 48 : Sinking velocity of aggregates in m.day^{-1} versus their equivalent spherical diameter (mm) at all stations.

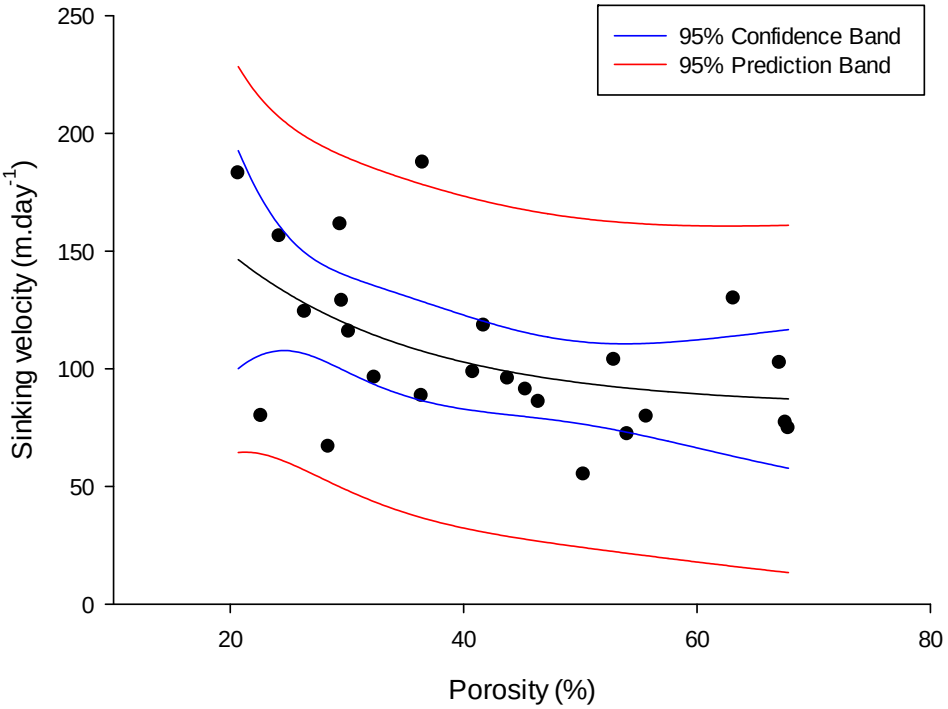

Figure 49 : Sinking velocity of aggregates in $m.day^{-1}$ versus their porosity in % at stations F-L and E3 (total)

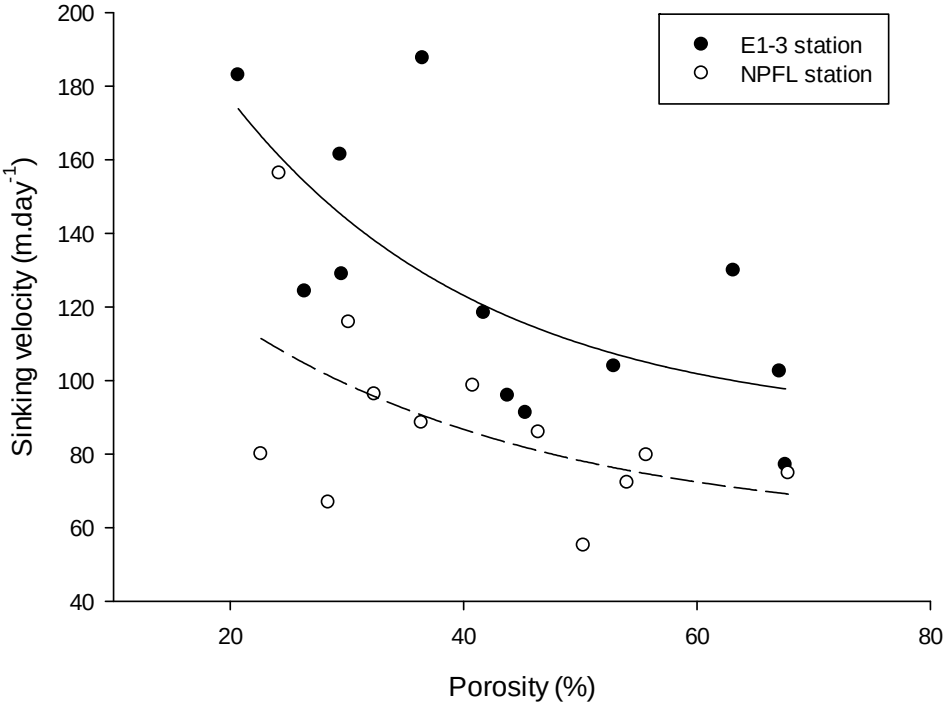

Figure 50 : Sinking velocity of aggregates in $m.day^{-1}$ versus their porosity in % at stations F-L and E3.

29.5 Post-cruise sampling analyses and dead-lines

TEP calibration and BSi sampling analyses: unknown at this time since depending from possible collaborations between Hobart and Brest.

POC samples will be analysed approximately in February in Hobart labs.

29.6 Data base organization

A specific data base has been constructed and will be refined to be shared on the public space.

29.7 References

Alldredge AL, Gotschalk CC (1989) Direct observations of the mass flocculation of diatom blooms: characteristics, settling velocities and formation of diatom aggregates. Deep-Sea Research Part A: Oceanographic Research Papers 36:159-171.

Blain S, Quéguiner B, Armand L, Belviso S, Bombled B, Bopp L, Bowie A, Brunet C, Brussaard C, Carlotti F, Christaki U, Corbiere A, Durand I, Ebersbach F, Fuda JL, Garcia N, Gerringa L, Griffiths B, Guigue C, Guillerm C, Jacquet S, Jeandel C, Laan P, Lefevre D, Lo Monaco C, Malits A, Mosseri J, Obernosterer I, Park YH, Picheral M, Pondaven P, Remenyi T, San-droni V, Sarthou G, Savoye N, Scouarnec L, Souhaut M, Thuiller D, Timmermans K, Trull T, Uitz J, van Beek P, Veldhuis M, Vincent D, Viollier E, Vong L, Wagener T (2007) Effect of natural iron fertilization on carbon sequestration in the Southern Ocean. Nature 446:1070-1074.

Boyd P, Trull T (2007) Understanding the export of biogenic particles in oceanic waters: Is there consensus? Progress In Oceanography 72:276-312.

Ebersbach F, Trull TW (2008) Sinking particle properties from polyacrylamide gels during the KErguelen Ocean and Plateau compared Study (KEOPS): Zooplankton control of carbon export in an area of persistent natural iron inputs in the Southern Ocean. Limnology and Oceanography 53:212-224.

Jouandet M-P, Trull TW, Guidi L, Picheral M, Ebersbach F, Stemmann L, Blain S (2011) Optical imaging of mesopelagic particles indicates deep carbon flux beneath a natural iron-fertilized bloom in the Southern Ocean. Limnology and Oceanography 56:1130-1140.

Passow U, Alldredge AL (1995) A dye-binding assay for the spectrophotometric measurement of transparent exopolymer particles (TEP). Limnology and Oceanography 40:1326-1335

Ragueneau O, Tréguer P (1994) Determination of biogenic silica in coastal waters: applicability and limits of the alkaline digestion method. Marine Chemistry 45:43-51.

30 Carbon export and remineralisation fluxes

Principal investigator

Frédéric Planchon
LEMAR, Technopole Brest Iroise Place Nicolas Copernic 29280 Plouzané
☎ +33 298 498 698
🖷 +33 298 498 645
frederic.planchon@univ-brest.fr

Names of other participants

- F. Dehairs, Vrije Universiteit Brussel (VUB)
- T. Trull, ACE-CRC, Hobart
- D. Davies, ACE-CRC, Hobart
- A.-J. Cavagna, VUB
- D. Cardinal, LOCEAN, Paris VI
- S. Jacquet, LOPB, Marseille

Abstract:

The focus of this work is on assessing the export flux of particles and carbon and the remineralisation of exported matter in the subsurface, mesopelagic waters during early season. Two main proxy-tools are used: (1) the ^{234}Th-deficit method to assess the export flux and (2) The build-up of the biogenic particulate Ba stock in subsurface waters to assess remineralisation. Sampling strategy consisted in resolving as much as possible the features in the upper 1000m of water column. In addition ^{234}Th activity ($t_{1/2}$ 24.1 days) was measured on (i) size fractionated suspended matter from vertical profiles; (ii) size fractionated matter from surface waters and (iii) material collected by free-drifting sediment traps to identify the POC/^{234}Th ratios of those particles most likely responsible for the export flux. While samples for biogenic Ba were saved for analysis later, beta-activity of the short-lived ^{234}Th isotope was measured directly on board for all samples, but final results await corrections for background activity and recovery, which can only be carried out after 6 to 7 ^{234}Th decay periods.

First results for ^{234}Th deficit indicate moderate export (relative to the reference station 'R') for the whole of KEOPS 2 area (including shelf station A3), and little change during these early stages of bloom development. 'E' stations showed evidence for increased ^{234}Th excess at mesopelagic depths over time, possibly indicating remineralisation.

30.1 Scientific context (1/2 page max.)

During KEOPS 1, the efficiency of the carbon export, defined as the ratio of particulate organic carbon at depth to primary production, was lower above the Kerguelen plateau (28%) than in HNCL-waters (58%) (Savoye *et al.*, 2008). These observations raise important questions on the processes that are responsible for the remineralisation of the organic matter in surface waters and how they are affected by iron fertilisation. The understanding of the structure and functioning of the food web is critical in this context. Studying export and remineralisation in an early bloom situation and under differing regimes of Fe supply to off-shelf waters east of Kerguelen during KEOPS 2 is expected to shed further light on this.

30.2 Overview of the project and objectives (1/2 page max.)

The focus is on assessing the export flux of particles and carbon and the remineralisation of exported matter in the subsurface, mesopelagic waters during the first stages of the spring bloom, the development of which was followed from MODIS imagery. The purpose of this work package is to contribute in conjunction of inputs by others, to answering the following questions put forward in the overall KEOPS 2 project: (1) Can we characterize the pathways that lead to the remineralisation or export of organic matter produced in surface waters? (2) What is the magnitude of the enhancement of the carbon export due to natural iron fertilisation during the early stages of the bloom? (3) What is the flux of carbon exported below the winter mixed layer? (4) What is the fate of carbon exported in deep water? (5) How does the export of particulate organic matter relate with bloom state and the intensity of vertical mixing (aggregation processes etc)?

Two main proxy-tools are used: (1) the ^{234}Th-deficit method to assess the export flux and (2) The build-up of the biogenic particulate Ba stock in subsurface waters to assess remineralisation. Sampling strategy consisted in resolving as much as possible the features in the upper 1000m of water column. In addition ^{234}Th activity ($t_{1/2}$ 24.1 days) was measured on (i) size fractionated suspended matter from vertical profiles; (ii) size fractionated matter from surface waters and (iii) material collected by free-drifting sediment traps to identify the POC/^{234}Th ratios of those particles most likely responsible for the export flux.

30.3 Methodology and sampling strategy:

30.3.1 ^{234}Th activity and export flux

Naturally occurring ^{234}Th is the decay product of ^{238}U, which is conservatively distributed in open ocean and proportional to salinity. Unlike ^{238}U, ^{234}Th has a strong affinity for particulate matter and its activity distribution through the water column offers a means for quantifying fluxes and aggregation/disaggregation rates of particles on a regional and seasonal scale (Buesseler *et al.*, 1992). Combined with the POC/^{234}Th ratio of sinking particles, calculated fluxes of ^{234}Th enable to quantify upper ocean and mesopelagic export of POC (Cochran et Masqué, 2003; Savoye *et al.*, 2004, 2008; Maiti *et al.*, 2010).

Sampling strategy consisted in resolving as much as possible the features in the upper 1000m of water column. In addition of total ^{234}Th activity measurements, we also measured beta activity of (i) two size fractions (1< < 53 µm and >53µm) of suspended matter from vertical profiles from large volume in-situ pump sampling; (ii) 6 size fraction (>350; 350>>210; 210>>50; 50>>20; 20>>5; 5>>1) of surface water suspended matter sampled via a high flow rate on-board pump when at station (see cruise report by T. Trull); (iii) sinking particles collected by short-term (2 – 6 days) PPS3 sediment trap deployment, in order to identify the POC/^{234}Th ratios of those particles most likely responsible for the export flux (see cruise report by T. Trull). Total ^{234}Th (i.e., dissolved + particulate; from 4L seawater samples) is precipitated with Mn-oxide and collected on QMA filters (1 µm nominal pore size) following Pike *et al.* (2005). Recovery is checked by spiking with a known amount of ^{230}Th, and will be assessed later, once samples have been counted for background activity. Suspended material collected on large diameter screens or filters is resuspended in filtered seawater and re-filtered on Ag filters of 1 µm pore size.

Beta-activity of the short-lived ^{234}Th isotope of all types of samples was measured directly on board, though final results await corrections for recovery, background activity, POC analysis, which will be done after 6 to 7 ^{234}Th half-lives (~6 months). POC analysis will be carried out by Elemental Analyser at VUB, Brussels (in-situ pump samples) and ACE-CRC, Hobart (surface filtrations and traps).

^{234}Th flux (obtained by integrating the deficit of activity relative to ^{238}U activity) is multiplied by the POC/^{234}Th ratio of sinking particles. Usually the >53µm size fraction is used for that purpose.

30.3.2 Particulate barium

Profiles of particulate biogenic Ba (Ba_{xs}) in the open ocean generally display a maximum in the upper mesopelagic (~ 150 – 500m) (Jacquet *et al.* 2008; Dehairs *et al.*, 2008). This Ba_{xs} is mostly present as microcrystalline barite ($BaSO_4$), which forms inside oversaturated microenvironments, mostly aggregates of organic material where bacterial activity is intense. When these particles are remineralised in the mesopelagic zone, barites are spread over the water layer and Ba_{xs} content can be related to carbon remineralisation activity. The time-scale involved in this process integrates a period of a few weeks.

5-10L of seawater was filtered onto 0.4 µm polycarbonate membranes (∅ 47mm) using Perspex filtration under slight overpressure of filtered air (0.4µm). Membranes were rinsed with a few mL of Milli-Q water to remove most of the sea salt, dried overnight at ~60°C and stored in plastic Petri dishes. Filtration blanks, consisting of 5 L filtered Milli-Q water and re-filtered seawater were processed on-board.

In the home-based laboratory particles are digested with a tri-acid mixture (1.5 ml HCl 30%, 1.0 ml HNO_3 65% and 0.5ml HF 40%, all Suprapur grade) in closed teflon beakers overnight at 90°C (Cardinal *et al.*, 2001; 2005). Samples are evaporated close to dryness and redissolved into ~13ml of HNO_3 2%. These solutions are analysed by ICP-MS X Series 2 (Thermo) equipped with a Collision Cell Technology (CCT) or by HR-SF-ICP-MS. Ba, Na and Al contents are analysed simultaneously (with CCT for Al and without for Ba and Na) and concentrations calculated using linear calibration curves made by analysing certified standards of diverse origins to check that matrix effect, if present, is adequately corrected by internal standards (^{99}Ru, ^{115}In, ^{187}Re, ^{209}Bi). The standards used for calibration are dilute acid-digested rocks (e.g. BHVO-1, GA, SGR-1), natural water (SLRS-4) and multi-element artificial solutions.

A small part of every filter sample is saved for later SEM-EMP analysis of barite morphology and abundance (S. Jacquet, LOPB, Marseille).

Table XL : Exhaustiv list of measured parameters

Parameter	code of operation	units
1. Total ^{234}Th actvity	CTD	dpm/l
2. Particulate ^{234}Th activity	ISP	dpm/l
3. Particulate ^{234}Th activity	Surface water filtration	dpm/l
4. Particulate ^{234}Th activity	Free drifting PPS3 Traps	dpm/l
5. Particulate Ba	CTD	pmol/l

30.4 Preliminary results

Figure 1 shows the preliminary (un-corrected) total ^{234}Th activity profiles for stations E1, E2, and E3. Total ^{234}Th activity (in cpm/sample) appears depleted in surface waters relative to its parent nuclide ^{238}U, indicating that export of ^{234}Th-bearing particles from the upper water column already occurred before the first visit to site "E" (E1). Total ^{234}Th deficit in surface waters remains relatively unchanged during the second and third visits to "E" site (E2 and E3), indicating that the system was close to a steady state condition. Note that deficit of ^{234}Th activity reaches till 300m horizon,

extending well below the upper mixed layer. Some excess ^{234}Th activity can be discerned at 300m and below for E2 and E3 possibly indicating increasing remineralisation over time. Confirmation of such features, however, awaits correcting data for background counting and ^{234}Th recovery.

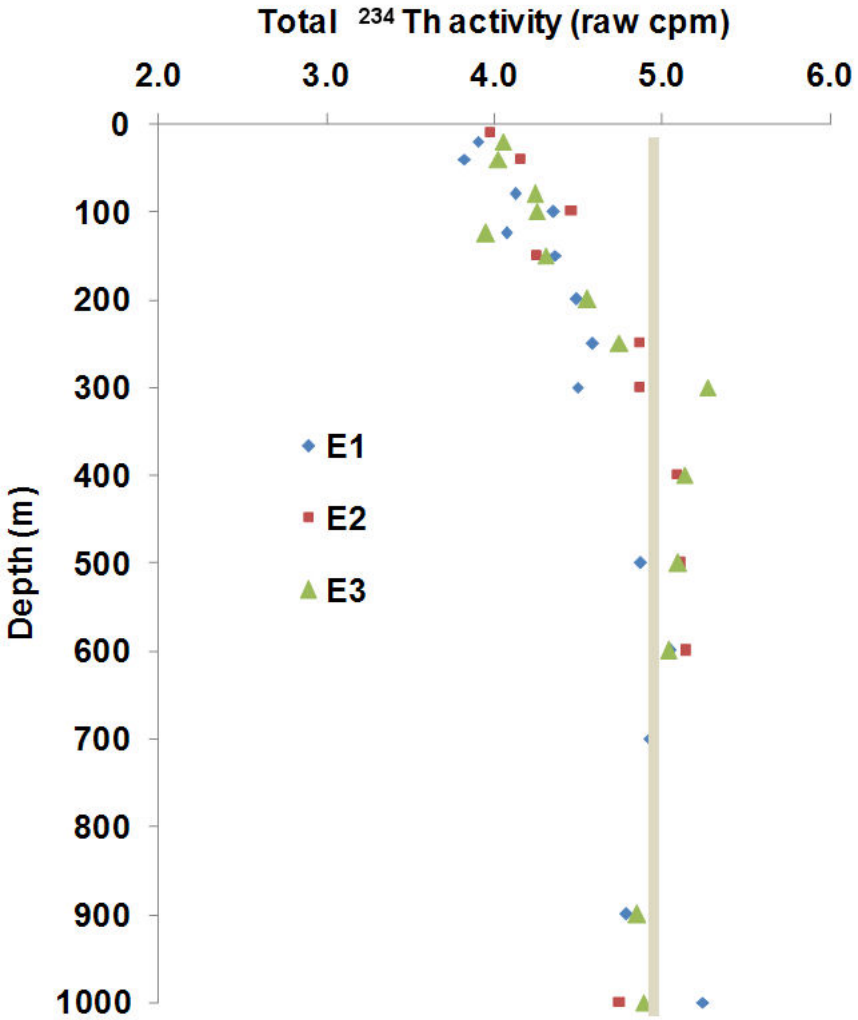

Figure 51 : Total ^{234}Th activity (cpm/per sample) measured as a function of depth at E1, E2, and E3. The grey bar represents the secular equilibrium between ^{238}U and ^{234}Th.

30.5 Post-cruise sampling analyses and dead-lines

- ^{234}Th: After 6 to 7 decay periods (April-May 2012) all samples are re-counted to correct for any background, ^{238}U-sustained activity. Subsequently samples for total ^{234}Th activity are dissolved after spiking with ^{229}Th for recovery assessment and ^{230}Th/^{229}Th ratio is measured by HR-SF-ICP-MS, either in Brussels or at IUEM, Brest (June-July 2012). After background counting the particulate matter samples from on-board filtrations and free-drifting sediment traps these will be send to ACE-CRC, Hobart for further analysis there (May-June 2012). Background counted particulate matter samples collected by in-situ pumps will be analysed for POC at VUB (May-June 2012).
- Samples for particulate Ba will be analysed either in Brussels, Marseille or LOCEAN, depending on access to HR-ICP-MS facilities (summer – autumn 2012). A small part of every filter sample is saved for later SEM-EMP analysis of barite morphology and abundance (S. Jacquet, LOPB, Marseille; in the course of 2013).

30.6 References of methods

Buesseler K.O., M.P. Bacon, J.K. Cochran and H.D. Livingston, 1992. Carbon and nitrogen export during the JGOFS North Atlantic Bloom experiment estimated from ^{234}Th: ^{238}U disequilibria, *Deep-Sea Research Part A*, 39(7-8), 1115-1137.

Cardinal D., F. Dehairs, T. Cattaldo and L. André, 2001. Constraints on export and advection in the Subantarctic and Polar Front Zones, south of Australia from the geochemistry of suspended particles, *Journal of Geophysical Research*, 106, 31,637.

Cardinal, D.B., N. Savoye, T.W. Trull, L. André, E. E. Kopczynska and F. Dehairs, 2005. Variations of carbon remineralisation in the Southern Ocean illustrated by the Ba_{xs} proxy, *Deep-Sea Research I*, 52, 355-370.

Dehairs, F., S. Jacquet, N. Savoye, J.K.B Bishop, B.A.S. van Mooy, K.O. Buesseler, C.H. Lamborg, M. Elskens, P.W. Boyd, K. Casciotti, W. Baeyens, 2008. Barium in twilight zone suspended matter as a proxy for particulate organic carbon remineralization: results for the North Pacific, *Deep-Sea Research II*, 55, 1673-1683.

Jacquet S.H.M, P.J. Lam, T.W. Trull and F. Dehairs, 2011. Carbon export production in the Polar Front Zone and Subantarctic Zone south of Tasmania, *Deep-Sea Research II,* 58, 2277-2292.

Maiti, K., C.R. Benitez-Nelson and K.O. Buesseler, 2010. Insights into particle formation and remineralization using the short-lived radionuclide, Thorium-234, *Geophysical Research Letters*, 37(15), L15608, doi:10.1029/2010GL044063.

Pike, S. M., K.O.Buesseler, J. Andrews and N. Savoye, 2005. Quantification of ^{234}Th recovery in small volume sea water samples by inductively coupled plasma-mass spectrometry, *Journal of Radioanalytical and Nuclear Chemistry*, 263(2), 355-360.

Planchon F., A.-J. Cavagna, D. Cardinal, L. André and F. Dehairs, Late summer particulate organic carbon export from mixed layer to mesopelagic twilight zone in the Atlantic sector of the Southern Ocean, to be submitted to *Biogeosciences* (BONUS-GoodHope special volume).

Savoye, N., K. O. Buesseler, D. Cardinal, D. and F. Dehairs, 2004. ^{234}Th deficit and excess in the Southern Ocean during spring 2001: Particle export and remineralization, *Geophysical Research Letters*, 31(12), L12301, doi:10.1029/2004GL019744

Savoye, N., T. W. Trull, S. H. M. Jacquet, J. Navez and F. Dehairs, 2008. ^{234}Th-based export fluxes during a natural iron fertilization experiment in the Southern Ocean (KEOPS), *Deep-Sea Research II*, 55(5-7), 841-855.

31 Sterols and their carbon isotopic composition in whole water column suspended matter

Principal investigator

Anne-Julie Cavagna
ANCH & ESS depts. – Vrije Universiteit Brussel – Pleinlaan 2 – Brussels, Belgium
☎ +32-2 629 39 71
🖷 +32-2 629 18 11
acavagna@vub.ac.be

Names of other participants (+affiliation)

- F. Dehairs (ANCH & ESS dept. – VUB)
- F. Planchon (LEMAR)

Abstract:
The combination of organic matter composition (sterols for this study) and $\delta^{13}C$ signatures is a powerful approach for addressing the nature of ecological and environmental changes. It allows studying the fate and origin of organic matter throughout the oceanic water via Compound Specific Isotope Analysis (CSIA). Samples for CSIA were taken at each In-Situ Pump (ISP) deployment during KEOPS.

Résumé : Combiner la composition de la matière organique (étude des sterols pour ce projet) avec la signature isotopique naturelle $\delta^{13}C$ est une approche puissante pour comprendre la nature des changements écologiques et environnementaux dans le système étudié (changements temporels et / ou spatiaux). Cela permet en effet d'étudier l'origine et le devenir de la matière organique à travers la colonne d'eau via CSIA. Pour cela, des échantillons ont été prélevés à chaque déploiement de pompes in-situ lors de l'expédition KEOPS 2.

31.1 Scientific context

Gaining information about source and fate of sinking and suspended biogenic particles is necessary to improve our knowledge on what is happening below the euphotic layer where the attenuation of the export flux is the strongest. Wakeham *et al.* (2009) state that one way to improve our understanding about mechanisms controlling interrelated biogeochemical processes involved in particle sinking and decomposition is to determine the chemical composition of those particles sinking rapidly through the water column as well as of the suspended fine particles with longer residence time. The study of selected sterols & their $\delta^{13}C$ in the context of CSIA allows gaining such information and, to the best of our knowledge, only one study documents the whole water column distribution of selected sterols and their $\delta^{13}C$ in the Southern Ocean (Cavagna *et al.*, *to be submitted*; Cavagna, 2011). In this study, cholesterol and brassicasterol were chosen as ideal biomarkers of the heterotrophic and autotrophic carbon pools because of their ubiquity and relative refractory nature.

31.2 Overview of the project and objectives

The objectives are here (1) to document the fate and origin of biogenic particles in 2 size fractions (small particles = 53> diameter >1 µm; and large particles = diameter > 53 µm) in the whole water column at each long station occupied during KEOPS 2; (2) to document spatial variation of the studied biomarkers through the Kerguelen site in the early productive season; and (3), to improve the database preliminary obtained for cholesterol and brassicasterol $\delta^{13}C$ and relative content distribution in the Southern Ocean whole water column (Cavagna *et al.*, *to be submitted*).

31.3 Methodology and sampling strategy

On board *R/V* Marion Dufresne, particulate organic matter is sampled using in situ large volume filtration systems (Challenger Oceanics and McLane WTS6-1-142LV systems) fitted with 142 mm diameter filters holders. Water is pumped through two successive filters: (i) a 53 µm mesh nylon screen (filter SEFAR-PETEX®; polyester) and (ii) a QMA quartz fiber filter (~1 µm porosity, Pall Life). Prior to use PETEX screens were conditioned by soaking in HCl 5 %, rinsed with Milli-Q grade water, dried at ambient temperature under a laminar flow hood and were stored in clean plastic zip-bags till use. QMA filters were conditioned for trace-metal analysis (pre-combustion and acid bath – see cruise report by Andrew Bowie and Pier van der Merwe). Filters were sub-sampled for the analysis of: (i) trace-metals (see report by Bowie *et al.*); ^{234}Th activity (see report by Planchon *et al.*) and Chl-a (report by V. Cornet) using sterile scalpels for the PETEX screens and a plexiglass punch of Ø = 25.30 mm for the QMA filters. Aliquots dedicated to compound specific isotope analysis (CSIA) were packed in cryotubes and stored at -80°C till processing in the home-laboratory. Aliquots dedicated to the analysis of $\delta^{13}C_{POC}$ were dried at 50°C and stored in Petri dishes at ambient temperature till processing in the home laboratory.

Particulate organic carbon (POC) concentration along with its carbon isotopic composition ($\delta^{13}C_{POC}$) will be analyzed via elemental analyzer – isotope ratio mass spectrometer (EA-IRMS). Prior to this, inorganic carbon (carbonates) is removed by exposing the filters to concentrated HCl vapor inside a closed-glass container during 4 h. After drying at 50°C the samples are packed in silver cups and analyzed with a Carlo Erba NA 2100 elemental analyzer configured for C analysis and coupled on-line via a Con-Flo III interface to a Thermo-Finnigan Delta V isotope ratio mass spectrometer (IRMS). Acetanilide and IAEA-CH-6 reference materials are used for calibrating concentrations and isotopic composition, respectively.

Samples for sterols analysis are processed following the method described in Boschker (2004). Briefly, total lipids are extracted using a modified method from Bligh and Dyer (1959) with chloroform / methanol / Milli-Q water mixture. The total lipid extract is then separated into neutral (eluted with chloroform), glyco- (eluted with acetone), and polar lipids (eluted with methanol) on silica chromatographic column (0.5 g Kieselgel 60; Merck). Neutral phases containing sterols are completely dried under gentle inert N_2 flow (to avoid degradation) while the glyco-lipids and the polar phases are stored at -20°C for further possible analyses; and a known quantity of squalane used as internal standard IS (i.e. stable compound which does not co-elute with natural compounds present in the samples) is added. Dried neutral lipids are then derivatized using bis-(trimethylsilyl)-trifluoroacetamide (BSTFA, 99%) / toluene (v:v, 1:1). Trimethylsylil (TMS) groups are substituted to the hydrogen of the hydroxyl groups of the compounds to form trimethylsyliloxy groups [-O-Si-$(CH_3)_3$]. In practice, derivatization is achieved by adding 50 µL of BSTFA-toluene to the dried samples (and squalane) and heating during 60 min at 60°C. All the TMS-derivatized neutral fractions (+IS) are analyzed using a Trace GC Ultra coupled to Trace Plus MS (Interscience) for compound identification and a Thermo Finnigan GC equipped with a combustion furnace (CuO/NiO/Pt reactor at 940°C) coupled to a Delta*Plus* XL isotope ratio mass spectrometer (IRMS), for $\delta^{13}C$ and concentration measurements. Compound identification is achieved by (i) retention time matching between standard mix and sample, (ii) GC-MS mass spectrometry characterization (matching with Goad and Akihisa, 1997).

Table XLI : Exhaustive list of measured parameters

parameters	code of operation	units
1. sterols biomarkers $\delta^{13}C$	ISP	‰
2. sterols biomarkers concentration	ISP	ng L^{-1}
3. POC-bulk $\delta^{13}C$	ISP	‰
4. POC-bulk concentration	ISP	µg L^{-1}

31.4 Post-cruise sampling analyses and dead-lines

Start post-cruise analyses in early summer 2012. Deadline post-cruise analyses mid-2013.

Data will be included in the general cruise base.

31.5 References of methods

Bligh, E.G., Dyer, W.J. A rapid method of total lipid extraction and purification. Can. J. Biochem. Physiol. 31, 911-917, 1959.

Boschker, H. T. S. Linking microbial community structure and functioning: stable isotope (13C) labeling in combination with PLFA analysis, pp. 1673–1688, in: Molecular Microbial Ecology Manual II, edited by: Kowalchuk, G. A., de Bruijn, F. J., Head, I. M., Akkermans, A. D., and van Elsas, J. D., Kluwer Academic Publishers, Dordrecht, The Netherlands, 2004.

Cavagna, A.-J., Dehairs, F., Woule-Ebongué, V., Delille, B., Bouloubassi, I., Bouillon, S. Whole water column distribution and carbon isotopic composition of POC-bulk, cholesterol and brassicasterol from the Cape Basin to the northern Weddell Gyre. *To be submitted to Biogeosciences, BONUS-GoodHope special issue*.

Cavagna, A.-J., 2011. The biological pump in the Southern Ocean: three study-cases, three stable isotope tools. PhD thesis, Vrije Universiteit Brussel, 188pp.

Goad L.J., Akihisa, T. Analysis of sterols. Eds. Blackie Academic & Professional, 437 pp, 1997.

Wakeham, S.G., Lee, C., Peterson, M.L., Liu, Z., Szlosek, J., Putnam, I.F., Xue, J. Organic biomarkers in the twilight zone - Time series and settling velocity sediment traps during MedFlux. Deep Sea Res. Part II, 56(18), 1437-1453, 2009.

32 Biogeochemistry of Kerguelen plateau sediments

Principal investigator

Marie Lise DELGARD
Laboratoire EPOC, UMR 5805, Université Bordeaux 1
m.delgard@epoc.u-bordeaux1.fr

Names of other participants

- P. Anschutz, Ph.D. supervisor (EPOC)
- B. Deflandre, Ph.D. supervisor (EPOC)

Abstract:
Sediment cores were collected in 6 contrasting stations situated on the Kerguelen plateau and in the surrounding area. Several experiments were performed to get some key biogeochemical parameters: oxygen microprofiles, sediment water interface fluxes measurements, solid phase and porewaters key redox species concentration. Study of coastal stations should help to better characterize the potentiel source of iron that promotes recurrent phytoplankton bloom. Samples from stations out of the plateau would help to understand the impact of deposition of the bloom material on deep sediment.

32.1 Scientific context

During Keops 1, bottom waters above the plateau was systematically enriched in dissolved total iron. Sediment could thus be a potential supply of iron that promotes recurrent phytoplankton bloom. In order to characterize this source, sediments were collected during Keops 1 on several stations on the plateau. Only one coring was made outside the plateau at 3350 m depth (station C11).

During Keops 2, we focused on an eddy structure next to Kerguelen plateau and thus studied deeper stations than those of Keops 1.

32.2 Overview of the project and objectives

We investigate the biogeochemistry of sediments of the Kerguelen plateau and the surrounding area.

More specifically, we aim to understand the spatial variability of sediment biogeochemistry of coastal and oceanic stations in link with the complex circulation of water masses, in particular by taking into account the eddy dynamic and the presence of the polar front.

Two coastal stations were sampling to characterize the potential source of iron. Shallower stations were visited in order to study the potential impact of the deposition of bloom material on deep sediment.

32.3 Methodology and sampling strategy

32.3.1 Sampling strategy:

Cores were collected in contrasted stations in order to characterize the sediment biogeochemistry of the Kerguelen plateau and surrounding area. Two stations are on the plateau: one in the south of the polar front (A3: 535 m depth) that was visited twice and one in the north of the polar

front (TEW1: 84 m depth). Four deeper stations were sampled: a reference station located in the HNLC area (R: 2445 m depth), a station in the polar front (F: 2741 m depth) and 2 stations located in the eddy (E3: 1920 m depth, E4W: 1410 m depth).

All the deployments provided at least 4 high quality sediment cores (undisturbed sediment-water interface, clear overlying water, length > 10 cm).

32.3.2 Methodology:

On deck:

Overlying water was sampled for dissolved oxygen, nutrients (after filtration at 0.2 µm), phytoplankton identification and counting (L. Armand).

Immediate cores treatment sequence in the lab:

- Oxygen microprofiles: 1 to 4 dissolved oxygen profiles per station with a vertical resolution of 1mm to 250 µm.
- Incubation set up: one core was incubated with an optode (D. Lefevre) to follow in real time the consumption of oxygen and to optimise the incubation time. Samples of overlying water were collected at the beginning and at the end of the incubation to measure Sediment Water Interface fluxes of several dissolved redox species: oxygen, NH4, NO2, NO3, PO4, Fe, Si(d). Samples were filtered through acetate cellulose membrane (0.2 µm, MINISART).
- Core slicing under N_2: One core was sliced under N_2 few hours after sampling with 0.5 cm resolution for the top 2 cm, with 1 cm resolution in the 2 to 10 cm layer, with 2 cm resolution in the 10 to 24 cm and with 3 cm resolution down to the core bottom (until 30 cm depth maximum). For each level, a sub-sample was sealed in a pre-weight vial and frozen for later chemical analyses of the solid fraction. Another sub-sample was centrifuged to extract porewater at 4,000 rpm for 15 min and filtered through acetate cellulose membrane (0.2 µm, MINISART). An aliquot of filtered interstitial water was immediately acidified with HN03 to prevent precipitation of reduced iron. A second aliquot was refrigerated at 4°C for Si(d) and ΣCO_2 analysis. A third aliquot was frozen at -20°C for NO_2, NO_3, NH_4 analysis.

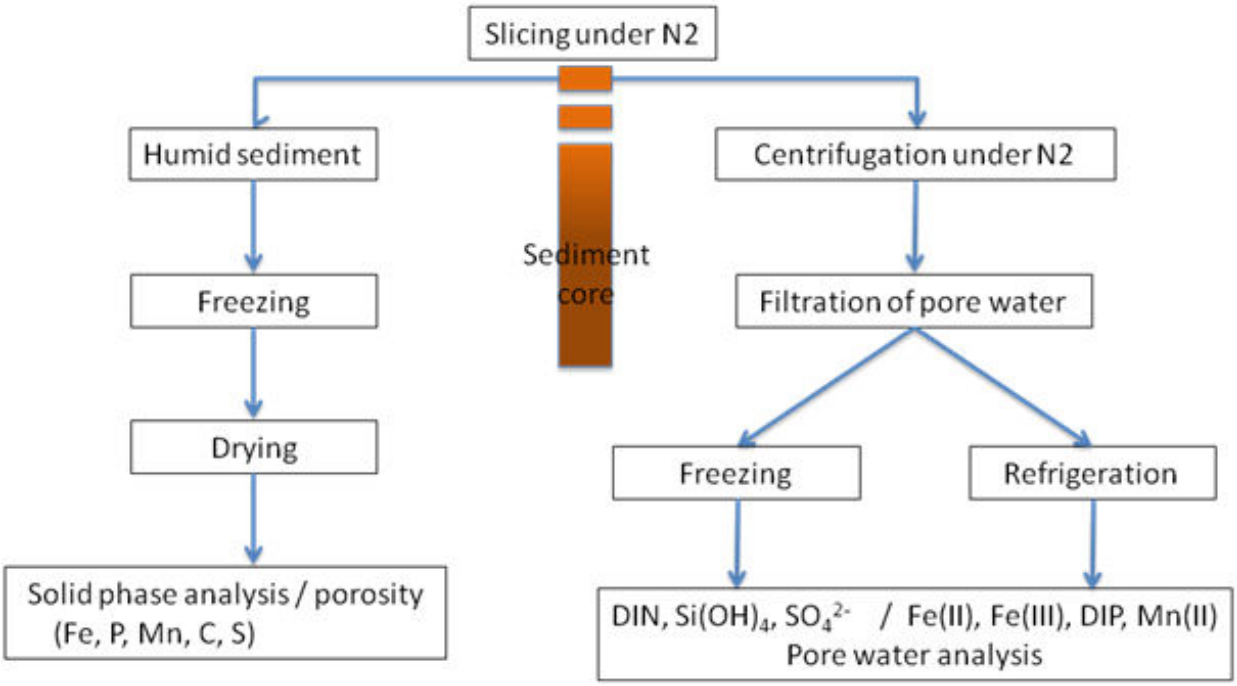

Figure 52 : Sediment core sample treatments.

At the end of the incubation (after 2 days at least), 3 cores were sliced (with the same vertical resolution previously described) for analysis of the following parameters:

- One core for Pa/Th (Jeanne Gerardhi),
- One core for Biogenic Si (Bernard Quéguiner), Alkenones (Anne-Julie Cavagna) and Phytoplankton (Leanne Armand),
- One core for Radioelements (Pieter van Beek).

Table XLII : Exhaustiv list of measured parameters

Parameter	code of operation	units
1. overlying water temperature	CORER	°C
2. dissolved oxygen concentration in PW	CORER	µmol/L or % sat
3. dissolved oxygen concentration in OW	CORER	µmol/L
4. NH_4 concentration in OW	CORER	µmol/L
5. Total Fe(d) concentration in OW	CORER	µmol/L
6. H_4SiO_4 concentration in OW	CORER	µmol/L
7. NO_2 concentration in OW	CORER	µmol/L
8. NO_3 concentration in OW	CORER	µmol/L
9. PO_4 concentration in OW	CORER	µmol/L
10. Total Fe(d) concentration in PW	CORER	µmol/L
11. PO4 concentration in PW	CORER	µmol/L
12. H_4SiO_4 concentration in PW	CORER	µmol/L
13. NO_2 concentration in PW	CORER	µmol/L
14. NO_3 concentration in PW	CORER	µmol/L
15. NH_4 concentration in PW		
16. Mn(II) concentration in PW	CORER	µmol/L
17. P ascorbate concentration (solid phase)	CORER	µmol/g
18. P HCl concentration (solid phase)	CORER	µmol/g
19. Fe ascorbate concentration (solid phase)	CORER	µmol/g
20. Fe HCl concentration (solid phase)	CORER	µmol/g
21. Mn ascorbate concentration (solid phase)	CORER	µmol/g
22. Mn HCl concentration (solid phase)	CORER	µmol/g
23. porosity	CORER	No units
24. Particulate Organic Carbon (POC)	CORER	%
25. Total carbon	CORER	%
26. Total sulfur (TS)	CORER	%

Abbreviations: PW: porewaters; OW: overlying water

- Parameter 2: Microprofiles of dissolved oxygen concentration in porewaters were measured on board at 250-1000 µm depth increments with Clark-type sensors (Revsbech 1989) manufactured by Unisense. The sensor tip diameter is 100 µm and the 90% response time is shorter than 7 s. Microelectrodes are connected to a high-sensitivity picoammeter (Unisense) via an A/D converter. Linear calibrations were done in air saturated water (the oxygen concentration was precisely determined by the Winkler titration) and zero oxygen in the anoxic part of the sediment.
  Oxygen profiles will be processed using the PRO_2FLUX software (Deflandre and Duchêne, 2010). Oxygen diffusive fluxes will be calculated with this software.
- Parameter 3: Dissolved oxygen concentration in overlying water was determined on board by Winkler titration with the D. Lefevre titration system.
- Parameter 4: Ammonium concentration in overlying water was measured on board by fluorimetry method (see 'nutrient analysis' report Stephan Blain et Louise Oriol).
- Parameter 5: Total dissolved iron concentration in overlying water will be measured by the 'trace metal team' (FIA method, See Geraldine Sarthou report).
- Parameters 6/7/8/9: Nutrient measurements (NO_2, NO_3, PO_4, H_4SiO_4) of overlying waters were made on board by Louise Oriol with a nutrient autoanalyser. (See nutrient report).
- Parameters 10/11: Dissolved inorganic phosphate and iron were measured in porewaters by colorimetric procedures a few days after sampling with a precision of ± 5% (Murphy & Riley 1962, Stookey 1970, Strickland & Parsons 1972).
- Parameters 12 to 15: H_4SiO_4, NO_2, NO_3 and NH_4 in porewaters will be measured with a nutrient microflow autoanalyser.
- Parameter 16: Flame atomic adsorption spectrometry will be used for porewaters Mn(II) concentration determination.
- Parameters 17 to 22: Sediment samples from core slicing under N_2 will be freeze-dried. The weight loss will be used to calculate porosity after sea salt correction. The dried sediment will be homogenized and kept for solid-phase analysis. An ascorbate reagent will be added to remove the most reactive Fe(III) phases (Fe ascorbate) and the associated phosphorus (P ascorbate) from the sediment (Kostka *et al.* 1994, Anschutz *et al.* 1998). This reagent also remove the most reactive Mn(III)/Mn(IV) phases (Mn ascorbate) from the sediment. A separate extraction will be carry out with HCl to determine acid-soluble iron (Fe HCl). This reagent is used to dissolved amorphous Fe oxides, FeS, Fe phyllosilicates and carbonates (Kostka *et al.* 1994). Phosphorus extracted with HCl (P HCl) come from detrital and authigenic phosphate minerals, and from carbonates (Kostka *et al.* 1994, Anschutz *et al.* 2007). Manganese extracted with HCl (Mn HCl) come from Mn oxides and carbonates. For both extractions, about 100 mg of dry sample will be leach with 10 ml soution during 24h while shaking continuously at room temperature. After each extraction, the samples will be centrifuged and the Fe, P and Mn contents of the supernatant will be determined spectrometrically.
- Parameters 23/24/25: POC, total carbon and TS will be measured on freeze-dried samples by infrared spectroscopy using a LECO C-S 125 gas chromatography analyser. POC will be measured after removal of carbonates with HCl. Particulate inorganic carbon (PIC) will be calculated as the difference between total carbon and POC.

32.4 Preliminary results

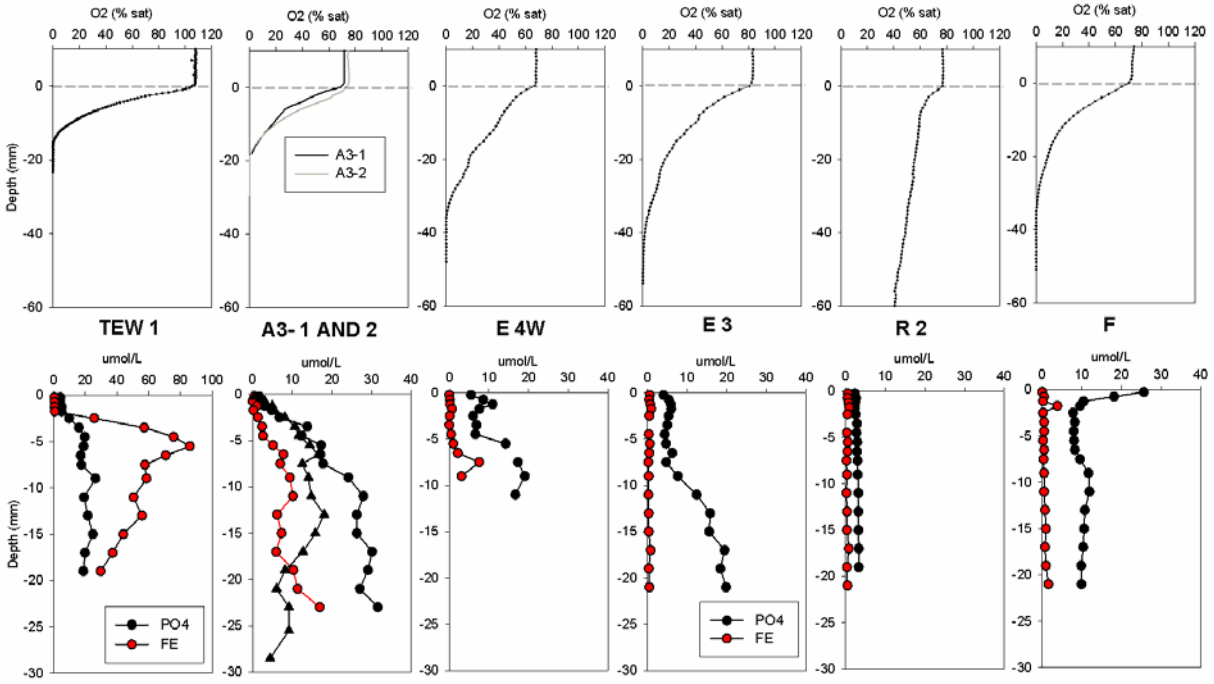

Figure 53 : For each stations, vertical distribution of oxygen (top graphs), PO_4 and total Fe(d) (bottom graphs) concentration measured in porewaters. Note that A3 was visited twice: no Fe(d) was detected at A3-1; black triangles : concentration of PO_4 measured at A3-1; black and red circle : PO_4 and Fe(d) measured at A3-2.

32.5 Post-cruise sampling analyses and dead-lines

Post-cruise analyses:

- Total Fe(d) concentration in OW
- Nutrient (NO_2, NO_3, NH_4, H_4SiO_4) and Mn(II) concentration in PW
- Solid phase analysis: ascorbate and HCl extraction for particulate P, Fe and Mn; Total sulphur, total carbon and POC analysis

32.6 Data base organization

General data base + specific processing database for cores (see excel file : MULTICORERdatabase_KEOPS2)

32.7 References of methods

Anschutz P., Zhong S., Sundby B., Mucci A., Gobeil C., 1998. Burial efficiency of phosphorus and the geochemistry of iron in continental margin sediments. Limnology and Oceanography 43: 53-64.

Deflandre B., Duchene J.C. (2010) PRO2FLUX : a software for PRofile quantification and diffusive O2 FLUX calculation. Environmental Modelling & Software, 25, 1059-1061.

Kostka J. E., Luther G. W., 1994. Partitioning and speciation of solid phase iron in saltmarsh sediments. Geochimica et Cosmochimica Acta 58: 1701-1710.

Murphy J., Riley J. P., 1962. A modified single solution method for the determination of phosphate in natural waters. Analytica Chimica Acta 27: 31-36.

Stookey L. L., 1970. Ferrozine - A new spectrophotometric reagent for iron. Analytical Chemistry 42: 779-781.

33 Export fluxes

Principal investigator

Tom Trull
UTAS-CSIRO, ACE CRC
☎ 61 3 6226 2988
🖷 61 3 6226 2973
Tom.Trull@utas.edu.au

Names of other participants

- D. Davies (ACE CRC)
- S. Bray (ACE CRC)
- A. Passmore (ACE CRC)
- E. Laurenceau (UTAS)

Abstract:

Particle export processes were examined directly and indirectly using several approaches:
1. deployments of a PPS3 sediment trap at a ~200 depth to collect a time series of multiple samples into a carousel of cups.
2. deployments of cylindrical polyacrylamide-gel traps at multiple depths (~100, 200, 300, 400m) for particle imaging
3. separation of surface particles into 6 size classes (350, 210, 50, 20, 5, 1 um) for characterization of their compositions, for comparison with the trap-collected particles, including both elemental (POC/BSI/PIC) and isotopic (15N, 13C) analyses.
4. deployment of an autonomous profiling float with sensors to repeatedly measure phytoplankton (fluorescence) and total (backscatter) biomass distributions as they evolved over time, relative to temperature, salinity and dissolved oxygen distributions.
5. using underway sensors to map spatial distributions of biomass (again via fluorescence and back-scatter) and its influence on export via measurement of dissolved nitrate.

This work was coordinated with:

1. the 234Th deficit method to estimate export – by using samples from the traps and surface size-classes to determine C/Th ratios for conversion of Th export to C export, as described in the voyage report from F. Dehairs and others.

2. particulate trace metal analyses - by using samples from the PPS3 trap to determine export of Fe and other elements, as part of the broader program of particulate and dissolved trace metal studies as described in the report from A. Bowie and others.

3.study of diatoms collected with nets, as described in the report from L. Armand and others.

33.1 Scientific context and overview of the project and objectives

The efficiency of the carbon export (defined as the ratio of particulate organic carbon at depth to primary production) was lower above the Kerguelen plateau (28%) than in HNCL-waters (58%) (Savoye *et al.*, 2008), This raised the question of whether the efficiency of Fe use decreases with its availability an aspect that would significantly affect the calculation of seasonal carbon export budgets from ecosystem models (Mongin *et al.*, 2008). Lower efficiency of iron use could be driven by

luxury iron uptake by phytoplankton and/or enhanced abiotic Fe scavenging by exported organic matter. Determination of the C/Fe ratio of suspended and sinking particles addresses this issue.

The understanding of the structure and functioning of the food web is critical in this context. Development of trophic complexity tends to increase community respiration relative to phytoplankton primary production and thus to lower export efficiency, but it also increases the diversity of particle export pathways, some of which may lead to greater penetration of carbon into the ocean interior. The polyacrylamide gel traps address this issue. Additional information on the extent of recycling is obtained f-ratios calculated from the size-fractionated particle samples via 15N measurements (Trull *et al.*, 2008; and detailed in the voyage report on nitrate isotopic compositions from F. Dehairs et al).

The complex circulation and water mass mixing that occurs downstream of the Kergulen plateau in the region targeted by KEOPS2 makes determination of production and export difficult, and also raises the issue of whether this stirring increases the magnitude of export beyond that which would occur is a less dynamic zone, such as over the Kerguelen plateau. This is a difficult issue to address, and the first issue is to attempt to map the relationships between mixing structures and biomass. The bioprofiler and underway sensors address this issue.

33.2 Methodology and sampling strategy:

The traps were suspended below surface floats using an elastic link to dampen wave motions with pressure sensors to verify deployment depths following the methods of Trull *et al.*, 2008. Separate systems were used for the PPS3 trap (P-string) and gel traps (G-string) After loss of a P-string (possibly as a result of sinking of the hollow surface float), and to optimise logistics a second PPS3 trap was deployed twice on the IODA array (see the voyage report from D. Lefevre) which uses a string of small floats to achieve similar dampening of wave motions. The deployments were carried out at the following sites (Table XLIII).

Table XLIII : Characteristics of the floating trap moorings deployed

Site	Deployed	Instruments	Status	Gel#
R	G-string	RBR PT logger	recovered	1-4
R	P1-string	RBR PT logger	lost	
E2	G-string	RBR PT logger	recovered	5-8
E2	P2 trap with IODA	RBR PT logger and Inclinometre	recovered	
E3	G-string	RBR PT logger	recovered	9-11
E3	P2 trap with IODA	RBR PT logger and Inclinometre	recovered	
F	G-string	RBR PT logger	recovered	12-14
A3-2	P2 string with 1 gel	RBR logger and Inclinometre	recovered	15
E5	G-string	RBR PT logger	recovered	16-18
E5	P2-string	RBR logger and Inclinometre	recovered	

Table XLIV : Exhaustive list of measured parameters

Parameter	code of operation	units
ISUS nitrate sensor	UP - Underway Pump	umol/L
WETLABS FLNTUS sensor - fluorescence	UP	ugChl/L
WETLABS FLNTUS sensor-backscatter	UP	%
CSTAR sensor - beam transmission	UP	%
Aanderaa oxygen sensor (D. Lefevre)	UP	umol/L
WETLABS FLBB sensor - fluorescence	BIOPROFILER	ugChl/L
WETLABS FLBB sensor - backscatter	BIOPROFILER	%
Seabird sensor - oxygen	BIOPROFILER	umol/L
Seabird sensor - temperature	BIOPROFILER	C
Seabird sensor - salinity	BIOPROFILER	psu
Size fractionated POC	UP	umol/L
Size fractionated PON	UP	umol/L
Size fractionated BSi	UP	umol/L
Size fractionated PIC	UP	umol/L
Size fractionated ^{13}C-POC	UP	umol/L
Size fractionated ^{15}N-PON	UP	umol/L
Total POC	UP	umol/L
Total particulate Ca (a few test samples only)	UP	umol/L
Total nitrate	UP	umol/L
Total ^{13}C-DIC	UP	umol/L
Total ^{15}N-NO_3	UP	umol/L
POC, PON, BSi	PTRAP	umol/L
Particle Images and statistics	GTRAP	

Collection of size-fractionated surface samples was done at all stations (except TNS04 an d TNS07) using the pumped water supply in *"Cale 2"*, following methods used in Trull *et al.*, 2008. The pump filter screen (800um) was cleaned immediately prior to every sample collection. The water was sequentially filtered through 142mm diameter plastic meshes (350, 200, 50, 20 and 5 um) and a quartz fibre filter (QMA, 1um nominal size). More water (several hundred litres) was run through the two largest sizes than the other sizes (approx 100 litres). The material collected on the plastic meshes was then transferred to 25mm 1um pore size silver filters.

The pumped water supply in *"Cale 2"* was also used for the underway sensor mapping. The water was run continuously through an insulated tank with the sensors submerged in it. The sensors were:

1) ISUS nitrate sensor.
2) WETLABS FLNTUS phytoplankton fluorescence and particulate backscatter sensor
3) WETLABS CSTAR transmissometer
4) Aanderaa optode oxygen sensor (provided by D. Lefevre)

The FLNTUS had an automated wiper. The CSTAR and ISUS sensor heads were manually cleaned at least once per day. The ISUS was calibrated by running a set of 4 standards several times during the voyage, and by collecting samples for nitrate analyses run onboard by the hydrochemistry team. POC samples were collected at most stations for calibration of the CSTAR. Oxygen samples were collected daily for calibration of the optode (see voyage report of D. Lefevre).

The "bioprofiler" autonomous float was deployed at the E1 site. It is a Teledyne Webb APEX IPF9 float fitted with the standard pumped CTD for T,S, and pressure, and the following additional sensors:

1) SBE43 oxygen electrode
2) WETLABS FLBBAP2 unwiped bio-optical sensor

The float was initially operated to do 4 profiles from 300m depth to the surface daily, and this frequency was then reduced to 2 profiles per day after 2 weeks. The float will continue to operate for several months.

The gels were examined under a binocular microscope and the particles photographed for later image analysis following the methods in Ebersbach and Trull, 2008 and Ebersbach *et al.*, 2011.

33.3 Preliminary results

The only preliminary results available at this time are from the bioprofiler deployed at E1, as presented in the onboard science conferences. Its track is shown in Figure 54, with a selection of profiles shown inFigure 55.

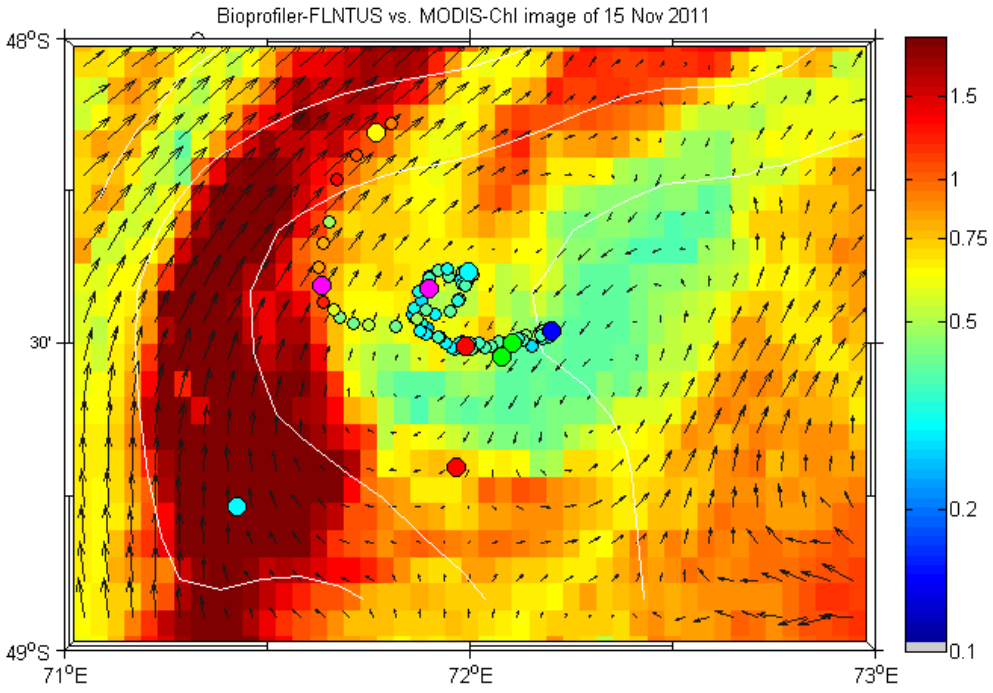

Figure 54 : Bioprofiler maximum fluorescence values along its track compared to a satellite chlorophyll image and velocity field estimated from surface drifter data. The colored circles along the track represent 6 profiles selected for presentation in Figure 2. The colored

circles off the track are the corresponding positions of ship stations at the same time.

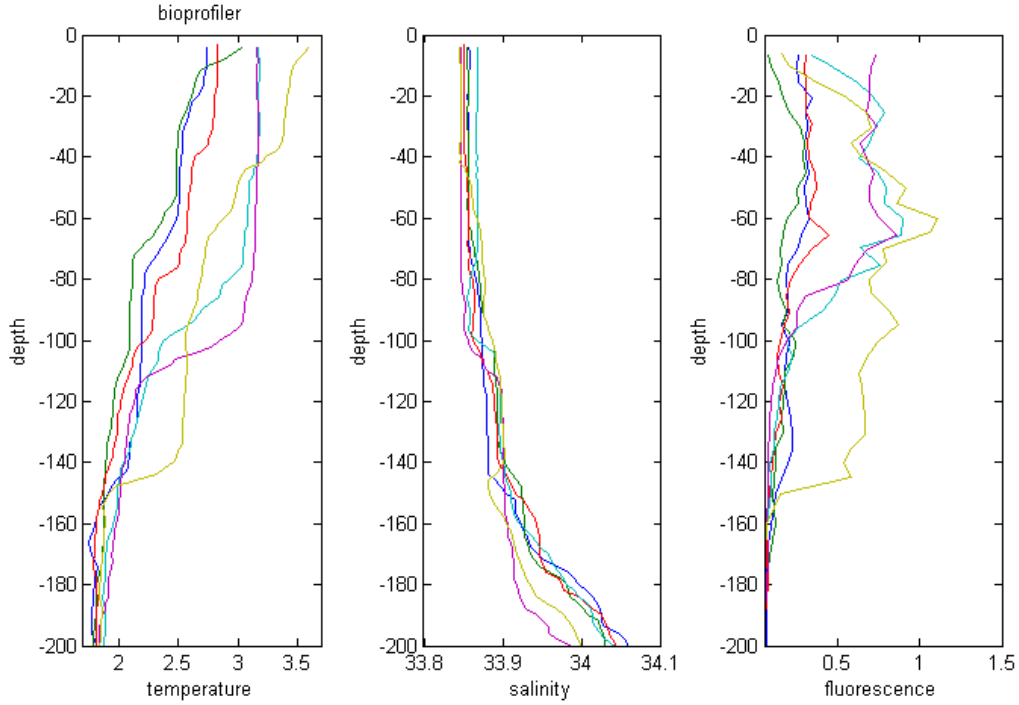

Figure 55 : Selected profiles from the bioprofiler, at the times of the following stations. Blue – E1, Green – E2, Red – E3, Cyan – E4, Magenta – E5, Yellow – leaving the region in the northward flowing jet.

33.4 Post-cruise sampling analyses and dead-lines

The trap and size-fractionated particle samples will be analysed for ^{234}Th backgrounds in Europe in mid 2012, and then returned to Australia for chemical analyses. Some of this data (POC, PON, BSi) may be ready for the September 2012 meeting depending on when the samples arrive. Other analyses are likely to be completed later in 2012. The underway sensor maps will be completed by June 2012 and bioprofiler results will be available continuously as collected. Image analysis of the gel particles will be ready for the September 2012 meeting

33.5 Data base organization (general cruise base and/or specific data base(s))

The data will initially be compiled into specific databases as follows, and then guidance will be sought on the best way to transfer the information into the general cruise data base .

- Underway pump sensor results
- Trap and Size-fractionated sample chemical analysis results
- Bioprofiler results
- Gel photos and particle image analysis statistics

33.6 References of methods

Ebersbach F., and T. W. Trull. 2008. Sinking particle properties from polyacrylamide gels during the KErguelen Ocean and Plateau compared Study (KEOPS): Zooplankton control of carbon export in an area of persistent natural iron inputs in the Southern Ocean. Limnology and Oceanography **53**: 212-224.

Ebersbach F., T. W. Trull, D. M. Davies, and S. G. Bray. 2011. Controls on mesopelagic particle

fluxes in the Sub-Antarctic and Polar Frontal Zones in the Southern Ocean south of Australia in summer--Perspectives from free-drifting sediment traps. Deep Sea Research Part II: Topical Studies in Oceanography **58,** 2260-2276.

Mongin M., E. Molina, and T. W. Trull. 2008. Seasonality and scale of the Kerguelen plateau phytoplankton bloom: a remote sensing and modeling analysis of the influence of natural iron fertilization in the Southern Ocean. Deep Sea Research II **55**: 880-892.

Savoye N., T. W. Trull, S. H. M. Jacquet, J. Navez, and F. Dehairs. 2008. ^{234}Th-based export fluxes during a natural iron fertilization experiment in the Southern Ocean (KEOPS). Deep Sea Research II **55**: 841-855.

Trull T. W., D. Davies, and K. Casciotti. 2008. Insights into nutrient assimilation and export in naturally iron-fertilized waters of the Southern Ocean from nitrogen, carbon, and oxygen isotopes. Deep Sea Research II **55**: 820-840, doi:810.1016/j.dsr1012.2007.1012.1035.

Trull T. W., S. G. Bray, K. O. Buesseler, C. H. Lamborg, S. Manganini, C. Moy, and J. Valdes. 2008. In-situ measurement of mesopelagic particle sinking rates and the control of carbon transfer to the ocean interior during the Vertical Flux in the Global Ocean (VERTIGO) voyages in the North Pacific. Deep Sea Research II **55**: 1684-1695, doi:1610.1016/j.dsr1682.2008.1604.1021.

34 Mesozooplankton community spatial distribution, taxonomy structure, size structure, biomass and role in carbon transformation during the functioning during KEOPS2

Principal investigator

François Carlotti
MIO, Campus de Luminy, case 901
F–13288 Marseille Cedex 09
☎ +33 491 829 111
🖷 +33 491 826 548
francois.carlotti@univmed.fr

Names of other participants

- M.P. Jouandet (MIO)
- A. Nowaczyk (MIO)
- D. Lefèvre (MIO)
- M. Harmelin (MIO)
- M. Zhou (U. Mass. Boston/MIO)
- Y. Zhu (U. Mass. Boston/MIO)

Abstract:

During the KEOPS2 cruise, zooplankton sampling was made with Bongo net using two mesh size nets (120 µm and 300 µm). 42 net tows deployed in all stations and with a "midnight-midday" timing on long stations (> 24 hours). Collected samples have been preserved for further taxonomic counting with binocular, sizing with ZOOSCAN, weighting from dry weight, for measuring 13C and 15N ratios, for assessing the content in chlorophyll or derived pigments in gut. In addition, experiments were done on board on living animals maintained for 20 to 36 hours to estimated oxygen consumption and CO2 production. In four among these experiments, ammonium production was measured additionally.

All these data will be interpreted in the context in connections with various data : sea surface temperature and chlorophyle, hydrodynamics, physical, chemical and biological parameters from CTD / Rosette profiles.

The different treatment would conduct to an understanding of :

– the mesozooplankton community spatial distribution, in relation to water masses during KEOPS2. The questions will be to understand how hydrodynamics during KEOPS2 alter frontiers between pelagic bioregions. The method will be to study species cluster vs. stations cluster.
– the role of zooplankton in the carbon transformation during the functioning during KEOPS2. Biomass stocks, zooplankton consumption on autotrophs (from gut content, zooplankton trophic interactions from 13C/15N in size fractions, respirations rates 02/CO2 of key species, will serve to estimate this role
– In addition, zooplankton specific determination and sizing will serve to calibrate and interpret images / signals from PVM, ZOOSCAN, ADCP and Echosounding. Migration pattern of key species might be derived.

34.1 Scientific context

During the KEOPS2 cruise, zooplankton sampling was made with Bongo net using two mesh size nets (120 µm and 300 µm). 42 net tows deployed in all stations and with a "midnight-midday" timing on long stations (> 24 hours).

Collected samples have been preserved for taxonomic counting with binocular, sizing with ZOOSCAN, weighting from dry weight, for measuring ^{13}C and ^{15}N ratios, for assessing the content in chlorophyll or derived pigments in gut.

In addition living animals were maintained for 20 to 36 hours to estimated oxygen consumption and CO2 production. In four among these experiments, ammonium production was measured additionally

All these data will be interpreted in the context of the pluridisciplinary research activities realized during the KEOPS2 cruise.

34.2 Overview of the project and objectives

The zooplankton data from nets will be used in connections with various data : sea surface temperature and chlorophyle, hydrodynamics, physical, chemical and biological parameter profiles from CTD

1) One objective will be to look at mesozooplankton species distribution in relation to water masses during KEOPS2. The questions will be to understand how hydrodynamics during KEOPS2 alter frontiers between pelagic bioregions. The method will be to study species cluster vs. stations cluster. This tudy should bring together the physicist and biologist. Potential co-authors: F. Carlotti, M.Zhou, F. Dovidio, Park, J., Jouandet M., Nowaczyk A.
2) A second objective will be to understand the role of zooplankton in the carbon transformation during the functioning during KEOPS2. Biomass stocks, zooplankton consumption on autotrophs (from gut content, zooplankton trophic interactions from $^{13}C/^{15}N$ in size fractions, respirations rates 02/CO2 of key species, will serve to estimate this role. F. Carlotti, Nowaczyk, A., Jouandet, M.P., Lefèvre, D. M. Zhou, Y. Zhu, Harmelin M.
3) If the analysis of isotopes delivers a large sets of interesting data, an independent paper could be proposed on Trophic interactions within mesozooplankton derived from C and N stable isotopic ratios in 5 mesosooplankton, to be prepared by Harmelin.
4) In addition zooplankton specific determination and sizing will serve to calibrate and interpret images / signals from PVM, ZOOSCAN, ADCP and Echosounding. Migration pattern of key species might be derived.

34.3 Methodology and sampling strategy

34.3.1 Echantillonnage.

42 opérations (Tableau 1) utilisant le double filet « Bongo ». Filets montés de maille de 330 µm et de 120 µm. Hormis lors des deux premières stations, les traits de filet ont été verticaux à une vitesse de remontée de 0,4-0,5 m/s.

Un grand nombre d' « opération » ont constitué une série de 3 traits de filets, 2 traits à 250 m, l'un pour la fixation au formol et les poids secs globaux, l'autre pour les isotopes. Le troisième trait, jusqu'à 100 m, était utilisé pour récupérer des individus pour des expériences de respiration (voir plus bas).

Table XLV : Sampled stations for mesozooplankton

Code BONGO	Station	Latitude	Longitude	Date	Heure Début (LT)
1	OISO7	47°40.00	56°00.3000	16-oct	14h30
2	A3-1	50°37.800	72°04.800	20-oct	03h38
3	A3-1	50°37.800	72°04.800	20-oct	14h47
4	TSN10	50°13.000	72°08.000	21-oct	09h09
5	TSN9	49°47.942	72°12.012	21-oct	14h41
6	TNS8	49°27.770	72°14.405	21-oct	20h05
7	TNS7	49°08.006	72°17.014	22-oct	03h07
8	TNS6	48°46.788	72°16.654	22-oct	13h10
9	TNS5	48°28.07	72°12.10	22-oct	19h14
10	TNS4	48°09.97	72°03.92	23-oct	02h36
11	TNS3	47°50.0114	71°55.1674	23-oct	07h50
12	TNS2	47°19.9	71°42	23-oct	13h00
13	TNS1	46°49.9884	71°30.0636	23-oct	19h24
14	RK2-2	50°21.5266	66°21.5266	26-oct	00h40
15	RK2-2	50°21.5264	66°42.9959	26-oct	13h50
16	RK2-2	50°21.5266	66°21.5266	27-oct	non réalisée
17	E1-1-D	48°30.6845	72°15.1721	29-oct	12h53
18	E1-1-N	48°27.4364	72°11.2665	30-oct	01h05
19	TEW1	49°08.9376	69°50.0104	31-oct	09h40
20	TEW2	48°53.9224	70°39.9719	31-oct	16h26
21	TEW3	48°47.93	71°01.06	31-oct	20h00
22	TEW4	48°37.98	71°37	01-nov	09h00
23	E1-2	48°31.4022	73°31.4022	01-nov	20h00
24	TEW5	48°28.0694	72°47.9267	01-nov	21h06
25	TEW6	48°27.9731	73°23.9907	02-nov	06h05
26	TEW7	48°27.9960	73°59.9655	02-nov	11h56
27	TEW8	48°28.3892	74°59.9576	02-nov	21h40
28	E1-3-N	48°42.1335	71°58.0025	03-nov	22h42
29	E1-3-D	48°42.2407	74°58.1966	04-nov	10h56
30	NPF-L	48°31.3813	74°40.0062	06-nov	12h20
31	NPF-L	48°31.9045	74°39.4807	06-nov	23h19
32	NPF-L	49°54.0099	71°53.9813	09-nov	01h28

Table XLV (continued)

33	NPF-L	49°07.9882	70°38.9813	09-nov	18h29
34	E1-4W	48°45.9974	71°25.7763	11-nov	11h05
35	E1-4W	48°45.9310	71°25.5104	11-nov	22h34
36	E1-4E	48°42.8355	72°34.1984	12-nov	21h47
37	E1-4E	48°43.0075	72°33.9974	13-nov	10h13
38	A3-2	50°37.4550	72°03.3261	16-nov	12h13
39	A3-2	50°37.4663	72°03.3465	16-nov	22h30
40	E1-5	48°24.7137	71°54.1538	18-nov	17h57
41	E1-5	48°24.6964	712°53.9917	19-nov	01h59
42	A1-5	48°24.7137	71°54.1538	19-nov	19h02

Table XLVI : Exhaustiv list of measured parameters

Parameter	code of operation	units
1. Taxons - densities	BONGO NET	#/ m3
2. Biovolume size spectrum	BONGO NET	mm3 / m3
3. Dry weight	BONGO NET	mgDW / m3
4. ^{13}C, ^{15}N in 5 size fractions	BONGO NET	‰
5. Gut content	BONGO NET	µg Chla / ind
6. Respiration rate	BONGO NET	µmol O2 / ind / d
5. Gut content	BONGO NET	µmolCO2 / ind / d

34.4 Traitements des échantillons de mesozooplancton

Traitement à bord :

Opérateurs : F. Carlotti ; M.P. Jouandet

- Fractionnement de l'échantillon à l'aide d'une boite de Motoda en fonction de la densité observée du zooplancton.
- Conditionnement d'une fraction dans des pots de 250 ml d'eau de mer à 5% de formaline tamponnée.
- Filtration d'un fragment sur filtre pour mesure de poids sec global
- Fractionnement sur 5 classes de tailles 80 µm, 200 µm, 500 µm, 1000 µm, 2000 µm pour mesures d'isotopes stables
- Fractionnement sur 4 classes de tailles 200 µm, 500 µm, 1000 µm, 2000 µm pour mesures de contenus stomacaux.

Traitement ultérieur :

Opérateurs : F. Carlotti ; M.P. Jouandet ; A. Nowaczyk, M. Harmelin

- Dénombrement des espèces à la loupe binoculaire pour obtenir les abondances par espèces et par station et étudier la diversité (cf. Carlotti *et al.*, 2008)
- Dénombrement des organismes par le ZOOSCAN pour obtenir le spectre de taille (cf. Nowaczyk *et al.*, 2011)
- Pesée pour poids sec de la biomasse totale échantillonnée (cf. Carlotti *et al.*, 2008 ; Nowaczyk *et al.*, 2011)
- Quantification des isotopes stables dans les fractions de taille du mesozooplancton (cf. Banaru & Harmelin 2009 pour la méthode de mesure des isotopes). Les isotopes stables du carbone et de l'azote se sont révélés être de bons traceurs des relations trophiques au sein des écosystèmes. L'utilisation de cet outil repose sur le principe qu'il existe une discrimination ou fractionnement isotopique prédictible entre un prédateur et sa proie. Cet enrichissement isotopique-trophique est habituellement considéré comme constant.
- Fluorescence des Contenus stomacaux (cf. Carlotti *et al.*, 2008 ; Nowaczyk *et al.*, 2011)

34.5 Mesures de la respiration d'organismes zooplanctoniques

Traitement à bord :

Opérateurs : F. Carlotti ; D. Lefèvre., M.P. Jouandet

86 mesures de respiration sur des groupes de copépodes, salpes, cténophores, chaetognathes, euphausiacés, amphipodes et gymnosomes.

Les organismes ont été prélevés aux stations RK2, E1-1, E1-3, E1-4, A3-2.

Les expériences en incubation de 24h à 36h ont été réalisées après la capture des organismes.

Les animaux étant placés dans de l'eau de mer filtrée à 0,2 µm et incubés pendant des périodes de 18 heures à 36 h. Les paramètres mesurés sont la consommation d'oxygène et de la production de CO_2. Les méthodes sont décrites dans Carlotti et al (2008), Nowaczyk *et al.*(2011). Pour la mesure de CO_2 (voir aussi le rapport de D. Lefèvre).

Traitement ultérieur :

Opérateurs : F. Carlotti ; D. Lefèvre.,

Traitement des données.

34.6 Post-cruise sampling analyses and dead-lines

Septembre 2012 : Résultats brut en Taxonomie, Poids secs, Isotopes, Gut content, Analyse sur les premiers résultats

Juin 2013 : Articles rédigés.

34.7 References of methods

Banaru D. & , Harmelin-Vivien, M., 2009. Trophic links and riverine effects on food webs of pelagic fish of the north-western Black Sea. Marine and Freshwater Research, 60, 529–540

Carlotti, F., Thibault-Botha, D., Nowaczyk, A, Lefèvre D. (2008) Zooplankton community structure, biomass and role in carbon transformation during the second half of phytoplankton bloom on the Kerguelen shelf (January –February 2005) and comparison with the oceanic areas. Deep-Sea Research II, 55 : 720–733.

Nowaczyk A., Carlotti F. , Thibault-Botha D., Pagano M. (2011) Metazooplankton diversity and spatial distribution across the Mediterranean Sea in summer (BOUM Cruise). Biogeoscience (in press). Paper available in Biogeoscience discussion.

35 OISO20: Spatial and temporal variability of oceanic CO_2

Principal investigator

Claire Lo Monaco
LOCEAN-IPSL, UPMC case100, 4 place Jussieu, 75252 Paris cedex 5, France
☎ +33 1 44 27 33 94
eclaire.lomonaco@locean-ipsl.upmc.fr

Names of other participants (+affiliation)

- J. Llort (LOCEAN-IPSL)
- C. De La Vega (IPEV)
- D. Lefèvre (LMGEM)
- L. Chirurgien (LMGEM)
- L. Oriol (LOMIC)
- A. Gueneugues (LOMIC)
- J. Caparros (LOMIC)

Résumé :
Le Service d'Observation OISO vise a maintenir sur une longue durée l'évaluation des flux air-mer de CO_2 et de l'invasion de CO_2 anthropique dans l'Océan Indien Austral. Pendant la campagne KEOPS2, les propriétés hydrologiques et biogéochimiques ont été mesurées dans les eaux de surface (en continu) et dans la colonne d'eau (stations CTD), incluant le CO_2 océanique et atmosphérique, le carbone inorganique dissous, ainsi que les paramètres complémentaires qui permettront de mieux comprendre l'origine des variations observées (température, salinité, alcalinité totale, oxygène dissous, chlorophylle-a, sels nutritifs, $\delta^{13}C_{DIC}$ et $\delta^{18}O_{H2O}$).

Abstract:
The OISO program aims at monitoring the evolution of air-sea CO_2 fluxes and evaluating the invasion of anthropogenic CO_2 in the Southern Indian Ocean. During the KEOPS2 cruise, hydrological and biogeochemical properties were measured in surface waters (underway measurements) and in the water column (CTD stations), including oceanic and atmospheric CO_2, dissolved inorganic carbon, as well as that the complementary parameters that will allow to investigate the origin of the observed changes (temperature, salinity, total alkalinity, dissolved oxygen, chlorophyll-a, nutrients, $\delta^{13}C_{DIC}$ and $\delta^{18}O_{H2O}$).

35.1 Scientific context

"The Kyoto Protocole requires nations to monitor their "national" carbon sources and sinks, and that interannual and seasonal resolution is required to constraint both oceanic and terrestrial budgets versus emissions" (conclusions from the Ocean Observation Panel for Climate).

Observing and understanding the seasonal, interannual and decadal variations of the oceanic carbon cycle is crucial to better estimate the global carbon budget and to validate diagnostic and prognostic climate models. Although the importance of the Southern Ocean in the carbon cycle and climate change is widely recognized, observations of the carbon dioxide (CO_2) system are still rela-

tively sparse in the southern high latitudes regions compared to other key regions such as the North Atlantic Ocean. The OISO program (Service d'Observation INSU/IPSL) was initiated in 1998, and was later associated to the MINERVE program conducted onboard the R.V. L'Astrolabe (IPEV), as part of the French Observatory CARAUS (Carbone Austral). The OISO and MINERVE cruises are conducted every year onboard the R.V. Marion-Dufresne and L'Astrolabe (respectively) in the South Indian and Southern Oceans. The CARAUS Observatory makes a significant contribution toward resolving the role of the Southern Ocean in the uptake of atmospheric CO_2 and its evolution with time.

The OISO program is supported by three French Institutes (INSU, IPSL and IPEV), and it is linked to the international research programs IGBP, IMBER, CLIVAR, SOLAS, and the European Integrated Program CARBOCHANGE.

35.2 Overview of the project and objectives (1/2 page max.)

The objective of the OISO program is to monitor the evolution of air-sea CO_2 fluxes over different regions of the Southern Indian Ocean (subtropical, subantarctic and antarctic zones) at the seasonal to decadal scales, and to evaluate the decadal changes in dissolved inorganic carbon in the ocean interior attributed to both the invasion of anthropogenic CO_2 and natural variability. In this, the OISO program is part of the international collaborative effort for the monitoring of oceanic CO_2 (figure 1). Detailed information about the OISO Program can be found on the Web: http://www.caraus.ipsl.jussieu.fr/oiso-accueil.html.

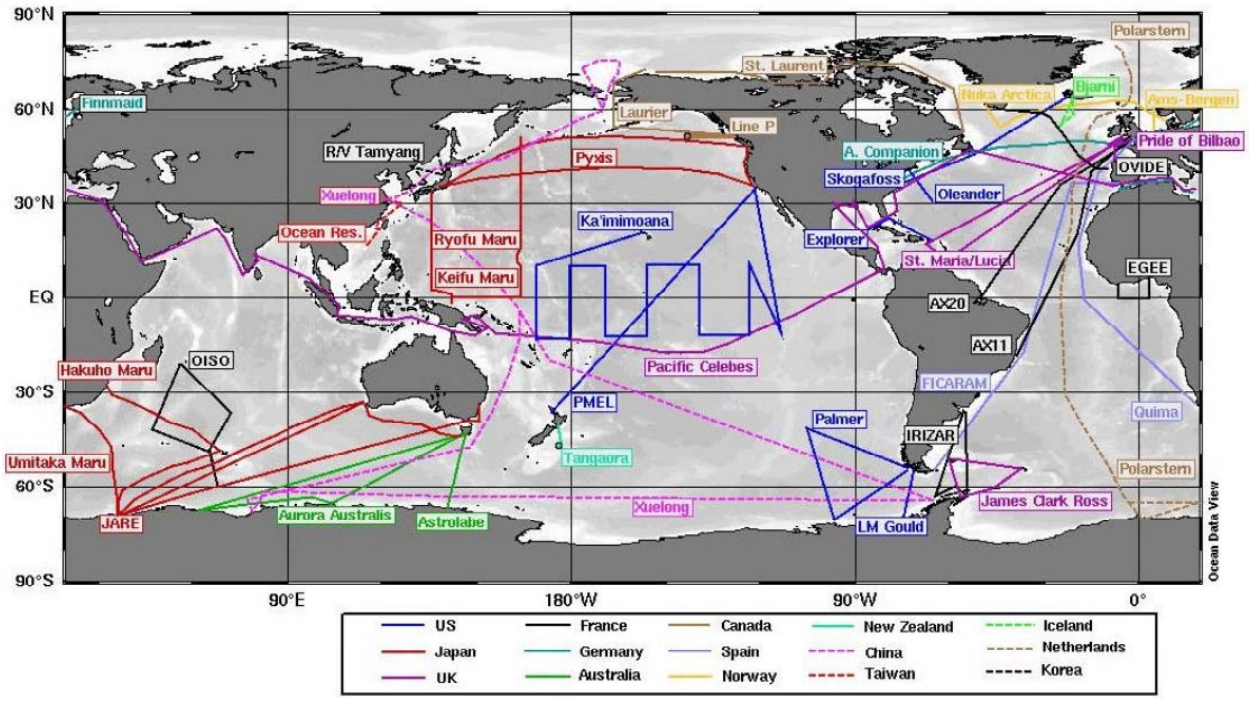

Figure 56 : Compilation of sea surface measurements of CO_2 at the international level, including the OISO and MINERVE (Astrolabe) cruises in the South Indian and Southern Ocean. Source: IOCCP report, 2007, www.ioc.unesco.org/ioccp/pCO2_2007.htm.

35.3 Methodology and sampling strategy

During the cruise MD188-KEOPS2 onboard R.V. Marion-Dufresne (IPEV), hydrological and biogeochemical properties were measured in surface waters and in the water column. Continuous sea surface measurements were obtained between October the 10th and Novembre the 22nd for temperature (SST), salinity (SSS), fluorescence, dissolved oxygen (O_2, from Oct. the 14th), and the fu-

gacity of CO_2 (fCO_2, from Oct. the 17th). Atmospheric CO_2 was also measured every 4 hours, and surface water samples were colleted regularly for dissolved inorganic carbon (DIC), total alkalinity (TA), salinity, dissolved O_2, nutrients (nitrates, nitrites, silicates, phosphate), chlorophyll-a (chl-a) and the stable isotopes $\delta^{13}C$ of DIC and $\delta^{18}O$ of H_2O. In addition to surface data, the water column was sampled at 34 stations, including two OISO stations north and east of Crozet Islands (Subantarctic and Antarctic zones). At the OISO stations, samples were collected in the first 1000m of the water column (22 Niskin bottles) for salinity, dissolved O_2, DIC, TA, nutrients, chl-a, $\delta^{13}C_{DIC}$ and $\delta^{18}O_{H2O}$. At the KEOPS stations, samples were collected from 6 to 14 Niskin bottles for DIC and TA. Water column samples were also collected for $\delta^{13}C_{DIC}$ and $\delta^{18}O_{H2O}$ at a few stations as a complement to KEOPS sampling.

Table XLVII : Exhaustiv list of measured parameters

Parameter	code of operation	Units
1. oceanic fCO_2	Underway	µatm
2. atmospheric pCO_2	Underway	ppm
3. temperature	Underway	Degree C
4. salinity	Underway	
5. fluorescence	Underway	volt (not calibrated)
6. dissolved oxygen	Underway	µmol/kg
7. nitrate	Underway	µmol/kg
8. nitrite	Underway	µmol/kg
9. silicate	Underway	µmol/kg
10. phosphate	Underway	µmol/kg
11. chlorophyll *a*	Underway	µg/L
12. dissolved inorganic carbon	Underway + CTD	µmol/kg
13. total alkalinity	Underway + CTD	µmol/kg
14. $\delta^{13}C_{DIC}$	Underway + CTD	Per mil
15. $\delta^{18}O_{H2O}$	Underway + CTD	Per mil

Total alkalinity (TA) and dissolved inorganic carbon (DIC) were measured onboard for both surface and water column samples using a potentiometric method with a closed cell (details on the method can be found on the web : http://soon.ipsl.jussieu.fr/SNAPOCO2/). DIC and TA measurements were calibrated using Certified Referenced Materials (CRMs, Batch 111) provided by Dr. A. Dickson (SIO, University of California). The precision estimated from the CRMs values during OISO cruises is around 2.2 µmol/kg for TA and DIC.

The technique for fCO_2 measurements has been described in details by Poisson *et al.* (1993), Metzl *et al.* (1995, 1999), Jabaud-Jan *et al.* (2004). This instrumentation was also part of the international at-sea intercomparison of fCO_2 systems conducted in the late 1990's (Körtzinger *et al.*, 2000). In short, sea surface water is continuously equilibrated using a "thin film" type equilibrator thermostated with surface seawater. The CO_2 in the dried gas is measured with a non-dispersive infrared analyser (NDIR, Siemens Ultramat 5F until the 27th of Oct. and Ultramat 6 from the 29th of Oct.). Standard gases (270 ppm, 375 ppm, 480 ppm) were used for calibration. Based on previous cruises analysis, the oceanic fCO_2 data are accurate to about ± 0.7 µatm.

Nutrients, dissolved O_2 and salinity were measured onboard. Techniques and accuracy are described in details in the KEOPS2 cruise reports by Blain *et al.*, Lefèvre *et al.* and Park *et al.*, respectively.

Water samples for $\delta^{13}C_{DIC}$ measurements were collected in 125 ml glass bottles and poisoned with 1 ml of saturated solution of $HgCl_2$ for storage. Water samples for $\delta^{18}O_{H2O}$ were collected in 25 ml tinted glass bottles. $\delta^{13}C_{DIC}$ and $\delta^{18}O_{H2O}$ samples will be measured at LOCEAN following the methods described by Racapé *et al.* (2010) and Pierre *et al.* (2011), respectively.

35.4 Post-cruise sampling analyses and dead-lines

Chlorophyll *a*, $\delta^{13}C_{DIC}$ and $\delta^{18}O_{H2O}$ will be measured at LOCEAN and will be available before the end of the year.

35.5 Data base organization (general cruise base and/or specific data base(s))

In addition to the general KEOPS database, the CO_2 data collected during the cruise will be available at the Carbon Dioxide Information Analysis Center (http://cdiac.ornl.gov/oceans/)

35.6 References of methods

Jabaud-Jan A., N. Metzl, C. Brunet, A. Poisson and B. Schauer, 2004. Variability of the Carbon Dioxide System in the Southern Indian Ocean (20°S-60°S): the impact of a warm anomaly in austral summer 1998. Global Biogeochemical Cycles, Vol. 18, No. 1, GB1042,10.1029/2002GB002017.

Körtzinger, A., L. Mintrop, D.W.R. Wallace, K.M. Johnson, C. Neill, *et al.*, 2000. The international at-sea intercomparison of fCO2 systems during the R/V Meteor Cruise 36/1 in the North Atlantic Ocean. Marine Chemistry 2 (2–4), 171–192.

Metzl, N., A.Poisson, F. Louanchi, C. Brunet, B. Schauer, B. Brès, 1995. Spatio-temporal distributions of air-sea fluxes of CO2 in the Indian and Antarctic Oceans: a first step. Tellus, 47B, 56-69.

Metzl, N., B.Tilbrook and A. Poisson, 1999. The annual fCO_2 cycle and the air-sea CO2 flux in the sub-Antarctic Ocean. Tellus, 51B, 4, 849-861.

Pierre C., J-F. Saliege, M-J. Urrutiaguer, and J. Giraudeau, 2001. Stable isotope record of the last 500 ky at site 1087 (Southern Cape Basin). in: Wefer G., Berger W.H., Richter C. *et al.*, Proceedings of the ocean Drilling Program, Scientific Results, vol. 175, chapter 12, 1-22.

Poisson, A., N. Metzl, C. Brunet, B. Schauer, B. Brès, D. Ruiz-Pino and F. Louanchi, 1993. Variability of sources and sinks of CO2 and in the western Indian and Southern Oceans during the year 1991. J. Geophys. Res. 98, C12, 22,759-22,778.

Racapé, V., C. Lo Monaco, N. Metzl, and C. Pierre, 2010. Summer and winter distribution of δ13CDIC in surface waters of the South Indian Ocean (20°S-60°S). Tellus B 62, 5, 660-673. DOI: 10.1111/j.1600-0889.2010.00504.x